Strategies for dynamic vision in the *Drosophila* peripheral visual system

Dissertation
for the award of the degree

Doctor rerum naturalium (Dr.rer.nat)

of the Georg-August-Universität Göttingen

within the doctoral program *Neurosciences*
of the Georg-August University School of Science (GAUSS)

submitted by

Madhura D. Ketkar

from Thane, India

Göttingen/Mainz, 2021

Thesis Committee

Prof. Dr. Marion Silies
Neural Circuits Lab, Institute of Developmental Biology and Neurobiology (iDN), Johannes Gutenberg University of Mainz

Prof. Dr. Tim Gollisch
Sensory Processing in the Retina, Department of Ophthalmology, University Medical Center Göttingen

Dr. Viola Priesemann
Neural Systems Theory, Max Planck Institute for Dynamics and Self-Organization, Göttingen

Members of the Examination Board

First referee: Prof. Dr. Marion Silies
Neural Circuits Lab, Institute of Developmental Biology and Neurobiology (iDN), Johannes Gutenberg University of Mainz

Second referee: Prof. Dr. Tim Gollisch
Sensory Processing in the Retina, Department of Ophthalmology, University Medical Center Göttingen

Further members of the Examination Board

Dr. Viola Priesemann
Neural Systems Theory, Max Planck Institute for Dynamics and Self-Organization, Göttingen

Prof. Dr. Tobias Moser
Institute for Auditory Neuroscience, University Medical Center Göttingen

Prof. Dr. Martin Göpfert
Department of Cellular Neurobiology, Schwann-Schleiden Research Centre, University of Göttingen

Dr. Jan Clemens
Neural Computation and Behavior group, European Neuroscience Institute Göttingen

Date of oral examination: 05.11.2021

Table of Contents

Abstract

Changes in luminance over space and time drive visual behaviors across species. Thus, sensitivity to luminance changes or *contrast* is fundamental to visual perception. Visual perception has to work in many different conditions, and these conditions can change rapidly. For perception unaffected by viewing conditions, contrast sensitivity must remain constant despite changing visual statistics, such as changes in mean luminance. Across species, photoreceptor gain control maintains the system sensitive enough to capture light changes over vastly varying illumination, however the gain control often does not meet the goal of constant contrast sensitivity, especially in dynamic conditions. Yet, animals across the evolutionary tree seem to reliably interpret visual cues when they navigate environments, suggesting a role of post-receptor visual circuitry in revising contrast sensitivity through additional layers of luminance gain control. Furthermore, gain correction must occur across parallel divisions of visual processing hierarchies, such as in both the ON and OFF pathways, within their differential circuit architectures and physiology. How the post-receptor gain control operates towards a robust contrast sensitivity evident in behavior, and how this is organized across parallel pathways is not understood in any visual system.

In this thesis, I study how the peripheral visual system of fruit flies *Drosophila melanogaster* organizes information processing to support robust contrast computation and guide behavior. In the first manuscript, we show that fly behavior is luminance invariant in dynamic conditions, although peripheral contrast computation is not. Two first-order interneurons L2 and L3 in parallel convey luminance and contrast information respectively, and the luminance information is key to revise contrast computation in downstream circuitry. Luminance information scales up contrast signals in sudden dim light, when photoreceptors and the first-order interneurons do not increase their gain sufficiently fast. Thus, the peripheral processing stages themselves do not achieve a fixed contrast sensitivity in dynamic conditions, but they preserve and relay the forms of information required for contrast refinement in downstream circuitry. Here, parallel processing of the features contrast and luminance is the strategy that helps tackle the challenge of processing visual cues dynamically (Ketkar et al., 2020).

I next explore how ON and OFF pathways compare in the ways they implement parallel feature processing and enable luminance invariance, especially considering their anatomical and physiological distinctions. Whereas the OFF pathway in *Drosophila* receives both luminance and contrast inputs through L2 and L3, the ON pathway was known to rely on input from a single contrast-sensitive first-order interneuron, L1. In the second manuscript, we show that the interneurons L1, L2 and L3 do not form ON- or OFF-specific inputs, but rather specialize in encoding contrast and luminance differently. Both ON and OFF pathways then benefit from this diversified luminance information as they compute luminance-invariant contrast in further processing stages. Therefore, the peripheral fly visual circuitry seems to first filter the photoreceptor signals differentially and then distribute them across ON and OFF pathways. In both pathways, luminance is required for behaviorally relevant contrast correction downstream of L1-L3.

Finally in the third manuscript, I perform a comprehensive analysis of behaviorally relevant luminance gain across many different contrast and luminance conditions. This work demonstrates that post-receptor gain correction is a two-way process that can both enhance and reduce gain to restore the behavioral relevance of different contrasts. The correction is generally required across both fast and slow illumination changes. L2 contrast sensitivity scales with luminance even in fully adapted conditions, and the fixed contrast sensitivity seen in behavior is a result of post-L2 gain control. L3-mediated gain correction plays a dichotomous role, wherein particularly dim stimuli are amplified, and contrast signals in bright conditions are either scaled up or down to make up for the nature of contextual gain deficit. Based on behavioral data, an algorithmic model proposes a multi-channel circuitry to explain the multitude of gain correction operations led by luminance signals. Therefore, the circuitry seems to adopt a strategy of parallel computations up to an advanced circuit element, where the features must eventually be integrated.

In sum, these findings reveal how behavioral responses to ON and OFF contrasts can achieve constancy beyond the first two processing stages, owing to downstream luminance gain control strategies. This work sheds light on the neural correlates of contrast constancy in a more proximal circuitry than photoreceptors, and the genetic access to cell types in *Drosophila* allows to dissect neural circuitry while directly correlating cell type physiology with behavioral output. Considering the common environmental challenges faced by different species and shared computational principles around which the systems have evolved, the involvement of gain control hierarchy in behavior is likely similar across visual systems, including our own.

Introduction

Vision is a major sensory modality in many animals. Biological vision has evolved to support survival of a great deal of species in vastly varying environments. Our own vision works efficiently across so many different viewing conditions where machine vision is still challenged to perform comparably well. It is no wonder that visual systems are immensely complex in terms of the cellular diversity that they host, and the physiological specializations that the diverse cell types develop in a hierarchical fashion. To understand how visual information guides behavior, it is essential to study how visual processing stages sequentially extract increasingly complex information. Such understanding would not only further our efforts of restoring biological vision, but also help improve algorithms of machine vision that are taking up increasingly crucial roles in our lives, such as in optical character or object recognition, or to develop autonomous navigation of cars.

Peripheral processing is generally considered to extract basic features such as contrast, by adapting their gain to luminance. However, cellular constraints at each stage imply that contrast computation expected from a behavioral standpoint occurs in a distributed fashion across multiple processing stages. To delineate the circuitry underlying the orchestrated computation, it is necessary to understand the constraints on the peripheral contrast computation and the strategies that the circuitry adopts to overcome these limitations. In this thesis, I study the physiological role of peripheral processing stages in relaying information useful for perception and behavior.

In the following sections, I recollect our current understanding of what perception and behavior demand from visual processing, and how different processing stages contribute to meeting these demands in varying visual environments. In the beginning, I argue that the visual feature 'contrast', which is considered to be an outcome of peripheral processing, forms the basis of visual perception and must be computed in specific ways to accurately represent visual cues. I proceed with reviewing how contrast is encoded by peripheral visual systems and how it is processed further in the visual hierarchy to derive behaviorally useful information. At this stage, I take a comparative approach to consider how visual systems of flies and vertebrates organize contrast processing in comparable ways, while noting dissimilarities stemming from the evolutionary distances between them. Lastly, I go through the common challenges in contrast processing and known strategies, before defining my aims for this thesis.

1. Contrast: the most basic visual information

Visual information arrives at the eyes as photons, but it must undergo several processing steps before it takes a useful form to guide perception or behavior. Photons arriving at a retinotopic location at a single time point are loaded with information, yet being uninformative before they are compared with another location or another time point. Only a difference in their number (intensity) or their energy (wavelength/color) is truly informative. Thus, to see is to see a difference, either spatially or temporally, in incoming photons.

Detecting a mere difference between the numbers of photons is neither possible nor useful. It is not possible because light intensities vary over ~10 orders of magnitude throughout the day, and by 4-5 orders within a natural scene (Naka and Rushton, 1966; Pouli et al., 2010; Rieke and Rudd, 2009a). In contrast, the operating range of our light sensors – photoreceptors – is limited to two orders of voltage levels (Naka and Rushton, 1966; Normann and Perlman, 1979; Schnapf et al., 1990). Mere photon difference is also not useful for object recognition, a prime goal of visual processing, since the same objects reflect very different amounts of photons in different viewing conditions (Figure 1). Thus, capturing a vast range of differences in a perceptually useful way with a constrained apparatus is the first challenge our photoreceptors must tackle. They do so by detecting a photon difference relative to prevailing light conditions, generally termed as contrast (Laughlin and Hardie, 1978; Normann and Perlman, 1979; Normann and Werblin, 1974; Shapley and Enroth-Cugell, 1984). Thus, contrast is one of the first informative features that enters the processing pipeline.

As contrast helps the detection of edges between objects or between differently lit areas, it forms the basis for extracting several features along the visual hierarchy, including edges, shape, orientation, motion and so on. All these features ultimately shape object recognition and other interpretations of visual cues including motion. Besides providing the substrate for feature extraction, the amplitude of contrast also encodes the strength of visual cues. For example, the temporal contrast cue generated by dark clouds sweeping over the sun is stronger than white clouds doing so, and the two cues may influence behavioral decisions differently. In line with this, behavioral responses scale with contrast in diverse species including humans, monkeys, mice, zebrafish, bees and fruit flies (Busse et al., 2011; Chakravarthi et al., 2016; Dakin and Turnbull, 2016; Keleş et al., 2019; Palmer et al., 2007; Rinner et al., 2005). In hoverflies, descending neurons that are adapt to visual motion also rely on stimulus contrast, and they adapt to visual motion (Nicholas and Nordström, 2020).

Contrast can be both chromatic (color contrast) and achromatic (brightness contrast), i.e. between two hues or between two intensities of the same hue. Purely temporal contrasts, emerging from illumination changes over a static scene, are largely achromatic. This thesis mainly concerns the encoding of achromatic contrasts, including and preferentially temporal contrasts, at the neural level and the question how this guides animal behavior. Before delving into contrast encoding by visual systems, I will summarize different ways of defining contrast as a physical parameter to describe visual scenes.

1.1 Measures of contrast

Contrast is the difference in luminances relative to mean luminance. Depending on stimulus structure over which to calculate mean luminance, different measures of contrasts are used. For example, Weber contrast C_{Weber} is a suitable description, when one of two surfaces under comparison occupies a greater portion of the visual field, such as this white page with black text. The greater portion is considered background (white page), and the other surface makes an object (black text). The contrast is then denoted as

$$C_{Weber} = \frac{L_{object} - L_{background}}{L_{background}}$$

where L is the luminance of object or background. The definition assumes background luminance as the mean luminance, which thus normalizes the difference between object and background intensity. When surfaces cannot be classified as objects and backgrounds, but rather have a periodic structure such as square-wave gratings, Michelson contrast $C_{Michelson}$ is computed as

$$C_{Michelson} = \frac{L_{max} - L_{min}}{L_{max} + L_{min}}$$

where L_{max} and L_{min} are the luminances of the relatively more reflective and less reflective of the two surfaces. When describing light differences for a more intricate spatial structure embedding a range of reflecting properties – a case often found in natural environments – root-mean-square (RMS) contrast is particularly useful (Drews et al., 2020; Frazor and Geisler, 2006). RMS contrast is a measure of deviation around mean luminance of a scene, and for pairs of surfaces it is equivalent to Weber contrast.

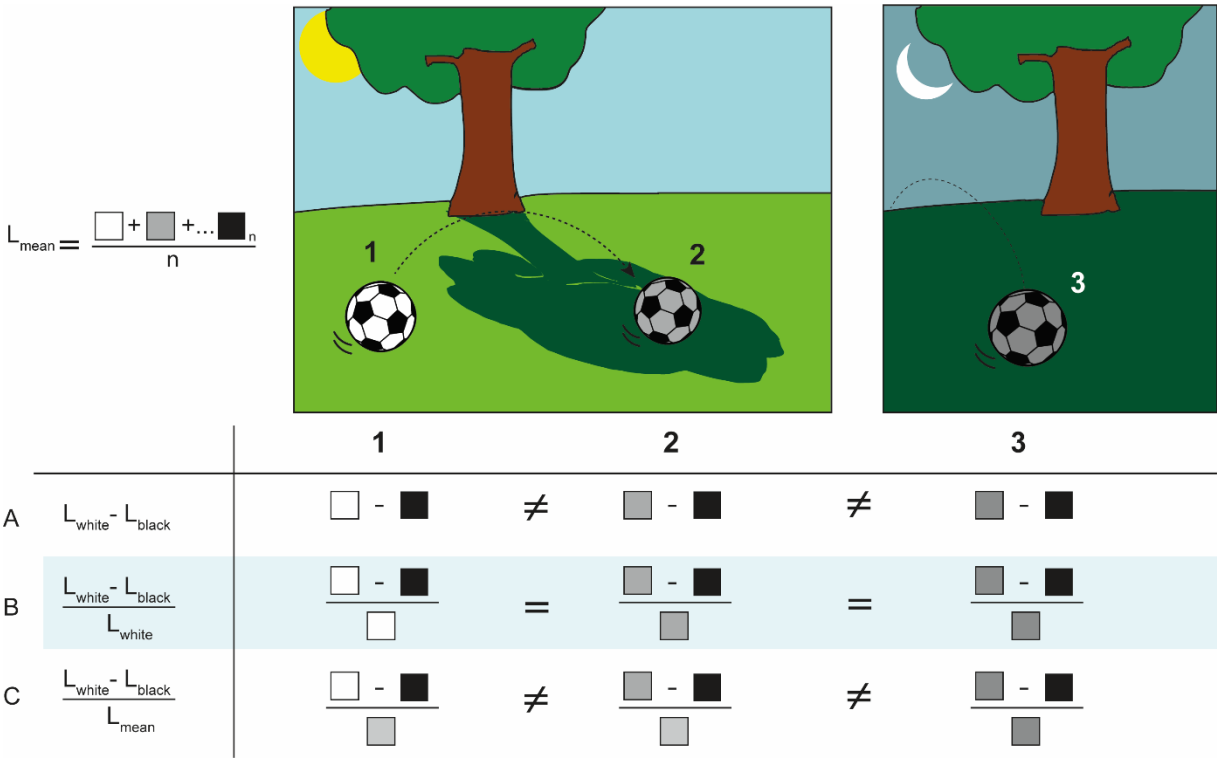

Figure 1: Contrast computed with reference to rapidly updating luminance is useful for object recognition. (A) Illumination changes rapidly due to motion, e.g. movements during a soccer game across sunlight and shadows (1 and 2) or slowly due to day-night changes (3). Consequently, the black and white patches of the soccer ball reflect different amounts of light in all three conditions. Yet the ball is perceived to be the same object, implying mere luminance difference (L_{white} -L_{black}) that changes with illumination does not drive our perception. (B) Luminance difference normalized by the current reference (here, L_{white}) leads to a measure of contrast (here, Weber contrast) that remains constant across illumination conditions, thus supporting object recognition. (C) If a mean luminance over a large spatial/temporal window (L_{mean}) is used as reference, the

resulting contrast estimate would again vary in rapidly changing conditions. Thus, rapidly updating the luminance reference is essential for perceptually relevant contrast estimation across conditions.

By any of these definitions, contrast is a luminance-invariant description of a stimulus, since contrast computation normalizes the raw luminance difference by mean luminance. However, mean of luminance values can be computed across different spatiotemporal scales. Weber contrast is sometimes defined for stimuli comprising more than two luminance values changing over time, where the mean of all values is taken as the normalizing parameter (Baden et al., 2013). Some other measures such as percent contrast or fractional contrast also often rely on a range of luminance values displayed over time rather than the immediately preceding luminance as the reference (Rister et al., 2007; Silies et al., 2013a). How visual systems encode contrast and which contrast measures ultimately guide appropriate behavior is particularly important.

1.2 Behaviorally relevant estimation of contrast

For the goal of object recognition, contrast encoded by visual systems between two objects/surfaces should compare their fixed properties, especially reflectance. The luminance-invariant measures of contrast listed above essentially are comparisons of reflectance (Shapley and Enroth-Cugell, 1984). However, the spatiotemporal scales at which perception has to work robustly determine the useful extent of averaging luminance, which serves as the normalizing parameter for contrast computation. For perceptual invariance over slow day-night transitions, averaging luminance over long time windows (of the order of minutes) is sufficient. In contrast, exploratory saccadic eye movements occurring every few hundred milliseconds as well as self-motion result in rapid scene changes, implying the reference luminance must be updated dynamically, rather than relying on mean luminance over long temporal windows (Figure 1) (Andrews and Coppola, 1999; Frazor and Geisler, 2006; Rieke and Rudd, 2009a). Similarly, scene statistics can vary substantially between spatial locations, and thus local luminance values instead of global means must be used as reference for contrast computation (Rieke and Rudd, 2009a). In sum, contrast computation must be adaptive, such that the reference luminance should be updated by averaging on short temporal and spatial scales.

Focusing on the temporal domain, perceptual reports indeed revealed that adaptive contrast computation guides perception at multiple timescales. At slow timescales where exposure to background luminance was a few minutes-long, just-detectable stimulus strength scaled with background luminance for a range of luminance, thus constituting Weber region of the threshold-vs-luminance curves for both rod and cone vision (Aguilar and Stiles, 1954; Barlow, 1965; Koenderink and van Doorn, 1978; Nes and Bouman, 1967; Whittle and Challands, 1969). Similar measurements of cat behavior showed qualitative similarities with human contrast sensitivity (Pasternak and Merigan, 1981). When the time course of adaptation was specifically examined, contrast sensitivity recovered to a considerable extent within 200 ms of background viewing (Adelson, 1982; Crawford, 1947; Hayhoe and Wenderoth, 1991; Hayhoe et al., 1987), matching the timescales of fixation between consecutive saccades. Likewise, contrast amplitude could be accurately perceived if presented after ~400 ms of background exposure (Kilpelainen et al 2011). Thus, visual systems can compute contrast relative to

rapidly updating luminance, and support perceptual invariance across luminance changes. On the other hand, contrast sensitivity further adapts for several tens of seconds (Adelson, 1982), arguing for contrast-coding mechanisms acting also on longer timescales, potentially to account for slow but large day-night luminance transitions. Notably, contrast computation adapts differently over different ranges of background luminance. Unlike the Weber region, where detection thresholds are proportional to background luminance, low luminance ranges comprise regions of constant threshold ('dark light' region) or thresholds increasing less steeply than the Weber region (e.g. Rose-de Vries region), indicating limitations of adaptation in very low luminance (Aguilar and Stiles, 1954; Barlow, 1965; Rieke and Rudd, 2009a).

Admittedly, accurate contrast estimation regardless of light changes is just one step towards object recognition. Perceptual invariance is achieved by the entire brain and also involves top-down control, however visual processing mechanisms alone explain many psychophysical observations related to contrast perception (Adelson, 2000; Blakeslee and McCourt, 2015). Especially, constant perception of contrast regardless of luminance i.e. contrast constancy is considered to emerge mainly due to adaptive visual processing, specifically peripheral processing.

2. Neural basis of contrast processing

Where in the visual circuitry is behaviorally relevant contrast computed? The earliest psychophysical assessments proposed 'adaptation pools' past photoreceptors, within which spatially summated signals enable adaptation by negative feedback (Rushton, 1965). Direct measurements of photoreceptor response demonstrated that photoreceptors themselves adapt to luminance and compute contrast, albeit with limitations.

2.1 Photoreceptors

Photoreceptors are entry points to visual systems and the entire visual perception is limited by their information capture (with the exception of ipRGCs in the vertebrate retina, considered below). To capture massive input changes with limited operating range, photoreceptor types across visual systems adapt their gain, defined as ratio of physiological response (e.g. voltage) to luminance changes. Gain increases at low luminance so that luminance changes do not go undetected, and decreases at high luminance so as to avoid saturation. In an ideal case of gain control the system follows Weber's law, i.e. when the gain is inversely proportional to the mean luminance. Photoreceptor gain follows Weber's law, at least after prolonged exposure to background (Baylor et al., 1980; Burkhardt, 1994). Adapted photoreceptor intensity-response functions measured at different background luminances appear copies of each other shifted along the log-luminance axis (Burkhardt, 1994; Laughlin and Hardie, 1978; Normann and Perlman, 1979; Normann and Werblin, 1974), indicating background-invariant encoding of (Weber) contrast (Figure 2).

Mechanisms underlying photoreceptor gain control are diverse, ranging from rearrangement of screening pigments to modulation of the phototransduction cascade to membrane conductance changes and neuronal feedback (Abbas and Vinberg, 2021; Burkhardt, 1994; Fain et al., 2001; Frixione

and Pérez-Olvera, 1991; Kirschfeld and Franceschini, 1969; Zheng et al., 2006). Besides, adaptation of pupil size in vertebrates and eye optics in compound eyes of invertebrates add pre-receptor adaptation (Kirschfeld, 1976; Laughlin, 1989; Nilsson, 1989). The different mechanisms work at different timescales, ranging from a few milliseconds (e.g. Ca^{2+} homeostasis) to several minutes or even hours (e.g. photopigment regeneration). Especially, dark adaptation (recovery after photobleaching) requires extensive regeneration of photopigments, which may result in reduced sensitivity for several minutes after bleaching (Fain et al., 2001; Normann and Werblin, 1974). Fly photoreceptors complete a rapid phase of adaptation in 100ms, but the slow phase lasts up to 60s (Laughlin and Hardie, 1978). Therefore, contrast computed by photoreceptors, at least at light offset, is relative to a considerable luminance history and thus not always accurate enough for perceptual requirements.

Importantly, photoreceptor response waveforms include a luminance-sensitive sustained component that marks their steady state (Figure 2). The steady-state response scales with luminance until it asymptotically attains a constant value at high luminance (Burkhardt, 1994; Laughlin and Hardie, 1978; Normann and Werblin, 1974). Whereas the sustained component is captured by some classes of first-order interneurons, its function in image-forming computations is not clear. In the vertebrate retina, the sustained component from the rod-bipolar cell pathway may enter the cone pathway via the AII amacrine cells, where it is thought to enable contrast computation in scotopic conditions (Oesch and Diamond, 2011). Besides, sustained components are thought to constitute surround inhibitory fields of first-order interneurons, thus helping the subtraction of constant illuminant information (Laughlin, 1989).

Unsurprisingly, different receptor systems have different gain control properties and accordingly show different limitations with respect to contrast computation. Vertebrate rods specialize to deal with scotopic luminances and have a dynamic range of 1-1000 photons/s. They can theoretically relay single photon information, but adapt to very limited extent and saturate (Normann and Werblin, 1974). Cones in most species can control their gain effectively over a dynamic range of 100-10^7 photons/s (Abbas and Vinberg, 2021; Burkhardt, 1994; French et al., 1993; Normann and Perlman, 1979). Whereas vertebrate photoreception splits photopic and scotopic processing, invertebrate photoreceptors accommodate a wide dynamic range (1 to 10^6 photons/s in *D. melanogaster*) without pathway splitting (Abbas and Vinberg, 2021; French et al., 1993). These receptors efficiently control gain over many orders of high intensities, but not adapt at low intensities (Laughlin and Hardie, 1978; Laughlin et al., 1987). Thus, additional mechanisms are required to modulate gain at dim light, in case that such gain control is behaviorally relevant. In nocturnal species, mechanisms such as spatiotemporal summation improve signal-to-noise ratio, while trading off acuity (Stöckl et al., 2016a; Warrant and McIntyre, 1992).

In vertebrates, intrinsically photosensitive retinal ganglion cells (ipRGCs) also capture photons by means of melanopsin, and their role in image processing has recently been uncovered (Reviewed by Spitschan 2019). A class of ipRGCs distributes sensitivity to different luminance regimes among the population, thus collectively achieving high resolution across a broad luminance range (Milner and Do,

2017). Besides providing luminance information for non-image forming functions, ipRGCs contribute to diverse visual tasks including brightness discrimination and color perception. Furthermore they undergo light adaptation, suggesting they signal contrast in addition to luminance (Brown et al., 2012; Do and Yau, 2013; Zele et al., 2018). However, similar to rods and cones, ipRGCs also adapt with variable time constants that go up to 20 s, and complete recovery of dark sensitivity takes up to 15 minutes (Do and Yau, 2013). Thus, although potentially more sensitive across a broad luminance range, ipRGCs do not encode contrast with reference to rapidly updating luminance and thus may not support contrast constancy in dynamic conditions.

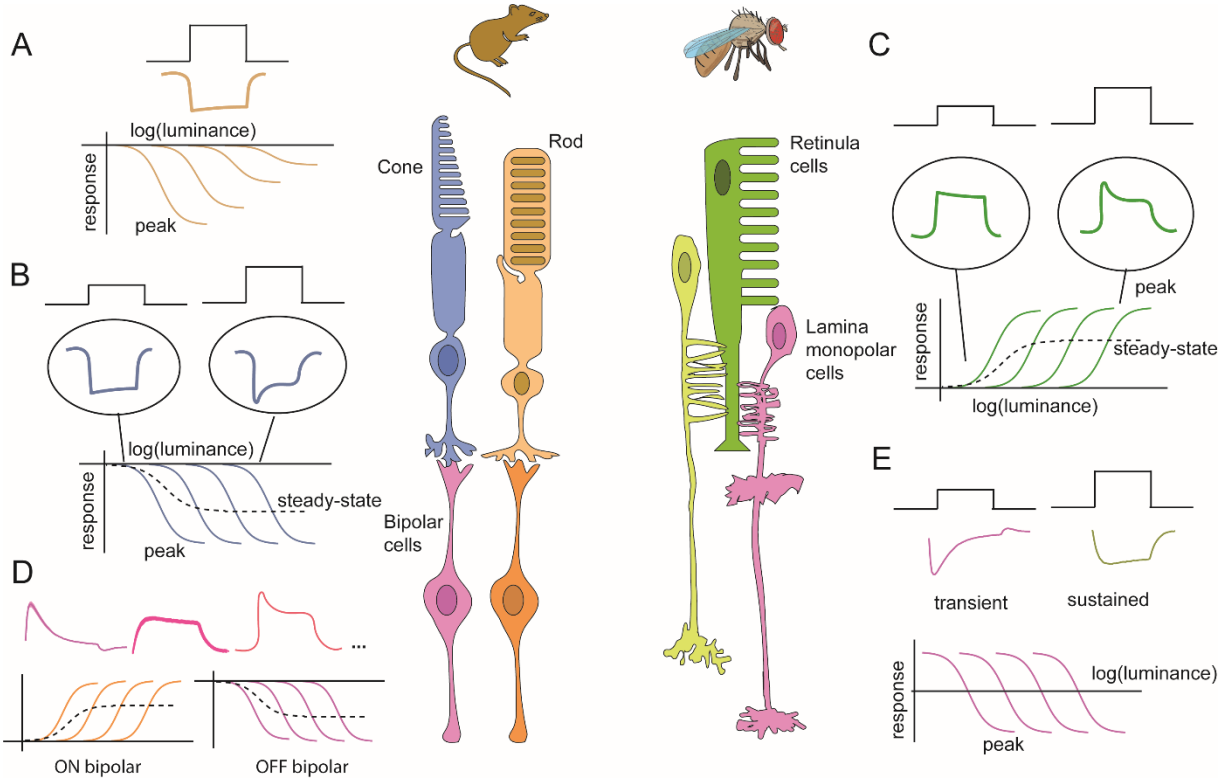

Figure 2: Photoreceptors and the first-order visual interneurons of vertebrates and invertebrates share physiological properties, and also have some differences. Schematic of the peripheral visual systems and their response properties. (A) Most vertebrate retinae have two classes of photoreceptors, rods and cones. Rods respond to luminance increments with hyperpolarization, and in many species they do not adapt to sustained luminance. As a result, their responses saturate and show dynamic range compression at higher luminance values. (B) Cones also respond to luminance increments with hyperpolarization, and their transience increases with increasing luminance. Cones adapt to a broad range of luminance, and their peak responses shift along the log(luminance) axis without compression, representing luminance-invariant contrast coding. The steady-state responses of cones (dashed line) also initially increase with luminance and eventually attain a fixed value. (C) Photoreceptors in flies, known as retinula cells respond to light increments with depolarization. They do not adapt strongly at low luminance, where their response is also mostly sustained, but adapt efficiently over a range of luminance, with their response getting increasingly transient. Retinula responses also encode luminance in their steady state (dashed line), similar to the vertebrate cones. (D) First-order interneurons of the vertebrate retina – bipolar cells – show a range of luminance- and contrast-sensitivity (example waveforms). Distinct classes of bipolar cells acquire ON and OFF selectivity. Depending on the luminance sensitivity of different classes, they capture luminance information in the steady-state response (dashed line). (E) Lamina monopolar cells (LMCs) in flies capture photoreceptor signals. They respond to light increments with

hyperpolarization, and can be classified as transient and sustained LMCs. The transient LMCs are described to subtract the luminance information and maintain a luminance-independent baseline, thus their responses are plotted as the deviation from the maintained baseline.

2.2 First-order interneurons

First-order interneurons capture luminance and contrast signals relayed by photoreceptors, with a range of sensitivities for the two features. In vertebrates, different bipolar cell classes have sustained and/or transient properties and thus both luminance and contrast features are relayed to different degrees (Awatramani and Slaughter, 2000; Baden et al., 2013; Euler et al., 2014a; Ichinose et al., 2014; Oesch and Diamond, 2011). Additionally, subtractive sensitivity modulations at this stage take place through surround inhibition, where lateral interactions are mediated by horizontal cells (Normann and Werblin, 1974; Werblin, 1974). Besides temporal specializations, bipolar cell classes also split processing of light increments and decrements, as well as chromatic and achromatic information (Euler et al., 2014a). Thus, highly specialized signaling properties emerge in the array of several bipolar cell classes (e.g. 14 in mouse), which instead of merely relaying photoreceptor signals, provide a rich substrate to the downstream processing stages. In line with this diversity, adaptation dynamics of bipolar cell classes also vary considerably, with their time constants ranging from 400 ms to 4 s (Awatramani and Slaughter, 2000; Baden et al., 2013). Therefore, at least some bipolar cell classes would relay luminance-dependent contrast signals under rapid changes.

First-order interneurons of flies are also well-characterized. The main interneuron types, known as Large Monopolar Cells (LMCs) are canonically described as principally contrast sensitive, and discarding the steady-state luminance component (Laughlin and Hardie, 1978; Laughlin et al., 1987). However, more sustained characteristics of an LMC type L3 and its more monophasic temporal filter different to other LMCs are known (Fisher et al., 2015a; Hardie and Weckström, 1990; Silies et al., 2013a). The sign-inverting photoreceptor-LMC synapses amplify contrast signals with a factor of 6-6.5, and LMC contrast responses are described as “more transient versions of photoreceptor responses” (Laughlin, 1989; Laughlin et al., 1987), suggesting they implement further temporal filtering. Subtraction of sustained components via mechanisms including surround suppression is also a part of LMC adaptation (Freifeld et al., 2013a; Laughlin, 1989; Laughlin and Osorio, 1989). For one, this helps LMCs get rid of constant illuminant information, thus opening their entire operating range to efficiently code the amplified contrast signals. Secondly, by not encoding luminance, the steady-state response level of LMCs can be maintained constant, allowing LMCs to stay at the midpoint of their operating curve and thus be sensitive to most probable intensity changes in the prevailing conditions (Laughlin, 1981). Moreover, LMCs also account for the skewed probability distribution of ON and OFF contrasts in natural scenes (Dyakova and Nordström, 2017; Van Hateren, 1997). Thus, LMCs seem to match their coding capacity to environmental statistics, better than the photoreceptors. However, with the additional mechanisms of adaptation at work, recovery of sensitivity in LMCs still remains slow. LMC sensitivity to light onset recovers within 200 ms, whereas adaptation to light offset even takes at least two minutes (Laughlin and Hardie, 1978). Moreover, the LMCs also seem to inherit the lack of adaptation at low intensities from photoreceptors, in that their contrast sensitivity increases with increasing adapting luminance

over 3-4 orders of magnitude. This imposes another challenge to contrast constancy in dim conditions, assuming that achieving constancy is behaviorally relevant under those light conditions.

Altogether, different first-order interneurons of different visual systems may not provide accurate contrast information necessary for behavior. On the other hand, how the distinct physiologies of the interneuron classes, especially their sustained response components contribute to behaviorally relevant computations remains to be tested.

2.3 More advanced processing steps

Contrast signals past the second synapse contribute to the extraction of several other visual features, while they also get further refined. For example, retinal ganglion cells (RGCs) in vertebrates acquire feature specificity such as motion or orientation selectivity, while they also sharpen spatial contrast computation with the help of center-surround receptive fields (Baden et al., 2020; Enroth-Cugell and Lennie, 1975; Kaplan et al., 1979). Thus, further gain controls are at work, and may have multiple time constants (Wark et al., 2009). RGCs and cells at more advanced processing stages host both luminance and contrast gain control processes (Barlow and Levick, 1969; Beaudoin et al., 2007; Enroth-Cugell and Shapley, 1973; Garvert and Gollisch, 2013; Khani and Gollisch, 2017). Contrast gain control aims at optimal use of the neuronal operating range to encode prevailing luminance variances, and thus is not a primary requirement for contrast constancy (Carandini and Heeger, 2012). On the other hand, luminance gain control - even at the advanced stages - may help achieving luminance-invariant contrast computation, especially when photoreceptors and the first-order interneurons do not fulfill this requirement. Under one such condition, where low backgrounds lead to high noise and cones may spuriously adapt to noise, the site of rapid adaptation switches to RGCs where relatively noise-free signals are available due to spatial summation (Dunn et al., 2007; Rieke and Rudd, 2009a). Such background-dependent coordination of luminance gain controls can ensure contrast constancy across varying environments. In line with this, cat LGN neurons can respond to contrast in a luminance-invariant manner, with sensitivity adapting almost instantaneously (Mante et al., 2005).

Unlike vertebrate systems, post-LMC gain controls in fly visual systems are seldom described. Besides recently discovered contrast gain controls (Drews et al., 2020; Matulis et al., 2020a), adaptation to velocity in order to encode ‘velocity contrast’ has been found in wide-field motion-sensitive neurons H1 (Maddess and Laughlin, 1985). Although post-LMC luminance gain controls are not explicitly studied, center-surround receptive fields of several neuron types indicate a scope of contrast refinement through spatial summation (Keleş and Frye, 2017; Ramos-Traslosheros and Silies, 2021). Wide-field neurons, e.g. dorsal medulla (Dm) neurons, analogous to vertebrate amacrine cells are also present in the fly eye to pool signals from the first-order interneurons (Fischbach and Dittrich, 1989; Nern et al., 2015a). Besides spatial mechanisms, contrast may also undergo refinement through the integration of distinctly filtered temporal signals, similar to the signal integration by motion-sensitive neurons (Borst, 2009; Egelhaaf and Reichardt, 1987; Ibbotson and Clifford, 2001; Silies et al., 2014). If such circuit interactions can lead to an improved constancy at advanced processing stages and in behavior has been unexplored.

2.4 Parallel ON and OFF contrast processing

Light increments (ON contrast) and decrements (OFF contrast) are processed in parallel pathways in many visual systems (Clark et al., 2011a; Gollisch and Meister, 2008; Hubel and Wiesel, 1962; Joesch et al., 2010; Wässle and Boycott, 1991; Werblin and Dowling, 1969). In vertebrates, the pathways split at the stage of bipolar cells, as cone bipolar cell classes acquire ON and OFF selectivity through different glutamate receptor signaling. Fly LMCs do not acquire ON and OFF contrast selectivity, but the second-order interneurons do (Behnia et al., 2014a; Serbe et al., 2016; Silies et al., 2013a; Strother et al., 2017). Among the *Drosophila* LMC classes, L2 and L3 make sign-conserving synapses with their downstream OFF-selective cells, whereas L1 forms a sign-inverting synapse with most of the downstream cells that constitute ON pathway (Arenz et al., 2017; Fisher et al., 2015b; Joesch et al., 2010; Molina-Obando et al., 2019; Silies et al., 2013a; Yang et al., 2016). This adds a first evidence from the fly eye to the common observation that OFF pathway elements are more numerous than the ON pathway, mirroring the dominance of dark pixels in natural scenes (Dyakova and Nordström, 2017; Odermatt et al., 2012; Ratliff et al., 2010). Visual systems continue to process the two contrast polarities in parallel and extract further features such as motion for both polarities separately (Baden et al., 2018; Maisak et al., 2013; Vaney et al., 2012).

Processing of the two polarities has evolved in response to different environmental challenges, such as asymmetrical ON-OFF statistics of the visual world (Clark et al., 2014; Ruderman and Bialek, 1994) and comprises several structural and physiological asymmetries (Chichilnisky and Kalmar, 2002; Jin et al., 2011; Leonhardt et al., 2016; Ratliff et al., 2010). Consequently, gain control works differently when light level increases than when it decreases. For example, detection thresholds are lower for decrements than for increments (Boynton et al., 1964; Krauskopf, 1980). Even phototransduction machinery adapts asymmetrically to the two polarities, with dark adaptation taking several tens of minutes (Abbas and Vinberg, 2021). Yet, perceptual contrast constancy is evident symmetrically for ON and OFF contrasts (Burkhardt et al., 1984), suggesting that visual circuitries fulfill perceptual demands similarly for the two polarities despite different resources and adaptation dynamics available.

3. Studying contrast processing strategies in *Drosophila* in challenging conditions

3.1 Challenges to contrast estimation

Two fundamental discrepancies are evident, when perceptual requirements of contrast estimation are compared with the contrast signals generated by visual periphery i.e. photoreceptors and first-order interneurons. One, the peripheral systems compute contrast relative to seconds- to minutes-long luminance history, whereas stable perception despite environmental and self-motion requires rapidly changing luminance to be the reference for contrast computation. On the one hand, adapting to scene statistics over a large enough temporal window is a useful strategy to avoid inappropriate adaptation to noisy stimuli. On the other hand, the resulting luminance-dependent contrast estimate does not represent constant object properties in dynamic environments, thus challenging contrast computation. The second discrepancy is relevant specifically to the visual systems where classes of photoreceptors

dealing with dim light poorly adapt their sensitivity in a luminance range relevant for active behavior. For example, flies have such photoreceptors, and their unadjusted sensitivities in dim light would likely lead to lack of contrast constancy (Laughlin and Hardie, 1978; Laughlin et al., 1987). Thus, improving detection of dim light contrasts downstream of photoreceptors is another challenge to behaviorally useful contrast estimation.

To tackle both of these challenges, visual systems must recruit more proximal processing stages to compensate for the limitations of the periphery. To establish contrast constancy in dynamic environments, the proximal stages must implement a corrective gain control that functions at rapid timescales and also circumvent the deleterious effects of adapting to noise. RGCs in some visual systems seem to implement such adaptation, although in very specific conditions (Dunn et al., 2007). How the presynaptic network may organize such conditional switch in gain control site is unclear. More importantly, if and how behavior benefits from post-receptor gain correction remains unexplored. The second challenge of improving dim light vision requires extensive spatiotemporal summation to improve signal-to-noise ratio, as has been suggested for nocturnal insects (Stöckl et al., 2016a; Warrant, 2017). However, peripheral circuit organization required to implement this strategy is again largely unknown.

Additionally, the challenges must be tackled in all parallel pathways specializing in distinct feature extraction. Specifically, visual systems encounter ON and OFF contrast polarities in both dim light as well as dynamic environments. Segregated processing of ON and OFF contrasts is an energy-efficient strategy (Gjorgjieva et al., 2014), but implies that the contrast-corrective operations must take place in both ON and OFF pathways. Also, these operations have to compensate for pathway-specific deficits that emerge from asymmetrical adaptation mechanisms. If post-receptor gain correction is a common solution recruited by the two pathways is an intriguing question. For such shared solution, peripheral visual systems would need to feed the required information into both pathways.

The Drosophila visual system offers an attractive model to address these open questions, for the reasons elaborated in the following section.

3.2 The *Drosophila* visual system as a model

Drosophila visual system is studied thoroughly to unravel various aspects of vision, ranging from luminance and contrast adaptation to local and global motion detection (Borst, 2014; Drews et al., 2020; Matulis et al., 2020a; Ramos-Traslosheros et al., 2018; Silies et al., 2014; Song and Juusola, 2017; Zheng et al., 2006). The anatomy of the visual system and morphology of the cell types is known with exceptional detail (Fischbach and Dittrich, 1989). Even the connectivity between the cell types is getting progressively better understood, thanks to more recent connectomics approach (Shinomiya et al., 2014a, 2019; Takemura et al., 2013a, 2017a). Genetic and molecular tools developed in *D. melanogaster* are unmatched and allow cell-type specific access to dissect individual circuit components, on molecular and physiological levels. For example, cell-type specific expression of fluorescent calcium indicators such as GCaMP allows measurements of calcium activity of the specific

neuronal population. Moreover, an array of behavioral paradigms informs about (fly-) perceptual relevance of various visual stimuli (Reiser and Dickinson, 2008; Silies et al., 2013a).

The compound eyes of *Drosophila* encompass a hexagonal arrangement of visual units, named ommatidia (Figure 3A). Each of the ~750 ommatidia per eye has a separate lens, under which it hosts six identical photoreceptors, the retinula cells R1-R6, which constitute the achromatic visual pathway (Heisenberg and Buchner, 1977). Two other receptors R7 and R8 are major inputs to chromatic processing (Chou et al., 1996; Heisenberg and Buchner, 1977; Salcedo et al., 1999). Unlike the photopic-scotopic split in vertebrate retinae, the same photoreceptors in flies deal with dim and bright light intensities (Asteriti et al., 2017), and R1-R6 provide sufficient information for achromatic visual behaviors over a broad luminance range (Heisenberg and Buchner, 1977). Like other dipteran eyes, *Drosophila* eyes are 'neural superposition' eyes, and combine high spatial resolution with high sensitivity (Agi et al., 2014; Katz and Minke, 2009; Kirschfeld, 1967).

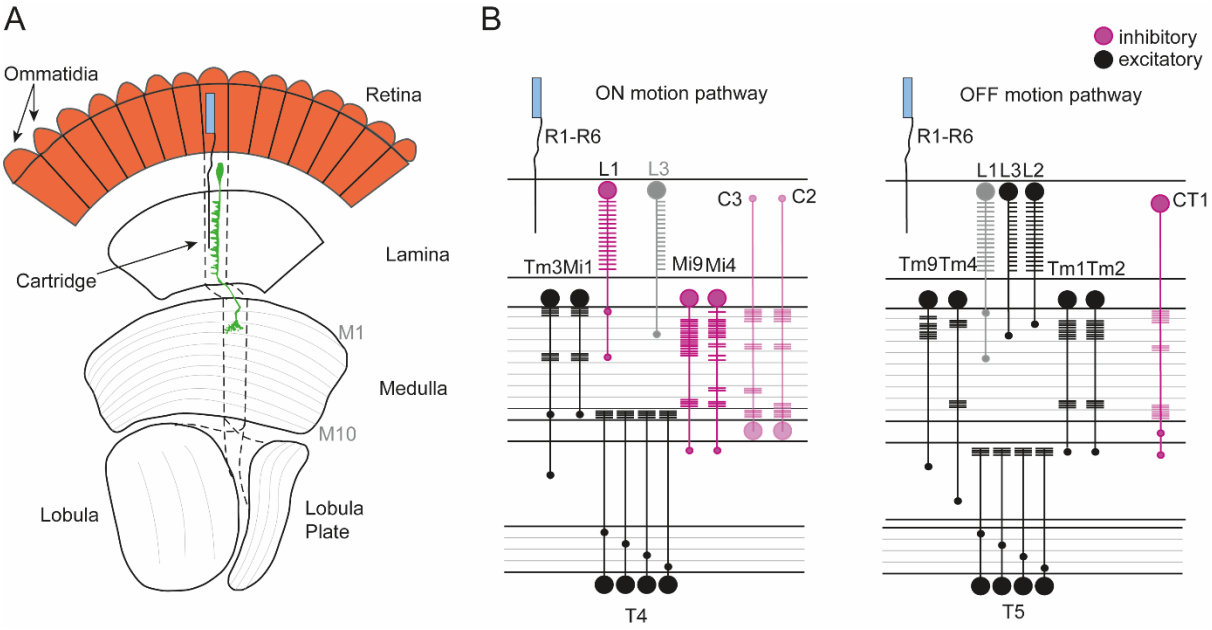

Figure 3: The *Drosophila* visual system processes ON and OFF contrasts in separate pathways. (A) The fly eye comprises retinotopic arrangement of visual units named ommatidia (red). Each ommatidium houses photoreceptors R1-R6 as well as R7 and R8. Among them, R1-R6 project to the corresponding 'cartridge' in the lamina (dashed lines) and innervate predominantly LMCs (shown here in green, L3). LMCs project to the medulla that comprises layers M1-M10. Retinotopy is further maintained in the downstream neuropils lobula and lobula plate. (B) ON and OFF pathways emerge downstream of LMCs. L1 is the major input to the ON pathway, however L3 can contribute to the ON-motion selective T4 responses through Mi9. Mi1, Tm3, Mi9 and Mi4 are principal medulla interneurons that converge onto T4 dendrites. Besides, feedback neurons C2 and C3 (pale pink) also shape ON responses. In the OFF pathway, L2 and L3 are the major inputs, whereas T5 are the motion-selective neurons. L1 contributes to T5 function through Tm9, however its anatomical connection to Tm9 is unknown. Tm1, Tm2, Tm4 and Tm9 converge onto T5. Besides, CT1 – a wide-field amacrine cell is the only known inhibitory input to T5. Inhibitory inputs are shown in magenta, and the excitatory ones in black. Adapted from (Silies et al., 2014).

Photoreceptors are part of the retina, and they project to the first neuropil called lamina, where they synapse with the first-order interneurons L1, L2 and L3, collectively known as lamina monopolar cells

(LMCs), as well as an amacrine cell (Fischbach and Dittrich, 1989; Meinertzhagen and O'Neil, 1991). LMCs receive photoreceptor input through a histaminergic synapse, and Ort is the main histamine receptor known to mediate the transmission (Gengs et al., 2002). Whereas photoreceptors depolarize with light increments, the inhibitory synapses lead to hyperpolarization in LMCs in response to the same stimulus. The lamina neuropil is also divided into retinotopically arranged columns called cartridges. This columnar retinotopic arrangement extends below the corresponding ommatidia. Thus, the eye includes ~750 copies of L1, L2 and L3 each, and the same applies to columnar neurons in further neuropils (Figure 3A).

LMCs project to different layers of the downstream neuropil named medulla, where they innervate several columnar and multi-columnar (wide-field) neurons (Fischbach and Dittrich, 1989; Nern et al., 2015a; Takemura et al., 2013a). L1 makes glutamatergic synapses with medulla interneurons Mi1 and Tm3, among other post-synaptic partners, which acquire ON contrast selectivity through sign-inverting synapses (Behnia et al., 2014a; Molina-Obando et al., 2019; Strother et al., 2017; Yang et al., 2016), and L1 is thus considered the ON pathway input (Figure 3B). L2 and L3 make cholinergic synapses, e.g. with Tm1, Tm2, Tm4 (post-L2) and Tm9, Mi9 (post-L3), and their post-synaptic partners retain OFF selectivity (Behnia et al., 2014a; Serbe et al., 2016; Yang et al., 2016). The second-order interneurons project to other layers of the medulla or downstream lobula complex, where some of them converge on the first direction-selective cells – T4 and T5 – that acquire sensitivity to local ON and local OFF motions, respectively (Behnia et al., 2014a; Shinomiya et al., 2019; Takemura et al., 2013a, 2017a). Here, neurons selectively processing a contrast polarity can contribute to motion processing of the other polarity too, since contrast-opponent receptive fields of T4/T5 are shown necessary for direction selectivity (Leong et al., 2016; Ramos-Traslosheros and Silies, 2021; Wienecke et al., 2018). The local motion cues are integrated by several classes of wide-field motion-sensitive neurons, commonly referred to as lobula plate tangential cells (Bahl et al., 2013; Maisak et al., 2013; Strother et al., 2017). LPTCs carry the motion information to central brain and eventually inform the motion-guided behavior (Boergens et al., 2018; Schnell et al., 2010; Wei et al., 2020a).

Motion-guided behaviors are useful to assess several visual functions. Particularly, optomotor response of both walking and flying Drosophila has been examined as a readout of visual processing outcome (Buchner, 1976; Creamer et al., 2018; Götz, 1964; Silies et al., 2013a; Tuthill et al., 2013). Optomotor behavior is a reflex, by which flies attempt to counteract environmental motion, and this ability helps them in navigational course stabilization. Behavioral assays measuring optomotor response parallel human psychophysical assays, plus they can be combined with other neurophysiological measurements as well as manipulations (Chiappe et al., 2010; Seelig et al., 2010). Extremely valuable is the possibility of genetically silencing specific neuron types or connections and observing the impact of such manipulations on behavior. For example, cell-type specific expression of Shibire^{ts}, a temperature-sensitive, dominant-negative Dynamin mutation, can block synaptic transmission of the particular neuron type (Kitamoto, 2001). Behavioral measurements of Shibire^{ts}-expressing flies can shed light on the silenced neuron's overall contribution to the visual output. Using such tools, functions of neurons can be causally linked to behavior.

When studying the first-order interneurons, the *Drosophila* visual system offers an additional convenience – it comprises fewer of these interneurons as compared to the wide variety present in vertebrate retina. Thus, it is possible to understand the physiology of all principal channels of the transmission layer between photoreceptors and the downstream circuitry. This is of enormous importance, especially when we plan to exhaustively understand limitations of this layer in providing behaviorally relevant contrast information.

4. Aim of the study and thesis structure

Peripheral visual processing stages, namely photoreceptors and the first-order interneurons adapt their luminance gain and encode contrast, but they don't reach the goal of contrast constancy due to their physiological constraints, both in dynamic conditions and in specific illumination conditions. If behavior still exhibits constancy under these conditions, more proximal circuitry has to implement corrective gain control and the peripheral circuitry has to organize transmission of relevant information. Exploiting the genetic accessibility of the *Drosophila* cell types, I aim to understand the extent to which contrast computation in *Drosophila* LMCs meets the behavioral expectation and when not, how their physiology and connectivity shape downstream contrast correction. Besides, I aim to study how contrast computation compares across parallel ON and OFF pathways.

Together with my colleagues, I addressed these aims over three individual studies. In the first study, we aimed to explore if and how flies tackle the challenge of dynamic conditions. Inspecting motion-guided behaviors of fruit flies *Drosophila melanogaster*, we aimed to define the behavioral expectation of contrast encoding that the visual system as a whole needs to fulfill. Given that the fly behavior was contrast constant when luminance changed rapidly, we examined how peripheral processing stages meet this expectation. Thus, we predicted contrast-sensitive responses of the first-order interneurons – LMCs – under the same dynamic conditions. Since the LMCs had very different temporal characteristics, we explored their individual coding properties and their distinct roles in driving behavior. As the contrast-sensitive LMC responses were insufficient to guide behavior under dynamic conditions, we tested the hypothesis that the OFF-pathway input with sustained properties – L3 – transmits the information necessary for contrast correction. For this purpose, we asked if genetically silencing L3 output abolishes contrast constancy in behavior. L3 encoded luminance, and the luminance information was indeed key to contrast-constant behavior across multiple luminance regimes.

Knowing that fly behavior is contrast constant in dynamic conditions, I aimed to understand in a second study if this property generalizes across ON and OFF pathways. We first asked if and how the single major ON pathway input L1 could support contrast constancy in the ON pathway. Testing the temporal properties of L1 showed that contrast and luminance information was encoded differently by L1, L2 and L3. Based on this, and informed by connectomics, we thus revisited the contribution of the three channels to distributing luminance information across ON and OFF pathways. To test the relevance of the two differentially encoded functions of luminance in L1 and L3, we genetically tested their necessity and sufficiency to ON and OFF contrast-constant behaviors.

In the last study, we focused on the OFF pathway and asked how LMC contrast sensitivity varies with adapting luminance and how it influences behavior across many different conditions, including various contrasts and also especially in dim conditions. We first explored if L2 responses would be sufficient to guide contrast-constant behavior if allowed to adapt nearly completely. Since L2 contrast signals showed luminance dependence even in adapting conditions, we asked how L3-mediated gain correction should vary across a range of luminance. For this purpose, we combined a computational modelling approach with behavioral measurement across a wide contrast-luminance space. L3 was required in seemingly contradictory ways across the luminance range and in rapidly changing conditions. To understand the implementation of the diverse gain control operations, we trained a model to predict the behavioral responses measured at different stimulus paradigms, and compared its output with behavior of wild type flies, as well as flies lacking the L3 channel.

Manuscript 1: Luminance Information Is Required for the Accurate Estimation of Contrast in Rapidly Changing Visual Contexts

This manuscript is published as a research article in Current Biology and is available under DOI: https://doi.org/10.1016/j.cub.2019.12.038.

Authors and affiliations

Madhura D Ketkar[#1,2,3], Katja Sporar[#1,2,3] Burak Gür[1,2,3], Giordano Ramos-Traslosheros[1,2,3], Marvin Seifert[2] and Marion Silies*[1,2]

[1]Institute of Developmental Biology and Neurobiology, Johannes Gutenberg-Universität Mainz, Hanns-Dieter-Hüsch-Weg 15, 55128 Mainz, Germany

[2]European Neuroscience Institute Göttingen, University Medical Center Göttingen and the Max Planck Society, Grisebachstr. 5, 37077 Göttingen, Germany

[3]International Max Planck Research School and Göttingen Graduate School for Neurosciences, Biophysics, and Molecular Biosciences (GGNB) at the University of Göttingen, Justus-von-Liebig-Weg 11, 37077 Göttingen, Germany

[#]these authors contributed equally to this work

* Lead contact: msilies@uni-mainz.de

Contribution statement

Marion Silies, Katja Sporar and I conceptualized and planned the study. Giordano Ramos-Traslosheros contributed to designing a stimulus for imaging. Katja Sporar and Marvin Seifert performed the imaging experiments. Katja Sporar, Burak Gür and Giordano Ramos-Traslosheros analyzed the imaging data. I performed and analyzed the behavioral experiments, and calculated predictions of neuronal responses. I wrote the manuscript together with Marion Silies and Katja Sporar. We included edits from all authors.

Article

Current Biology

Luminance Information Is Required for the Accurate Estimation of Contrast in Rapidly Changing Visual Contexts

Graphical Abstract

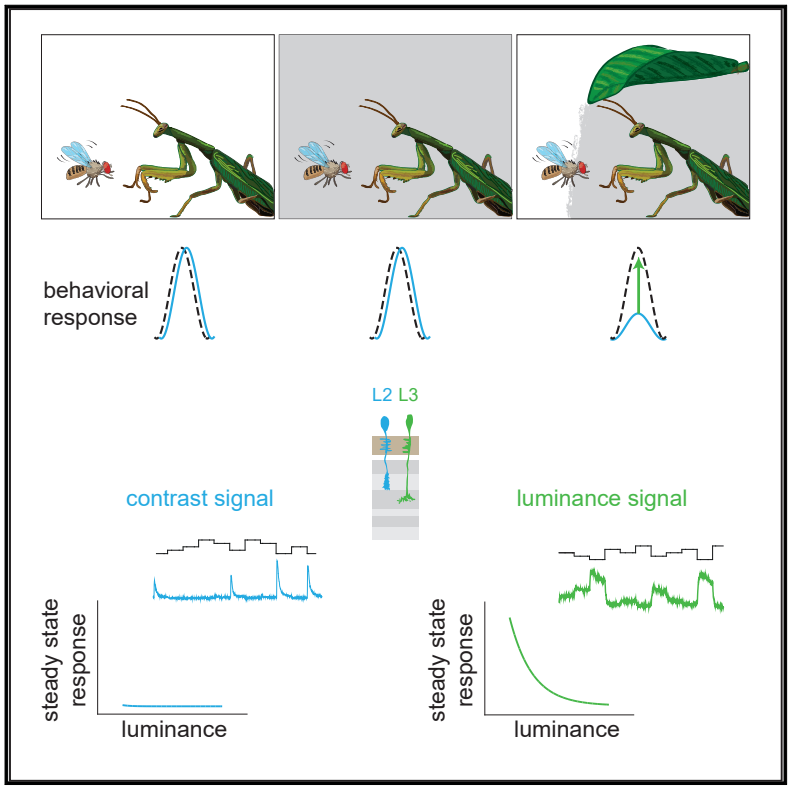

Authors

Madhura D. Ketkar, Katja Sporar, Burak Gür, Giordano Ramos-Traslosheros, Marvin Seifert, Marion Silies

Correspondence

msilies@uni-mainz.de

In Brief

Ketkar and Sporar et al. reveal a novel mechanism in which visual systems can mediate accurate behavioral responses to visual cues under changing light conditions. Luminance information is preserved in a distinct pathway past photoreceptors. This pathway is required for visual behavior when pure contrast-sensitivity underestimates a visual stimulus.

Highlights

- Lamina neurons underestimate contrast when light levels suddenly decline
- Distinct visual pathways postsynaptic to photoreceptors encode contrast and luminance
- The luminance-sensitive pathway via L3 is necessary for behavior in sudden dim light
- L3 scales behavioral responses in contextual dim light across adaptation states

Ketkar et al., 2020, Current Biology *30*, 1–13
February 24, 2020
https://doi.org/10.1016/j.cub.2019.12.038

CellPress

Please cite this article in press as: Ketkar et al., Luminance Information Is Required for the Accurate Estimation of Contrast in Rapidly Changing Visual Contexts, Current Biology (2019), https://doi.org/10.1016/j.cub.2019.12.038

Current Biology
Article

Luminance Information Is Required for the Accurate Estimation of Contrast in Rapidly Changing Visual Contexts

Madhura D. Ketkar,[1,2,3,4] Katja Sporar,[1,2,3,4] Burak Gür,[1,2,3] Giordano Ramos-Traslosheros,[1,2,3] Marvin Seifert,[2] and Marion Silies[1,2,5,*]

[1]Institute of Developmental Biology and Neurobiology, Johannes Gutenberg-Universität Mainz, Hanns-Dieter-Hüsch-Weg 15, Mainz 55128, Germany

[2]European Neuroscience Institute Göttingen, a Joint Initiative of the University Medical Center Göttingen and the Max Planck Society, Grisebachstr. 5, Göttingen 37077, Germany

[3]International Max Planck Research School and Göttingen Graduate School for Neurosciences, Biophysics, and Molecular Biosciences (GGNB) at the University of Göttingen, Justus-von-Liebig-Weg 11, Göttingen 37077, Germany

[4]These authors contributed equally

[5]Lead Contact

*Correspondence: msilies@uni-mainz.de

https://doi.org/10.1016/j.cub.2019.12.038

SUMMARY

Visual perception scales with changes in the visual stimulus, or contrast, irrespective of background illumination. However, visual perception is challenged when adaptation is not fast enough to deal with sudden declines in overall illumination, for example, when gaze follows a moving object from bright sunlight into a shaded area. Here, we show that the visual system of the fly employs a solution by propagating a corrective luminance-sensitive signal. We use *in vivo* 2-photon imaging and behavioral analyses to demonstrate that distinct OFF-pathway inputs encode contrast and luminance. Predictions of contrast-sensitive neuronal responses show that contrast information alone cannot explain behavioral responses in sudden dim light. The luminance-sensitive pathway via the L3 neuron is required for visual processing in such rapidly changing light conditions, ensuring contrast constancy when pure contrast sensitivity underestimates a stimulus. Thus, retaining a peripheral feature, luminance, in visual processing is required for robust behavioral responses.

INTRODUCTION

Sensory systems have evolved to detect changes rather than absolute inputs from their environment. For example, while we might forget that glasses are perched on top of our head, we can feel an insect landing on our skin. Similarly, visual systems are well suited to detect changes in light intensity. In many contexts, changes in perception are proportional to relative changes in a stimulus (Weber contrast) [1, 2]. The ability to process such changes in sensory input under changing conditions is crucial to the behavior and survival of many organisms.

In vision, the most basic characteristic of a visual stimulus is the distribution of luminance, which is the luminous intensity per unit area. Rather than responding to luminance, many cells in the visual system instead respond to contrast [3–5]. Contrast can be defined in the temporal or spatial domain. Here, we study temporal contrast, which corresponds to the relative change in luminance (Weber contrast) over time at a single point in space. We will describe a mechanism that ensures contrast constancy, a visual phenomenon that allows discrimination of a visual feature from its background solely based on its contrast, regardless of the global light level [2, 6–8].

Many visual systems are well suited to function at dusk, dawn, or in daylight as well as in rapidly changing environments. In both vertebrates and invertebrates, photoreceptor adaptation is a key mechanism that ensures contrast computation irrespective of background illumination [3, 6, 9]. Photoreceptor adaptation happens across different timescales that range from tens of milliseconds to tens of seconds [6, 10–13]. However, animals frequently encounter close-to-instantaneous changes in luminance that far exceed photoreceptor adaptation. For example, during self-motion, saccadic eye movements, or when gaze follows a moving object into the shade, background luminance changes within milliseconds. A failure to adjust light sensitivity equally fast would lead to inaccurate calculation of contrast and a misinterpretation of salient cues (Figure 1A). Therefore, the timescale of adaptation might limit the capability of the visual system to ensure contrast constancy in fast-changing light conditions, and thus may be alone insufficient to explain robust visual behaviors under changing conditions.

Core visual circuits have been mapped in the fruit fly *Drosophila*, which responds to visual cues at luminances spanning orders of magnitude [15–18]. Briefly, information passes from the retina through the lamina and medulla to the lobula complex. Visual information is computed in 800 parallel channels, together forming a retinotopic array. Downstream of photoreceptors, visual circuitry splits into pathways that are specialized to detect contrast increments (ON) or decrements (OFF). The lamina neuron L1 forms the principal input to the

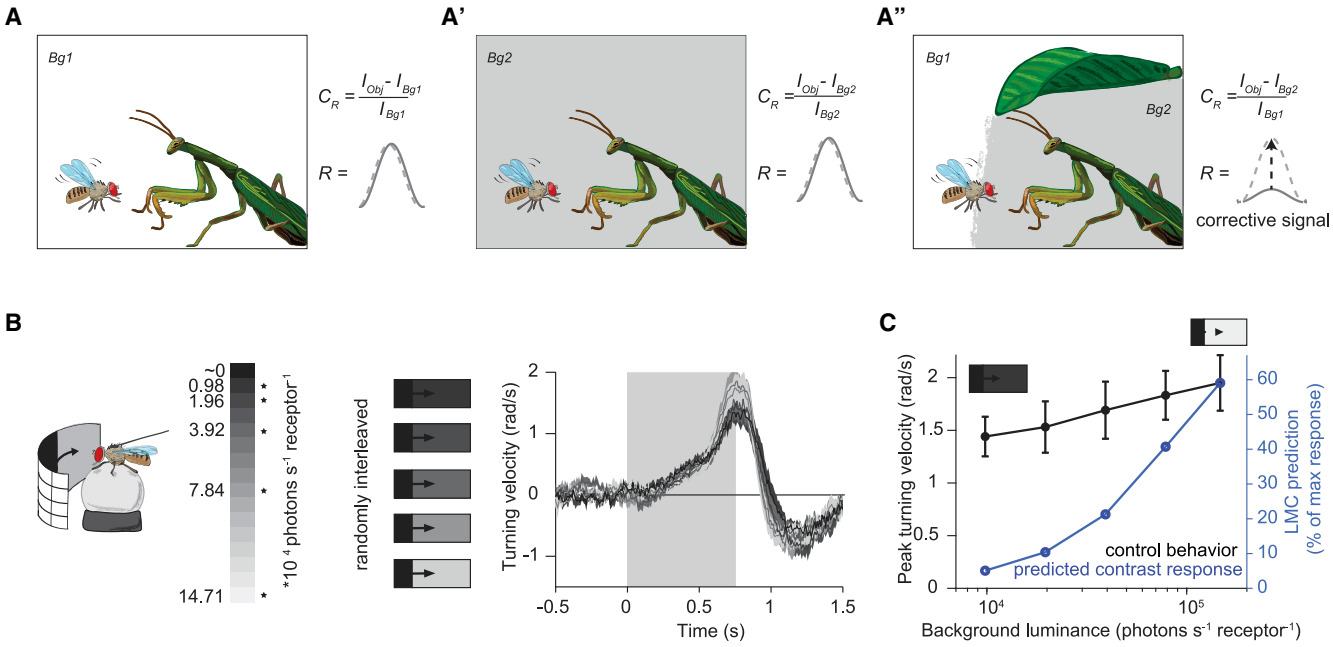

Figure 1. Contrast-Sensitive Neurons Underestimate a Visual Input in Sudden Dim Light

(A–A'') Schematic illustrating the contrast-sensitive responses generated by an object (a predator) under different light conditions. The response of contrast-sensitive neurons (C_R) is computed as the difference between object and background luminance ($I_{Obj} - I_{Bg}$), normalized by background luminance, (A and A'), unless the change in background luminance is faster than adaptation (A''). In (A''), a contrast-sensitive behavioral response (R, solid line) will be smaller than in (A and A') because of insufficient adaptation, and thus underestimate the visual stimulus generated by the predator (dashed line). This needs to be adjusted by a corrective signal (arrow).

(B) An LED arena surrounds a fly walking on an air-cushioned ball. The LEDs can show 16 different intensity levels. OFF edges move onto backgrounds of different luminances (stars). Turning responses to five moving OFF edges varying in onset luminance, the gray box region indicates motion duration. n = 10 flies.

(C) Contrast-sensitive responses of LMCs are calculated for the stimuli in (B) according to previous recordings of canonical LMCs [14] and are plotted together with peak turning velocities from (B). LMC response to the biggest contrast is aligned with the corresponding behavioral response. Traces and plots show mean ± SEM.

ON pathway, whereas L2 and L3 are major input neurons to the OFF pathway [19–21]. Together, L1–L3 are referred to as large monopolar cells (LMCs). Based on behavioral experiments, L2 and L3 were considered to mediate fast and slow motion-processing pathways, respectively [21, 22]. However, while L1 and L2 show transient responses to light and biphasic filtering properties, L3 responses are sustained and display a monophasic linear temporal filter [19, 21, 23, 24]. This argues that L2 and L3 are sensitive to entirely different features of the visual scene.

In flies, voltage recordings have shown that the photoreceptor cells respond to prolonged, bright illumination with an initial transient phase, which encodes contrast, followed by a luminance-sensitive plateau, which lasts for the duration of the stimulus [6]. Downstream LMCs are thought to amplify photoreceptor contrast signals while discarding information about constant illumination [13, 14]. Such contrast responses in LMCs have been extensively characterized in flies that were adapted to different mean luminances [14]. However, it is not known how the visual system deals with contrast signals in a non-adapted state. Ideally, an animal should be able to show invariant responses to contrast under rapidly changing light conditions. To achieve contrast constancy under such conditions, information about illumination might be advantageous. Interestingly, in the vertebrate retina, luminance sensitivity is retained past photoreceptors at the bipolar cell to amacrine cell synapse [25, 26]. Furthermore, intrinsically photosensitive retinal ganglion cells can contribute to image-forming visual functions [27–29]. However, in the *Drosophila* visual system, a luminance-sensitive component has not been described past photoreceptors. Furthermore, it is not known whether luminance indeed contributes to image processing past the initial detection stage.

Here, we uncover a luminance-sensitive pathway in the *Drosophila* visual system. Contrast-sensitive neuronal responses alone are insufficient to account for behavioral responses to changing visual stimuli, arguing for the presence of a corrective signal that scales contrast-sensitive responses when light levels suddenly decline. Through a series of *in vivo* calcium-imaging experiments, we show that the two input neurons to the OFF pathway, L2 and L3, encode contrast and luminance, respectively. Luminance information from L3 is necessary for appropriate behavioral responses to visual cues when background luminance suddenly becomes dim. This is true across a range of adaptation states. Our data demonstrate that luminance information is retained in a specialized L3 pathway and used as a corrective signal that ensures contrast constancy. This work thus highlights a novel mechanism that allows accurate image processing under dynamically changing light conditions.

RESULTS

Contrast-Sensitive Neurons Underestimate Visual Inputs in Sudden Dim Light

Contrast signals generally convey salient information about the visual scene, and adaptation is one mechanism to ensure that this is done accurately across light conditions (Figure 1A). To compute contrast in a system that is fully adapted, the difference in object and background luminance is normalized to background luminance. This ensures that the contrast signal remains similar irrespective of illumination (Figures 1A and 1A'). However, light conditions changing faster than neural adaptation mechanisms might challenge visual perception when pure contrast sensitivity underestimates a visual stimulus (Figure 1A''). We thus hypothesized the existence of a corrective signal that adjusts the behavioral response when flies suddenly enter a dim area, where objects appear to be of low contrast (Figure 1A''). To test this idea, we first asked if changing light conditions indeed provide a challenge for the visual system to accurately compute temporal contrast. Behavioral responses to visual stimuli scale predominantly with contrast. If contrast computation alone provides the relevant input to image processing when illumination suddenly changes, behavioral responses and contrast-sensitive LMC responses should vary together. We therefore compared contrast-sensitive LMC responses with behavioral responses to the same set of visual stimuli.

We examined the flies' behavioral response to OFF edges moving onto different bright backgrounds, using a fly-on-a-ball assay (Figure 1B). We showed one of a range of different background luminances for 500 ms, and then moved an OFF edge onto this background. The five different background luminances were randomly interleaved. Wild-type flies showed a co-directional turning response with the rotating OFF edge over the duration of the stimulus and displayed some counter-turning after the end of the motion epoch. Quantification of the response to the motion duration showed similar turning responses to all of these five OFF motion stimuli (Figure 1B). Similar turning responses to dark bars have been previously described [30].

Contrast-sensitive LMC responses have been thoroughly characterized under many adapting conditions [14]. Previous recordings of contrast-sensitive LMCs contain different lamina neuron subtypes (L1 and L2, which are both transient), and we will call their responses "canonical" LMC responses. These previous recordings allowed us to predict LMC responses to the stimuli used in the behavioral paradigm. In order to predict the responses, we first reconstructed a contrast-response curve for our behavioral stimulus set. From this curve, we predicted canonical contrast-sensitive LMC responses for all OFF edges used (Figure 1C). In brief, because flies were not given enough time to fully adapt to each background, we assumed adaptation to the mean luminance during the entire stimulus and generated a LMC response curve for this adaptation state from [14]. From this curve, we calculated LMC responses as if a step were taken from the adapted luminance to the luminance of the OFF edge and the background individually, and generated "predicted" LMC responses as the difference between these two.

Comparing those predicted LMC responses with the fly turning responses showed that LMC responses did not scale with behavior but underestimated the stimulus for motion onto dim backgrounds (Figure 1C). Therefore, another signal must indeed exist that, together with pure contrast sensitivity, provides accurate information about visual stimuli in changing light conditions.

Calcium Signals Are Contrast Sensitive in L2 but Not L3 Inputs to the OFF Pathway

A corrective signal that acts together with contrast-sensitive signals to generate appropriate behavioral responses could be provided by luminance information. Downstream of photoreceptors, LMCs have been described as inverted, transient versions of their photoreceptor inputs, which signal contrast [13]. However, the two major LMC input neurons to the OFF pathway, L2 and L3, differ in their filtering properties [19, 21]. We therefore asked if both L2 and L3 are indeed sensitive to contrast. We expressed the calcium indicator GCaMP6f specifically in L2 or L3 and recorded calcium signals in response to light flashes in their axon terminals using *in vivo* 2-photon imaging (Figures 2A and 2B). L2 and L3 showed the same response polarity to light flashes, but while L2 axon terminals responded to light flashes in a transient manner, L3 responses were sustained, even for light flashes lasting tens of seconds [23] (Figures 2B and 2C). Responses in both L2 and L3 neurons were no longer significantly different from the steady state 10.5 s (L2) and 11.7 s (L3) after the OFF step (Figure S1). To explicitly test the contrast sensitivity of L2 and L3, we presented different ON and OFF steps, all relative to an intermediate gray background (Figures 2D–2G). The gray-to-dark steps ranged from −20% to −100% temporal Weber contrast, $c = (I_{dark} - I_{gray})/I_{gray}$. Recordings from the axon terminals of both L2 and L3 showed that their responses varied with the contrast of the gray-to-dark step (Figures 2D–F). However, the stimulus contained another set of contrast changes, which occurred when returning to background gray following an ON step (bright-to-gray steps, $c = (I_{gray} - I_{bright})/I_{bright}$). L2 responses to these contrast decrements again increased with contrast, while L3 showed almost no response (Figures 2D, 2E, and 2G). Together, our data show that L2 and L3 axon terminals respond differently to visual inputs. Calcium signals in L2 are proportional to a wide dynamic range in terms of contrast sensitivity. L3 neurons hardly responded to stimuli that were returning from bright to gray.

L3 Is Luminance Sensitive and Particularly Active in Dim Light

L3 only responded to contrasts presented at dim background, but these stimuli also differed in luminance. To explicitly test contrast versus luminance sensitivity in L2 and L3, we adapted flies to a bright background and then provided two sequential OFF steps (A and B steps), in which the first OFF step varied in magnitude with respect to both contrast ($c = (I_A - I_{background})/I_{background}$) and luminance. The second step varied in luminance but always had 25% Weber contrast ($c = (I_B - I_A)/I_A$) (Figure 3A). A similar stimulus has been used to describe luminance and contrast coding at the bipolar-to-amacrine cell synapse in vertebrates [25]. Differences in response to the first step can be attributed to either luminance or contrast, whereas only a cell that measures fast temporal contrast will respond with the same magnitude to all B steps. L2 calcium signals scaled linearly with contrast, and all six responses to 25% contrast OFF steps

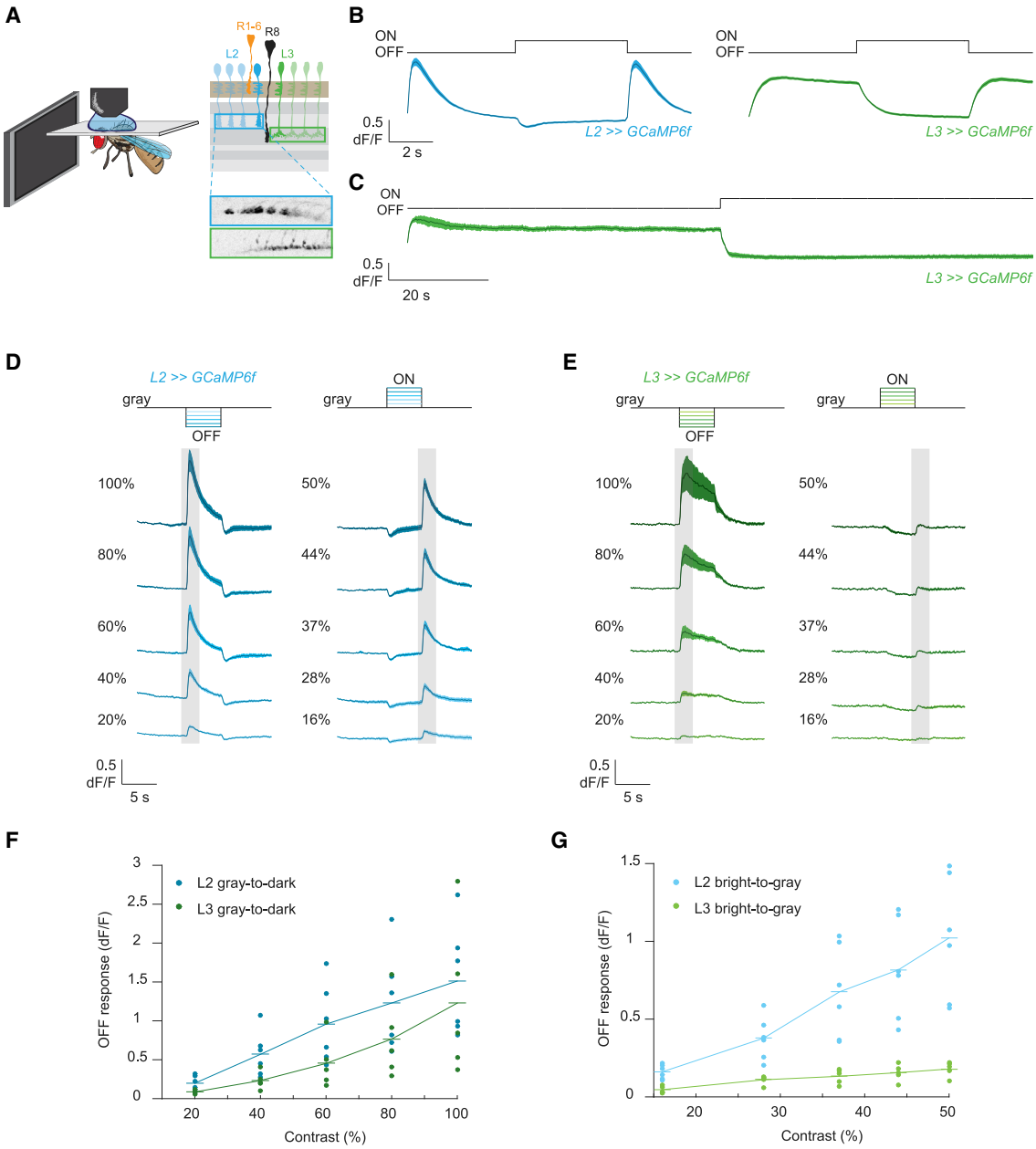

Figure 2. Calcium Signals Are Contrast Sensitive in L2 Inputs but Not L3 Inputs to the OFF Pathway

(A) Schematic of shaded neurons illustrate the columnar organization of the visual system. 2-photon images below show L2 and L3 axon terminals.

(B and C) Calcium signals from L2 or L3 axon terminals in response to 5 s (B) or 60 s (C) light flashes. n = 23(130) flies (ROIs) for L2, n = 20(224) for L3 in (B), and n = 5(79) for L3 in (C).

(D and E) Calcium signals in response to full-field flashes of different Weber contrast. Gray boxes mark the OFF responses.

(F and G) Quantification of the peak responses of the OFF steps shown in (D and E).

Sample sizes are n = 6(158) for L2 and n = 5 (93) for L3 in (D–G). All traces and plots show mean ± SEM. See also Figure S1.

were virtually indistinguishable from one another (Figures 3A–3C). Interestingly, L3 showed significant differences in response to the 25% contrast steps (Figures 3A and 3D). Plotting calcium signals as a function of luminance revealed that L3 responses to the A step were similar to the responses to the B step at a similar luminance (Figure 3E), indicating that calcium responses in L3 are sensitive to luminance but not contrast over the timescales of these stimuli.

We next tested L2 and L3 responses to the same luminance values but associated with different contrasts (Figure 3F). When flies were shown a stimulus that varied randomly between five different luminances, L2 neuron responses scaled with the magnitude of the recent step change in luminance. Furthermore, calcium signals in L2 returned to one fixed baseline within each 10 s window (Figure 3F). In contrast, calcium signals in L3 axon terminals did not adopt a single baseline but varied with

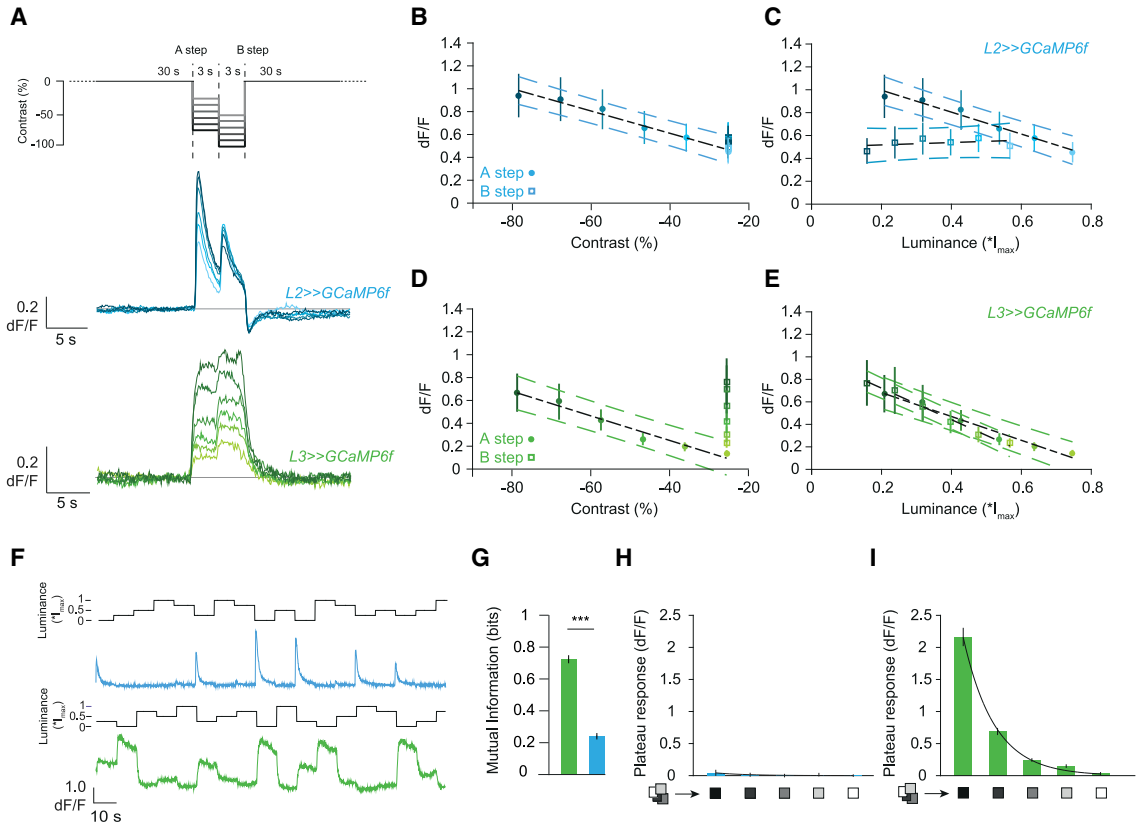

Figure 3. L2 Is Contrast Sensitive and L3 Is Luminance Sensitive

(A) Schematic of the stimulus. Six different A-B-step combinations are illustrated by the grayscale of the trace. Shown below are average calcium signals of L2 and L3; darker traces correspond to larger OFF steps.

(B–E) Peak calcium responses of L2 (B and C) or L3 (D and E) plotted as a function of contrast (B and D) or luminance (C and E). Linear regression model (black line) were fit to the responses to the A step (B and D) or the A and B steps (C and E). The dashed lines indicate the 95% confidence interval.

(F) Example calcium trace of single L2 (blue) or L3 (green) axon terminals to a stimulus comprising 10 s full-field flashes varying randomly between five different luminances.

(G) Mutual information between luminance and calcium signal, ***$p < 0.001$, two-tailed Student's t tests.

(H and I) L2 (H) and L3 (I) plateau responses (last 2 s of each epoch) pooled for all steps ending at a given luminance. The maximum screen luminance I_{max} was $1.87*10^5$ photons*s^{-1}*$receptor^{-1}$ in this figure.

Plots show mean ± SEM in (B–E and G–I). n = 10(132) flies (ROIs) for L2 and n = 10(126) for L3 in (A–E) and n = 26(436) for L2 and n = 31(512) for L3 in (G–I). See also Figure S2.

luminance and were most active at the lowest luminance (Figure 3F). When we calculated mutual information between stimulus and calcium signals, L3 showed significantly more information about luminance than L2 (Figure 3G). Mutual information was indistinguishable between 2 s and 10 s of stimulus presentation (Figure S2A). Analysis of the plateau component in many cells confirmed that the L2 baseline always returned to zero (Figures 3H and S2B). The plateau response of L3 was independent of the preceding step but indistinguishable when the stimulus ended at the same luminance (Figure S2C). Pooled L3 responses for steps ending at the same luminance were highest in dim light and showed a non-linear decline with increasing luminance (Figure 3I). Taken together, our data show that luminance information is retained in parallel to contrast information. L2 and L3 thus extract different components of the photoreceptor response. Whereas calcium signals in L2 are sensitive to contrast, L3 carries information about luminance.

L3 Neurons Are Required for Motion Responses when Light Levels Suddenly Decline

Comparing canonical LMC responses and fly turning showed that pure contrast sensitivity underestimated behavioral responses to moving stimuli (Figure 1C). Mechanisms such as spatial pooling or sensorimotor processing might account for this discrepancy [16, 31, 32]. Alternatively, the newly identified luminance information might provide a corrective signal to ensure contrast constancy. To test this, we selectively silenced L2 or L3 outputs using *shibire^{ts}* (*shi^{ts}*) and tested behavioral responses to the same OFF motion stimuli used above (Figures 1B and 1C). Compared with control turning responses, which were similar across all stimuli, flies lacking L2 outputs showed a significant reduction in response to all moving OFF edges (Figures 4A and 4B) [19, 21]. Whereas L3-silenced flies turned with normal response amplitude to stimuli starting with higher luminance, they showed response deficits when the luminance at

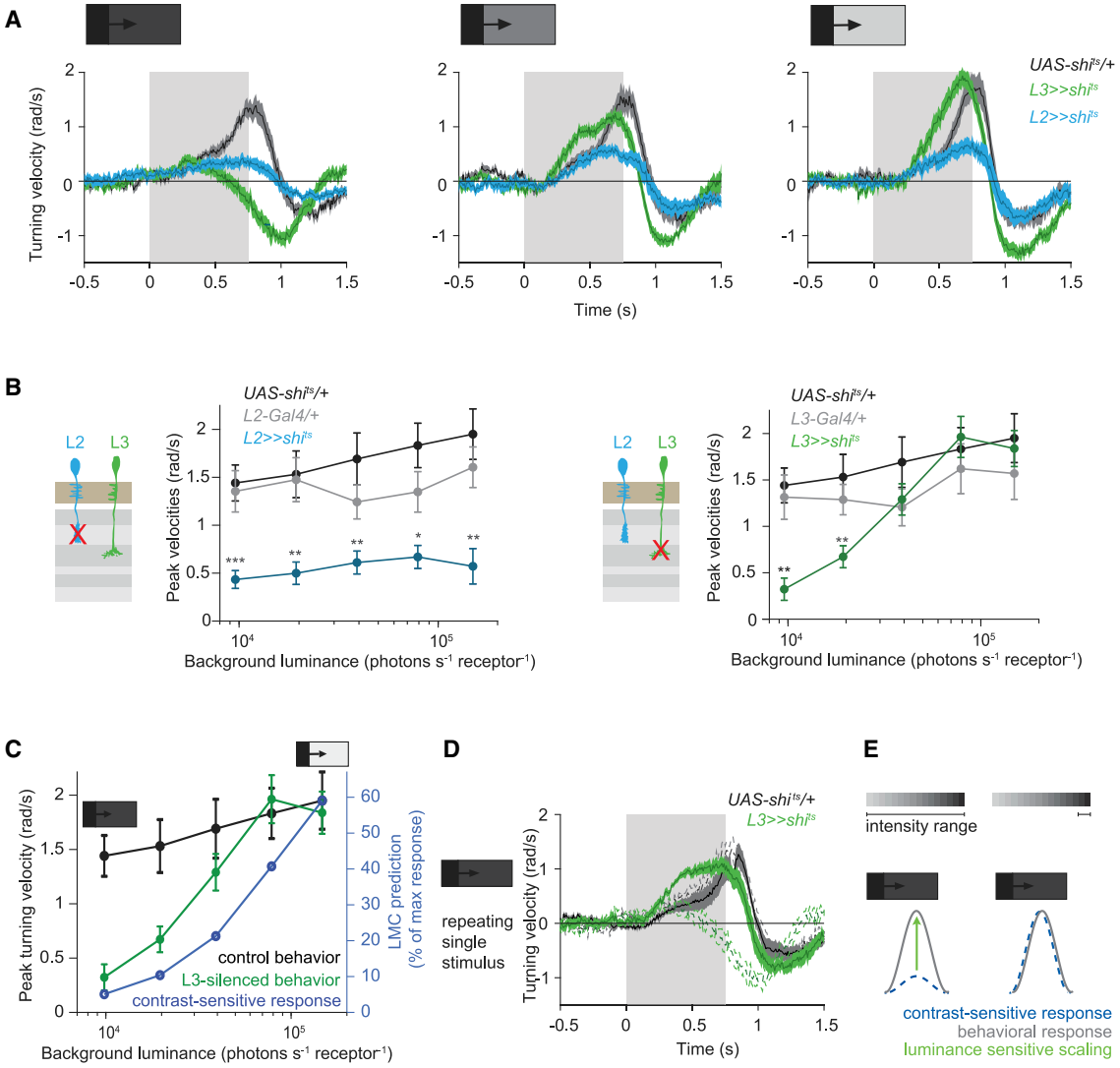

Figure 4. L3 Neurons Are Required for Behavioral Responses where Contrast-Sensitivity Underestimates a Stimulus

(A) Turning velocities for three OFF-edge motion stimuli (0.98, 3.92, or 14.71*10^4 photons*s^{-1}*receptor^{-1} background luminance, corresponding to the brightest, intermediate, and dimmest of the five OFF edges shown in Figure 1B).

(B) Peak turning velocities for five OFF-edge motion stimuli (see Figure 1B), quantified during the motion period, *p < 0.05, **p < 0.01, ***p < 0.001, two-tailed Student's t tests against both controls.

(C) Same data as in (Figure 1C), including peak turning velocities of L3-silenced flies.

(D) Turning velocities of control and L3-silenced flies in response to the dimmest OFF edge shown repeatedly. Dashed lines show data from (A). n = 10 flies each. Traces and plots show mean ± SEM.

(E) Schematic summary. When a contrast-sensitive response underestimates the salience of a stimulus at relative dim light, a luminance-sensitive corrective signal produces appropriate behavior. There is no luminance-sensitive scaling when the fly is presented with just the dimmest luminance. See also Figure S3.

motion onset was low (Figures 4A and 4B). This result was consistent when using a second L3-Gal4 line (Figure S3).

Strikingly, the behavioral response of L3-silenced flies closely resembled the predictions of canonical LMCs for all stimuli tested (Figure 4C). These data argue that L3 indeed accounts for most of the discrepancy between purely contrast-sensitive responses and behavior and provides a corrective signal in contexts where background illumination changes quickly. The remaining discrepancy can then be accounted for by subsequent sensorimotor processing. This finding further allows for two interpretations: L3 could be required in absolute dim light, or it could be required in contextual dim light for each adaptation state (i.e., the low end of the range of luminances encountered). To distinguish these possibilities, we used a stimulus with identical parameters to the previous set but only containing the darkest stimulus in which L3 silencing had the strongest effect. If L3 is required at low luminance regardless of the animal's adaptation state, blocking L3 outputs will have a similar phenotype for behavioral responses to this OFF edge moving onto a dark background. If the L3 requirement depends on the adaptation state, blocking L3 outputs will lead to different results depending on the range of stimuli that the fly is presented with.

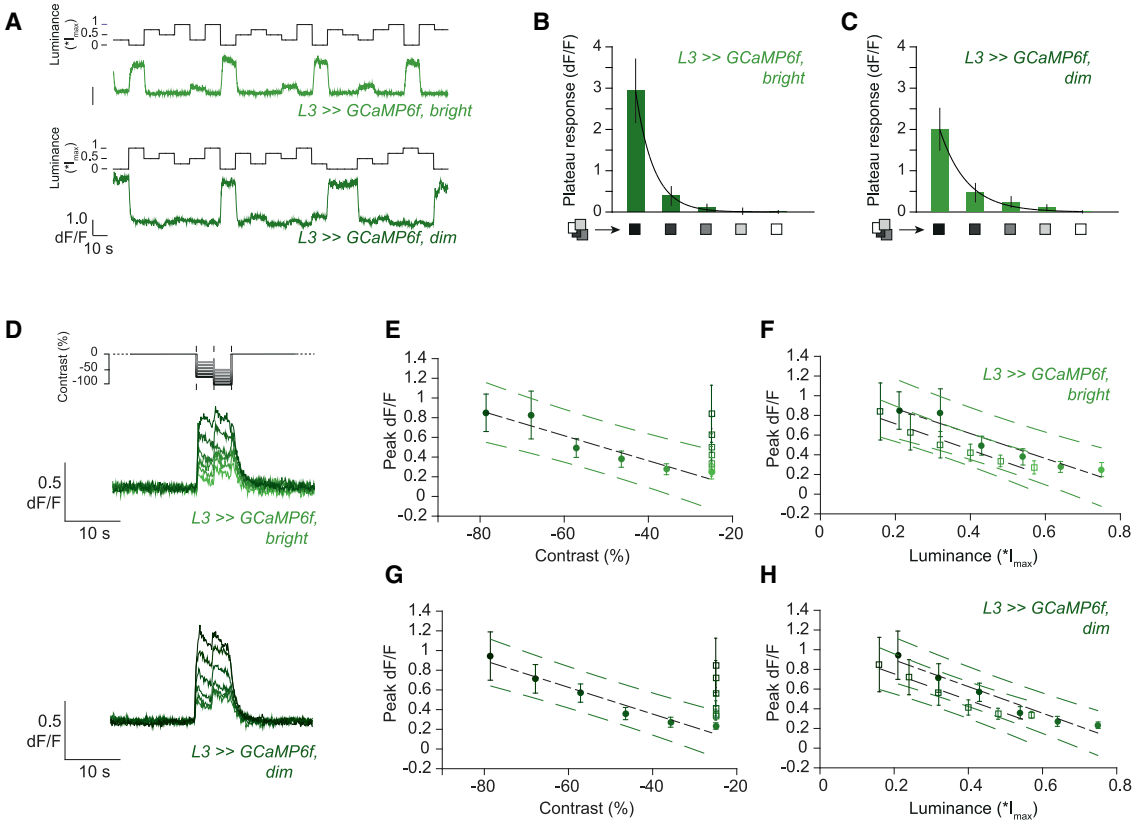

Figure 5. L3 Neurons Carry Information about Luminance at Different Adaptation States

(A) Calcium trace of single L3 axon terminals to a stimulus varying between five different luminances. Mean luminance varied ~4-fold between bright and dim conditions.

(B and C) L3 plateau responses pooled for all steps ending at a given luminance.

(D) Schematic of the stimulus. Six different A-B-step combinations are illustrated by the grayscale of the trace. Shown below are average calcium signals of L3 at two different light conditions.

(E–H) Peak calcium responses of L3 in bright (E and F) and dim (G and H) conditions plotted as a function of contrast (E and G) or luminance (F and H). Linear regression model (black line) were fit to the responses to the A step (E and G) or the A and B steps individually (F and H). The dashed lines indicate the 95% confidence interval.

I_{max} was *3.19*10^5 photons s^-1 photoreceptor^-1* for the bright and *7.55*10^4 photons*s^-1*photoreceptor^-1* for the dim condition. Plots show mean ± SEM in (B, C, and E–H). n = 6(40) for L3 in bright and n = 7(46) in dim conditions.

When flies were shown only the darkest background, the turning response of control flies was similar to their responses to the same stimulus from the full set comprising five different backgrounds (Figures 4A, 4B, and 4D). Interestingly, blocking the outputs of L3 when the fly only experienced this one background luminance did not result in a phenotype, contrasting with the effect of L3 silencing when using a set of stimuli that included brighter background luminances (Figure 4D). Thus, flies do not adapt to each individual trial when different background luminance levels are interleaved. Taken together, contrast-sensitive lamina neurons cannot fully account for behavior, and L3 neurons are functionally required for OFF edge motion detection in contextual dim light, relative to the range of stimuli that the fly is encountering (Figures 4D and 4E). This is consistent with the physiological specialization of L3 neurons, strongly responding to dim stimuli. Our data thus suggest that luminance information provided by a pathway via L3 scales behavioral responses when pure contrast sensitivity underestimates the visual input.

L3 Physiological Properties Are Maintained at Different Adaptation States

Calcium recordings showed that L3 neurons are luminance sensitive and mainly active in dim light, but so far, we tested this for one adaptation state in our imaging experiments. We next wanted to know whether L3 calcium signals provide information about luminance at different adaptation states. To test this, we used neutral density (ND) filters to change the overall mean luminance of the stimuli ~4-fold in our *in vivo* 2-photon recordings. We recorded the same flies in bright and dim conditions. Using the stimulus that varied randomly between five different luminances, L3 calcium responses were sustained in both regimes and most active in dim light (Figure 5A). L3 neurons showed a nonlinear decline with increasing luminance for both conditions (Figures 5B and 5C). After adapting flies to a bright background and then providing the two sequential OFF steps, L3 responses to both the A and B steps scaled as a function of luminance in

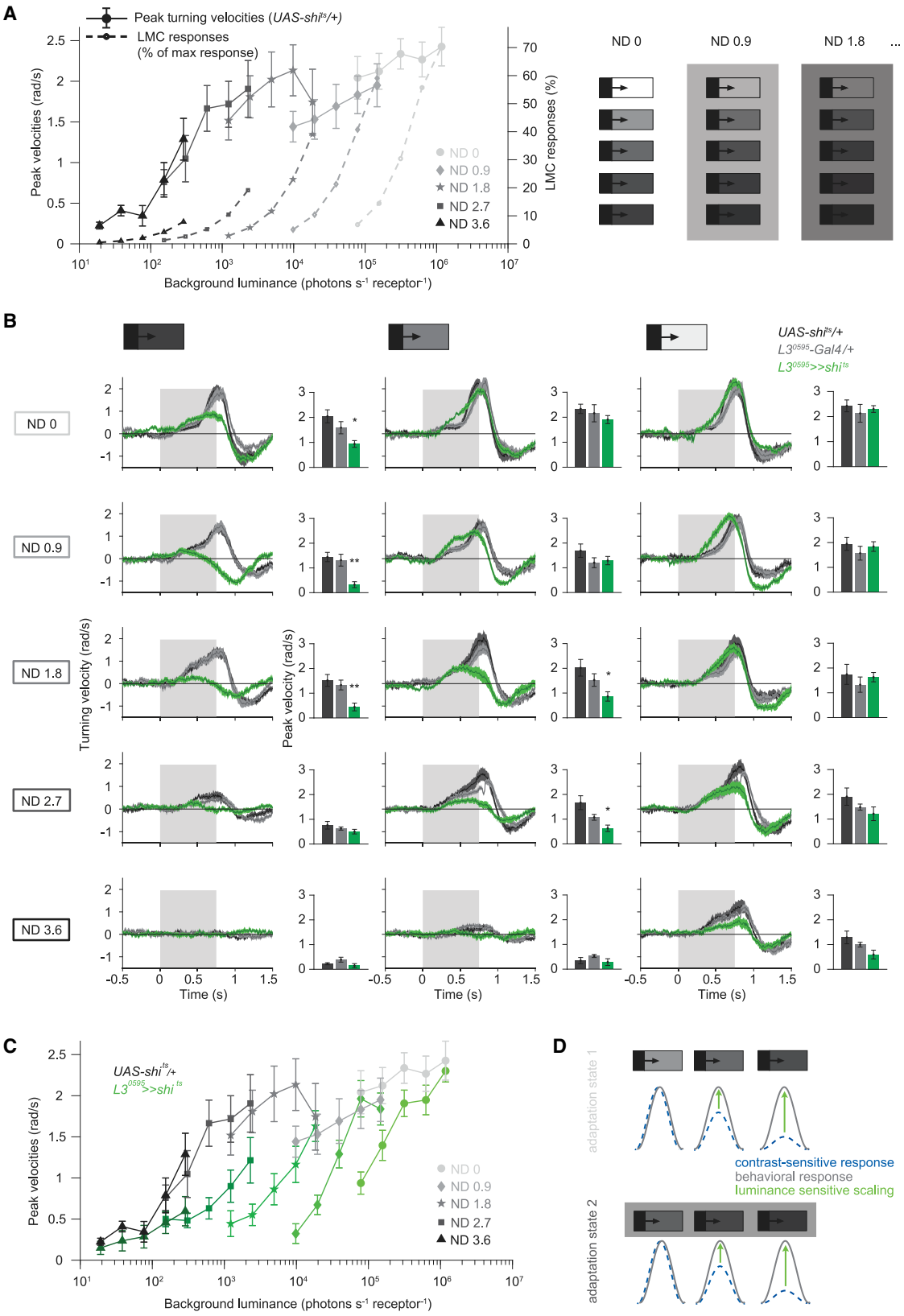

Figure 6. L3 Neurons Are Required for Behavioral Responses at Different Adaptation States

(A) Contrast-sensitive responses of canonical LMCs are predicted for different luminance regimes and plotted together with measured peak turning velocities. Each curve corresponds to one adaptation state.

(legend continued on next page)

bright and dim conditions (Figures 5D–5H). These data suggest that L3 neurons are luminance sensitive, such that their calcium signals are highest in contextual dim light, for different adaptation states.

L3 Neurons Scale Behavioral Responses to Match Stimulus Contrast Under a Range of Light Conditions

We next asked if the luminance-based scaling of the LMC response is required for behavioral responses at many different light adaptation states. The behavioral assay allowed us to examine a wider range of luminances compared with imaging. We altered the luminance range of the stimulus using neutral density filters, such that background luminance covered four orders of magnitude (Figure 6A). Contrast sensitivity of LMCs varies with adaptation to the mean of the luminance history [14]. Previous LMC measurements again allowed us to predict contrast-sensitive, canonical LMC responses under any of the individual adaptation regimes [14] (Figure 6A).

We measured optomotor responses to the same set of OFF edges as above. For low filter densities, corresponding to moderate-to-high background luminances, wild-type responses to moving OFF edges did not differ significantly from each other (Figure 6A). At low luminance, the turning amplitude decreased, indicating that flies were reaching visibility threshold. The behavioral responses appeared to be a continuous function of luminance across the five adaptation states tested (Figure 6A). In contrast to behavior, predicted canonical LMC responses dropped to near zero at the lower end of each regime. LMC prediction curves appeared shifted relative to each other. Within each adaptation state, predictions of canonical LMC responses were low for dim OFF edge stimuli, relative to the current luminance range (Figure 6A).

To test if this discrepancy can be accounted for by L3 function, and if L3 is required for motion responses in all of these regimes, we next silenced L3 under all stimulus conditions (Figure 6B). Strikingly, we found that L3 was not required for motion responses in bright conditions for each adaptation state (Figure 6B, right column). In contrast, L3 silencing led to deficits in motion detection at contextual dim light under all conditions that still produced wild-type turning (Figure 6B). Moreover, behavioral curves for turning responses in L3-silenced flies showed remarkable similarity to predictions based on contrast-sensitive LMC responses (Figures 6A and 6C). Together, luminance information from the L3 pathway ensures appropriate behavioral responses to contrast at different individual adaptation states (Figure 6D).

L3 Function Is Sufficient for Behavioral Responses to Motion in Dim Light

Having established that L2 and L3 are contrast- and luminance-sensitive inputs to the OFF pathway and that L3 is required for appropriate behavioral responses to contrast, we asked whether L3 is merely facilitating motion responses computed by parallel pathways or whether an L3 pathway alone could play a more active role in motion processing. The temporal constraints of calcium imaging do not allow us to measure the temporal properties of L2 and L3 to the immediate onset of visual stimuli. We therefore optically recorded voltage signals using the genetically encoded voltage sensor ASAP2f [33]. Both L2 and L3 displayed a fast voltage response to the onset of light (Figure 7A), consistent with previous LMC voltage recordings [34, 35]. This argues that an L3 pathway alone could process visual motion cues and L3 neurons might be sufficient to generate behavioral responses.

To test this hypothesis, we performed behavioral experiments in which photoreceptor signaling to all but one lamina neuron type were disrupted, using L3 *ort* (*outer rhabdomeres transientless*) rescues. *ort* is the gene encoding a histamine-gated chloride channel, the major receptor transmitting photoreceptor signals to lamina interneurons [36]. Cell-type-specific expression of *ort* in L3 in an *ort* mutant background enabled us to restore photoreceptor inputs selectively onto L3 (Figure 7B). We found that flies lacking Ort channels hardly responded to dim moving OFF edges but could still respond to brighter stimuli (Figures 7C and 7D). Although this is in contrast to previous reports that found that *ort* mutants to be motion blind [20, 37], we for the first time used a defined null allele containing a 569-bp deletion within the *ort* gene and leading to a premature Stop codon in *trans* to a deficiency deleting the entire *ort* locus (ort^{1}/ort^{Df}). Our results argue in favor of an *ort*-independent phototransmission (see also [38, 39]). Since responses to dim OFF edges were small in *ort* mutants, this allowed us to test L3′s ability to rescue optomotor responses relative to this background. L3 *ort* rescue completely re-established the responses to dim OFF edge motion (Figures 7C and 7D). These findings show that the L3 pathway is sufficient for behavioral responses to motion stimuli, again in dim light, indicating that fast contrast computation is still present in the L3 pathway in addition to its luminance sensitivity.

DISCUSSION

In this study, we have demonstrated that contrast sensitivity alone is not sufficient to explain the behavioral response to visual stimuli. Luminance, the primary input to the visual system, is additionally required for behavioral responses. We have shown that the two OFF pathway neurons, L2 and L3, are sensitive to fundamentally different visual features, contrast, and luminance. The presence of a luminance-sensitive pathway boosts behavioral performance where contrast pathways prove inadequate, demonstrating a role for luminance in image processing. The specific requirement of luminance signals in behavior, along with the underlying L3 physiology, are consistent across a range of adaptation states. Together, our data suggest that visual processing can handle changing light conditions because the basic luminance feature is passed on by the early fly visual system and is utilized to modulate further computations in a behaviorally relevant way.

(B) Time traces and peak turning velocities of control and L3-silenced flies, to the same stimuli as in Figure 4A. Rows correspond to five different adaptation states, generated by ND filters. *$p < 0.05$, **$p < 0.01$, ***$p < 0.001$, two-tailed Student's t tests against both controls.
(C) Peak turning velocities from data in (B).
(D) A luminance-sensitive signal is scaling the contrast-sensitive response to produce appropriate behavioral responses at different adaptation states.
All data show mean ± SEM. n = 10 flies each.

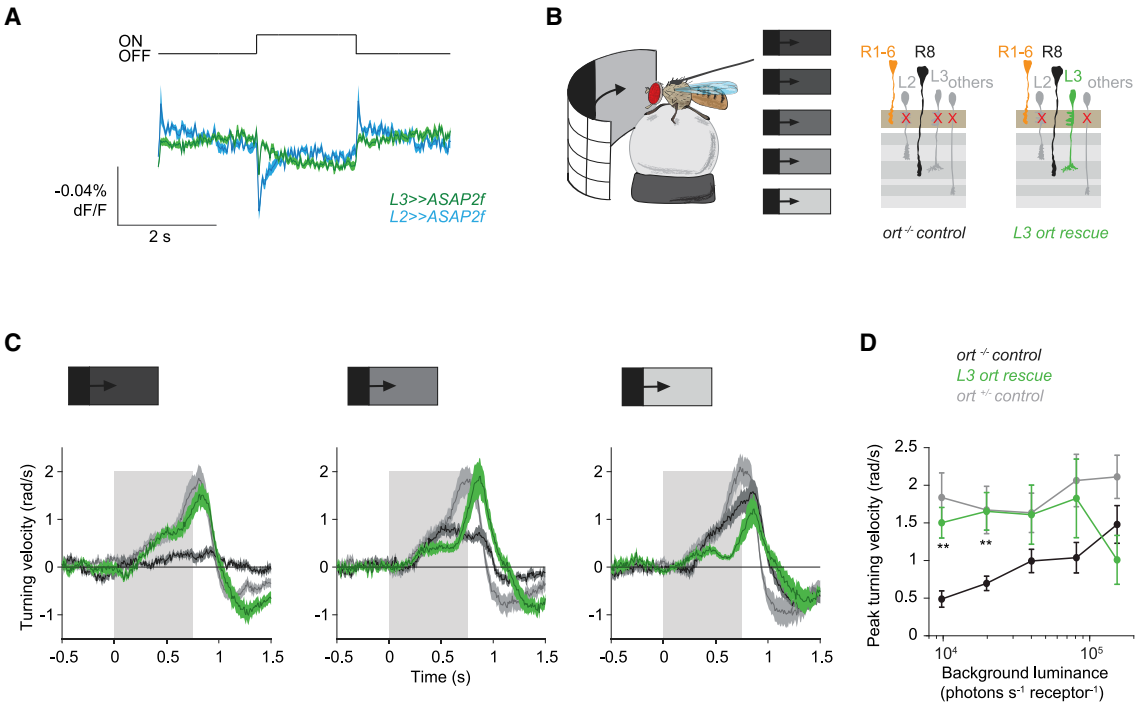

Figure 7. L3 Function Is Sufficient for Behavioral Responses to Motion in Sudden Dim Light

(A) ASAP2f signals recorded from L2 and L3 axon terminals. n = 11(72) for L2 and n = 14(74) for L3.

(B) Schematic showing the assay and genotypes for (C and D).

(C) Turning velocity time traces of $ort^{-/-}$ negative controls, $ort^{+/-}$ positive controls, and L3 *ort* rescue flies for three OFF edge stimuli.

(D) Peak turning velocities of L3 *ort* rescue flies and controls; stimulus parameters are as in Figure 4. **p < 0.01, two-tailed Student's t tests against both controls. Data show mean ± SEM. n = 9 flies each.

Transient and Sustained Signals Co-exist in the Visual System and Other Sensory Systems

Here, we have shown that a sustained component in the lamina neuron L3 is sensitive to luminance. First-order visual interneurons have been characterized extensively, and canonical LMCs are generally thought to be "amplified and more transient versions of photoreceptor responses" [13] and, therefore, contrast sensitive. This contrast sensitivity is visible in L2 calcium responses. However, it was noted that L3 is physiologically distinct and has a more pronounced sustained component and a slower temporal filter compared with those of L1 and L2 [19, 21, 34, 35]. Electrophysiological recordings showed that the L3 membrane potential did not return to baseline upon prolonged visual stimulation [34, 35]. Our data show that this is more pronounced for calcium signals and that L3 responds to a step change in luminance with a step change in GCaMP signal. Luminance information is retained in a specialized L3-mediated pathway in parallel to contrast-sensitive pathways to facilitate visual processing under conditions that are challenging for purely contrast-sensitive pathways.

The parallel presence of sustained (tonic) and transient (phasic) responses has been observed in different neural systems. Examples include proprioceptive neurons, where tonic and phasic neurons encode joint position and movement, or mechanosensory neurons from Johnston's organ, where tonic and phasic responses encode antennal deflection and vibration, respectively (e.g., [40, 41]).

Luminance Information Ensures Contrast Constancy when Light Levels Suddenly Decline

Our findings suggest that a behavioral response to a stimulus of varying temporal contrast in the *Drosophila* OFF pathway is computed in two phases—first, contrast-sensitive LMCs, such as L2, report the luminance difference relative to the adapted luminance, and this signal is then subjected to corrective modulation with the luminance information from the L3 pathway. In species ranging from flies to humans, photoreceptor adaptation mechanisms operate on different timescales, typically a faster one that takes a fraction of a second and a slower one that lasts several seconds or minutes [6, 10]. These processes allow visual systems to operate under a wide range of luminances to detect contrast as a salient feature in the environment. However, fast changes in mean luminance caused by a shadow or by an animal's own movement would cause high contrasts to elicit only very small photoreceptor responses if the adaptation state was not yet fully caught up. Consequently, signals encoded by contrast-sensitive neurons would underrepresent the physical contrast. The presence of a luminance-sensitive pathway appears to overcome these limitations to ensure accurate motion detection in sudden dim light. This could happen through excitatory interactions between the L3 and the L2 pathways. At low luminance, when L3 is most active, such an interaction would amplify signals from contrast-sensitive neurons and thereby allow for a behaviorally adequate response. Such an interaction between luminance- and contrast-sensitive channels might be a

general mechanism implemented in visual systems to explain robust behavioral responses when adaptation timescales are insufficient.

Mechanisms of Luminance and Contrast Processing Downstream of the Lamina

Luminance and contrast signals must ultimately be combined to control motion-guided behaviors. This could for example happen in the transmedullary (Tm) or medulla intrinsic (Mi) neurons that are postsynaptic to LMCs [42]. One major postsynaptic partner of L3, Tm9, possesses similarly sustained responses to those seen in L3 [23]. Interestingly, Tm9 has wide receptive field properties, potentially receiving input from several neighboring columns [23]. Thus, Tm9 could serve to integrate over space to identify a change in illumination and help to distinguish global from local changes in signal. Tm9 responses further depend on the biphasic ON pathway input L1 [23], arguing that transient and sustained responses are combined at this stage. All other major medulla OFF pathway interneurons receive predominant input from L2 and have transient response kinetics [33, 42, 43, 44]. Medulla neurons of the ON pathway can also be separated into sustained and transient types, and connectomics suggests that L3 could provide luminance information to both ON and OFF pathways [45]. Thus, relative lamina neuron contributions might determine downstream response properties. Further integration could happen in the dendrites of the downstream direction-selective T4 and T5 cells. Luminance information might simply act on contrast signals to scale them before they are spatiotemporally compared. The addition of a DC component also enhanced predictions of motion responses to slow apparent motion stimuli and reverse-phi illusion [46, 47]. Luminance-sensitive L3 responses may thus provide the neural substrates for conveying this DC component to downstream visual circuitry.

Finally, L3 feeds into the color pathway by for example providing input to Dm9 cells [48] and could thus help establish color constancy.

A Role for Luminance in Image Processing Might Be a Common Feature of Visual Systems

Our finding that the presence of luminance information downstream of photoreceptors allows for appropriate behavioral response could suggest a selective advantage for animals living in certain environments. It will be interesting to see if different species with specific ethological constraints have evolved similar luminance-sensitive pathways and how they facilitate visual behaviors. The requirement for such a pathway appears to be greater in animals encountering broad luminance variance over short time periods. Although local mean and variance in natural scenes vary independently, a positive correlation between them sometimes exists because of shadows [49]. Because objects in bright sunlight tend to cast darker shadows, diurnal animals are more likely to encounter wide variance and to possess a luminance-sensitive channel. Nocturnal animals, on the other hand, may require luminance information to tackle challenges posed by low light levels. Therefore, luminance information preserved beyond photoreceptors might facilitate behavior in different ways depending on the species' ethology.

Physiologically different LMC subtypes have been described in different species. For example, LMCs in bumblebees and butterflies exhibit sustained components [50, 51], and motion-sensitive neurons perform better than photoreceptor responses predict in the nocturnal hawkmoth [32, 52]. Interestingly, presynaptic L2 and L3 calcium signals are highly reminiscent of sustained and transient calcium signals in bipolar cells of the vertebrate retina [53–55]. Information about luminance is retained past vertebrate photoreceptors at the rod bipolar cell to the AII amacrine cells synapse [25]. The rod bipolar cell pathway is an important player specifically in dim light conditions. Together, these findings suggest that luminance information in the vertebrate retina is also used to aid image processing. In line with this idea, human eyes come across substantial variation in luminance every few milliseconds when inspecting natural scenes with saccades [49, 56]. It has been suggested that gain control to luminance fluctuations also occurs within the retinal circuitry and past photoreceptor adaptation [57, 58]. Therefore, our finding that the visual system uses luminance information to aid contrast computation may reveal a general image processing strategy utilized across phyla.

STAR★METHODS

Detailed methods are provided in the online version of this paper and include the following:

- KEY RESOURCES TABLE
- LEAD CONTACT AND MATERIALS AVAILABILITY
- EXPERIMENTAL MODEL AND SUBJECT DETAILS
- METHOD DETAILS
  - Behavioral experiments
  - Visual stimulation for behavior
  - Two-photon imaging
  - Visual stimulation for imaging
  - Prediction of contrast-sensitive LMC responses
- QUANTIFICATION AND STATISTICAL ANALYSIS
  - Two photon calcium imaging analysis
  - Behavioral analysis
- DATA AND CODE AVAILABILITY

SUPPLEMENTAL INFORMATION

Supplemental Information can be found online at https://doi.org/10.1016/j.cub.2019.12.038.

ACKNOWLEDGMENTS

We thank Christine Gündner, Lennart Schlieder, and Frank Kötting for excellent technical assistant and Carsten Duch, Roland Strauss, Jan Clemens, Yvette Fisher, Julijana Gjorgjieva, Carlotta Martelli, Iain Patten, and members of the Silies lab for discussions and comments on the manuscript. This work was supported by the German Research Foundation (DFG) through the Emmy-Noether program (SI 1991/1-1) and the collaborative research center 889 (project C08) to M. Silies.

AUTHOR CONTRIBUTIONS

K.S., M.D.K., and M. Silies designed and planned the study; M.D.K., K.S., and M. Seifert performed experiments; K.S., M.D.K., B.G., G.R.-T., and M. Silies analyzed the data; K.S., M.D.K., and M. Silies wrote the manuscript with input from all authors.

DECLARATION OF INTERESTS

The authors declare no competing interests.

Received: August 18, 2019
Revised: November 1, 2019
Accepted: December 11, 2019
Published: January 30, 2020

REFERENCES

1. Fechner, G.T. (1860). Element der Psychophysik (Breitkopf and Härtel).
2. Shapley, R., and Enroth-Cugell, C. (1984). Chapter 9 Visual adaptation and retinal gain controls. Prog Retin Res *3*, 263–346.
3. Clark, D.A., and Demb, J.B. (2016). Parallel Computations in Insect and Mammalian Visual Motion Processing. Curr. Biol. *26*, R1062–R1072.
4. Gollisch, T., and Meister, M. (2010). Eye smarter than scientists believed: neural computations in circuits of the retina. Neuron *65*, 150–164.
5. Burkhardt, D.A., Fahey, P.K., and Sikora, M. (1998). Responses of ganglion cells to contrast steps in the light-adapted retina of the tiger salamander. Vis. Neurosci. *15*, 219–229.
6. Laughlin, S.B., and Hardie, R.C. (1978). Common strategies for light adaptation in the peripheral visual systems of fly and dragonfly. J. Comp. Physiol. *128*, 319–340.
7. Davidson, E.H., and Freeman, R. (1965). Brightness constancy under a gradient of illumination. Psychon. Sci. *2*, 349–350.
8. Whittle, P., and Challands, P.D.C. (1969). The effect of background luminance on the brightness of flashes. Vision Res. *9*, 1095–1110.
9. Normann, R.A., and Werblin, F.S. (1974). Control of retinal sensitivity. I. Light and dark adaptation of vertebrate rods and cones. J. Gen. Physiol. *63*, 37–61.
10. Adelson, E.H. (1982). Saturation and adaptation in the rod system. Vision Res. *22*, 1299–1312.
11. Calvert, P.D., Govardovskii, V.I., Arshavsky, V.Y., and Makino, C.L. (2002). Two temporal phases of light adaptation in retinal rods. J. Gen. Physiol. *119*, 129–145.
12. Dowling, J.E., and Ripps, H. (1972). Adaptation in skate photoreceptors. J. Gen. Physiol. *60*, 698–719.
13. Laughlin, S.B. (1989). The role of sensory adaptation in the retina. J. Exp. Biol. *146*, 39–62.
14. Laughlin, S.B., Howard, J., and Blakeslee, B. (1987). Synaptic limitations to contrast coding in the retina of the blowfly Calliphora. Proc. R. Soc. Lond. B Biol. Sci. *231*, 437–467.
15. Dubs, A. (1982). The spatial integration of signals in the retina and lamina of the fly compound eye under different conditions of luminance. J. Comp. Physiol. *146*, 321–343.
16. Pick, B., and Buchner, E. (1979). Visual movement detection under light- and dark-adaptation in the fly, Musca domestica. J. Comp. Physiol. *134*, 45–54.
17. Silies, M., Gohl, D.M., and Clandinin, T.R. (2014). Motion-detecting circuits in flies: coming into view. Annu. Rev. Neurosci. *37*, 307–3271.
18. Yang, H.H., and Clandinin, T.R. (2018). Elementary Motion Detection in *Drosophila*: Algorithms and Mechanisms. Annu. Rev. Vis. Sci. *4*, 143–163.
19. Clark, D.A., Bursztyn, L., Horowitz, M.A., Schnitzer, M.J., and Clandinin, T.R. (2011). Defining the computational structure of the motion detector in Drosophila. Neuron *70*, 1165–1177.
20. Joesch, M., Schnell, B., Raghu, S.V., Reiff, D.F., and Borst, A. (2010). ON and OFF pathways in Drosophila motion vision. Nature *468*, 300–304.
21. Silies, M., Gohl, D.M., Fisher, Y.E., Freifeld, L., Clark, D.A., and Clandinin, T.R. (2013). Modular use of peripheral input channels tunes motion-detecting circuitry. Neuron *79*, 111–127.
22. Tuthill, J.C., Nern, A., Holtz, S.L., Rubin, G.M., and Reiser, M.B. (2013). Contributions of the 12 neuron classes in the fly lamina to motion vision. Neuron *79*, 128–140.
23. Fisher, Y.E., Leong, J.C.S., Sporar, K., Ketkar, M.D., Gohl, D.M., Clandinin, T.R., and Silies, M. (2015). A Class of Visual Neurons with Wide-Field Properties Is Required for Local Motion Detection. Curr. Biol. *25*, 3178–3189.
24. Hardie, R.C., and Weckström, M. (1990). Three classes of potassium channels in large monopolar cells of the blowfly Calliphora vicina. J. Comp. Physiol. A Neuroethol. Sens. Neural Behav. Physiol. *167*, 723–736.
25. Oesch, N.W., and Diamond, J.S. (2011). Ribbon synapses compute temporal contrast and encode luminance in retinal rod bipolar cells. Nat. Neurosci. *14*, 1555–1561.
26. Odermatt, B., Nikolaev, A., and Lagnado, L. (2012). Encoding of luminance and contrast by linear and nonlinear synapses in the retina. Neuron *73*, 758–773.
27. Schmidt, T.M., Alam, N.M., Chen, S., Kofuji, P., Li, W., Prusky, G.T., and Hattar, S. (2014). A role for melanopsin in alpha retinal ganglion cells and contrast detection. Neuron *82*, 781–788.
28. Milner, E.S., and Do, M.T.H. (2017). A Population Representation of Absolute Light Intensity in the Mammalian Retina. Cell *171*, 865–876.
29. Spitschan, M. (2019). Melanopsin contributions to non-visual and visual function. Curr. Opin. Behav. Sci. *30*, 67–72.
30. Keleş, M.F., Mongeau, J.-M., and Frye, M.A. (2019). Object features and T4/T5 motion detectors modulate the dynamics of bar tracking by *Drosophila*. J. Exp. Biol. *222*, jeb190017.
31. Duistermars, B.J., Chow, D.M., Condro, M., and Frye, M.A. (2007). The spatial, temporal and contrast properties of expansion and rotation flight optomotor responses in Drosophila. J. Exp. Biol. *210*, 3218–3227.
32. O'Carroll, D.C., and Warrant, E.J. (2017). Vision in dim light: highlights and challenges. Philos. Trans. R. Soc. Lond. B Biol. Sci. *372*, 20160062.
33. Yang, H.H.H., St-Pierre, F., Sun, X., Ding, X., Lin, M.Z.Z., and Clandinin, T.R.R. (2016). Subcellular Imaging of Voltage and Calcium Signals Reveals Neural Processing In Vivo. Cell *166*, 245–257.
34. Rusanen, J., and Weckström, M. (2016). Frequency-selective transmission of graded signals in large monopolar neurons of blowfly *Calliphora vicina* compound eye. J. Neurophysiol. *115*, 2052–2064.
35. Uusitalo, R.O., Juusola, M., and Weckström, M. (1995). Graded responses and spiking properties of identified first-order visual interneurons of the fly compound eye. J. Neurophysiol. *73*, 1782–1792.
36. Gengs, C., Leung, H.T., Skingsley, D.R., Iovchev, M.I., Yin, Z., Semenov, E.P., Burg, M.G., Hardie, R.C., and Pak, W.L. (2002). The target of Drosophila photoreceptor synaptic transmission is a histamine-gated chloride channel encoded by ort (hclA). J. Biol. Chem. *277*, 42113–42120.
37. Rister, J., Pauls, D., Schnell, B., Ting, C.Y., Lee, C.H., Sinakevitch, I., Morante, J., Strausfeld, N.J., Ito, K., and Heisenberg, M. (2007). Dissection of the peripheral motion channel in the visual system of Drosophila melanogaster. Neuron *56*, 155–170.
38. Schnaitmann, C., Haikala, V., Abraham, E., Oberhauser, V., Thestrup, T., Griesbeck, O., and Reiff, D.F. (2018). Color Processing in the Early Visual System of Drosophila. Cell *172*, 318–330.
39. Zheng, L., de Polavieja, G.G., Wolfram, V., Asyali, M.H., Hardie, R.C., and Juusola, M. (2006). Feedback network controls photoreceptor output at the layer of first visual synapses in *Drosophila*. J. Gen. Physiol. *127*, 495–510.
40. Kamikouchi, A., Inagaki, H.K., Effertz, T., Hendrich, O., Fiala, A., Göpfert, M.C., and Ito, K. (2009). The neural basis of Drosophila gravity-sensing and hearing. Nature *458*, 165–171.
41. Mamiya, A., Gurung, P., and Tuthill, J.C. (2018). Neural Coding of Leg Proprioception in Drosophila. Neuron *100*, 636–650.
42. Takemura, S.Y., Bharioke, A., Lu, Z., Nern, A., Vitaladevuni, S., Rivlin, P.K., Katz, W.T., Olbris, D.J., Plaza, S.M., Winston, P., et al. (2013). A visual

motion detection circuit suggested by Drosophila connectomics. Nature *500*, 175–181.

43. Behnia, R., Clark, D.A., Carter, A.G., Clandinin, T.R., and Desplan, C. (2014). Processing properties of ON and OFF pathways for Drosophila motion detection. Nature *512*, 427–430.
44. Serbe, E., Meier, M., Leonhardt, A., and Borst, A. (2016). Comprehensive Characterization of the Major Presynaptic Elements to the Drosophila OFF Motion Detector. Neuron *89*, 829–841.
45. Takemura, S.Y., Nern, A., Chklovskii, D.B., Scheffer, L.K., Rubin, G.M., and Meinertzhagen, I.A. (2017). The comprehensive connectome of a neural substrate for "ON" motion detection in Drosophila. Elife *6*, e24394.
46. Eichner, H., Joesch, M., Schnell, B., Reiff, D.F., and Borst, A. (2011). Internal structure of the fly elementary motion detector. Neuron *70*, 1155–1164.
47. Leonhardt, A., Meier, M., Serbe, E., Eichner, H., and Borst, A. (2017). Neural mechanisms underlying sensitivity to reverse-phi motion in the fly. PLoS ONE *12*, e0189019.
48. Heath, S.L., Christenson, M.P., Oriol, E., Saavedra-Weisenhaus, M., Kohn, J.R., and Behnia, R. (2019). Circuit mechanisms underlying chromatic encoding in Drosophila photoreceptors. bioRxiv. https://doi.org/10.1101/790295.
49. Frazor, R.A., and Geisler, W.S. (2006). Local luminance and contrast in natural images. Vision Res. *46*, 1585–1598.
50. Rusanen, J., Frolov, R., Weckström, M., Kinoshita, M., and Arikawa, K. (2018). Non-linear amplification of graded voltage signals in the first-order visual interneurons of the butterfly *Papilio xuthus*. J. Exp. Biol. *221*, jeb179085.
51. Rusanen, J., Vähäkainu, A., Weckström, M., and Arikawa, K. (2017). Characterization of the first-order visual interneurons in the visual system of the bumblebee (Bombus terrestris). J. Comp. Physiol. A Neuroethol. Sens. Neural Behav. Physiol. *203*, 903–913.
52. Stöckl, A.L., O'Carroll, D.C., and Warrant, E.J. (2016). Neural summation in the hawkmoth visual system extends the limits of vision in dim light. Curr. Biol. *26*, 821–826.
53. Borghuis, B.G., Looger, L.L., Tomita, S., and Demb, J.B. (2014). Kainate receptors mediate signaling in both transient and sustained OFF bipolar cell pathways in mouse retina. J. Neurosci. *34*, 6128–6139.
54. Euler, T., Haverkamp, S., Schubert, T., and Baden, T. (2014). Retinal bipolar cells: elementary building blocks of vision. Nat. Rev. Neurosci. *15*, 507–519.
55. Baden, T., Berens, P., Bethge, M., and Euler, T. (2013). Spikes in mammalian bipolar cells support temporal layering of the inner retina. Curr. Biol. *23*, 48–52.
56. Rieke, F., and Rudd, M.E. (2009). The challenges natural images pose for visual adaptation. Neuron *64*, 605–616.
57. Freeman, D.K., Graña, G., and Passaglia, C.L. (2010). Retinal ganglion cell adaptation to small luminance fluctuations. J. Neurophysiol. *104*, 704–712.
58. Dunn, F.A., Lankheet, M.J., and Rieke, F. (2007). Light adaptation in cone vision involves switching between receptor and post-receptor sites. Nature *449*, 603–606.
59. Timofeev, K., Joly, W., Hadjieconomou, D., and Salecker, I. (2012). Localized netrins act as positional cues to control layer-specific targeting of photoreceptor axons in Drosophila. Neuron *75*, 80–93.
60. Hong, S.-T., Bang, S., Paik, D., Kang, J., Hwang, S., Jeon, K., Chun, B., Hyun, S., Lee, Y., and Kim, J. (2006). Histamine and its receptors modulate temperature-preference behaviors in Drosophila. J. Neurosci. *26*, 7245–7256.
61. Reiser, M.B., and Dickinson, M.H. (2008). A modular display system for insect behavioral neuroscience. J. Neurosci. Methods *167*, 127–139.
62. Seelig, J.D., Chiappe, M.E., Lott, G.K., Dutta, A., Osborne, J.E., Reiser, M.B., and Jayaraman, V. (2010). Two-photon calcium imaging from head-fixed Drosophila during optomotor walking behavior. Nat. Methods *7*, 535–540.
63. Dubs, A., Laughlin, S.B., and Srinivasan, M.V. (1981). Single photon signals in fly photoreceptors and first order interneurones at behavioral threshold. J. Physiol. *317*, 317–334.
64. Gonzalez-Bellido, P.T., Wardill, T.J., and Juusola, M. (2011). Compound eyes and retinal information processing in miniature dipteran species match their specific ecological demands. Proc. Natl. Acad. Sci. USA *108*, 4224–4229.
65. Ross, B.C. (2014). Mutual information between discrete and continuous data sets. PLoS ONE *9*, e87357.

STAR★METHODS

KEY RESOURCES TABLE

REAGENT or RESOURCE	SOURCE	IDENTIFIER
Experimental Models: Organisms/Strains		
D. melanogaster: L3[MH56]-Gal4	[59]	N/A
D. melanogaster: L2[21Dhh]-Gal4	[37]	N/A
D. melanogaster: UAS-ASAP2f	[33]	RRID: BDSC_65414
D. melanogaster: ort [1], ninaE[1]	[36]	RRID: BDSC_1946
D. melanogaster: UAS-ort	[37]	N/A
D. melanogaster: UAS-GCaMP6f	Bloomington Drosophila Stock Center (BDSC)	RRID: BDSC_42747
D. melanogaster: L3[0595]-Gal4	[21]	N/A
D. melanogaster: Df(3R)BSC809	BDSC	RRID: BDSC_27380
D. melanogaster: UAS-shi[ts]	BDSC	RRID: BDSC_44222
Software		
MATLAB	Mathworks	http://www.mathworks.com/
ImageJ	National Institutes of Health	https://imagej.nih.gov/ij

LEAD CONTACT AND MATERIALS AVAILABILITY

This study did not generate new unique reagents. Further information and requests for resources and reagents should be directed to and will be fulfilled by the Lead Contact, Marion Silies (msilies@uni-mainz.de).

EXPERIMENTAL MODEL AND SUBJECT DETAILS

Flies used for 2-photon imaging and behavioral experiments were raised on a standard molasses-based food on a 12:12 h light-dark cycle at 25°C and 55% humidity. Imaging experiments were conducted at room temperature (20°C) and behavioral experiments at 34°C. Female flies, 2-3 days after eclosion, were used for both types of experiments.

L2[21Dhh]-Gal4 was described in [37], *L3[MH56]-Gal4* in [59], *L3[0595]-Gal4* in [21]. *UAS-GCaMP6f, UAS-shi[ts], Df(3R)BSC908* are from BDSC, *UAS-ASAP2f* is from [33]. The *ort [1]* chromosome described in [36] also carries the *ninaE [1]* mutation (see also [38], and was therefore used in *trans* to a deficiency uncovering the *ort* but not the *ninaE* locus (*ort [1],ninaE [1]/Df(3R)BSC809*) for *ort* mutant analysis. *UAS-ort* was first described in [60]. Full genotypes are given in the table below.

Genotypes Used in this Study

Name	Genotype	Figure
Imaging		
L3>>GCaMP6f	*w+; L3[MH56]-Gal4 / +; UAS-GCaMP6f / +*	Figures 2, 3, 5, S1, and S2
L2>>GCaMP6f	*w+; UAS-GCaMP6f / +; L2[21Dhh]-Gal4 / +*	Figures 2, 3, 5, S1, and S2
L3>>ASAP2f	*w+; L3[MH56]-Gal4 / +; UAS-ASAP2f / +*	Figure 7
L2>>ASAP2f	*w+; UAS-ASAP2f +; L2[21Dhh]-Gal4 / +*	Figure 7
Behavior		
UAS-shibire[ts] control	*w+; + / +; UAS-shi[ts] / +*	Figures 1, 4, and 6
L3-*Gal4* controls	*w+; +/ +; L3[0595]-Gal4 /+*	Figures 4 and 6
	w+; L3[MH56]-Gal4 / +; + / +	Figure S3
L3 block	*w+; +/ +; L3[0595]-Gal4 /UAS-shi[ts]*	Figures 4 and 6
	w+; L3[MH56]-Gal4 / +; UAS-shi[ts] / +	Figure S3
L2-*Gal4* control	*w+; + / +; L2[21Dhh]-Gal4 / +*	Figure 4
L2 block	*w+; + / +; L2[21Dhh]-Gal4 / UAS-shi[ts]*	Figure 4
L3 *ort* rescue	*w+; UAS-ort / +; L3[0595]-Gal4, ort [1], ninaE[1] / Df(3R)BSC809*	Figure 7
ort mutant	*w+; UAS-ort / +; ort [1], ninaE[1] / Df(3R)BSC809*	Figure 7
L3 *ort* ± control	*w+; + / +; L3[0595]-Gal4, ort [1], ninaE[1] / +*	Figure 7

METHOD DETAILS

Behavioral experiments

All behavioral experiments were conducted at 34°C, a temperature at which flies walk reliably and the restrictive temperature for *shibire^{ts}*, and at 55% humidity. Female flies were cold anesthetized and glued to the tip of a needle at the dorsal side of the thorax using a UV-hardened Norland optical adhesive. A 3D micromanipulator positioned the fly above an air-cushioned polyurethane ball (Kugel-Winnie, Bamberg, Germany), 6 mm in diameter, located at the center of a semi-cylindrical LED arena [61]. The LED panels arena (IO Rodeo, CA, USA) consisted of 570 nm LEDs that spanned 192° in azimuth and 80° in elevation and was enclosed in a dark chamber. The pixel resolution was 2° at the fly's elevation. Rotation of the ball was sampled at 120 Hz with two wireless optical sensors (Logitech Anywhere MX 1, Lausanne, Switzerland), positioned toward the center of the ball and at 90° to each other (described in [62]). Stimulus and data acquisition were coordinated using MATLAB. Data for each stimulus sequence were acquired for 15 min (see 'visual stimulation' for details).

Visual stimulation for behavior

The LEDs can show 16 different, linearly spaced, intensity levels. The luminance of each of these levels was measured at the fly's position using a LS-100 luminance meter (Konica Minolta, NJ, USA). These values, originally recorded in candela/m^2, were converted to photons incident per photoreceptor per second, following the procedure described by [63]. In short, photon flux (*570 nm for the LED arena and 475 nm for the screen at the 2-photon microscope*) available per unit area, solid angle and time, were calculated. Estimating the fraction of this flux that enters each ommatidium required its average diameter, measured in *D. melanogaster* to be 16-17 μm and the half width of its angular sensitivity function, which was estimated to be 8.23° [64]. Native luminance corresponding to the highest LED intensity, computed this way, was approximately 11.77 * 10^5 photons s^{-1} photoreceptor^{-1} (corresponding to a measured luminance of 51.34 cd/m^2). The 15 dimmer luminances scaled linearly between this value and close to complete darkness.

Flies were tested in an open-loop paradigm. Each epoch in a stimulus sequence consisted of an OFF edge moving at 192°/s on a uniformly lit background. Epochs with five such background luminances were presented in a randomized order, showing 60 to 80 trials each. In each epoch, the background intensity lasted 500 ms before motion of the OFF edge began. A 750 ms motion period was followed by a 1 s inter-stimulus interval, where the LEDs remained dark. Stimuli were presented in mirror-symmetric fashion (i.e., clockwise and anti-clockwise) to account for potential biases. When five OFF edge stimuli were interleaved, the display stepped to complete dark from 7%, 14%, 27%, 54% and 100% of the highest LED intensity (corresponding to five different background luminances: (0.98, 1.96, 3.92, 7.84 or 14.71 *10^4 photons*s^{-1}*receptor^{-1} background luminance). When a single OFF edge was repeated (Figure 4D), only the 7% of maximum intensity step was used. Neutral density filter foils (Lee filters) were placed in front of the LED arena to attenuate stimulus luminance. The foils were used individually or in combinations to achieve optical densities of 0.9 (Figures 1,6,7, S2), 1.8, 2.7 and 3.6 (Figure 6), thus creating luminance regimes that spanned about four orders of magnitude. Data for each stimulus sequence were acquired for 15 min.

Two-photon imaging

Female flies were anesthetized on ice and then glued with a UV-sensitive glue (Bondic) onto a sheet of stainless steel foil, containing a hole for the head and thorax of the fly. Mounting and dissection was done at room temperature. Flies were positioned in a way that the head was tilted downward, looking toward the screen and exposing the back of the head. The cuticle on the back of the head was removed using breakable razor blades and fine forceps. The flies were perfused with a carboxygenated saline-sugar imaging solution. The saline composition was as follows: 103 mM NaCl, 3 mM KCl, 5 mM TES, 1 mM NaH_2PO_4, 4 mM $MgCl_2$, 1.5 mM $CaCl_2$, 10 mM trehalose, 10 mM glucose, 7 mM sucrose, and 26 mM $NaHCO_3$. The pH of the saline equilibrated near 7.3 when bubbled with 95% O_2/5% CO_2. Imaging experiments were performed on a Bruker Investigator 2-photon microscope (Bruker, Madison, WI, USA), equipped with a 25x/1.1 objective (Nikon, Minato, Japan). The excitation laser (Spectraphysics Insight DS+) was set to 920 nm in order to excite *GCaMP6f*, applying 5-15 mW of power at the sample. Emitted light was sent through a SP680 short-pass filter, a 560 lpxr dichroic filter and a 525/70 emission filter. Data was acquired using PrairieView software at a frame rate of ~20Hz using a frame size ~60x200 pixels and 8x optical zoom.

Visual stimulation for imaging

For calcium imaging experiments, custom-written software using C++ and OpenGL was used to generate visual stimuli. For the stimulus projection, we used a LightCrafter (Texas Instruments, Dallas, TX, USA) running at a frame rate of 100 Hz. Stimulus light was sent through a 482/18 band pass filter onto an 8 cm x 8 cm rear projection screen, positioned anterior to the fly. The projection screen spanned 60° of the fly visual field in azimuth and 60° in elevation. For imaging experiments in Figures 2 and 3 and 7, a ND1.0 neutral density filter (Thorlabs) was used to minimize stimulus bleedthrough, such that the brightest luminance measured at the fly's position was *1.87 * 10^5 photons s^{-1} photoreceptor^{-1}*. For imaging experiments at different adapting luminances (Figure 5), neutral density filters were used to change the mean luminance of the visual stimuli. Luminances between the two conditions varied ~4-fold with *3.19 * 10^5 photons s^{-1} photoreceptor^{-1}* maximum luminance for the bright condition and *7.55 * 10^4 photons s^{-1} photoreceptor^{-1}* maximum luminance for the dim condition. We recorded the same flies in bright and dim conditions, and randomly switched the order between the two conditions for different flies.

Visual stimuli are described below. All temporal contrast values were calculated using the definition of Weber contrast:

$$C = \frac{I_{after} - I_{before}}{I_{before}}$$

Full-field flashes

Periodic, alternating, full-contrast light and dark flashes were presented. Each 5s stimulus period was presented for ~10 trials, each 60 s period for ~3 trials.

ON or OFF steps from intermediate gray:

The stimulus consisted of a 10 s gray period, followed by 5 s ON or OFF flashes of 20%, 40%, 60%, 80% or 100% contrast increments or decrements (Weber contrast). The light offset to gray backgrounds following ON steps thus included contrast decrements of 16%, 28%, 37%, 44% and 50%.

Flashes of different luminances

The stimulus consisted of 10 s full-field flashes of 5 different luminances (0, 0.25, 0.5, 0.75 and 1* of the maximal luminance I_{max}). The order between the periods was randomized, resulting in 20 different step combinations with varying Weber contrast.

Contrast steps from adapted background stimulus:

To distinguish contrast and luminance sensitivity, we designed a stimulus after [25] containing a 30 s adapting period max luminance, followed by two consecutive 3 s OFF steps: the A and B steps. The A step took one of 6 linear decreasing luminance values, resulting in 6 different contrast steps relative to the adapting step. The luminance of the next OFF steps, the B step was one of 6 linear decreasing luminance values, depending on the previous A step, all of which resulted in 6 equally sized 25% contrast steps. The order of the different A steps and their associated B steps was randomized.

Prediction of contrast-sensitive LMC responses

Contrast-sensitive LMC responses were calculated for the stimuli tested in behavior (Figures 1,4,6). Different luminance regimes were generated using ND filters, and thus corresponded to different respective adapting luminances.

LMC responses to different contrast steps at different mean adapting background luminances have been extensively characterized [22], and the response of LMCs per unit contrast (contrast response) is shown to vary with background luminance [14].

In our behavioral paradigm, contrast steps during OFF edge motion followed briefly displayed background luminances that differed from the adapting luminance. We calculated the adapting luminance I_{mean} as the mean luminance of a stimulus trace, comprising equal occurrences of the five OFF edges and the dark inter-stimulus intervals.

To generate predicted LMC values for each adapting luminance, we fitted published data of LMC contrast response versus adapting luminance [14] with a sigmoid function using the method of least-squares:

$$f(x) = \frac{a}{1 + e^{-b*(x-c)}}$$

where $a = 133.9$, $b = 1.095$, $c = 4.505$.This function was used to generate contrast response values (k) as a function of the adapting luminances calculated for each luminance regime in our experiment. Contrast–response curves for an LMC can be best approximated by logistic sigmoid curves [14] centered at zero contrast and having a slope parameter equivalent to -k. Thus, the following logistic function gave the predicted LMC responses, if a step was taken from I_{mean} to the individual background or OFF edge luminances:

$$R_{LMC} = \frac{1}{1 + e^{-(-k)*C}}$$

LMC contrast-response curves in [16] were obtained by adapting the flies to a particular luminance and then exposing them to steps of different Weber contrast. Here, contrast c is the temporal Weber contrast of either the luminance of the OFF edge or the background as if steps were taken from the adapted luminance to either of these luminances. Therefore, contrast of the OFF edge was always −1, and contrast of the background varied.

Contrast-sensitive LMC responses to the OFF edge moving onto a background were then calculated as

$$R = R_{LMC(OFF)} - R_{LMC(background)}$$

where R_{OFF} is the contrast-sensitive LMC response if the step was taken from I_{mean} to the OFF edge intensity (0), and $R_{background}$ is the LMC response if the step was taken from I_{mean} to the background luminance.

Contrast-sensitive LMC responses (R) were compared against behavioral responses measured for the same OFF edge stimuli (Figures 1C, 4C, 6A).

QUANTIFICATION AND STATISTICAL ANALYSIS

Analyses of calcium imaging data as well as behavioral data were done using MATLAB (Mathworks, Natick, MA).

Two photon calcium imaging analysis

To correct for movement during the imaging experiments, cross-correlation upon Fourier transformation was used to align the acquired images to a reference stack composed of a maximum intensity projection of the first 30 frames. All responses and visual stimuli were interpolated to 10 Hz and then averaged across the repeating trials. Regions of interest (ROIs) were selected manually and an average intensity within individual ROIs was computed for each frame in order to generate a time trace of the response of each ROI. All responses and visual stimuli were interpolated to 10 Hz and then averaged across the repeating trials. An exception was ASAP2f voltage recordings, which were interpolated at 30 Hz. For all the stimuli, single ROI responses from L2 and L3 neurons were correlated with the stimulus, and only the ones that were negatively correlated with the stimulus were used for the analysis [23]. Mean responses were calculated for all ROIs within a fly, and then between flies. All statistical analysis was performed between flies.

Full field flashes

For calculating $dF/F = (F - F_0)/F_0$, the mean fluorescence intensity signal of the whole trace was used as F_0.

ON or OFF flashes from intermediate gray

For calculating dF/F, the mean fluorescence intensity signal of the trace to the gray step was used as F_0. Peak OFF responses to the OFF-to-gray or ON-to-gray steps were calculated relative to the mean response over the 2.5 s before the step. A two-tailed Student's t test was used to test for statistical differences between equivalent OFF steps.

Flashes of different luminances

To calculate dF/F, the mean fluorescence intensity signal of the trace to the 100% ON step was used as the F_0. The plateau response was calculated as the maximal difference in the calcium signal at the last 2 s of the response compared to the mean baseline response during 2 s before the step. One-way analysis of variance (ANOVA) was used to test for differences between responses to different steps ending at the same luminance. We used Shannon's information theory to estimate which cell encodes more information about luminance according to [65]. Mutual information was calculated either for the whole response trace, or for 2 s time bins.

Contrast steps from the adapted background stimulus:

To calculate dF/F, F_0 was calculated as the mean calcium response at the last 5 s of the 30 s adaptation period. Calcium responses were calculated as the maximal calcium response in the first 3 s after the step (for both A and B step) compared to the mean baseline response over the period of 5 s before the step. One-way ANOVA was used to estimate whether responses to the B step were significantly different within the same genotype.

Behavioral analysis

To analyze behavioral responses of flies to moving stimuli, yaw velocities of the flies were derived as described in [62]. Velocities in the direction of stimulus motion were deemed positive and those against the stimulus, negative. Fly responses to each mirror-symmetric stimulus pair were aggregated while computing mean response of the fly to that stimulus category. Time series of turning responses presented here consist of velocities averaged across flies ± SEM (Figures 1B, 4A,D, 6B, 7C, Figure S3A). Flies with a forward walking speed less than 3 mm/s were discarded from the analysis, resulting in rejection of approximately 20% of all flies. Peak turning velocities were extracted for each fly from trial-averaged instantaneous yaw velocities over the stimulus motion interval (750 ms), considering a 100 ms response latency. These peak velocities were then adjusted for baseline turning separately for each fly, by subtracting the maxima of the trial-averaged velocities over the last 200 ms of the preceding inter-stimulus intervals. Mean turning of flies from control and experimental genotypes was first tested for normal distribution using a Kolmogorov-Smirnov test. To examine statistical differences between genotypes, two-tailed Student's t tests were used. Data points were considered significantly different only when the experimental group differed from both genetic controls significantly (Figures 4B, 6B, 7D; S3B).

DATA AND CODE AVAILABILITY

The datasets generated during this study are available at Mendeley Data https://dx.doi.org/10.17632/p7xskvwktk.1. Analysis code corresponding to the key analyses is available at https://github.com/silieslab/KetkarSporar_CurrBiol_2020. Further information is available upon request by Lead Contact, Marion Silies (msilies@uni-mainz.de).

Current Biology, Volume *30*

Supplemental Information

Luminance Information Is Required for the Accurate Estimation of Contrast in Rapidly Changing Visual Contexts

Madhura D. Ketkar, Katja Sporar, Burak Gür, Giordano Ramos-Traslosheros, Marvin Seifert, and Marion Silies

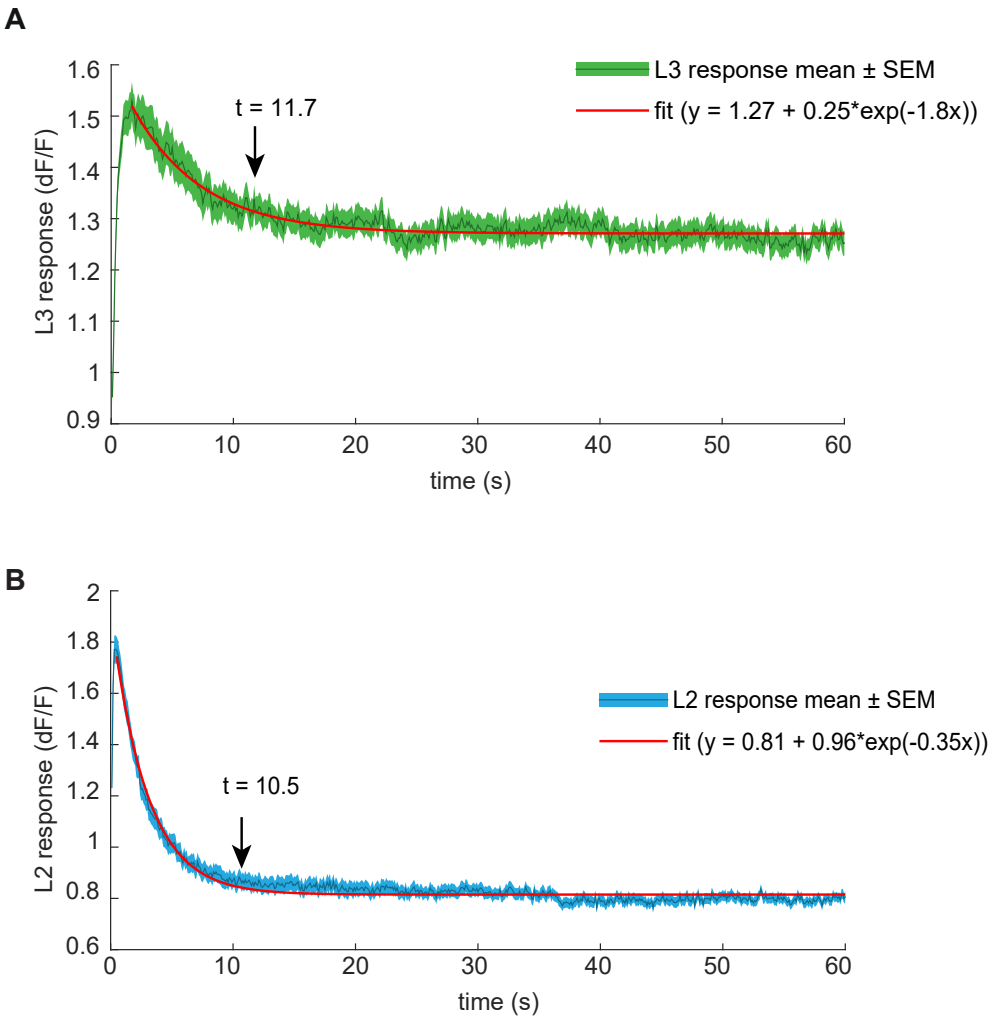

Figure S1: Analysis of L2 and L3 neurons' steady state after a prolonged OFF flash. Related to Figure 2.

(A,B) Calcium signals from L3 (A) or L2 (B) axon terminals in response to 60 s OFF flashes of 100% contrast were fit with an exponential decay function (y = c + a*ebx) using the method of least squares. The constant 'a' represents the steady-state response. The arrow denotes the time point at which calcium signals are no longer significantly different from the steady state, determined with a one-sample t-test. N = 8(68) for L2, N = 5(89) for L3.

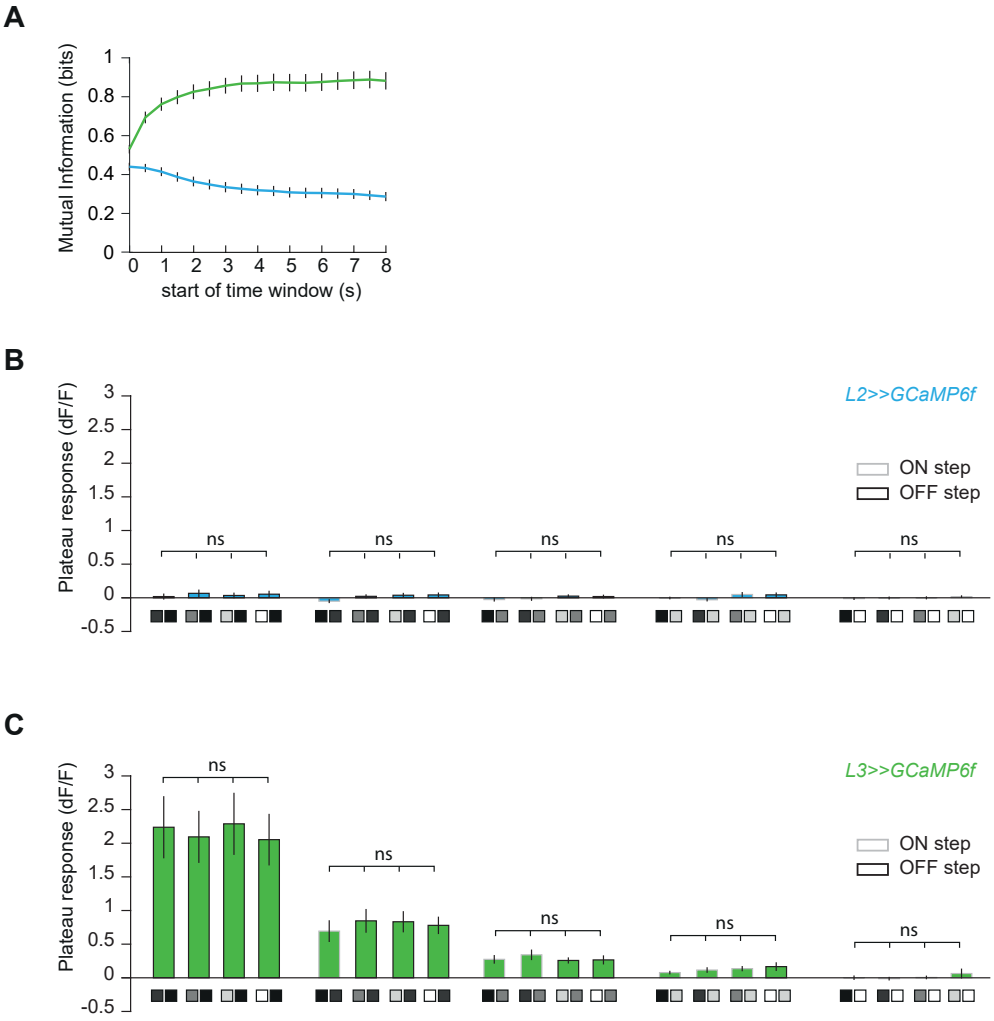

Figure S2: L3 neurons are luminance sensitive. Related to Figure 3.
(A) Mutual information between stimulus luminance and calcium signal, calculated for 2 s time windows. **(B,C)** Bar plot showing the L2 (B) or L3 (C) plateau responses measured for all steps ending at -100% OFF, -50% OFF, gray, 50% ON and 100% ON, calculated as the average response across the last 2 s of stimulus presentation. Gray lines surrounding the bars represent the ON steps and black lines represent the OFF steps. One-way analysis of variance (ANOVA) was used to test for differences between responses to different steps ending at the same luminance. Sample sizes given as N = # flies (# cells) are N = 26 (436) for L2 and N = 31 (512) for L3 in (A-C).

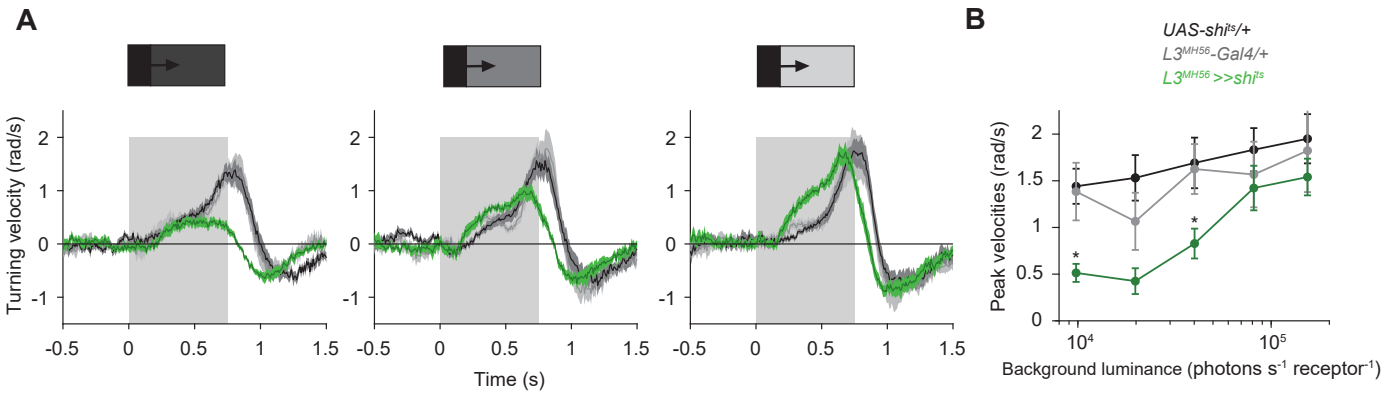

Figure S3: L3 neurons are required for motion responses in dim light. Related to Figure 4.
Same experiment as in Figure 4, but using another L3-Gal4 driver line. **(A)** Time traces showing turning velocities of controls and L3-silenced flies for three of the OFF edge motion stimuli as in Figure 1B. Traces show mean ± SEM; the gray box region indicates motion duration. **(B)** Quantification of the results shown in (A). Peak turning velocities during the motion period are plotted against background luminance. Curves show mean ± SEM. *p<0.05, ***p<0.001, tested with two-tailed Student t tests against both controls. N=10 for UAS-shits/+, N=7 for L3MH56-Gal4/+ and N=7 for L3MH56-Gal4>> shits.

Manuscript 2: Peripheral visual circuitry segregates behaviorally relevant features across ON and OFF pathways

The following manuscript is under review in eLife.

Authors and affiliations

Madhura D Ketkar*[1,2], Burak Gür*[1,2], Sebastian Molina-Obando*[1,2], Maria Ioannidou[1,3], and Marion Silies[1]

[1] Institute of Developmental Biology and Neurobiology, Johannes-Gutenberg University Mainz, 55128 Mainz, Germany

[2] Göttingen Graduate School for Neurosciences, Biophysics, and Molecular Biosciences (GGNB) and International Max Planck Research School (IMPRS) for Neurosciences at the University of Göttingen, 37077 Göttingen, Germany

[3] Present address: School of Physics, Faculty of Sciences, Aristotle University of Thessaloniki, 54124, Greece

*these authors contributed equally to this work

Contribution statement

Marion Silies, Burak Gür, Sebastian Molina-Obando and I designed and planned the study. Burak Gür performed the imaging experiments and analyzed the imaging data (Figure 4). I performed most behavioral experiments (Figures 2, 3, 4, 5, 6, 7, S1, S2) with help from Sebastian Molina-Obando (Figure 5) and Maria Ioannidou whom I supervised during her internship. I analyzed the behavioral experiments, and wrote the manuscript together with Sebastian Molina-Obando and Marion Silies. The manuscript was revised based on the input from all authors.

Abstract

In vision, the accurate processing of contrast information is the basis for all visually-guided behaviors. A particular challenge in visual scenes with quickly changing illumination is the luminance-invariant computation of contrast. This computation relies on the processing of luminance information itself and has to be achieved in parallel ON and OFF contrast-selective pathways. How different feature extraction mechanisms, that are either ON or OFF selective, and either encodes luminance or contrast are coordinated across visual pathways is not understood. Here we show that postsynaptic to *Drosophila* photoreceptors, the L1, L2 and L3 neurons distribute distinct contrast and luminance signals to both ON and OFF pathways. Contrast constancy in both pathways requires luminance information, which is provided by the known luminance-sensitive neurons L3, as well as L1. L1 supports contrast computation linearly across the luminance range, whereas L3 non-linearly amplifies contrasts at dim luminance. *In vivo* calcium imaging experiments reveal that the physiological specializations of L1 and L3 directly inform their behavioral requirements. Together, L1 and L3 do not form ON- or OFF-specific inputs but differentially support behaviorally relevant computations in both contrast-selective pathways.

Introduction

Animals extract different sensory features from the environment to guide proper behavior needed for survival. Distinct sensory features are commonly processed in parallel sensory pathways. Very early in signal processing, sensory systems split the processing of increases and decreases in a stimulus into two distinct pathways, the ON and OFF pathways. This dichotomy, which is found across sensory systems including vision, olfaction, audition, thermosensation and electrolocation (Bennet MVL, 1971; Clark et al., 2011a; Gallio et al., 2011; Joesch et al., 2010; Scholl et al., 2010; Tichy and Hellwig, 2018; Werblin and Dowling, 1969) is computationally and metabolically advantageous (Gjorgjieva et al., 2014). In vision, positive and negative luminance changes (i.e. ON and OFF contrasts) are split and processed in parallel first by contrast-selective neurons (Werblin and Dowling, 1969), and this split is subsequently passed on along visual circuitry (Baden et al., 2020; Popova, 2015). Besides the ON vs. OFF dichotomy, visual systems process several other features in parallel, including chromatic vs. achromatic information and luminance vs. contrast (Kaplan, 2008; Thoreson and Dacey, 2019), which have to intersect with the ON and OFF pathways. The feature luminance, in particular, is shown to be crucial for an accurate estimation of contrast in vision. It provides a corrective signal that scales contrast computation when background luminance quickly changes, a condition under which contrast-sensitive neurons alone cannot accurately compute contrast (Ketkar et al., 2020). Thus, this corrective luminance signal is likely to interact with both contrast polarities. However, the ON and OFF pathways are not mere sign-inverted versions of each other. They face different environmental challenges, such as asymmetrical ON-OFF statistics of the visual world (Clark et al., 2014; Ruderman and Bialek, 1994) and have evolved several structural and physiological asymmetries (Chichilnisky and Kalmar, 2002; Jin

et al., 2011; Leonhardt et al., 2016; Ratliff et al., 2010). How luminance and contrast information distribute across ON and OFF pathways and how these impact behavior remains unexplored.

In humans, visual perception scales with contrast. This property is invariant to changes in luminance, and therefore contrast constant. Contrast constancy is accomplished symmetrically across positive and negative contrasts (Burkhardt et al., 1984). Consistent with the idea that this might be a general feature of visual systems, the OFF motion pathway in fruit flies also displayed such luminance-invariant, contrast-constant behavior. In fly visual circuitry, a luminance-sensitive pathway scales contrast responses and is required for luminance-invariant behavioral responses (Ketkar et al., 2020). Luminance information is preserved in a dedicated pathway immediately downstream of photoreceptors, mediated by the first order interneuron L3. Similarly, in vertebrates, the two fundamental features contrast and luminance are also retained in parallel, either as components of the same neuronal responses or in distinct neurons (Kaplan, 2008; Oesch and Diamond, 2011). Luminance information is likely available to both ON and OFF pathways, as first order interneurons with sustained characteristics exist in both pathways (Ichinose and Lukasiewicz, 2007; Odermatt et al., 2012; Oesch and Diamond, 2011). However, the functional role of luminance in the ON pathway is not understood in any system.

In the fruit fly *Drosophila melanogaster*, the ON and OFF motion pathways have been well characterized on the cellular, circuit and behavioral levels (Silies et al., 2014; Yang and Clandinin, 2018). Thus, the fruit fly offers a promising model system to study the pathway-specific function of luminance. In the fly visual system, neurons were assigned to distinct ON or OFF pathways based on their physiological properties (Behnia et al., 2014b; Serbe et al., 2016; Silies et al., 2013a; Strother et al., 2017), anatomical reconstructions of the visual system (Shinomiya et al., 2014, 2019; Takemura et al., 2013, 2015; Takemura et al., 2017), and behavioral studies (Clark et al., 2011a; Silies et al., 2013a; Strother et al., 2017). ON and OFF contrast selectivity first arises two synapses downstream of photoreceptors, in medulla neurons (Behnia et al., 2014b; Molina-Obando et al., 2019; Yang et al., 2016). They receive photoreceptor information through the lamina neurons L1-L3 which project to specific medulla layers (Fischbach and Dittrich, 1989; Meinertzhagen and O'Neil, 1991). Although L1-L3 all show the same response polarity and hyperpolarize to light onset and depolarize to light offset, L1 projects to layers where it connects to ON-selective medulla neurons and its glutamatergic synapse mediates the sign inversion required to become ON selective. Cholinergic L2 and L3 project to distinct layers where OFF-selective medulla neurons get most of their inputs (Shinomiya et al., 2014; Takemura et al., 2013). L1 was thus thought to be the sole major input of the ON pathway, whereas L2 and L3 are considered the two major inputs of the OFF pathway (Figure 1A) (Clark et al., 2011a; Joesch et al., 2010; Silies et al., 2013a). Among these, L3 has been shown to maintain luminance information that shapes OFF-motion guided behavior in parallel to the contrast-sensitive L2 (Ketkar et al., 2020). It remains unexplored so far, whether the ON-motion driven behavior also requires luminance information and if yes, whether the single input L1 can provide it along with its contrast signal (Figure 1B).

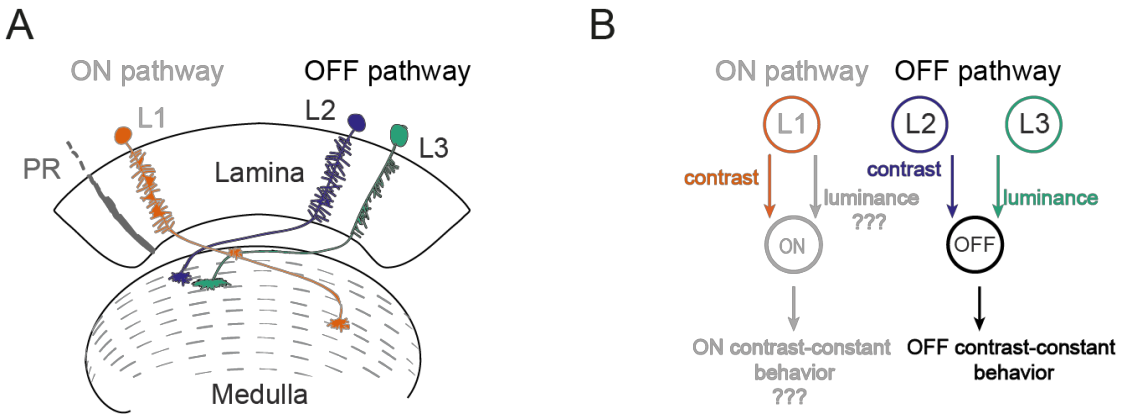

Figure 1: Current model of the major ON and OFF pathway inputs behind contrast-constant behavior. (A) Schematic of lamina neurons projecting from the lamina to the medulla neuropils. L1 as the main input to the ON-pathway and L2+L3 to the OFF pathway. (B) Different visual features as signals from L1 L2 and L3 to downstream partners required to elicit contrast-constant behavior.

Notably, motion-sensitive neurons with contrast opponent receptive fields exist in visual pathways (Ramos-Traslosheros and Silies, 2021), arguing that ON and OFF pathways maybe are not as clearly segregated. Interactions between ON and OFF pathways must further exist because of behavioral responses to visual illusions containing both ON and OFF stimuli (Salazar-Gatzimas et al., 2018). Furthermore, anatomical reconstructions reveal multiple interactions between the canonically defined pathway splits (Shinomiya et al., 2019; Takemura et al., 2013). For example, L3 makes synaptic connections with ON-selective medulla neurons of core motion detection circuitry, suggesting that L3 could provide luminance input to ON motion processing. At the functional or behavioral level, it is not understood if or how luminance and contrast information are relayed across the ON-OFF pathway split.

Here, we show that luminance information is distributed to, and is of behavioral relevance for, both ON and OFF pathways. First, an offset between contrast-sensitive responses of the major ON pathway input L1 and behavioral responses to moving ON stimuli argues that luminance information is required in the ON pathway. A combination of behavioral experiments and *in vivo* calcium imaging experiments show that two of lamina neuron cell types provide this information: the luminance-sensitive channel L3, as well as L1, which encodes both contrast and luminance in distinct response components. While L1 signals have a linear relationship with luminance, L3 non-linearly amplifies contextual dim light, and these differential luminance-encoding properties translate into distinct behavioral roles. Additionally, both luminance-sensitive neurons are required and sufficient for OFF behavior. Together, our work argues that L1 and L3 do not constitute ON- or OFF-specific inputs, as previously thought. Instead, the three first order interneurons encode luminance and contrast differentially, such that both ON and OFF pathways benefit from differentially extracted peripheral visual features. Together, our data demonstrate how the most peripheral visual feature luminance is distributed to both ON and OFF pathways to guide behavior.

Results

L1 responses to contrast do not explain ON behavior

Across species, behavioral responses to ON and OFF contrasts can be luminance invariant (Burkhardt et al., 1984; Pasternak and Merigan, 1981). Such contrast-constant behavioral responses have for example been shown in the Drosophila OFF pathway (Ketkar et al., 2020). We first asked if constancy is achieved in the ON pathway as well. To test this, we measured turning behavior of walking flies in a fly-on-a-ball assay. Flies were shown moving ON edges of different luminances, but all comprising the same 100% Michelson contrast. Fly turning responses were highly similar across edge luminances (Figure 2A,B, anova: p=0.09) suggesting constancy. We still noticed that low-luminance edges elicited slightly larger turning responses than brighter edges. We next examined if contrast responses of the sole ON pathway input L1 carry sufficient information to drive this behavior. We expressed GCaMP6f cell-type specifically in L1 and measured *in vivo* calcium responses to visual stimuli using a two-photon microscope. We presented the fly with moving ON edges that had comparable parameters and overlapping luminance values as those used in the behavioral assay (Figure 2C).

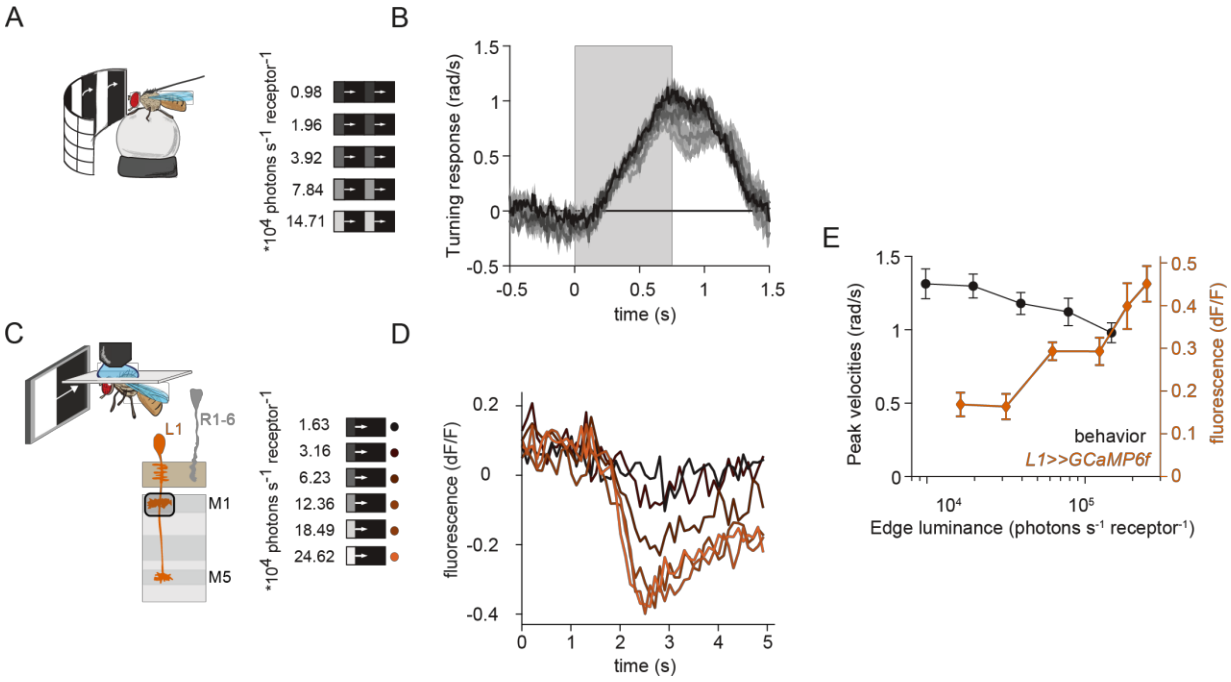

Figure 2: L1 responses to contrast do not explain ON behavior across luminance. (A) Schematic of the behavioral assay and stimuli. Multiple moving ON edges of 100% contrast are displayed on the LED arena that surrounds a fly walking on an air-cushioned ball. The edge luminance takes five different values shown next to the edges, and the background screen is always dark (~0 luminance). (B) Turning responses of *UAS-shi^{ts}/+* flies to the moving ON edges varying in edge luminance, color-coded according to the edge luminance (based on A). The gray box indicates motion duration. n = 10 flies. (C) For *in vivo* calcium imaging of L1 activity, single ON edges of six different luminances were shown. L1 axon terminals in medulla layer 1 were imaged. L1 is thought to be the sole major input to the ON pathway. (D) Calcium responses of L1 aligned to edge timing. Sample size is n=6(15). (E) Absolute step responses of L1 are plotted together with peak turning velocities calculated from (B). Highest mean responses from both categories are aligned. Traces and plots in B-E show mean ± SEM.

As described previously, L1 responded negatively to contrast increments, in line with the inverted response polarity of lamina neurons (Figure 2D) (Clark et al., 2011a; Laughlin and Hardie, 1978; Molina-Obando et al., 2019).The absolute response amplitude of the L1 calcium signals scaled with luminance and did not co-vary with the response amplitude measured in behavior (Figure 2E). Thus, L1 responses are fundamentally different from behavioral responses under these stimulus conditions. This data shows that contrast constancy observed in behavior cannot solely be explained by contrast inputs from L1, suggesting that the ON-pathway gets luminance-sensitive input to mediate ON-behavior.

The luminance-sensitive L3 is an ON-pathway input

In the OFF pathway, the luminance-sensitive L3 neuron provides the necessary luminance gain to achieve contrast constancy (Ketkar et al., 2020). Connectomics data suggest that the luminance-sensitive OFF-pathway input L3 could provide input to the ON pathway as well (Takemura et al., 2013). To test this hypothesis, we measured behavioral responses to a set of ON edges of 100% contrast at five different luminances while silencing L3 synaptic outputs using Shibire^{ts} (Kitamoto, 2001). Both control and L3-silenced flies turned with the direction of the moving edges at all luminances (Figure 3A,B). Interestingly, unlike controls, L3-silenced flies responded stronger to all ON edges and did no longer show a trend of responding stronger with lower edge luminance, indicating a luminance-dependent role of L3. To pinpoint this role, we quantified slopes of linear fits to the peak turning velocities of individual flies from each genotype (Figure 3C). The slopes from the control flies represented a negative correlation between luminance and response, whereas the L3-silenced velocities had little correlation with luminance, and their slopes were significantly more positive. Thus, L3 function did not account for the discrepancy between L1 contrast-sensitive responses and ON behavior than the controls, but L3 inputs to the ON pathway still contribute to behavior in a luminance-dependent manner (Figure 3D).

Intriguingly, L3 appears to provide an inhibitory signal to the ON pathway. We next examined if the inhibitory role generalizes across contrasts. For this purpose, we measured behavioral responses to moving ON edges of different contrasts, ranging from 11% to 100% Michelson (Figure S1 A,B). Behavioral responses of controls scaled with contrast in the low contrast range but were indistinguishable between 33% and 100% contrast. Responses of L3-silenced flies were again larger relative to the controls, especially for smaller contrasts (11 % and 25%), rendering responses to 25% contrast undistinguishable from higher contrast. Based on this, we tested the idea that L3 help to discriminate smaller contrasts and tested another set of stimulus set ranging 9% to 36% contrast (Figure S1C). Here, responses of L3 silenced flies were increased compared to controls for all ON edges (Figure S1C,D). Our data propose L3 as a second important input to the ON-pathway and reveal an inhibitory role of L3 that helps to discriminate different ON contrast steps in the low contrast range.

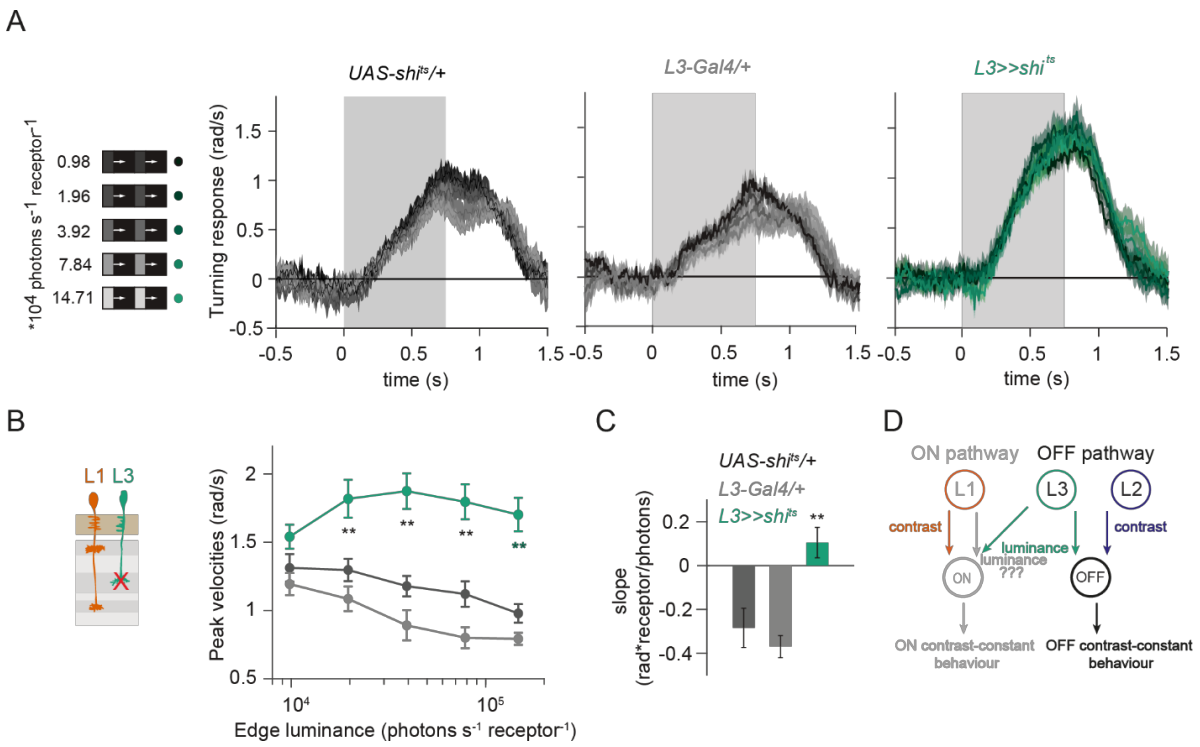

Figure 3: **The luminance-sensitive L3 is an ON-pathway input.** (A) Turning velocities of the controls (gray) and L3-silenced flies (green) in response to the five moving ON edges of 100% contrast (same stimuli as in Figure 2A). The gray box region indicates motion duration. (B) Peak turning velocities for five ON edges quantified during the motion period, **p < 0.01, two-tailed Student's t tests against both controls. (C) Relationship of the peak velocities with luminance, quantified as slopes of the linear fits to the data in (B). Fitting was done for individual flies. Sample sizes are n = 10 (*UAS-shi^{ts}/+,L3>>shi^{ts}*) and n = 8 (*L3^{0595}-Gal4/+*). Traces and plots show mean ± SEM. (D) Schematic summary. The ON pathway receives a prominent input from L3. See also Figure S1.

L1 neuronal responses carry a luminance-sensitive component

The luminance contribution of L3 did not account for the discrepancy between L1 contrast-sensitive responses and ON behavior, in that the L3-silenced flies still showed contrast-constant behavior. Thus, we hypothesized the presence of further luminance-sensitive inputs to the ON pathway. To explore other sources of luminance information in first-order interneurons, we tested calcium signals in L1, L2 and L3. Flies were shown a staircase stimulus with luminance going sequentially up and down. L1 and L2 showed positive and negative transient responses when luminance stepped down and up, respectively (Figure 4A), consistent with its contrast sensitivity (Clark et al., 2011a; Silies et al., 2013a). L2 did not show any sustained component. L3 showed sustained responses to OFF step, and was nonlinearly tuned to stimulus luminance, mostly strongly responding to the darkest stimulus. Intriguingly, L1 showed a transient component followed by a sustained component, suggesting that it encodes luminance in addition to contrast (Figure 4A). The sustained components of L1 response were negatively correlated with luminance, such that the baseline calcium signal at each step sequentially increased with decreasing stimulus luminance.

To explicitly compare luminance information across the three input neurons, we measured responses to randomized luminance and calculated the mutual information between stimulus and the sustained response component (Figure 4B-D). L1, L2 and L3 responded as described for the staircase stimulus. L2 transient responses fully returned to one baseline within the 10s of the stimulus presentation, whereas both L1 and L3 displayed sustained components that varied with luminance (Figure 4B,C). L1 and L3 sustained response components carried similar mutual information with luminance, and both were higher than L2 (Figure 4D). Interestingly, the luminance-sensitive response components of L1 and L3 scaled differently with luminance. We quantified non-linearity using the difference of Pearson's linear and Spearman's correlation between response and luminance. This value will approach to zero if the relationship is linear and increase if non-linear. L1 responses were more linear than L3 responses, whereas non-linear L3 responses selectively amplified low luminance (Figure 4E). Thus, the two luminance-sensitive neurons carry different types of luminance information.

L1 and L3 together provide luminance signals required for ON behavior

Since the canonical ON pathway input L1 is also found to carry luminance information, we hypothesized that it plays a role in mediating the luminance-invariant behavior observed even in the absence of L3. To test this, we silenced L1 and L3 simultaneously. Turning responses of flies lacking both L1 and L3 functional outputs to the five 100% contrast edges were no longer luminance-invariant, but instead turned less than controls in a luminance-dependent manner (Figure 5A-B). Intriguingly, behavioral responses now scaled positively with the edge luminance qualitatively recapitulating the contrast-sensitive responses. This was reflected in the significantly positive slopes of the L1-L3-silenced responses, compared to the controls. (Figure 5C). Thus, L1 and L3 can together account for the luminance information available to the ON pathway.

We further tested the extent to which L1 luminance component alone contributes to behavior. Silencing L1 alone severely reduced turning responses when different ON contrasts were interleaved, consistent with previous behavioral studies that identified L1 as the major input to the ON pathway (Clark et al., 2011a; Silies et al., 2013a) (Figure S2A-D). However, the L1 silencing had little effect on the responses to 100% contrast presented at different luminances, suggesting that the L1 requirement is stimulus dependent (Figure 5D-F). Thus, silencing both L1 and L3 produces qualitatively different behaviors as silencing either one alone, suggesting complex interactions between the two input pathways. Importantly, responses of L1-silenced flies to the 100% contrast edges of different luminances overlapped, maintaining contrast constancy (Figure 5D-F). This argues that the L1 and L3 luminance components act redundantly, and the L1 pathway interacts with the L3 luminance component to exert this effect. Together, the data further stress the relevance of the luminance-sensitive L3 input in shaping behavioral responses in the ON pathway.

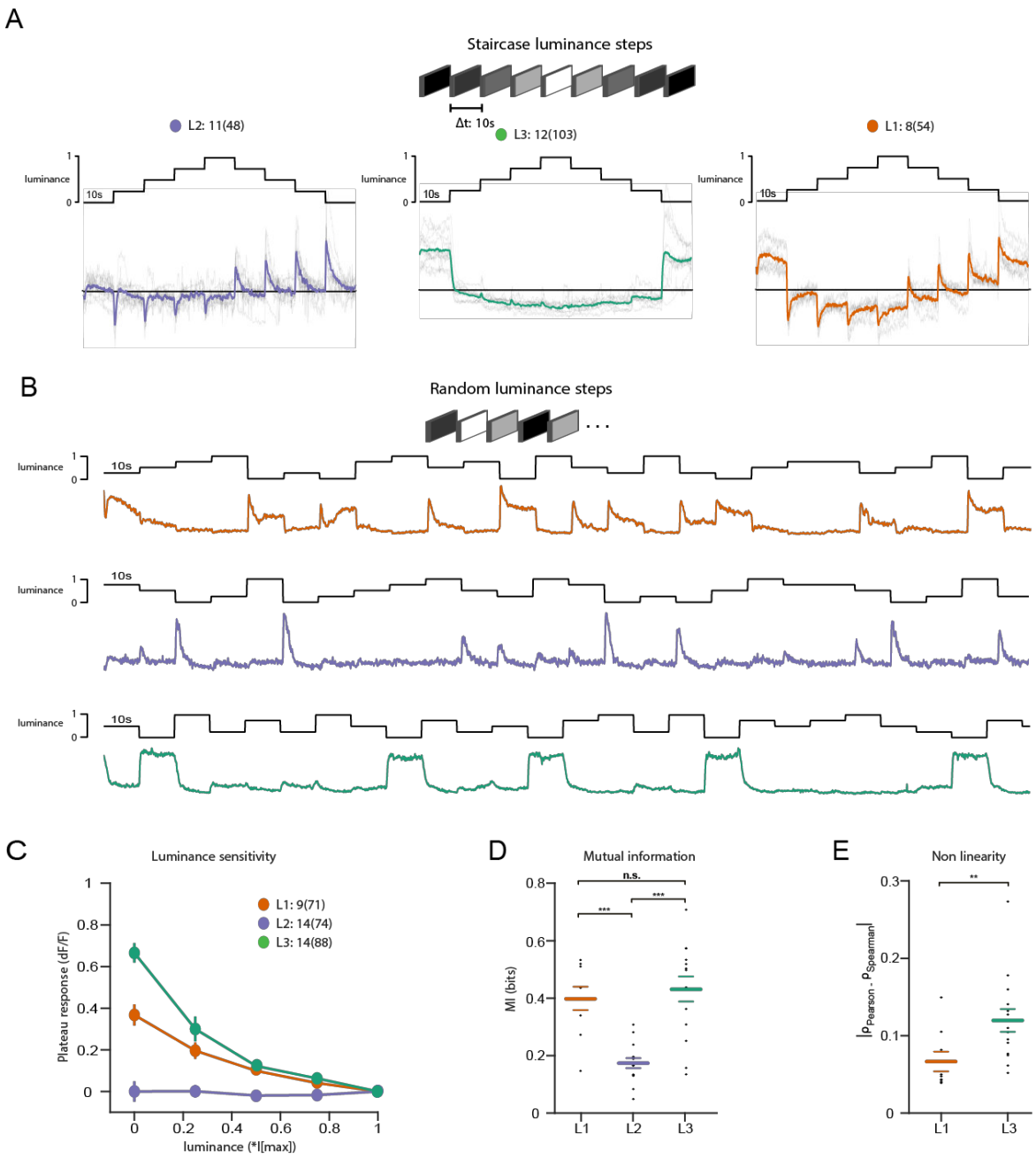

Figure 4: Lamina neuron types L1-L3 are differently sensitive to contrast and luminance. (A) Schematic of the 'staircase' stimulus. Luminance first sequentially steps up through five values and then sequentially steps down. Shown below are the plateau calcium responses of L1 (orange), L2 (purple) and L3 (green), plotted against luminance. (B) Example calcium traces of single L1, L2 and L3 axon terminals to a stimulus comprising 10 s full-field flashes varying randomly between five different luminances. (C) Plateau responses of the three neuron types, quantified from the responses to the stimulus in (B). (D) Mutual information between luminance and calcium signal, ***p<0.001, two-tailed Student's t tests. (E) Non-linearity quantification of luminance-dependent signals of L1 and L3 in (C), **p<0.01, two-tailed Student's t-test.

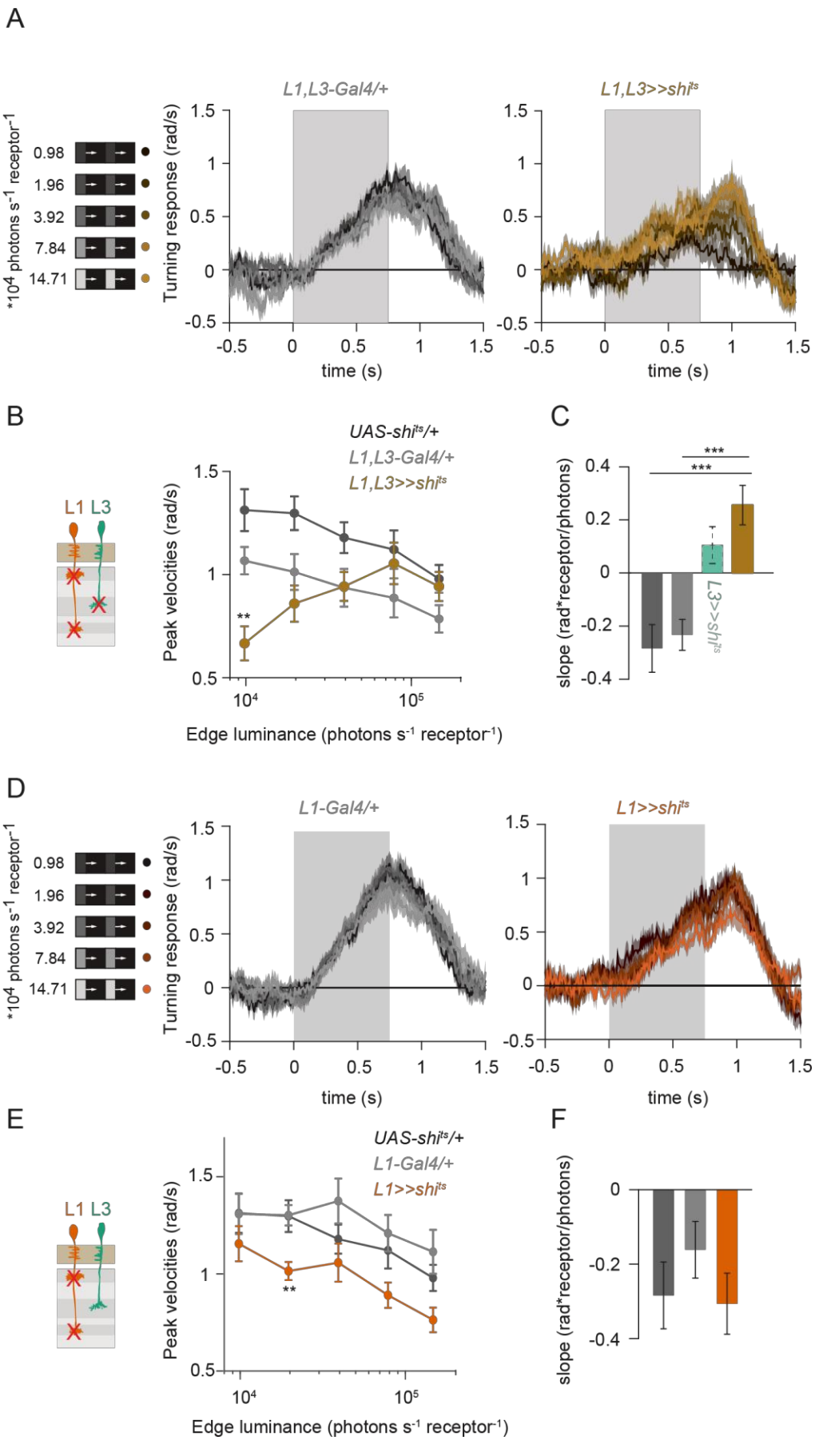
A
L1,L3-Gal4/+
L1,L3>>shi^ts
*10^4 photons s^-1 receptor^-1
0.98
1.96
3.92
7.84
14.71
Turning response (rad/s)
time (s)
B
UAS-shi^ts/+
L1,L3-Gal4/+
L1,L3>>shi^ts
L1 L3
Peak velocities (rad/s)
Edge luminance (photons s^-1 receptor^-1)
C
slope (rad*receptor/photons)
***
***
L3>>shi^ts
D
L1-Gal4/+
L1>>shi^ts
*10^4 photons s^-1 receptor^-1
0.98
1.96
3.92
7.84
14.71
Turning response (rad/s)
time (s)
E
UAS-shi^ts/+
L1-Gal4/+
L1>>shi^ts
L1 L3
Peak velocities (rad/s)
Edge luminance (photons s^-1 receptor^-1)
F
slope (rad*receptor/photons)

Figure 5: L1 and L3 together provide luminance signals required for ON behavior. (A) Turning responses of flies where L1 and L3 were silenced together (golden brown) and their specific Gal4 control (gray), color-coded according to the ON edge luminance. The same five moving ON edges of 100% contrast as in Figure 2A were shown. Responses of the other control UAS-shits/+ to these stimuli have been included in Figure 2B, Figure 3A. (B) Peak velocities quantified for each of the five edges during the motion period, also including the control UAS-shits/+, **p < 0.01, two-tailed Student's t tests against both controls. (C) Relationship of the peak velocities with luminance, quantified as slopes of the linear fits to the data in (B). Slopes from the L3-silenced flies (green, dashed) responding to the same stimuli (Figure 3C) are included again for comparison. Fitting was done for individual flies. Sample sizes are n = 10 (*UAS-shi^{ts}/+* and *L1,L3>>shi^{ts}*) and n = 7 (*L1^{c2025}-Gal4/+;L3^{0595}-Gal4/+*). (D) Turning responses of L1-silenced flies (orange) and their specific Gal4 control (gray) to the same moving ON edges. (E) Peak velocities quantified for each of the five edges during the motion period, also including the control *UAS-shi^{ts}/+*, **p < 0.01, two-tailed Student's t tests against both controls. (F) Relationship of the peak velocities with luminance, quantified as slopes of the linear fits to the data in (E). Sample sizes are n = 10 for each genotype. The gray box region in (A) and (D) indicates motion duration. Traces and plots show mean ± SEM.

L1 and L3 are individually sufficient for ON behavior across luminances

Neither of the two luminance-sensitive inputs to the ON pathway were alone required for contrast constant behavior. We thus further tested the idea that they can independently provide sufficient information about ON stimuli in dynamically changing luminance conditions. We measured contrast-constant behavioral responses after functionally isolating either L1 or L3 from other circuitry downstream of photoreceptors. To achieve this, we selectively rescued expression of the histamine-gated chloride channel Ort in *ort*-mutant flies, which otherwise lack communication between photoreceptors and its postsynaptic neurons. Behavioral responses of *ort* mutant control flies were absent, indicating that ON-motion behavior fully depends on Ort (Figure 6A). Heterozygous *ort* controls turned with the moving 100% contrast ON edges at all luminances (Figure 6B). Flies in which *ort* expression was rescued in L1 or L3 (i.e. L1 ort rescue flies and L3 ort rescue flies) both responded to ON motion at all luminances (Figure 6C). However, the extent of rescue was different for L1 and L3: Whereas L1 fully rescued turning behavior to ON edges at all luminances, L3 significantly rescued turning behavior selectively at low luminances (Figure 6C,D). We further confirmed this difference by computing rescue efficiency, defined as the fraction of the difference between positive and negative control behaviors enabled by the neuronal Ort rescue. Whereas the rescue of *ort* expression in L3 fully enabled responses to dimmer ON edges, rescue efficiency was much lower in brighter conditions, unlike L1's rescue efficiency (Figure 6E). This data confirms L1's general importance in the ON pathway, and further shows that L3 is sufficient at low luminances, reflecting L3's nonlinear preference for dim light seen at the physiological level. Thus, the differential feature extraction by L1 and L3 is mirrored at the level of ON behavior.

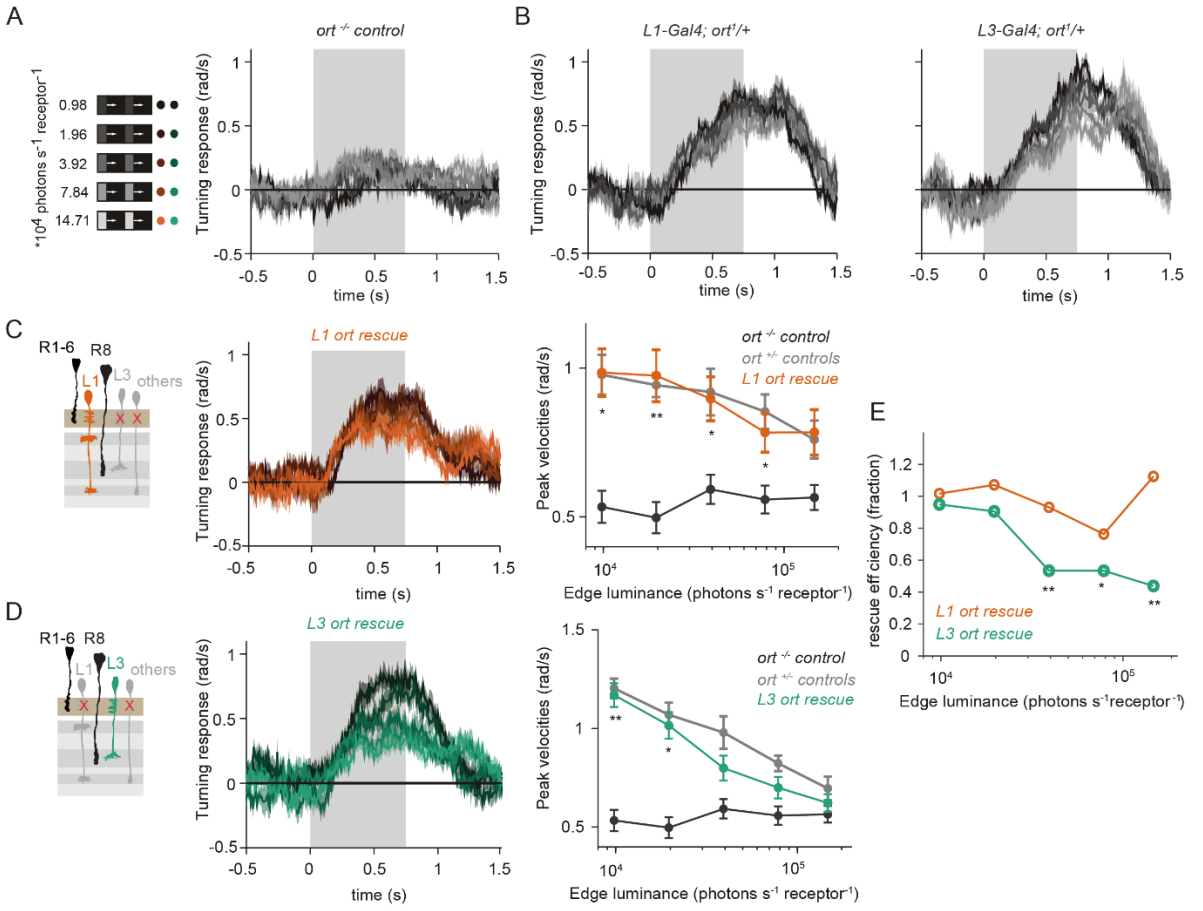

Figure 6: L1 and L3 are individually sufficient for ON behavior across luminances. (A) Schematic of the Ort mutant genotype (*ort*$^{-/-}$ control) and the moving ON edges. Stimulus parameters are as in Figure 2A. Shown below are the turning responses of the Ort mutant flies. (B) Turning responses of the heterozygous Ort controls (*ort*$^{+/-}$ controls). (C) Schematics of the genotypes followed by the turning responses of *L1 ort rescue* and *L3 ort rescue* flies. (D) Peak turning velocities of L1 ort rescue and L3 ort rescue flies and the respective controls; *p<0.05, **p < 0.01, two-tailed Student's t tests against both controls. (E) Efficiency of the L1 and L3 behavioral rescue, calculated for each edge luminance as (*rescue* - *ort*$^{-/-}$ *control*) / (*ort*$^{+/-}$ *control* - *ort*$^{-/-}$ control). *p<0.05, **p < 0.01, permutation test with 1000 permutations over the *L1 ort rescue* and *L3 ort rescue* flies. Data show mean ± SEM. Sample sizes are n = 11 flies (*ort*$^{-/-}$ control) and n =10 for every other genotype. The gray box region in A-C indicates motion duration.

An L1 luminance signal is required for OFF behavior

Given that three lamina neuron inputs encode visual stimuli differently, we next asked if L1 and its specific luminance sensitivity could also contribute to OFF pathway function. To test this, we silenced L1 neurons while showing moving OFF edges, all of -100% contrast, and moving across five different background luminances. Controls flies turned similar at all conditions, showing contrast-constant responses (Figure 7A). Previous work had shown that L3 is required to achieve contrast constancy by scaling behavioral responses when background luminance turned dark. Similarly, when L1 was silenced, behavioral responses were no longer invariant across luminance, but flies turned less to -100% contrast

at low luminance as compared to high luminance (Figure 7A,B). Our data demonstrate that L1 is required for contrast-constant behavior.

The slopes of L1-silenced fly responses were significantly steeper than controls, corroborating this finding (Figure 7B). However, underestimation of the dim OFF stimuli by L1-silenced flies was not as strong as was found with L3-silenced flies (Ketkar-Sporar et al, 2020), again highlighting the specialized role of L3 in dim light. Nevertheless, our data uncover L1 as an important input to the OFF pathway and argue that L1 also relays a luminance signal to the OFF pathway (Figure 7C).

L1 is sufficient for OFF behavior at low luminances

Although connectomics data do not suggest a direct input of L1 to OFF-selective neurons, our silencing experiments revealed L1 as an OFF-pathway input. To further test the idea that L1 can convey luminance information to both the ON and OFF pathway, we next asked if L1 could also be sufficient for OFF-behavior and measured behavioral responses to OFF edges in L1 ort rescue flies. Control flies showed contrast-constant behavioral responses to -100% OFF edges at five different luminances (Figure 7D). As described before (Ketkar et al., 2020), *ort* null mutants were not completely blind to this OFF-edge motion stimulus and responded especially at high luminance, but very little at low luminances. L1 ort rescue flies responded similar to positive controls, thus rescuing OFF edges at low luminances (Figure 7E). Therefore, L1 is even sufficient to guide OFF behavior under the same conditions as previously described for L3 (Ketkar et al., 2020). Taken together, our work reveals that the lamina neurons L1 and L3 provide behaviorally relevant, but differentially encoded luminance information to both ON and OFF pathways.

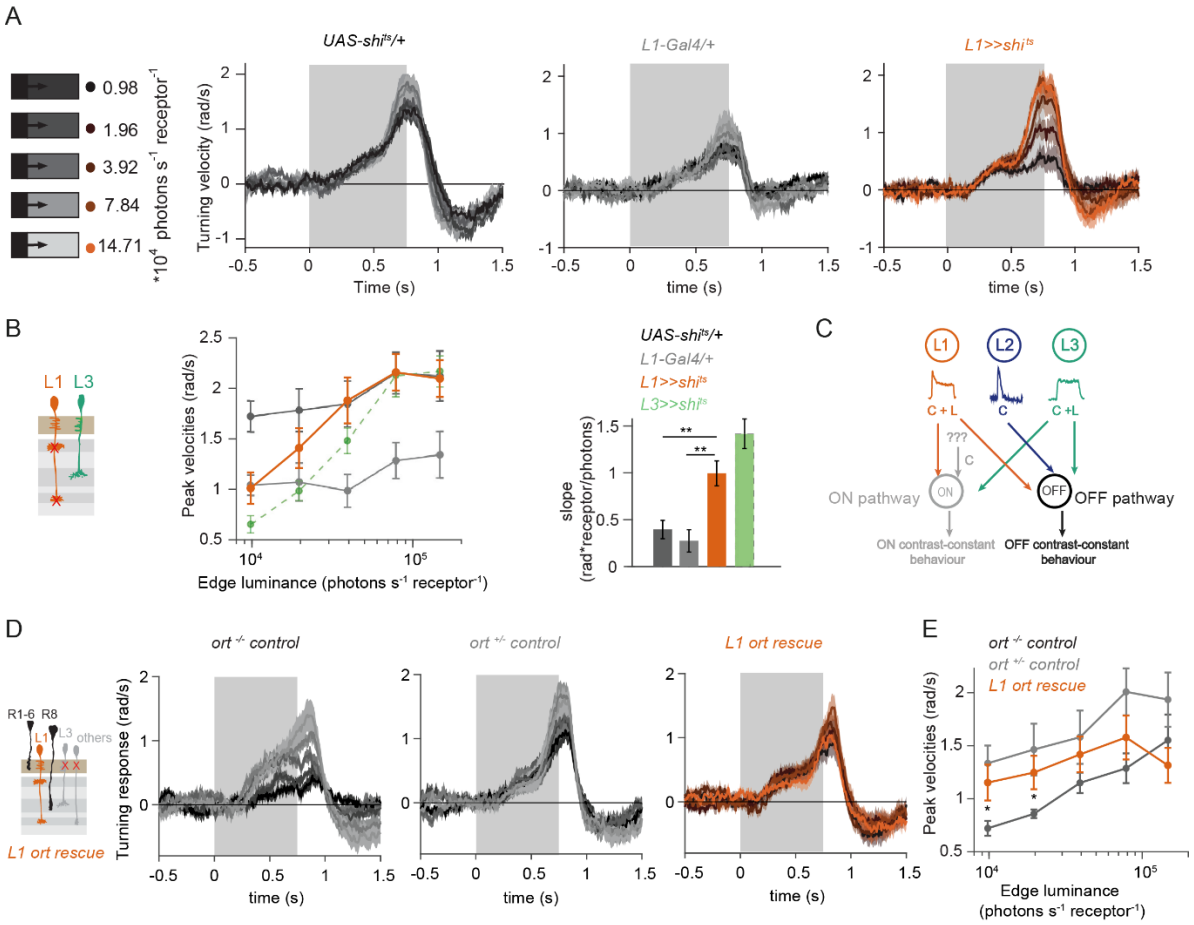

Figure 7: The L1 luminance signal is required and sufficient for OFF behavior. (A) Turning velocity time traces of L1-silenced flies (orange) and the controls (gray) to five OFF edges moving onto different backgrounds. (B) Peak velocities quantified for each of the five edges during the motion period, also including the peak velocities of L3-silenced flies (green dashed, re-quantified from the data in Ketkar et al. 2020. Shown next to it is relationship of the peak velocities with luminance, quantified as slopes of the linear fits to the data. **p < 0.01, two-tailed Student's t tests against both controls (not significant against the *L3>>shi^{ts}* slopes). Sample sizes are n = 7 *(L1-Gal4/+)* and n = 10 for other genotypes. (C) Summary schematic. Whereas the ON pathway has two confirmed inputs L1 and L3, the OFF pathway receives input from all three lamina neuron types L1-L3. The ON pathway has some unidentified contrast input. C= contrast, L= luminance. (D) Schematics of the *L1 ort rescue* genotypes followed by its turning responses to the moving OFF edges. (D) Peak turning velocities of *L1 ort rescue* flies and the respective controls; *p<0.05, two-tailed Student's t tests against both controls. Sample sizes are n = 11 flies (*ort$^{-/-}$* control) and n =10 for other genotypes. The gray box region in (A) and (D) indicates motion duration. Traces and plots show mean ± SEM.

Discussion

The present study establishes that contrast and luminance are basic visual features that interact with both ON and OFF pathways to guide visual behaviors. Lamina neurons act as the circuit elements segregating both contrast and luminance information. Behavioral experiments show that luminance information is required for contrast constancy in both ON and OFF behaviors, and the first order interneurons L1 and L3 convey this information. L1 and L3 encode luminance in two distinct ways. Whereas L3 activity non-linearly increases with decreasing luminance, L1 shows a linear relationship with luminance. Finally, L1 and L3 can both be sufficient for ON and OFF behaviors, further supporting the universal roles of these neurons across pathways. Together, we propose that specific ON and OFF pathways can only be defined downstream of lamina neurons, consistent with their emerging contrast selectivity. L1 – L3 neurons instead segregate the two most basic visual features contrast and luminance across pathways to enable behaviorally relevant computations.

L1 and L3 convey luminance information to multiple pathways

Our data expands the view of L1 being exclusively an ON-pathway neuron and of L3 being exclusively an OFF-pathway neuron to both neurons being relevant for both ON and OFF visual pathways. For L3, this functionally confirms anatomical prediction that suggested a role of L3 in the ON pathway based on synaptic contacts with ON-selective neurons (Takemura et al., 2013). L3 had mostly been considered an OFF pathway because it provides the strongest input to the OFF pathway neuron Tm9 (Fisher et al., 2015; Shinomiya et al., 2014; Takemura et al., 2013). Remarkably, L3 itself actually makes most synaptic connections with the ON-pathway neuron Mi9, and also synapses onto the ON-selective Mi1 neuron with similar strength as with Tm9 (Takemura et al., 2013).

Our findings further imply that the number of synapses may not be the best predictor of a neuron's contribution to specific computation. Although Mi1 receives more than 50% of its inputs from L1 and only 6% from L3 (Takemura et al., 2013), both of these input neurons play decisive roles in driving ON behavior. Thus, computation of relevant features does not solely depend on the input neuron with the highest number of synapses, but even a relatively low number of inputs can play physiologically relevant roles. Finally, L3 can potentially also convey information to the chromatic pathway, as Tm20 is its second strongest postsynaptic connection (Lin et al., 2016). There, L3 luminance sensitivity might play a relevant role in achieving color constancy, i.e., color recognition irrespective of illumination conditions. Altogether, anatomical and functional data urge to redefine L3 as part of a luminance-encoding system rather than a mere OFF-pathway input.

A role of L1 beyond the ON pathway was less obvious based on anatomical data. Connectomics did not identify any known OFF pathway neurons postsynaptic to L1 and presynaptic to the OFF-motion selective neuron T5 (Takemura et al., 2013). L1 thus has to connect to the OFF pathway via interneurons. Among the strongest postsynaptic partners of L1 are the GABAergic interneurons C2 and C3 that connect to the OFF pathway (Takemura et al., 2013). Intercolumnar neurons downstream of L1, such as Dm neurons (Nern et al., 2015a) could further carry information to OFF-selective neurons, likely through disinhibition from ON-selective inputs. In the vertebrate retina, intercolumnar amacrine

cells mediate interaction between ON- and OFF bipolar cells, which has been shown to extend the operating range of the OFF pathway (Manookin et al., 2008). Altogether, strategies appear to be shared across animals in what type of interneurons help to convey relevant features from one pathway to the other.

Novel input architecture of the ON pathway

Luminance signals from both L1 and L3 are required in both ON and OFF pathways, but the impact of the two neurons on behavior is pathway dependent. In the OFF pathway, losing either L1 or L3 function leads to a strong deviation from luminance invariances, such that the dim light stimuli are underestimated. On the contrary, the ON motion-driven behavior only failed to be luminance invariant if both L1 and L3 neuron types were not functional. However, even silencing L1 and L3 together did not completely abolish behavioral responses to bright ON edges. The residual responses match the expectation from contrast signals driving behavior alone, as they both scale with luminance. This raises the possibility that an additional, contrast-sensitive only input contributes to the ON pathway. In the absence of direct connections to the ON pathway, this could still be L2, which could indirectly mediate the information flow via L5 (Takemura et al., 2013). Alternatively, the amacrine cell (amc)- T1 pathway could carry some contrast information directly from the photoreceptors. This pathway has been shown to enhance the role of L1 pathway in a contrast-dependent way (Rister et al., 2007). A last option could be a direct input to medulla ON-pathway neurons from R8 photoreceptors, bypassing any lamina-mediated computation (Takemura et al., 2013).

L1 was still strictly required for ON responses if different contrasts were mixed with 100% contrast edges, but not when only 100% contrast edges of different luminances were interleaved. This is further in line with a more complex ON pathway input architecture, and hints at a role of the L1 pathway in contrast adaptation. Interestingly, an important post-synaptic partner of L1 – Mi1 – shows an almost instantaneous and strong contrast adaptation (Matulis et al., 2020b). Together, this work extends the input architecture of the ON pathway beyond L1, including L3 and potentially other neurons.

Neurons postsynaptic to photoreceptors encode contrast and luminance differently

Despite being postsynaptic to the same photoreceptor input, all lamina neurons respond differently to light stimuli. L1 was considered the ON pathway sibling of the contrast-sensitive L2, both with regard to its temporal filtering properties as well as at the transcriptome level (Clark et al., 2011a; Tan et al., 2015a). However, L1 calcium signals show a transient and a sustained response component, which are contrast- and luminance-sensitive, respectively. Compared to photoreceptors, which also carry both contrast and luminance components, L1 still amplifies the contrast signals received from the photoreceptors, since its transient component is more pronounced than the one seen in the photoreceptor calcium traces (Gür et al., 2020).

In other insect species, different types of lamina neurons have also been distinguished based on their physiological properties (Rusanen et al., 2017, 2018), although their specific luminance and contrast sensitivities are yet unknown. Notably, the first-order interneurons in the vertebrate retina also are

diverse array of physiological properties (Euler et al., 2014b). Many bipolar cell types resemble L1, in that they have both luminance and contrast signals in distinct response components (e.g., Oesch & Diamond, 2011). However, the extent of transiency varies from cell type-to-cell type, and some predominantly sustained bipolar cell types are also found, closely resembling the luminance-sensitive L3 (e.g., Awatramani & Slaughter, 2000; Ichinose & Hellmer, 2016).

The two luminance-sensitive neurons L1 and L3 also differ in their luminance encoding properties. L1's initial transient contrast response might reduce the operating range of the subsequent luminance-sensitive baseline. L3 calcium responses show little adaptation and can utilize most of its operating range for luminance encoding. L3 seems to invest this wider operating range into amplifying the darkest luminance values selectively and non-linearly. Thus, a predominantly luminance-sensitive channel among LMCs may have evolved to selectively process very dark stimuli. Together with the pure contrast sensitivity of L2, the second-order interneurons in both vertebrates and flies exhibit a wide range of sensitivities with respect to contrast and luminance, and our data confirm the functional relevance of the differential sensitivities.

First-order visual interneurons segregate different, behaviorally relevant features

The different combinations of transient and sustained characteristics of L1-L3 – responsible for their different contrast and luminance sensitivity – mainly stem from different temporal filter properties of the neuron types. In vertebrate retina, the bipolar cells show a spectrum of temporal filter properties rather than a strict transient-sustained dichotomy, thus capturing a diversity of temporal information in parallel channels (e.g., Baden et al., 2013; Ichinose et al., 2014). Such diversification of feature extraction at the periphery has been shown to be computationally advantageous, especially when processing complex natural scenes (e.g., (Odermatt et al., 2012; Schreyer and Gollisch, 2021). For example, during daylight, visual scenes can differ in intensity by 4–5 log units (Pouli et al., 2010; Rieke and Rudd, 2009a), while electrical signals in cone photoreceptors reach a dynamic range of only ~10^2 (Naka and Rushton, 1966; Normann and Perlman, 1979; Schnapf et al., 1990). This discrepancy can be solved by increasing the dynamic range of luminance signaling using linear and non-linear synapses (Odermatt et al., 2012), suggesting that different type of signals might be better suited for different environmental conditions varying in luminance statistics. In line with this, our data suggests that the non-linear luminance signal in L3 is particularly suited to detect stimuli in low luminance range. Thus, diversifying feature encoding through distinct temporal properties of the first-order interneurons is a strategy to reliably handle wide luminance ranges, across species.

ON and OFF pathways arise downstream of lamina neurons

Behavior is nearly contrast constant and requires luminance information in both ON and OFF pathways. Our data supports a model in which diversifying distinct information across several neurons serves as a strategy to reliably respond to contrast when luminance conditions vary. Whereas L2 appears to be truly contrast-sensitive, L3 shows a nonlinear relationship with luminance, and is both active and required in contextual dim light (Ketkar et al., 2020). L1 carries both luminance and contrast information, and its luminance signal is more linear compared to the one from L3. These distinct L1-L3

neuronal properties are then differentially utilized across pathways. How does this fit with the established notion, that they provide inputs to the ON (L1) and OFF (L2, L3) pathways? Lamina neuron types L1 to L3 all hyperpolarize to light onset and depolarize to light offset and are not contrast selective themselves. Contrast selectivity emerges downstream of these neurons: known post-synaptic partners of L1 acquire ON contrast selectivity due to inhibitory glutamatergic synapses, whereas cholinergic L2 and L3 synapses retain OFF contrast selectivity (Molina-Obando et al., 2019). Based on connectivity and on initial functional analyses, L1 had thus been classified as the ON pathway input, whereas L2 and L3 were thought to constitute OFF pathway inputs (Clark et al., 2011; Joesch et al., 2010; Silies et al., 2013; Takemura et al., 2013). Instead, it now appears that both ON and OFF circuitry truly exists in medulla neurons and downstream direction-selective cells, and that this circuitry benefits from distributed interactions with different inputs. The luminance and contrast features encoded differently in the lamina neurons are shared by both pathways. Importantly, the distinct features that are passed on by the specific inputs downstream of photoreceptors guide distinct behavioral roles.

In sum, our study provides a detailed account of how the parallel processing of the most basic features luminance and contrast is organized in a circuitry that handles the ON and OFF-contrast selectivity separately. The work further highlights the functional relevance of feature diversification in the visual periphery – a strategy found across species.

Methods

Experimental model

All flies were raised at 25 ºC and 65 % humidity on standard molasses-based fly food while being subjected to a 12:12h light-dark cycle. Two-photon experiments were conducted at room temperature (20 ºC) and behavioral experiments at 34 ºC. Female flies 2-4 days after eclosion were used for all experimental purposes. Lamina neuron driver lines used for genetic silencing and Ort rescue experiments were *L3^{0595}-Gal4* described in (Silies et al., 2013a), and *L1^{C202a}-Gal4* described in (Rister et al., 2007), and *UAS-shi[ts], ort^{1},ninaE^{1}* and *Df(3R)BSC809* were from BDSC (reference numbers 44222, 1946 and 27380 respectively). Since the *ort^{1}* mutant chromosomes also carries a mutation in *ninaE^{1}* (*Drosophila rhodopsin1*), we used *ort^{1}* mutation in trans to a deficiency that uncovers the *ort* but not the *ninaE* locus. *UAS-ort* was first described in (Hong et al 2006). For imaging experiments, GCaMP6f (42747) was expressed using *L1^{c202a}-Gal4*, *L2^{21Dhh}-Gal4* (Rister et al., 2007), and *L3^{MH56}-Gal4* (Timofeev et al., 2012). Detailed genotypes are given in Table 1.

Table 1: Genotypes used in this study.

Name	Genotype	Figure
Imaging		
L1>>GCaMP6f	*w+; L1^{c202a}-Gal4 / +; UAS-GCaMP6f / +*	Fig 2, 4
L2>>GCaMP6f	*w+; UAS-GCaMP6f / +; L2^{21Dhh}-Gal4 / +*	Fig 4
L3>>GCaMP6f	*w+; L3^{MH56}-Gal4 / +; UAS-GCaMP6f / +*	Fig 4
Behavior		
UAS-shibire^{ts} control	*w+; + / +; UAS-shi^{ts} / +*	Fig 2, 3, 5, 6, S1, S2
L3-Gal4 control	*w+; +/ +; L3^{0595}-Gal4 /+*	Fig 3, S1
L3 silencing	*w+; +/ +; L3^{0595}-Gal4 /UAS- shi^{ts}*	Fig 3, 7, S1
L1-Gal4 control	*w+; L1^{c202a}-Gal4 / +; + /+*	Fig 5, 7, S2
L1 silencing	*w+; L1^{c202a}-Gal4 / +; + /UAS- shi^{ts}*	Fig 5, 7, S2
L1-Gal4, L3-Gal4 control	*w+; L1^{c202a}-Gal4 / +; L3^{0595}-Gal4 /+*	Fig 5
L1, L3 silencing	*w+; L1^{c202a}-Gal4 / +; L3^{0595}-Gal4 /UAS- shi^{ts}*	Fig 5
ort mutants	*w+; UAS-ort / +; ort^{1},ninaE^{1} / Df(3R)BSC809*	Fig 6, 7

L3 ort +/- control	*w+; + / +; L3^{0595}-Gal4, ort^{1}, ninaE^{1} / +*	Fig 6
L3 ort rescue	*w+; UAS-ort / +; L3^{0595}-Gal4, ort^{1},ninaE^{1} / Df(3R)BSC809*	Fig 6
L1 ort +/- control	*w+; L1^{c202a}-Gal4 / +, ort^{1}, ninaE^{1} / +*	Fig 6, 7
L1 ort rescue	*w+; UAS-ort / +; L1[c202a]; ort^{1},ninaE^{1} / Df(3R)BSC809*	Fig 6, 7

Behavioral experiments

Behavioral experiments were performed as described in [Ketkar et al. 2020]. In brief, all experiments were conducted at 34 ºC, a restrictive temperature for *shibire^{ts}* (Kitamoto, 2001). Female flies were cold anesthetized and glued to the tip of a needle at their thorax using UV-hardened Norland optical adhesive. A 3D micromanipulator positioned the fly above an air-cushioned polyurethane ball (Kugel-Winnie, Bamberg, Germany), 6 mm in diameter, and located at the center of a cylindrical LED arena that spanned 192º in azimuth and 80º in elevation (Reiser and Dickinson, 2008). The LED panels arena (IO Rodeo, CA, USA) consisted of 570 nm LEDs and was enclosed in a dark chamber. The pixel resolution was ~2º at the fly's elevation. Rotation of the ball was sampled at 120 Hz with two wireless optical sensors (Logitech Anywhere MX 1, Lausanne, Switzerland), positioned toward the center of the ball and at 90º to each other (setup described in (Seelig et al., 2010). Custom written C#-code was used to acquire ball movement data. MATLAB (Mathworks, MA, USA) was used to coordinate stimulus presentation and data acquisition. Data for each stimulus sequence were acquired for 15-20 minutes, depending on the number of distinct epochs in the sequence (see 'visual stimulation' for details).

Visual stimulation for behavior

The stimulation panels consist of green LEDs that can show 16 different, linearly spaced intensity levels. To measure the presented luminance, candela/m^2 values were first measured from the position of the fly using a LS-100 luminance meter (Konika Minolta, NJ, USA). Then, these values were transformed to photons incidence per photoreceptor per second, following the procedure described by (Dubs et al., 1981). The highest native LED luminance was approximately 11.77 * 10^5 photons * s^{-1} * photoreceptor^{-1} (corresponding to a measured luminance of 51.34 cd/m2), and the luminance meter read 0 candela/ m^2 when all LEDs were off. For all experiments, a 0.9 neutral density filter foil (Lee filters) was always placed in front of the panels, such that the highest LED level corresponded to 14.71 *10^4 photons*s^{-1}*receptor^{-1}.

Fly behavior was measured in an open-loop paradigm where either ON or OFF edges were presented. For every set of ON or OFF edges, each epoch was presented for around 60 to 80 trials. Each trial consisted of an initial static pattern (i.e., the first frame of the upcoming pattern) shown for 500 ms followed by 750 ms of edge motion. Inter-trial intervals were 1s long. All edges from a set were randomly interleaved and presented in a mirror-symmetric fashion (moving to the right, or to the left) to account for potential biases in individual flies or introduced when positioning on the ball.

The ON edge stimuli comprised four edges, each covering 48º arena space. All ON edges moved with the angular speed of 160º/s. Thus, within a 750 ms stimulus epoch, the edge motion repeated thrice: After each repetition, the now bright arena was reset to the pre-motion lower LED level, and the next repetition followed immediately, picking up from the positions where the edges terminated in the first repetition. This way, each edge virtually moved continuously. The following sets of ON edges were presented:

1. 100% contrast edges: Here, the edges were made of 5 different luminance values (i.e. five unique epochs), moving on a complete dark background. Thus, the pre-motion LED level was zero, and the edges assumed the intensities 7%, 14%, 27%, 53% or 100% of the highest LED intensity (corresponding to the luminances: 0.98, 1.96, 3.92, 7.84 or 14.71 $*10^4$ photons$*s^{-1}*$receptor^{-1} luminance). Thus, every epoch comprised a 100% Michelson contrast. The inter-trial interval consisted of a dark screen.
2. Mixed-contrast edges – full range: The set comprised of seven distinct epochs, each with a different Michelson contrast value (11%, 25%, 33%, 43%, 67%, 82% and 100%). Here, the edge luminance was maintained constant at 67% of the highest LED intensity, across epochs, and the background luminance varied. The inter-trial interval showed a uniformly lit screen with luminance equivalent to the edge luminance.
3. Mixed-contrast edges – low contrast range: The set comprised of four distinct epochs, with contrasts from the range 9%, 18%, 27% and 36%. Here, edge luminances and background luminances both varied: The edge luminances assumed the intensities 80%, 87%, 93% and 100% of the highest LED intensity, whereas the background intensities were 67%, 60%, 53% and 47% of the highest LED intensity, respectively. The inter-trial interval consisted of a dark screen.

For the experiments concerning OFF edges, a set of five OFF edges comprising 100% Weber contrast was used as described in (Ketkar and Sporar et al 2020). Epoch consisted of a single OFF edge presented at one of the five different uniformly lit backgrounds. The edge luminance was always ~zero, whereas the five different background luminances were 7%, 14%, 27%, 54% and 100% of the highest LED intensity (corresponding to five different background luminances: 0.98, 1.96, 3.92, 7.84 or 14.71 $*10^4$ photons$*s^{-1}*$receptor^{-1}). The inter-trial interval consisted of a dark screen.

Behavioral data analysis

Fly turning behavior was defined as yaw velocities that were derived as described in (Seelig et al., 2010), leading to a positive turn when flies turned in the direction of the stimulation and to a negative turn in the opposite case. Turning elicited by the same epoch moving either to the right or to the left were aggregated to compute the mean response of the fly to that epoch. Turning responses are presented as angular velocities (rad/s) averaged across flies ± SEM. Peak velocities were calculated over the stimulus motion period (750ms), shifted by 100 ms to account for a response delay, and relative to a baseline defined as the last 200 ms of the preceding inter-stimulus intervals. For the moving edges of 100% contrast and varying luminance, relation between peak velocities and luminance was assessed by fitting a straight line (V = a*log(luminance) + b) to the peak velocities of individual flies and

quantifying the mean slope (a) ± SEM across flies. For the *ort* rescue experiments, rescue efficiency was calculated at each stimulus luminance as

$$E_{rescue} = \frac{rescue - control^{-}}{control^{+} - control^{-}}$$

where E_{rescue} is the fractional rescue efficiency, *rescue* is the mean peak velocity of the rescue genotype such as L1 rescue, $control^{-}$ is the mean peak velocity of the *ort* null mutant negative control and $control^{+}$ stands for the mean peak velocity of the positive heterozygous ort^{1} control (e.g., *L1-Gal4;* $ort^{1}/+$). Statistical significance of E_{rescue} differences was tested using permutation test. Specifically, flies of the genotypes L1 rescue and L3 rescue were shuffled 1000 times and the difference between their rescue efficiencies was obtained each time. The difference values so obtained gave a probability distribution that approximated a normal distribution. The efficiency difference was considered significant when it corresponded to less than 5% probability on both tails of the distribution.

Mean turning of flies as well as the slopes from control and experimental genotypes were first tested for normal distribution using a Kolmogorov-Smirnov test. Two-tailed Student's t tests subsequently examined statistical differences between genotypes. Data points were considered significantly different only when the experimental group significantly differed from both genetic controls. Flies with a baseline forward walking speed less than 2 mm/s were discarded from the analysis. This resulted in rejection of approximately 25% of all flies.

Two-photon imaging

Female flies were anesthetized on ice before placing them onto a sheet of stainless-steel foil bearing a hole that fit the thorax and head of the flies. Flies they were head fixated using UV-sensitive glue (Bondic). The head of the fly was tilted downward, looking toward the stimulation screen and their back of the head was exposed to the microscope objective. To optically access the optic lobe, a small window was cut in the cuticle on the back of the head using sharp forceps. During imaging, the brain was perfused with a carboxygenated saline-sugar imaging solution composed of 103 mM NaCl, 3 mM KCl, 5 mM TES, 1 mM NaH2PO4, 4 mM MgCl2, 1.5 mM CaCl2,10 mM trehalose, 10 mM glucose, 7 mM sucrose, and 26 mM NaHCO3. Dissections were done in the same solution, but lacking calcium and sugars. The pH of the saline equilibrated near 7.3 when bubbled with 95% O2 / 5% CO2. The two-photon experiments for Figure 3 were performed using a Bruker Investigator microscope (Bruker, Madison,WI, USA), equipped with a 25x/NA1.1 objective (Nikon, Minato, Japan). An excitation laser (Spectraphysics Insight DS+) tuned to 920 nm was used to excite GCaMP6f, applying 5-15 mW of power at the sample. For experiments in Figure 1, a Bruker Ultima microscope, equipped with a 20x/NA1.0 objective (Leica, Jerusalem, Israel) was used. Here the excitation laser (YLMO-930 Menlo Systems, Martinsried, Germany) had a fixed 930 nm wavelength, and a power of 5-15 mW was applied at the sample.

In both setups, emitted light was sent through a SP680 short pass filter, a 560 lpxr dichroic filter and a 525/70 emission filter. Data was acquired using PrairieView software at a frame rate of ~10 to 15Hz and around 6–8x optical zoom.

Visual stimulation for imaging

For the staircase stimuli and light flashes of different luminances, the visual stimuli were generated by custom-written software using C++ and OpenGL and projected onto an 8cm x 8cm rear projection screen placed anterior to the fly and covering 60º of the fly's visual system in azimuth and 60º in elevation. These experiments were performed with the Bruker Investigator microscope.

For ON-moving edges, the stimulus was generated by custom-written software using the Python package PsychoPy (Peirce, 2008), and then projected onto a 9cm x 9cm rear projection screen placed anterior to the fly at a 45 angle and covering 80 degrees of the fly's visual system in azimuth and 80 degrees in elevation. These experiments were performed with the Bruker Ultima microscope.

Both stimuli were projected using a LightCrafter (Texas Instruments, Dallas, TX, USA), updating stimuli at a frame rate of 100 Hz. Before reaching the fly eye, stimuli were filtered by a 482/18 band pass filter and a ND1.0 neutral density filter (Thorlabs). The luminance values are measured using the same procedure described above for the behavioral experiments. The maximum luminance value measured at the fly position was $2.17*10^5$ photons s^{-1} $photoreceptor^{-1}$ for the staircase and random luminance stimulation, and $2.4*10^5$ photons s^{-1} $photoreceptor^{-1}$ for the ON-moving edge stimulation. The imaging and the visual stimulus presentation were synchronized as described previously (Freifeld et al., 2013b).

Staircase stimulation

The stimulus consisted of 10s full-field flashes of 5 different luminances (0, 0.25, 0.5, 0.75 and 1^* of the maximal luminance I_{max}). The different luminance epochs were presented first in an increasing order (from darkness to full brightness) then in a decreasing order (full brightness to darkness). This sequence was repeated ~3-5 times.

Flashes of different luminances

The stimulus consisted of 10s full-field flashes of 5 different luminances (0, 0.25, 0.5, 0.75 and 1^* of the maximal luminance I_{max}). The order between the flashes was randomized and presented for ~300s.

ON moving edges at different luminances

Here, the edges were made of 6 different luminance values (corresponding to 0.16, 0.31, 0.62, 1.2, 1.8, 2.4 $*10^5$ photons$*s^{-1}*$receptor^{-1} luminance), moving on a complete dark background. The inter-stimulus interval was 4 seconds of complete darkness.

Two photon data analysis

Staircase stimulation and randomized flashes of different luminances

Data processing was performed offline using MATLAB R2019a (The MathWorks Inc., Natick, MA). To correct for motion artifacts, individual images were aligned to a reference image composed of a

maximum intensity projection of the first 30 frames. The average intensity for manually selected regions of interests (ROIs) was computed for each imaging frame and background subtracted to generate a time trace of the response. All responses and visual stimuli were interpolated at 10 Hz and trial averaged. Neural responses are shown as relative fluorescence intensity changes over time (ΔF/F0). To calculate ΔF/F0, the mean of the whole trace was used as F0. In some recordings, a minority of ROIs responded in opposite polarity (positively correlated with stimulus), as described previously (Fisher et al., 2015c). These ROIs have their receptive fields outside the stimulation screen (Fisher et al., 2015c; Freifeld et al., 2013b). To discard these and other noisy ROIs, we only used ROIs that were negatively correlated (Spearman's rank correlation coefficient) with the stimulus. Baseline responses were calculated as the mean of the last 2 seconds within each luminance presentation. In the randomized flashes of different luminances, full brightness epoch baseline values were subtracted for each baseline response to get a comparable relationship between each neuron for visualization (this leads to 0 baseline response for each neuron in full brightness condition). Mutual information between luminance and response is calculated according to (Ross, 2014). To characterize the distinct luminance-response relationships of L1 and L3, the difference of Pearson correlation and Spearman's rank correlation was used as a Non-linearity index. This value will increase if there is a non-linear relationship between luminance and response.

ON moving edges at different luminances

Data processing was performed offline using Python 2.7(Van Rossum 1995). Motion correction was performed using the SIMA Python package's Hidden Markov Model based motion correction algorithm (Kaifosh 2014). The average intensity for manually selected regions of interests (ROIs) was computed for each imaging frame and background subtracted to generate a time trace of the response. To calculate ΔF/F0, the mean of the whole trace was used as F0. The traces were then trial averaged. Responses of ROIs for each epoch was calculated as the absolute difference between the mean of the full darkness background epoch and the minimum of the ON edge presentation (minimum values are chosen because L1 neurons respond to ON stimuli with hyperpolarization).

Throughout the analysis procedure, mean of quantified variables were calculated first for all ROIs within a fly, and then between flies. All statistical analysis was performed between flies. For normally distributed data sets, a two-tailed Student *t* test for unpaired (independent) samples was used. For other data sets, Wilcoxon rank-sum was used for statistical analysis. Normality was tested using Lilliefors test. For multiple comparisons, one way ANOVA was used followed by multiple comparisons using the Bonferroni method for determining statistical significance between pairs of groups.

Supplemental figures

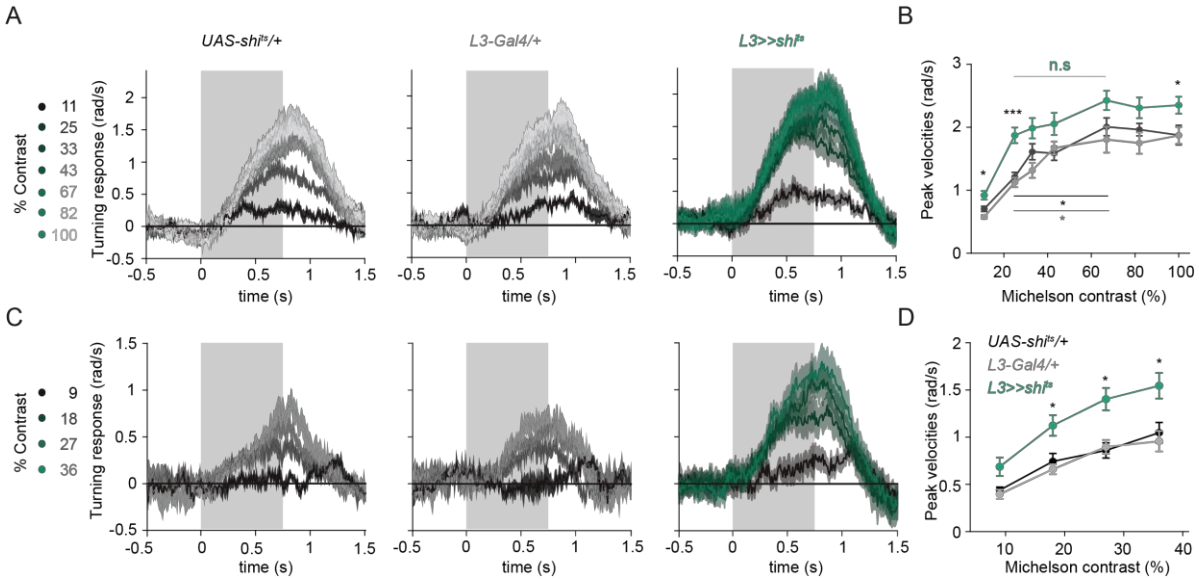

Figure S1: L3 contributes to ON behavior across a range of contrasts. (A) Turning velocity time traces of the controls (gray) and L3-silenced flies (green) in response to the moving ON edges of different contrasts, ranging from 11% to 100%. (B) Peak turning velocities quantified during the motion period, *p < 0.05, ***p < 0.01, ***p < 0.001, two-tailed Student's t tests against both controls. The horizontal lines mark the difference between 25% and 67% contrast responses within each of the three genotypes, tested for significance using multiple (pairwise) comparison test. Sample sizes are n = 9 (*UAS-shi^{ts}/+, L3>>shi^{ts}*) and n = 6 (*L3^{0595}-Gal4/+*). (C) Turning velocity time traces of the controls and L3-silenced flies in response to the moving ON edges of different contrasts, ranging from 9% to 36%. (D) Peak turning velocities quantified during the motion period, *p < 0.05, two-tailed Student's t tests against both controls. Sample sizes are n = 8 (*UAS-shi^{ts}/+),* n = 9 *(L3>>shi^{ts}*) and n = 5 (*L3^{0595}-Gal4/+*). Traces and plots show mean ± SEM. The gray box region in (A) and (C) indicates motion duration.

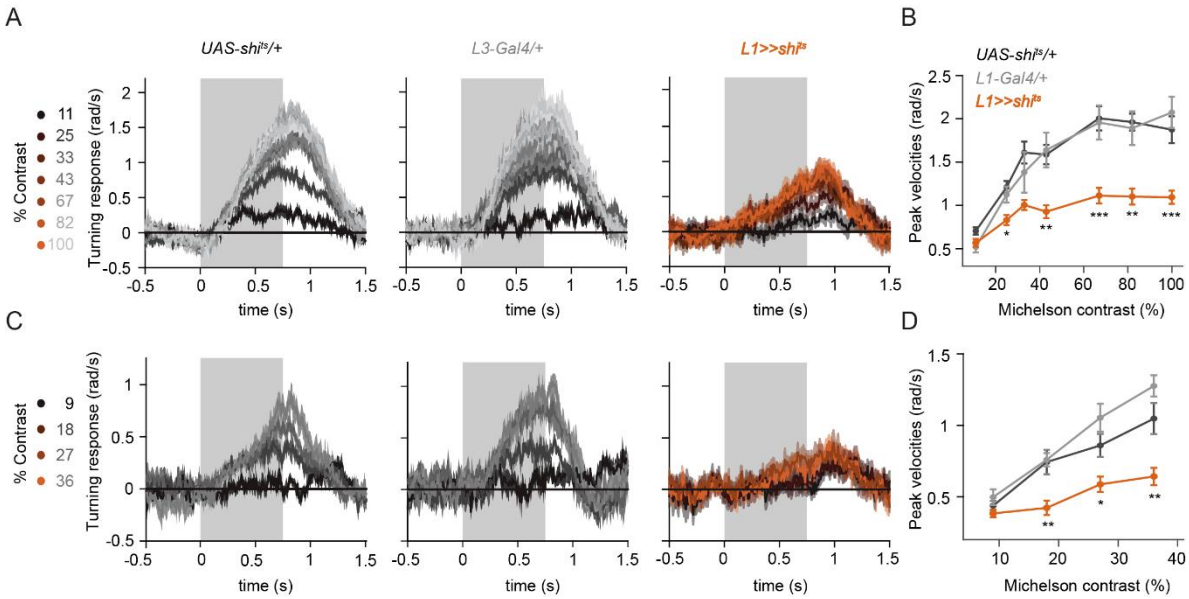

Figure S2 : L1 is required for ON behavior across a range of contrasts. (A) Turning velocity time traces of the controls (gray) and L1-silenced flies (orange) in response to the moving ON edges of different contrasts, ranging from 11% to 100%. (B) Peak turning velocities quantified during the motion period, *p < 0.05, ***p < 0.01, ***p < 0.001, two-tailed Student's t tests against both controls. Sample sizes are n = 9 (*UAS-shi^{ts}/+, L1^{c202a} >>shi^{ts}*) and n = 5 (*L1^{c202a}-Gal4/+*). (C) Turning velocity time traces of the controls and L3-silenced flies in response to the moving ON edges of different contrasts, ranging from 9% to 36%. (B) Peak turning velocities quantified during the motion period, *p < 0.05, two-tailed Student's t tests against both controls. Sample sizes are n = 8 (*UAS-shi^{ts}/+),* n = 8 *(L1^{c202a} >>shi^{ts}*) and n = 5 (*L1^{c202a} -Gal4/+*). Traces and plots show mean ± SEM. The gray box region in (A) and (C) indicates motion duration.

Manuscript 3: A two-way luminance gain control in visual circuitry enhances contrast constancy and dim light vision

The following manuscript is under preparation.

Authors and affiliations

Madhura D Ketkar *[1,2], Shuai Shao *[3,4], Julijana Gjorgjieva [#3,5] and Marion Silies [#1]

[1] Institute of Developmental Biology and Neurobiology, Johannes-Gutenberg University Mainz, 55128 Mainz, Germany.

[2] Göttingen Graduate School for Neurosciences, Biophysics, and Molecular Biosciences (GGNB) and International Max Planck Research School (IMPRS) for Neurosciences at the University of Göttingen, 37077 Göttingen, Germany.

[3] Max Planck Institute for Brain Research, Max-von-Laue-Straße 4, 60438 Frankfurt am Main, Germany

[4] Department of Neurophysiology, Radboud University, Nijmegen, Netherlands

[5] School of Life Sciences Weihenstephan, Technical University Munich, Munich, Germany

*, # These authors contributed equally to this work

Contribution statement

All four authors were involved in conceptualizing and planning the study. Shuai Shao devised the first version of the model, and revised it based on the inputs from other authors. I performed and analyzed the behavioral experiments, and wrote the first draft of the manuscript. The manuscript was revised with inputs from Marion Silies, Shuai Shao and Julijana Gjorgjieva.

A two-way luminance gain control in visual circuitry enhances contrast constancy and dim light vision

Madhura Ketkar *[1,2], Shuai Shao *[3,4], Julijana Gjorgjieva [#3,5] and Marion Silies [#1]

[1] Institute of Developmental Biology and Neurobiology, Johannes-Gutenberg University Mainz, 55128 Mainz, Germany

[2] Göttingen Graduate School for Neurosciences, Biophysics, and Molecular Biosciences (GGNB) and International Max Planck Research School (IMPRS) for Neurosciences at the University of Göttingen, 37077 Göttingen, Germany

[3] Max Planck Institute for Brain Research, Max-von-Laue-Straße 4, 60438 Frankfurt am Main, Germany

[4] Department of Neurophysiology, Radboud University, Nijmegen, Netherlands

[5] School of Life Sciences Weihenstephan, Technical University Munich, Munich, Germany

*, # these authors contributed equally to this work

Abstract

For perception unaffected by viewing conditions, visual systems must adapt their sensitivity to changing visual statistics, such as mean luminance. Sensitivity adjustment, or gain control, begins as early as in photoreceptors, but also occurs at many further stages of visual processing. Whereas photoreceptor gain control is insufficient to explain perceptual contrast constancy especially at fast timescales, how the downstream gain controls contribute towards constancy is not known. Here, we combine behavioral measurements and computational modelling approaches to reveal a circuit mechanism that revises gain adjustment past photoreceptors in the fly eye. When blocking the outputs of the first-order, luminance-sensitive interneurons L3, the major input to this corrective mechanism, the flies underestimate contrast in contextual dim light and overestimate contrast in contextual bright light. Thus, L3 is key input to a two-way gain control. Moreover, L3 enhances sensitivity to extremely dim stimuli, highlighting an additional role of the luminance-sensitive pathway reminiscent to the vertebrate rod-bipolar cell pathway. An algorithmic model suggests how the single luminance-sensitive signal shapes diverse gain control operations: on the one hand, it interacts nonlinearly with contrast information and on the other hand, it acts as a dark-sensitive contrast channel to improve detection of very dim stimuli. Together, our work demonstrates how luminance signals segregated in the periphery provide substrate for elaborate gain control operations at an advanced stage, aimed at robust perception.

Introduction

Animals have to recognize sensory cues in vastly changing environments. For vision, this means to recognize objects under different viewing conditions, especially changing illumination. For example, a soccer ball reflects different amounts of light from the black and white patches, comprising a contrast cue. The difference in reflected light is high in bright sunlight but reduces as the day approaches sunset or when the ball suddenly flies into a shadow of a tree (Figure 1A). Yet, we perceive the ball to be the same at different time scales of the change, indicating that our visual systems maintain constant perception of the black-and-white contrast despite different amounts of light reaching our eyes. Such contrast constancy is found not only in human reports of perception or behavioral responses of fruit flies, but in the neuronal responses in several species (Burkhardt et al., 1984; Ketkar et al., 2020; Laughlin, 1989; Normann and Werblin, 1974). To achieve constancy, visual systems adjust their sensitivity through gain control, thus determining the response size relative to the mean luminance rather than responding to mere light fluctuations. Gain control is a characteristic of many visual neurons, from photoreceptors to cortical cells (Carandini et al., 1999; Mante et al., 2005; Normann and Werblin, 1974; Werblin, 1974; Werblin and Dowling, 1969; Wienbar and Schwartz, 2018). The role of gain control at processing steps postsynaptic to photoreceptors for perceptual constancy and behavior remains unclear.

Gain control is a two-way process. For example, when a soccer ball flies into a shadow, the difference in light reflected by the black and white patches goes down, and vision thus requires a higher gain to perceive a similar contrast as compared to the non-shaded area. Conversely, a reduction in gain has to adjust contrast signals when the ball is back in the sunlight (Figure 1A). Gain control happens at different processing steps. Well studied is gain control implemented by photoreceptors, which is crucial to enable their limited operating ranges to deal with the vast range of environmental light intensities (Naka and Rushton, 1966; Pouli et al., 2010; Rieke and Rudd, 2009b). Specific photoreceptor types that lack gain control saturate with increasing intensity and thus lack sensitivity to changes at higher intensities (Normann and Werblin, 1974). Since light intensities vary not only with slow day-night changes but also with fast movements, such as saccadic eye movements or self-motion during a soccer game, rapid gain control mechanisms also have to be in place (Rieke and Rudd, 2009b). Fast gain control mechanisms acting on the order of 200-300 ms indeed modulate the sensitivity enough so as to not miss out changes in the new environment (Baylor and Hodgkin, 1974; Clark et al., 2013; Lee et al., 2003). However, the sensitivity continues to alter for another tens of seconds or even minutes, depending on the receptor system and the experimental settings (Laughlin and Hardie, 1978; Normann and Werblin, 1974). In line with this, neuronal responses are also more likely to obey Weber's law, indicative of constancy, when longer stimuli or stimuli of lower temporal frequency are shown (Barlow, 1957; Kelly, 1972). The downstream gain control processes could help achieve perceptual constancy at faster timescales, but this possibility is not causally explored.

Gain control is a universal process of vertebrate and invertebrate visual systems. In the fly visual systems (Juusola and Hardie, 2001; Laughlin and Hardie, 1978), photoreceptors R1-R6 implement a luminance gain and respond with a contrast-sensitive transient component followed by a luminance-sensitive component. The first-order interneurons, known as Lamina Monopolar Cells (LMCs) L1, L2

and L3, capture the photoreceptor signals in a sign-inverted manner. L2 and L3 constitute the major inputs to the OFF pathway, where L2 relays an amplified contrast signal crucial for OFF-motion guided behavior (Clark et al., 2011b; Ketkar et al., 2020; Silies et al., 2013b). However, LMCs cannot achieve luminance invariance in dynamic conditions (Ketkar et al., 2020; Laughlin and Hardie, 1978). Recently, a circuit mechanism was found necessary for behavioral constancy at fast timescales. This mechanism relied on a luminance-sensitive signal preserved past photoreceptors, in L3, in parallel to the contrast-sensitive L2 (Ketkar et al., 2020). This luminance gain control downstream of the first-order interneurons enables a fast adjustment of the system' sensitivity, required for contrast-constant behavioral responses. A system lacking this mechanism was less sensitive to changes comprising contextually dim values, indicating that the prevailing gain was lower than required. It remains to be tested if a gain control is also in place when contrast sensitivity postsynaptic to photoreceptors alone leads to too high responses in bright environment that deviate from constancy.

Whereas photoreceptors adjust their gain with the help of intrinsic properties and feedback inputs (Gu et al., 2005; Juusola and Hardie, 2001; Nikolaev et al., 2009), the post-receptor gain correction in flies is a circuit mechanism shaped by feed-forward inputs from the first-order interneurons. Post-receptor gain controls in vertebrates also involve non-intrinsic/ circuit components. For example, gain control in bipolar cells includes a potential input from horizontal cells (Thibos and Werblin, 1978). Gain control in retinal ganglion cells (RGCs) also involves upstream neurons that form the summation pool for RGCs (Shapley et al., 1972). Due to the greater extent of spatial summation leading to less noise, advanced visual processing stage such as RGCs is a more reliable site for rapid gain control than the periphery (Dunn et al., 2007; Rieke and Rudd, 2009b). Thus, the post-receptor gain controls are potentially involved in rapid sensitivity adjustment necessary for contrast constancy in dynamic environments.

Post-receptor gain adjustments might be necessary even in slowly changing light conditions. For example, LMCs increase their contrast sensitivity over several orders of adapting luminance, before the contrast sensitivity settles at a maximal value at high luminance (Laughlin et al., 1987). If behavior is limited by the varying sensitivity in this luminance range is not particularly tested. However, flies did not maintain contrast constancy in the low luminance regimes, indicating limitations of very dim light (Ketkar et al., 2020). Notably, L3 provides such a higher gain, as it non-linearly amplifies the dim stimuli. If and how L3 is able to provide a reduced gain, in bright conditions where it is least active, is an open question.

Here, behavioral studies combined with modelling approaches identified the circuit substrate for the two-way gain control occurring in downstream circuitry. Behavioral responses were both contrast constant on fast time scales when contrasts were presented at different adaptation states i.e. in different luminance regimes, and when the same contrast was presented at different luminances. Purely contrast-sensitive L2 responses deviated from constancy in both scenarios. In addition to the known underestimation of contrast in low luminance, predicted behavior driven by L2 alone overestimated many contrasts in high luminance, uncovering a circuit requirement for gain reduction. Interestingly, the L3 pathway was not only required for gain enhancement but also for gain reduction across many luminance regimes, and thus has a two-way role in contrast constancy. Additionally, the direction of gain control depended on absolute luminance. For very dim stimuli, L2 responses

underestimated contrasts and L3 enhanced these very dim stimuli. To explain how the luminance and contrast channels interact in the downstream circuitry to enable these seemingly diverse actions of L3, we devised an algorithmic model. The model predicts a circuitry where L2 and L3 interact non-linearly to implement the gain increment, whereas an inhibitory action of L3 implements gain decrement through a separate channel. Yet another L3-only channel acts as an additional contrast channel and confers a higher gain in extremely low luminance. In sum, our study describes a rapid gain control mechanism in fly vision that serves behavioral constancy and also improves vision in extremely dim conditions, reminiscent to the scotopic system in vertebrates.

Results

Adapted L2 responses deviate from contrast constancy

To achieve constant contrast sensitivity, the visual system's gain needs to increase or decrease when viewing conditions get dimmer or brighter. We first asked if the periphery of the fly eye meets these requirements. The first-order interneurons adapt slowly, and LMC contrast signals do not meet the gain control requirements for constancy in dynamic conditions (Ketkar et al., 2020; Laughlin and Hardie, 1978). But do they suffice for contrast-constant behavior when fully adapted? To explore how the contrast-sensitive LMC subtype L2 encodes contrast across adapting luminances, we examined *in vivo* calcium responses to different contrast steps in five luminance regimes together spanning four orders of luminance, using two-photon imaging (Figure 1B). Within each luminance regime, flies expressing GCaMP6f specifically in L2 neurons were adapted to a bright screen for 30 s, before luminance stepped down (6 OFF steps) or up (2 ON steps) to show one of 8 contrast values ranging from -25% to +50% Weber contrast. The step luminance again persisted for 30 s before the next adapting phase. Transient L2 responses negatively correlated with contrast, as shown previously (Figure 1C, Figure S1A, (Clark et al., 2011b; Laughlin et al., 1987)). The plateau signal, quantified within the last second of the step, showed little variance and almost completely returned to previous baseline within the 30s (Figure S1B). Within each luminance regime, the absolute change in L2 calcium scaled with contrast (Figure 1D). However, across regimes, the same contrasts did not elicit similar responses, but the response amplitude scaled with luminance for each of the contrasts. If the same data were plotted as a function of luminance, the operating range seemed to have expanded with adapting luminance (Figure 1E). Thus, even for long, static luminance exposures, L2 responses did not achieve constant contrast sensitivity, but retained luminance dependence.

We examined the timescales of L2 calcium adaptation by fitting an exponential curve to the mean response time traces obtained during each OFF step (Figure 1F-G, Figure S1C). A single exponential process captured the initial response decay well. A steady-state parameter obtained from the fit was small but non-zero for the bright stimuli, revealing an additional, slower adaptation process (Figure 1F, G middle). Adaptation time constants of the single exponential process varied across luminance regimes, with the brightest regime having the smallest time constants and adapting fastest, as has been shown for adaptation in the vertebrate retina (Figure 1G left, Dunn et al, 2007). Nevertheless, the fastest time constants were in the range 1.2 s - 1.7 s, meaning the responses required a minimum of 6 s - 8.5 s to reach steady state. The proportionality constant (or gain) of the exponential fit increasing with luminance again underlined the luminance-dependent contrast sensitivity (Figure 1G right). In sum, *Drosophila* L2 adapts its sensitivity over considerably long time scales, and does not attain contrast constancy even after long adapting exposures.

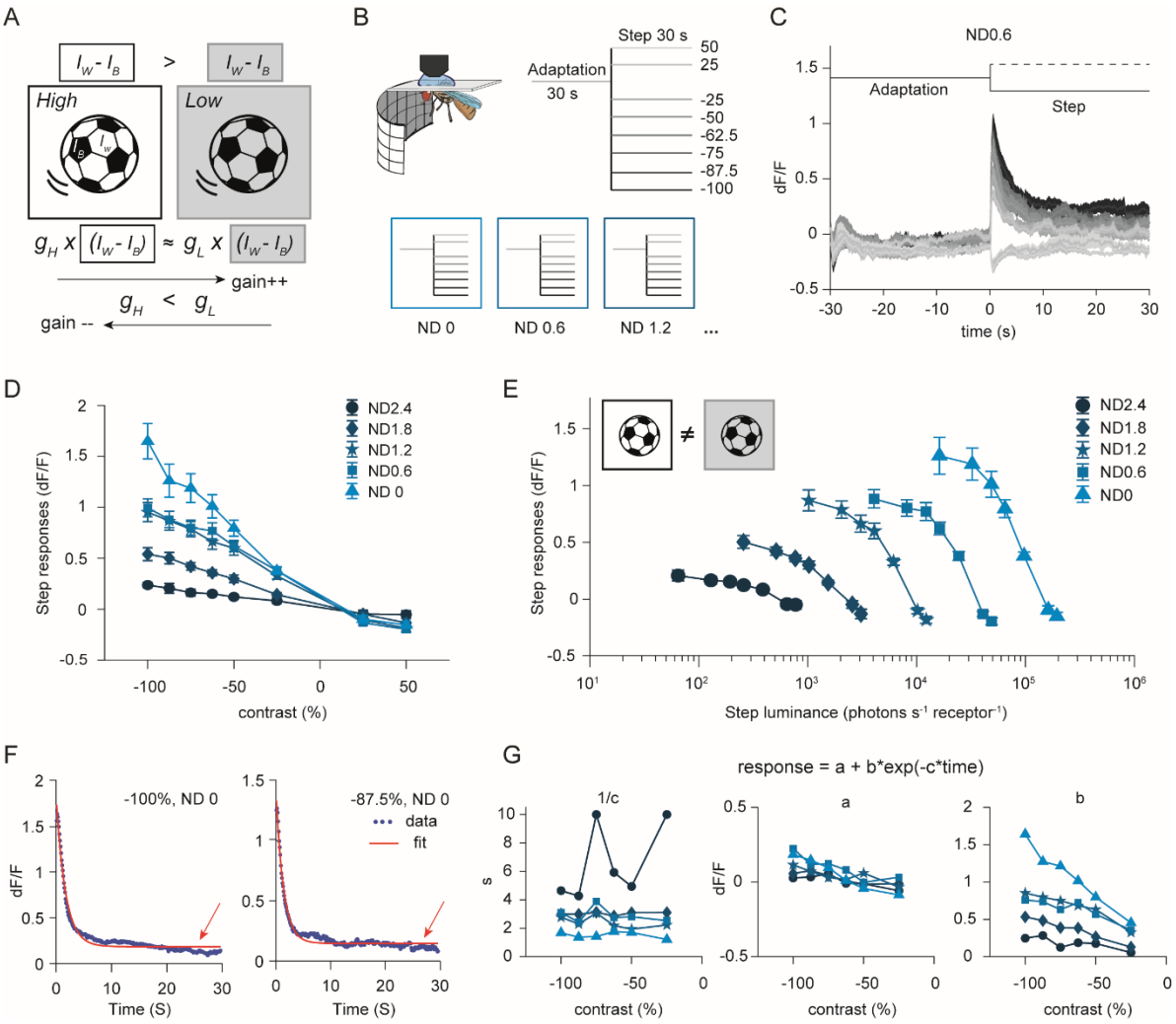

Figure 1: Adapted L2 responses deviate from constancy. (A) Difference of light reflected by the black and white patches on a soccer ball is higher in bright light and lower in dim light. To perceive the two differences similarly, gain should be increased when moving into a dim light region and vice versa. (B) Schematic of the stimulus for in vivo L2 calcium imaging. Within each luminance regime (denoted by neutral density (ND) 2.4, 1.8 etc.), flies were exposed to 30 s-long bright screen, followed by a 30 s-long step comprising one of eight different contrasts (% values are shown). (C) L2 calcium response time traces in one of the luminance regimes (ND 0.6). Gray shades represent contrasts. Black trace represents stimulus. (D) L2 step responses quantified as the difference between peak response and preceding plateau response, plotted against different contrasts, in five luminance regimes. (E) Same data as in D, plotted against step luminance. L2 responses do not sense contrast cues similarly across bright and dim conditions. (F) Example exponential fits to mean OFF step response traces (-100% and -87.5% contrasts) in the brightest luminance regime (ND 0). Orange arrows indicate deviations of the fit from the data in the plateau phase. (G) Parameters of the exponential decay as a result of fitting process – time constant (left), steady-state calcium level (middle) and proportionality constant (right). Sample size is n=10 (136), #flies (#ROIs). Traces and plots in B-E show mean ± SEM.

Fly behavior requires both gain increments and decrements for contrast constancy, at different absolute luminances

Given that L2 does not achieve constancy even at long timescales, we next asked if behavior too deviates from constancy at different adaptation states. We tested fly walking behavior with a similar, mixed-contrast stimulus set as the one used to characterize L2 physiology. Moving OFF edges of different contrasts (-50% to -87%) were randomly interleaved, and the same set was tested in five different luminance regimes (Figure 2A). Individual background and edge luminances did not persist long enough to allow complete gain adjustment. Flies positioned on an air-cushioned ball and surrounded by the stimulus turned in the direction of the edge motion, and turning scaled with contrast in all luminance regimes (Figure 2B,C). Across regimes, responses to each contrast were nearly the same, showing contrast constancy (Figure 2C). Only the lowest luminance regime was an exception, where responses to all contrasts were weak. When plotted against log(luminance), the response curves in the four brighter regimes appeared shifted versions of each other, indicating similar response ranges allocated to the fixed contrast range regardless of adaptation state (Figure 2D). Thus, unlike L2 responses, behavior was contrast constant across a broad luminance range, and implied additional gain control operating as a function of absolute luminance. The function of luminance may amplify or reduce L2 signals at different luminances. We next aimed at finding the direction of gain correction required.

Behavioral responses to -100% contrast required a corrective luminance gain across four orders of magnitude, provided by luminance-sensitive L3 neurons (Ketkar et al., 2020). In the absence of L3 function, behavior followed contrast-sensitive LMC responses, indicating a linear translation of the contrast-sensitive responses to purely contrast-driven behavior. We hypothesized that L3 might provide luminance-dependent gain required across all contrasts, and to predict the sign of gain correction, trained a linear model on the responses of L3-silenced flies to -100% contrast (data from (Ketkar et al., 2020)). To model behavior, contrast-sensitive LMC responses were predicted for all stimuli used in the behavioral assay based on previous LMC characterization in bigger flies, and with parameters adjusted to the *D. melanogaster* visual system ((Laughlin et al., 1987), see methods). Contrast-driven behavior was then modelled as a linear function of these LMC responses, and compared with the measured behavior (Figure 2E). Intriguingly, the pure contrast-driven behavior was bigger than measured behavior in the bright luminance regimes, indicating a requirement for gain reduction, and smaller in the dim regimes, indicating a requirement for gain enhancement. Thus, contrast-constant behavior relies on a two-way corrective gain control whose sign is based on absolute luminance.

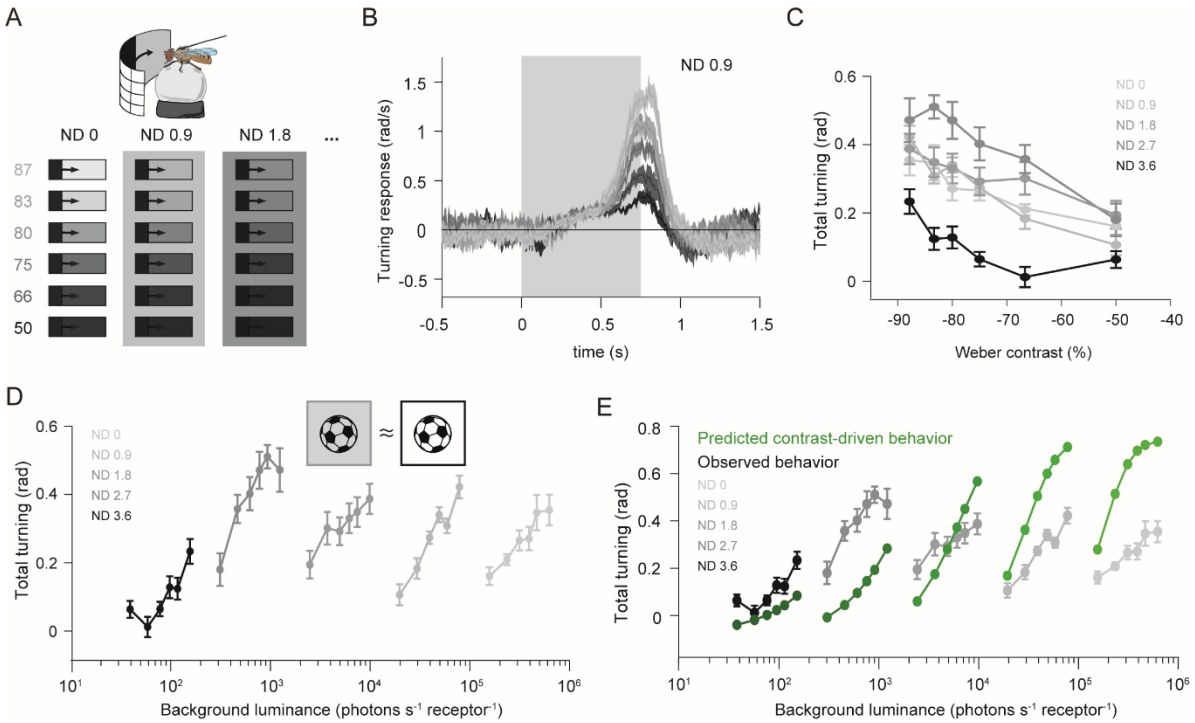

Figure 2: Fly behavior requires both gain increments and decrements for contrast constancy, at different absolute luminances. (A) Schematic of the mixed-contrast stimulus. Single moving OFF edges of varying contrast were randomly interleaved within each luminance regime (denoted by ND 0, ND 0.9 etc.) and turning responses of flies walking on a ball were measured. (B) Turning velocity time traces in response to different contrasts in one of the five luminance regimes (ND 0.9). (C) Quantification of total turning in all five regimes plotted against contrast. (D) Total turning in response to the contrast stimuli in all five regimes, plotted against edge luminance. Contrast cues are perceived similarly in bright and dim conditions. (E) The same data as in D, plotted together with predicted behavior based on LMC contrast responses alone. Discrepancy between the two can be abolished by increasing gain in dim luminance regimes and decreasing gain in bright regimes. Sample size is n=10 flies. Traces and plots in B-E show mean ± SEM.

LMC responses to multiple contrasts require corrective gain reduction in contextual bright light at fast timescales

For contrast-constant behavior in high luminance regimes, contrast-sensitive responses needed to be scaled down, for all contrasts we tested. This is unlike -100% contrast, which required a positive gain (Ketkar et al., 2020). We asked if the different requirements stemmed from distinct stimulus paradigms or distinct contrast values. For example, mixing contrast values could have involved contrast adaptation, leading to reduced behavioral responses to many contrasts. To test this possibility, we devised a stimulus where sets of moving OFF edges of one contrast (-50%, or -80%) was presented at different luminances. The background luminance lasted for only 500 ms, and thus each background did not induce complete luminance adaptation in LMCs. As a result, the stimulus also gave us an opportunity to simultaneously test if the challenge of rapid luminance changes contributed in deciding the direction of gain control.

When shown one contrast at different luminances, flies turned with comparable velocities and thus were contrast constant (Figure 3A, B). This was true for both the -50% and the -80% contrast set. Under

these conditions, theoretically predicted behavior driven by the LMC contrast information alone again did not show such constancy and instead scaled with contextual light, at both contrasts (Figure 3C, D). The predicted behavioral responses were stronger than the observed responses, and the discrepancy was more pronounced at contextual bright light. Thus, in the bright luminance regime, LMC gain was always higher than required to estimate the contrasts, and the required gain modulation was further stalled by the rapid luminance changes.

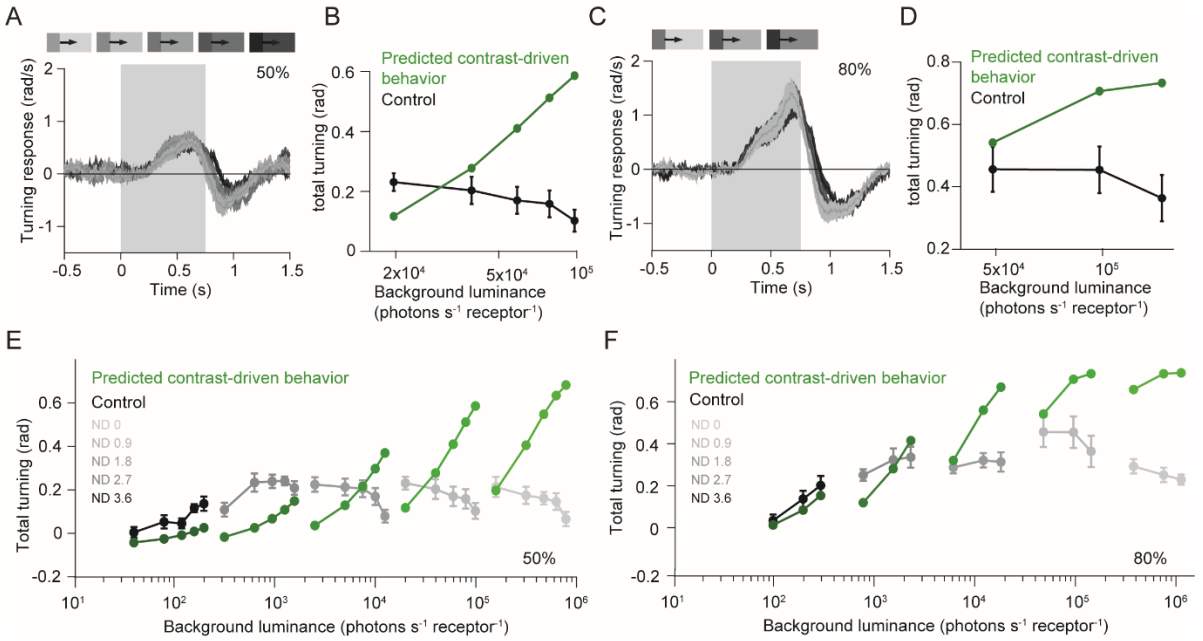

Figure 3: Contrast-constant fly behavior at multiple contrasts requires gain reduction in contextual bright light. (A-B) Turning velocity time traces in response to -50% (A) and -80% (B) contrasts, each presented at varying luminances (thus, 'uniform-contrast' stimuli). Shown here is one of the five luminance regimes (ND 0.9). (C-D) Quantification of total turning from the data in (A-B) plotted together with predicted behavior based on LMC contrast responses alone. (E-F) Total turning in response to the uniform-contrast stimuli in five luminance regimes, plotted together with predicted behavior based on LMC contrast responses alone. Discrepancy between the two can be abolished by increasing gain in dim luminance regimes and decreasing gain in bright regimes, especially contextual bright light. Sample size is n=10 flies. Traces and plots in A-F show mean ± SEM.

For any of the contrasts, gain correction was required to mainly scale down the contrast-driven behavior, and the contextual luminance only determined the extent of correction. We next tested if this observation generalizes over a broad luminance range (Figure 3E, F). Sets of both -50% and -80% contrast elicited nearly constant responses in all five luminance regimes tested. Predicted contrast-driven behavior underestimated stimuli in the low luminance regimes, overestimated the bright regimes, and a combination was seen in an intermediate regime – where the required gain correction 'reversed' its direction across the stimulus set. In the darkest regime, the predicted behavior did not vary much with contextual luminance variations. However, in the brighter regimes, contextual luminance determined the extent of correction, while adhering to the direction of correction demanded by the absolute luminance values. In summary, a two-way gain correction past LMCs was required to explain the observed behavior, at multiple contrasts and multiple timescales of luminance

change. The -100% contrast stimulus tested earlier was an exception, in that the LMC responses required only scaling up, and thus a one-way correction.

L3 signals implement the two-way gain control

We next wanted to understand how the two types of gain correction are implemented at the network level. Given that L3 is the only known neuron to provide luminance information to visual circuitry, we first asked if L3 could provide some luminance-dependent gain. We blocked L3 function by expressing the temperature-sensitive, dominant-negative dynamin allele *shibire*^{ts} (Kitamoto 2001) selectively in L3 neurons. We tested turning responses of L3-silenced flies to the mixed-contrast stimuli, as well as -50% and -80% stimuli in all five luminance regimes. Regardless of the stimulus set, L3-silenced flies turned less than controls to stimuli in the dim luminance regimes, resembling the pure contrast-driven behavior, confirming our hypothesis (Figure 4A, Figure S2 and Figure S3). To our surprise, L3-silenced flies turned more than controls in bright luminance regimes, as shown in the model prediction (Figure 4B, Figure S2 and Figure S3). Thus, L3 function appears to account for the discrepancy between pure contrast responses and behavior over the entire luminance range tested (Figure 4C-E). Furthermore, L3-silenced flies lost contrast constancy, and their turning responses instead scaled with contextual luminance, i.e. with luminances within one stimulus set (Figure 4C,D). Again, this behavior was as predicted by the pure contrast-driven behavior. In other words, L3 signal applied both gain increments and decrements onto the LMC contrast signal, at both fast and slow timescales, to meet the behavioral requirement across different luminances.

Since the absolute luminance values play key role in determining the direction of the post-receptor gain control, L3 must have absolute luminance information. We tested this hypothesis by expressing GCaMP6f selectively in L3 neurons and measured calcium signals in response to a broad range of luminances (Figure 4F). Flies were exposed to 30 s of adapting luminance before an OFF step to near-dark screen (~-100% contrast) was taken. The dark screen persisted for 3 s, before the next adapting luminance was displayed, making it an ON step. Five adapting intensities were tested over four luminance regimes each. Like L2, L3 also responded with an increase in calcium to the OFF steps (Figure 4G). The OFF screen-elicited calcium signal was taken as the baseline fluorescence (F) and the responses to different ON steps were quantified. The steady-state L3 responses gradually decreased with luminance within and across luminance regimes, showing that L3 encodes absolute luminance in its steady-state calcium level (Figure 4H). In the bright luminance regimes, L3 showed a certain degree of gain control making the steady-state response curve somewhat discontinuous, indicating a transition to encoding rather contextual luminance in bright light. Thus, L3 baseline calcium retains luminance information required for the gain correction mechanism that is shaped predominantly by the absolute luminance values, but also by contextual luminance in bright conditions.

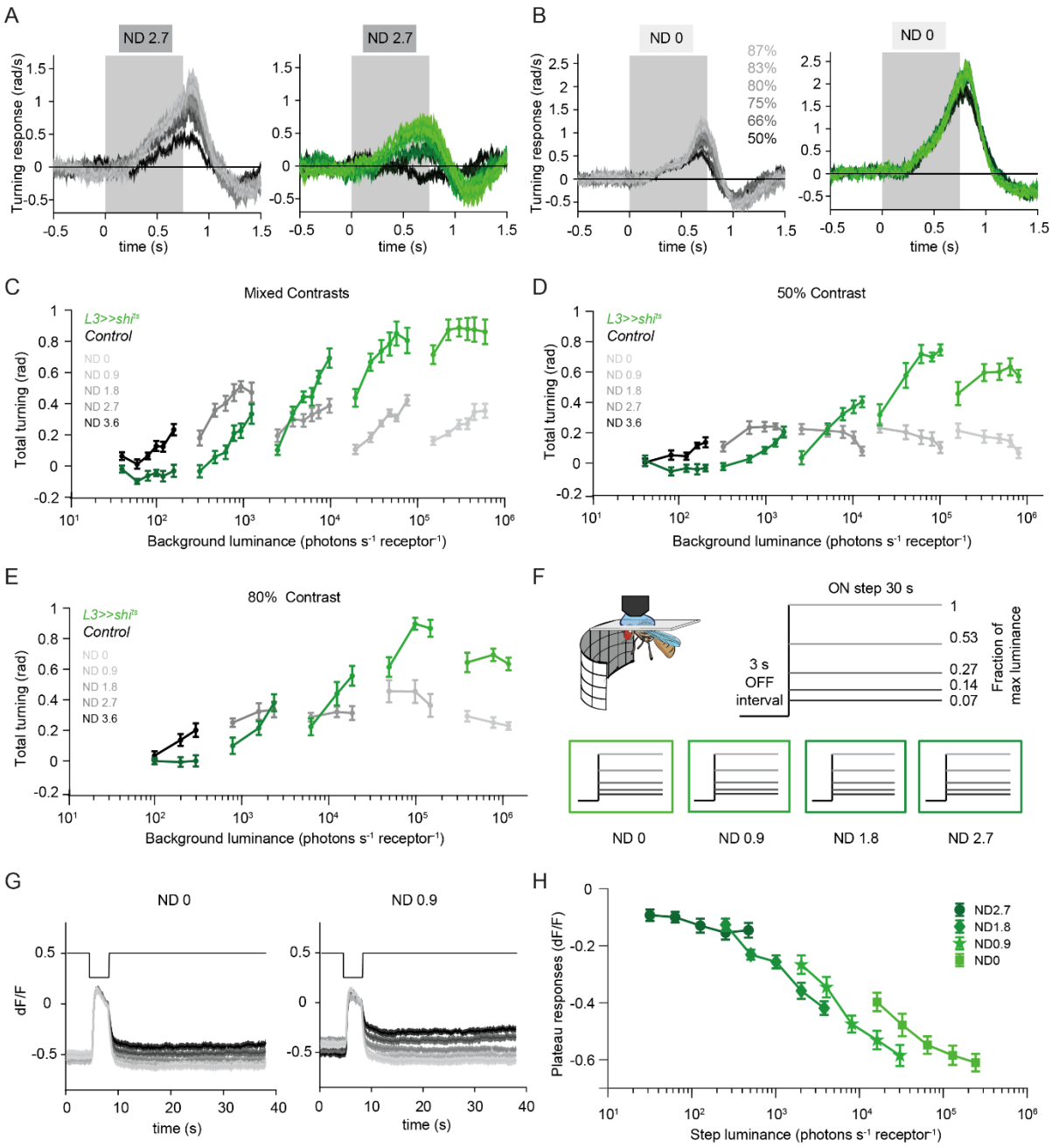

Figure 4: L3 signals implement two-way gain control. (A-B) Turning velocity time traces of control (gray) and L3-slenced (green) flies in response to mixed-contrast stimuli in a dim (A, ND 2.7) and a bright (B, ND 0) luminance regimes. (C-E) Turning responses (quantified as total turning) of control and L3-silenced flies to the mixed-contrast stimuli (C) and the uniform-contrast stimuli, at -50% (D) and -80% (E) contrast in five luminance regimes. Sample size is N=10 flies for each genotype and stimulus set. (F) Schematic of the stimuli used for *in vivo* calcium imaging in L3. 30s exposure to one of five different intensity values followed 3s OFF interval. The procedure was repeated in four different luminance regimes. (G) L3 response time traces for the five intensity values in the luminance regime ND 0 and ND 0.9. (H) L3 responses quantified in the last second of the 30s luminance exposures for all stimuli over the four regimes. Sample size is n=12 (192), #flies (#ROIs). All traces and plots show mean ± SEM.

A dichotomy-inspired, luminance-contrast integration model

L3 function appears to be dichotomous, providing a gain increment in absolute low luminance regimes, and a negative gain at absolute high luminance regimes. At first sight, this contradicts the role of L3 at -100% contrast, where flies did not overestimate stimuli at any luminance (Ketkar et al., 2020). If the same L3 neurons implement corrective operations in both stimulus paradigms, then a dichotomous impact of absolute luminance should be evident for all contrasts. To test for this explicitly, we quantified the 'L3 contribution' to behavioral responses to -100% contrast by subtracting total turning of L3-silenced flies from that of the control flies (Figure 5A, data from (Ketkar et al., 2020)). The difference indeed revealed two modes of L3 contribution, specific to high and low luminances: at high absolute luminance, L3 corrected for the response deficits in contextual dim light, i.e. the relatively dimmer stimuli of each luminance regime. There, the gain poorly adjusted due to dynamic stimulation needed a boost only when sudden dim light was encountered. In contrast, L3 contribution at absolute low luminances did not correlate with contextual luminance, but rather with absolute luminance. An L3-based correction at dim light did not lead to contrast constancy, but improved detection of the dim stimuli in general.

We then calculated L3 contribution for the other uniform-contrast stimulus sets used here. The sign of the L3 contribution for both the -50% and -80% contrasts was in line with the direction of gain correction: the L3 contribution was negative at -50% and -80% contrasts on the higher side of the partition, whereas all three contrasts required a positive L3 contribution on the lower side of the partition (Figure 5B). Therefore, L3 has a dichotomous role in adjusting behavioral responses across luminances for all contrasts tested. Importantly, the partitioning of the luminance axis occurred at similar luminances for the three contrasts, suggesting a common mechanism underlying the partition.

We wished to understand, algorithmically, how the luminance pathway interacts with the contrast pathway to implement the dichotomous correction. We modelled the role of luminance as guided by the dichotomy: two parallel channels constituted two distinct operations required at dim and bright luminances. A steep sigmoidal function of luminance *f(I)* with its midpoint at the partitioning luminance determined which of the parallel channels assumed a dominant role (Figure 5B, orange). The channel correcting the estimate of dim stimuli was a luminance-only channel, thus providing a contrast-independent signal to amplify all dim stimuli. In the other channel dealing predominantly with the brighter regimes, *f(I)* scaled LMC contrast signals to selectively tackle the challenges of dynamic conditions i.e. specific to contextual luminance variations. The output of the two channels, along with a contrast-only output, were linearly combined to predict control behavior. The model equation was

$$Turn = a_0 + a_1 L_2 + a_2 + a_3(1 - b_0 L_2) f(I) + a_4\big(1 - f(I)\big)\log I \quad \text{..... (1)}$$

where L_2 corresponds to the contrast-sensitive LMC output, I is background luminance, $f(I)$ is the sigmoidal function shown in (Figure 5B) and $a_0 - a_4$ and b_0 are constant parameters optimized when training the model. The contrast-only term combined with a constant term, $a_0 + a_1 L_2$ predicted L3-silenced behavior well, as shown in the previous sections. All terms together were expected to shape the control behavior. Among the luminance contributions, $a_3(1 - b_0 L_2) f(I)$ was the dominant term at high luminances, whereas $a_4(1 - f(I))\log I$ assumed the dominant role in dim light.

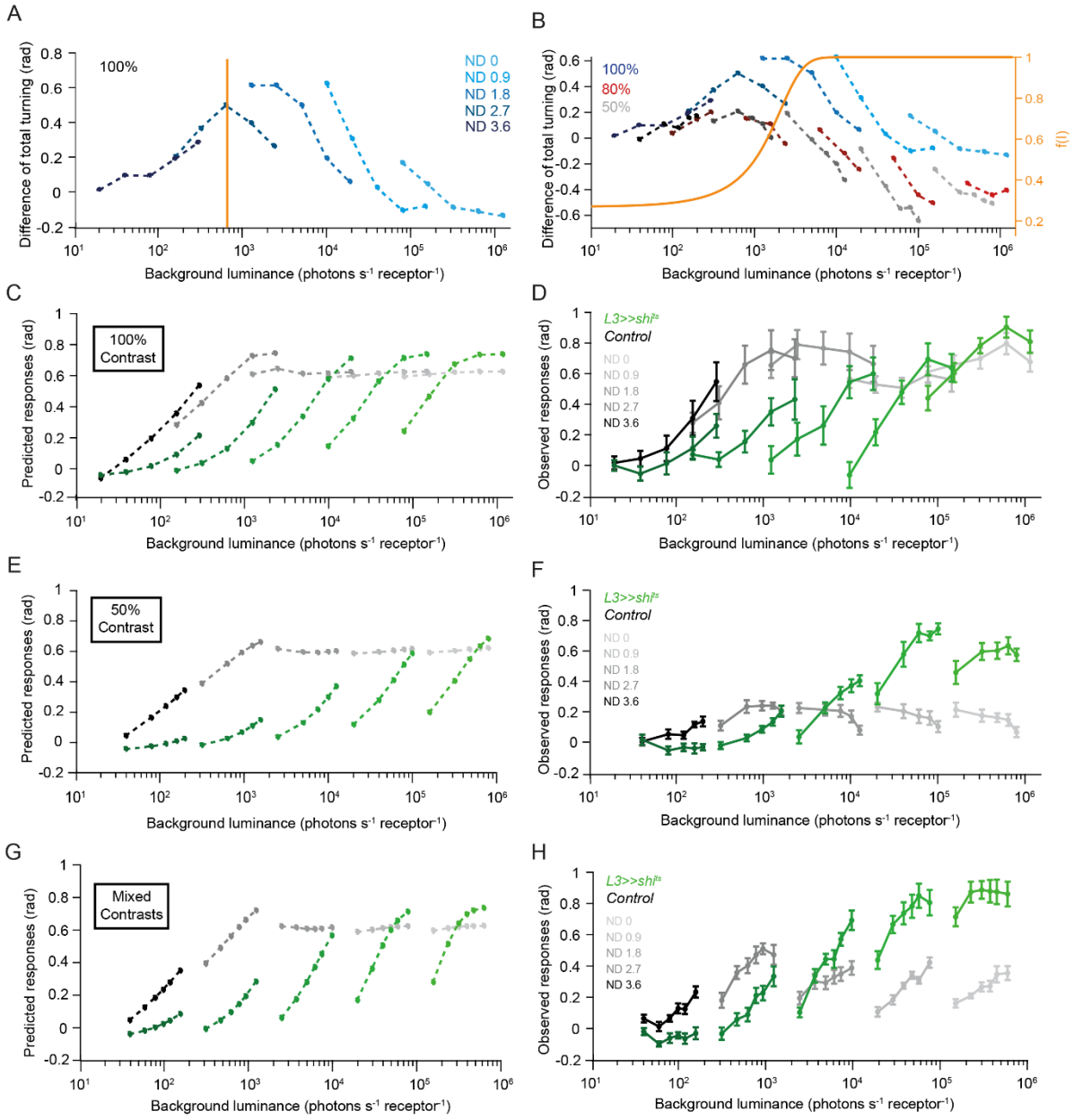

Figure 5: A dichotomy-inspired model captures -100% contrast undrestimation by L3 silenced flies, but not overestimation of other contrasts. (A) Difference between control responses and responses of L3-silenced flies to -100% OFF edge stimuli over five luminance regimes (data from Ketkar et al 2020). Red line partitions the luminance axis into two parts. Behavior in the brighter part requires L3 in contextual dim or bright light, whereas behavior in the dimmer part generally requires L3. (B) Difference between control responses and responses of L3-silenced flies to all three uniform-

contrast stimulus sets (-100%, -80%, -50%). Oragne curve shows *f(I)*, a sigmoidal function of luminance centered at the partitioning luminance (10^3 photons s^{-1} $receptor^{-1}$). (C-H) Behavior of control and L3-silenced flies in response to -100% (C), -50% (E) and mixed-contrast (G) stimuli as predicted by model (eqution 1). The corresponding observed behavioral responses are in (D, F, H), for comparison. (F,H) are the same as Figure 4C,E.

When the model was trained on the -100% dataset, it captured the control behavior at -100% contrast in all luminance regimes well (Figure 5C,D). However, it failed to predict responses to other stimulus sets, such that it overestimated control responses in bright conditions (Figure 5E-H). Thus, the model only captured L3-mediated gain increment, but not gain decrement. When the model was instead trained on a set comprising overestimation, it predicted overestimation for all sets – also for the 100% set. Thus, the model cannot capture bidirectional gain control at once The model also failed to discriminate contrasts in the mixed-contrast dataset, in the bright regimes (Figure 5G-H), hinting at insufficient information about contrast available to the model. Notably, the model captures responses to -100% OFF edges alone – the only condition where edge has no measurable luminance. Therefore, edge luminance could provide the information required to distinguish contrasts.

Inhibition by the OFF edge luminance signals is key to gain reduction

We next revised the model by including further contrast-related information. Edge luminance distinguishes -100% contrast from other contrasts, however, the model should distinguish between other contrasts too. To examine the utility of edge luminance to distinguish all contrasts, we explored if L3 contribution i.e. the difference between control and L3-silenced behavior varied as a function of edge luminance, at -50% and -80% contrasts. L3 contribution increased with luminance for both contrasts, however behavioral responses to the -50% contrast set generally required a higher L3 contribution than the -80% contrast set (Figure 6A). L3 contribution could be best fitted by a line $R = a * log_{10}(I_{edge})$, where I_{edge} is the OFF-edge luminance, suggesting that the logarithm of the edge luminance was a reliable feature distinguishing contrasts. Thus, we added to the model a term that solely depended on edge luminance. The model equation now took the form

$$Turn = a_0 + a_1 L_2 + a_2 + a_3(1 - b_0 L_2) f(I) + a_4\big(1 - f(I)\big)\log I - a_5 \log I_{edge} \tanh I_{edge}$$

…… (2)

We first trained the model on the uniform-contrast datasets. The model now captured both underestimation in the -100% set and overestimation in the -50% and -80% sets, with high accuracy (Figure 6B-F, Figure S4). We validated the model on the mixed-contrast set, where it also predicted both overestimation and underestimation equally accurately (Figure 6B,G,H). Conversely, the model trained on the mixed-contrast datasets was generally capable of capturing features of the uniform-contrast datasets, showing that the model was robust to the different stimulus paradigms tested (Figure S4).

Finally, we noticed that the responses to the mixed-contrast stimuli were slightly underestimated by the model, especially in high luminance regimes (arrows in Figure 6B, right). We thus considered the possibility that the mixture of contrasts leads to contrast adaptation or sensitization. To account for this, we added a scaling factor that operates on the terms involving L2 contribution in the equation 2,

although the scaling was only meant to operate when contrasts were mixed (see methods). The equation now read

$$Turn = a_0 + a_1 L_2 + a_2 + a_3(1 - b_0 L_2) f(I) + a_4\big(1 - f(I)\big)\log I \; - a_5 \log I_{edge} \tanh I_{edge} + k_{adapt} a_1 L_2 \quad \text{(3)}$$

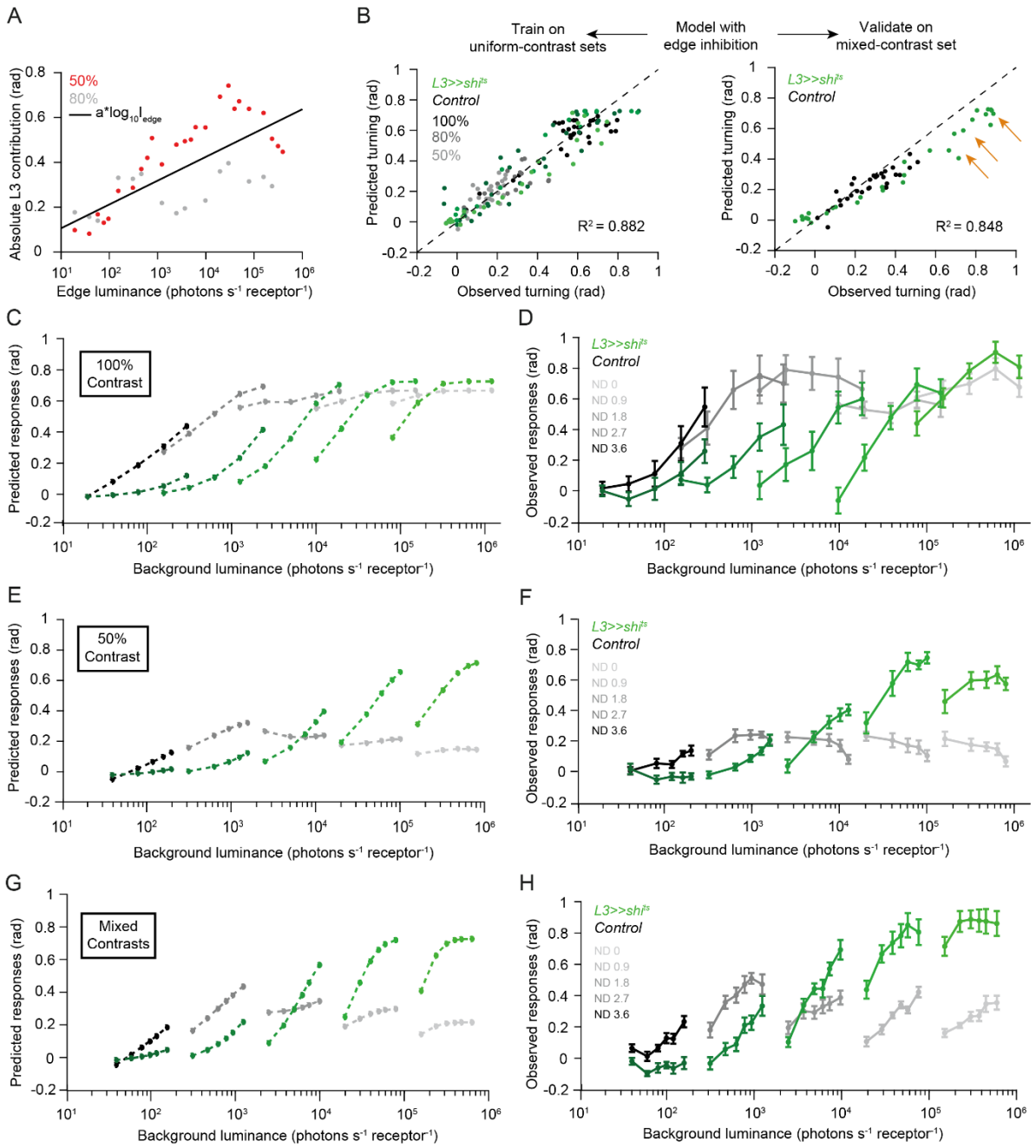

Figure 6: Inhibition by the OFF-edge luminance is key to gain reduction. (A) Difference between control responses and responses of L3-silenced flies to -50% (red) and -80% (gray) contrasts. Black line is a linear function of log(edge luminance). (B) The model including edge inhibition (equation 2) was trained on responses to the uniform-contrast stimuli and validated on responses to the mixed-contrast stimuli. Predicted vs observed responses are plotted separately for the training set (left) and the test set (right). Prediction accuracies are represented by the R-squared values. Dashed lines are unity lines; orange arrows indicate data points consistently deviating from the unity line. (C-H) Behavior of control and L3-silenced flies in response to -100% (C), -50% (E) and mixed-contrast (G) stimuli as predicted by the revised model (eqution 2). The corresponding observed behavioral responses are in (D, F, H), for comparison. (F,H) are the same as Figure 4C,E and Figure 5F,H.

This revised model, when trained on the uniform-contrast sets, predicted the mixed-contrast responses more accurately (Figure 7A-C). The model proposes that the post-receptor gain control operates in separate channels downstream of the lamina, which cater to distinct contrast- and luminance-dependent requirements of gain correction (Figure 7D).

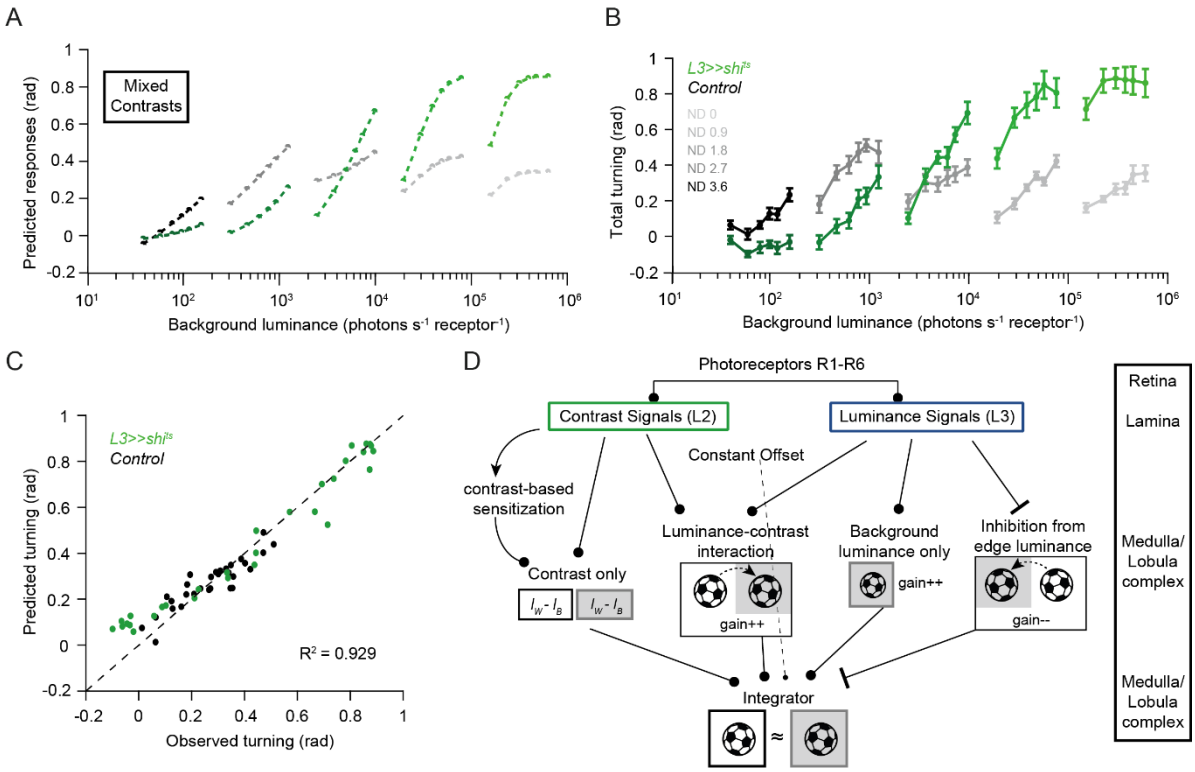

Figure 7: A multi-channel luminance-contrast integration model captures role of luminance in gain correction. (A) Behavior of control and L3-silenced flies in response to the mixed-contrast stimuli as predicted by a revised model that accounts for sensitization effects (eqution 3). (B) Observed behavioral responses are to the mixed-contrast stimuli, same as in Figure 4C, Figure 5H. (C) Predicted vs observed responses to the mixed-contrast stimuli. Dashed line is unity line. R-squared value represents prediction accuracy. (D) Summary schematic of the proposed circuitry implementing two-way gain correction. Lamina neurons L2 and L3 receive input from photoreceptors R1-R6. Downstream, four distinct channels process lumiance and contrast in different ways and their outputs are integrated. A constant offset independent of L2 or L3 also add to the overall summation. The processing channels as well as the integrating neuron may be found in the medulla or lobula complex.

In sum, our results provides an algorithmic and mechanistic understanding of vision in dynamically changing conditions, across a wide range of absolute luminances. Our work demonstrated that fly behavior achieves better constancy and better detection of dim stimuli than expected from contrast-sensitive (L2) physiology only, owing to the gain correction across luminances and contrasts. The luminance-sensitive L3 neurons provide signals necessary for the diverse gain control operations, and their interaction with contrast signals is well-captured by the algorithmic model.

Discussion

Luminance information retained past photoreceptors in known to correct contrast computation in flies (Ketkar et al., 2020). In the present study, we demonstrate how the role of luminance in post-receptor gain control generalizes over contrast-luminance space. Contrast computation in the first-order interneurons is not contrast constant at both fast and slow timescales, and challenges vision in distinct scenarios that require further gain modulation. Specifically, contrast-driven behavior requires (1) a gain increment in contextual dim light and (2) a gain decrement in contextual bright light to establish constancy. It further requires (3) gain increment at extremely low illumination to improve visibility of the stimuli. The luminance-sensitive L3 neurons provide signals for all these gain-corrective operations in their downstream circuitry. A computational architecture of this circuitry is provided by our modelling approach, which suggests how the contrast- and luminance-sensitive channels interact to tackle all these widely differing scenarios. Here, the luminance signal plays a dichotomous role: a contrast-dependent correction (i.e. in contextual dim or bright light only) is implemented in bright environments and a contrast-independent correction in dim environments, explaining the apparent dual role of L3.

Contrast computation in first-order interneurons is insufficient for constancy at multiple timescales

We show that the contrast-sensitive neurons L2 in *Drosophila* do not fully attain luminance invariance. They not only adapt their gain too slow to achieve constancy at fast timescales, but also exhibit a luminance-dependent contrast sensitivity at slow timescales of several tens of seconds, that allow adaptation of the sensory periphery / photoreceptor adaptation. LMCs in large flies also increase their contrast sensitivity over several log units of adapting luminance, although the contrast sensitivity of LMCs in bigger flies stabilizes at a maximal value at high luminance (Laughlin et al., 1987). It is possible that even *Drosophila* L2 attains a better stability at luminances higher than we have tested, however, behavior is contrast constant in the same luminance ranges where L2 is not. Thus, gain control in photoreceptors and LMCs combined is insufficient to explain constancy observed in behavior. Flies appear to have implemented a remarkable strategy to overcome the limitations in adaptation of the periphery. Fruit flies are preferentially active in twilight, and therefore the luminance range we tested is of their behavioral importance (Spitschan et al., 2016). Fly behavior only show an inability to maintain constancy at very low illumination, highlighting the requirement of additional gain control based on the absolute luminance scale.

In vertebrates, regions of luminance-dependent variation of contrast sensitivity are found in both rod and cone vision. For example, in the Rose-DeVries region of the threshold-vs-intensity curves, detection threshold rises less steeply than would be expected from Weber's law – the ideal case of sensitivity adjustment (Aguilar and Stiles, 1954; Brown and Rudd, 1998; Rieke and Rudd, 2009b). This is a low-intensity region, and Weber's law generally catches up at higher intensities. Importantly, observations regarding the Rose-DeVries region differ, and behavioral reports and physiological evidences often diverge. Our work examines behavior and physiology of the first-order interneurons using very similar stimulus parameters and hence offers a direct comparison between the two measures, demonstrating

that behavior achieves luminance-invariant contrast sensitivity where the peripheral contrast computation does not.

Contextual luminance as well as contrast determine the direction of gain correction

Contrast-driven behavior required a corrective gain increment in contextual dim light and decrement in contextual bright light, to achieve constancy. This is in line with the nature of challenges faced in dynamic conditions. When illumination suddenly goes down, a higher gain is required to perceive the same contrasts but is not achieved in slowly adapting L2. Conversely, sudden encounter with bright light would require lowering of gain. Whereas both requirements are expected to coexist within any luminance regime, only one of them is prominent in the bright regimes. Surprisingly, the contrast value determines which one of the two requirements exist: gain increment is required at -100% contrast, and gain decrement is required at lower contrasts (-50% and -80%). We interpret these differential requirements as representing the behavioral relevance of different contrasts. For example, -100% contrasts are the biggest negative changes and carry maximal relevance, and a higher gain might possibly not lead to stronger responses due to behavioral response ceiling. On the other hand, -50% contrasts might be less relevant, as evidenced by comparably weak fly turning responses, and a lower gain possibly does not lower the originally weak responses any further. Such low contrast is only overestimated, when the contrast signals are too high due to insufficient gain adjustment and lack of any other contrast cue. Our model hints at the edge luminance as an additional contrast cue. For any specific background luminance, the -100% contrast edge has a near-zero luminance, and the edge luminance increases with decreasing contrast values. Thus, inhibition proportional to the edge luminance is a plausible solution to enable responses correlating with relevance of different contrasts.

A single luminance-sensitive neuron provides both gain increments and decrements

L3 alone is able to implement the two-way gain control required for behavior. It scales up responses in contextual and absolute dim light, and scales them down in bright light. The bidirectional action is non-trivial, considering it is potentially a feed-forward mechanism. Feedback mechanisms rely on the neurons' own output (e.g., photoreceptor-horizontal cell feedback loop), and such feedback automatically goes up or down when the output itself goes up or down, thus allowing gain regulation in both directions. In contrast, the novel gain control in flies takes place downstream of the luminance-sensitive L3 neurons, which receive dominant input from photoreceptors and rely little on circuit interactions such as feedback (Sporar et al., unpublished). L3 is non-linearly more sensitive to dark, and consistently provides gain increment in both contextual and absolute low luminance (Ketkar et al., 2020). Paradoxically, the gain decrement in bright light requires an inhibitory role of L3 which is least active under these conditions. Reduced L3 activity cannot be directly linked with reduced gain either, because L3 silencing mimics its reduced activity in bright light but still leads to overestimation of stimuli. Interestingly, our model proposes a separate channel that relays inhibitory signal proportional to the OFF edge luminance. The separate channel could mediate the gain reduction through release of inhibition downstream of L3. This possibility requires an inhibitory neuron that receives inhibitory input from L3, however the known L3 post-synapses are excitatory (Takemura et al., 2013a), and the

hypothesis relies on indirect connections. For example, Mi9 is an inhibitory neuron downstream of L3, and CT1 links Mi9 to T5 – the OFF motion-sensitive neurons – through an inhibitory synapse (Shinomiya et al., 2019; Takemura et al., 2017a). Thus, different possible network solutions can implement the inhibitory role of L3.

Two other channels proposed by the model to convey luminance information are both excitatory, and employ background luminance. This indicates different temporal response properties of the neural elements underlying L3 inhibition and excitation: the inhibitory channel is faster than the excitatory channel such that it relays the latest (edge) information. In contrast, the excitatory channel employs background information to possibly regulate resting potential of a downstream integrating neuron, thereby changing its gain.

Post-receptor gain control is beneficial across species

Gain control is found at every stage of retinal processing in vertebrates. At some processing stages, gain regulation is primarily necessary to match the input range with neurons' operating range. For example, photoreceptors encode the natural scenes comprising ~ten orders of intensity variations, with just two orders of voltage response range (Naka and Rushton, 1966; Normann and Perlman, 1979; Schnapf et al., 1990). Even at advanced processing stages, the input from upstream neurons may exceed the operating range and gain control could be vital to prevent information loss stemming from this mismatch. However, regardless of this proposed requirement, post-receptor gain control is thought to be a more reliable rapid gain control, since it operates on a relatively noise-free, spatially pooled signal (Rieke and Rudd, 2009b). Interestingly, the major gain control operation is known to switch to the post-receptor cites such as RGCs, especially in low light that renders photoreceptor signals noisy and thus unreliable (Dunn et al., 2007). Since fly photoreceptors too have to deal with internal and external noise constraints (Dubs et al., 1981; Juusola and Hardie, 2001; Laughlin, 1989), the rapid gain control occurring at least two synapses downstream of photoreceptors may come with comparable benefits of spatial pooling, as in vertebrates. However, this needs wide-field neurons to sample information from single-columnar neurons of the compound eye. Distal medulla (Dm) neurons including Dm3, Dm4, Dm12 and Dm20 span several columns and also innervate medulla layer M3, where they could communicate with L3 axon terminals and pool luminance information (Nern et al., 2015b). Interestingly, Tm9 neurons downstream of L3 have a wide center-surround receptive field (Fisher et al., 2015b; Ramos-Traslosheros and Silies, 2021), in line with the idea that the L3-mediated gain control benefits from spatial summation.

Our results point at a possibility that the post-receptor gain controls in vertebrates are crucial for perceptual constancy under conditions where the visual periphery does not adapt rapidly. Furthermore, we highlight the role of the periphery, namely conserving luminance information parallel to contrast, in enabling the more proximal gain regulation.

Enhanced sensitivity to extremely dim stimuli

Unlike the bright luminance regimes, L3 always provided a gain increment in the low luminance regimes, for each stimulus set tested. This increased gain did not always achieve contrast constancy in behavior but helped improve detection of very dim stimuli. L3 physiology is especially suited to provide such gain increments. L3 non-linearly amplifies dim light signals, thus encoding the low luminance values with high resolution (Ketkar et al., 2020). Besides, spatial summation predicted to occur downstream of L3 can further enhance dim light detection, by improving signal-to-noise ratio. In line with this, nocturnal hawkmoth vision works better than the photoreceptors would allow, due to spatial summation (Stöckl et al., 2016b). Consistent with its role in absolute dim light, L3 encodes absolute luminance over a few orders of low luminance. Luminance sensitivity is also found in vertebrate retina e.g. in intrinsically photosensitive retinal ganglion cells (ipRGCs), however, different ipRGCs from the population tile the luminance space so that they can collectively encode the broad luminance range with sufficient resolution (Milner and Do, 2017). In contrast, L3 encodes nearly three orders of luminance with its limited operating range, compromising resolution. To still play the observed corrective roles with accuracy, L3 must respond to luminance with remarkable precision. L3 responses are a monotonous function of luminance. Yet, the direction of L3's gain control divides the luminance axis into two abrupt zones. How the downstream circuitry employs the purely luminance-sensitive signals in a dichotomous way remains to be explored. We hypothesize a luminance-dependent recruitment of wide-field neurons, such as the Dm neurons.

Integration of luminance and contrast features to implement the post-receptor gain control

The contrast- and luminance-sensitive channels must interact in the circuitry downstream of the first-order interneurons that segregate these features (Figure 7D). In the *Drosophila* visual system, transmedullary (Tm) neurons Tm1, Tm2, Tm4 and Tm9 comprise the main second-order interneurons in the OFF pathway, and they subsequently pass the information onto the first direction-selective T5 neurons (Fisher et al., 2015b; Joesch et al., 2010; Serbe et al., 2016; Shinomiya et al., 2019; Takemura et al., 2013a). Outputs of the local motion-sensitive T5 neurons are pooled by lobula plate tangential cells (LPTCs) to encode global motion that eventually guides behavior. Which of these processing stages integrates contrast and luminance, and where in the brain is contrast constancy truly established, remains to be explored. Our model provides some insights for this search. The different gain control operations rely on distinct processing channels, the outputs of which are eventually summed up. The Tm neurons could constitute these distinct channels that merge at T5 neurons. For example, Tm9 receives the main input from the luminance-sensitive L3 (Fisher et al., 2015b; Takemura et al., 2013a). It could either serve as the luminance-only channel to improve dim light vision, or it could scale up contrast information coming indirectly from L1 (Fisher et al., 2015b). Tm2, with its fast and transient properties, could act as the contrast-only channel. CT1, the only known direct inhibition onto T5, could mediate gain reduction through indirect connections with L3. The power of Drosophila genetics will allow to tease apart these different options in the future.

Together, our study uncovers a circuit-based, rapid gain control mechanism that ensures a better stimulus detection at low intensities and contrast constancy at high intensities, leading to better overall behavioral performance than supported by the visual periphery. This mechanism operates more proximally than at the noise-prone photoreceptor signals. Our work demonstrates how parallel processing of visual features in the periphery is key to overcoming specific visual challenges and opens up the possibility for examining the behaviorally relevant re-integration of these features at the physiological and molecular levels, well-guided by a computational modeling approach.

Materials and methods

Experimental model

Flies were raised at 25 ºC and 65 % humidity on standard molasses-based fly food in a chamber where 12h:12h light-dark cycle was maintained. Two-photon experiments were conducted at room temperature (20 ºC) and behavioral experiments at 34 ºC. Female flies 2-4 days after eclosion were used for all experimental purposes. Lamina neuron driver lines used for genetic silencing were *L3^{0595}-Gal4,* described in (Silies et al., 2013b), and *UAS-shi[ts]* from BDSC (reference numbers 44222). For imaging experiments, GCaMP6f (BDSC reference number 42747) was expressed using *L2^{21Dhh}-Gal4* (Rister et al., 2007) and *L3^{MH56}-Gal4* (Timofeev et al., 2012). Detailed genotypes are given in Table 1.

Table 1: Genotypes used in this study.

Name	Genotype	Figure
Imaging		
L2>>GCaMP6f	*w+; UAS-GCaMP6f / +; L2^{21Dhh}-Gal4 / +*	Fig 1, S1
L3>>GCaMP6f	*w+; L3^{MH56}-Gal4 / +; UAS-GCaMP6f / +*	Fig 4
Behavior		
UAS-shibire^{ts} control	*w+; + / +; UAS-shi^{ts} / +*	Fig 2, 3, 4, 5, 6, 7, S2, S3, S4
L3-Gal4 control	*w+; +/ +; L3^{0595}-Gal4 /+*	Fig S3, S4
L3 silencing	*w+; +/ +; L3^{0595}-Gal4 /UAS- shi^{ts}*	Fig 4,5,6,7, S3, S4

Behavioral experiments

Behavioral experiments were performed as described in [Ketkar et al. 2020]. In brief, all experiments were conducted at 34 ºC, a restrictive temperature for *shibire^{ts}* (Kitamoto, 2001). Female flies were cold anesthetized and glued to the tip of a needle at their thorax using UV-hardened Norland optical adhesive. A 3D micromanipulator positioned the fly above an air-cushioned polyurethane ball (Kugel-Winnie, Bamberg, Germany), 6 mm in diameter, and located at the center of a cylindrical LED arena that spanned 192º in azimuth and 80º in elevation (Reiser and Dickinson, 2008). The LED panels arena (IO Rodeo, CA, USA) consisted of 570 nm LEDs and was enclosed in a dark chamber. The pixel resolution was ~2º at the fly's elevation. Rotation of the ball was sampled at 120 Hz with two wireless optical sensors (Logitech Anywhere MX 1, Lausanne, Switzerland), positioned toward the center of the ball and at 90º to each other (setup described in (Seelig et al., 2010)). Custom written C# code was used to acquire ball movement data. MATLAB (Mathworks, MA, USA) was used to coordinate stimulus

presentation and data acquisition. Data for each stimulus sequence were acquired for 15-20 minutes, depending on the number of distinct epochs in the sequence (see 'visual stimulation' for details).

Visual stimulation for behavior

The stimulation panels consist of green LEDs that can show 16 different, linearly spaced intensity levels. The presented luminance was measured as previously described (Ketkar et al., 2020). Briefly, candela/m^2 values were first measured from the position of the fly using a LS-100 luminance meter (Konika Minolta, NJ, USA). Then, these values were transformed to photons incident per photoreceptor per second, following the procedure described by (Dubs et al., 1981) and using parameters specific to the *D. melanogaster* compound eye (Gonzalez-Bellido et al., 2011). The highest native LED luminance was approximately 11.77 * 10^5 photons * s^{-1} * $photoreceptor^{-1}$ (corresponding to a measured luminance of 51.34 cd/m2), and the luminance meter read 0 candela/ m^2 when all LEDs were off. Neutral density filter foils (Lee filters) were placed in front of the panels to attenuate luminance. The foils were used individually or in combinations to achieve optical densities of 0.9, 1.8, 2.7 and 3.6, thus creating luminance regimes that spanned about four orders of magnitude.

Fly behavior was measured in an open-loop paradigm where OFF edges varying in either contrast or luminance, depending on the experiment, were presented in a randomized order. For every set of OFF edges, each edge was presented for around 60 to 80 trials. Each trial consisted of an initial static pattern (i.e. the first frame of the upcoming pattern) shown for 500 ms as background, followed by 750 ms of edge motion. Inter-trial intervals were 1s long and always consisted of a dark screen. All edges from a set were presented in a mirror-symmetric fashion (moving to the right, or to the left) to account for potential biases in individual flies or introduced when positioning on the ball.

1. Uniform-contrast edges: These were two sets comprising -50% and -80% (Weber) contrast edges separately. In the -50% set, the edges were made of 5 different luminance values (i.e. five unique epochs), moving onto backgrounds twice as bright as the respective edges. The edges assumed the intensities 7%, 14%, 20%, 27% and 34% of the highest LED intensity (corresponding to the luminances: 0.98, 1.96, 2.94, 3.92 or 4.90 *10^4 photons*s^{-1}*$receptor^{-1}$ luminance). The -80% set comprised three unique edges with luminances 0.98, 1.96 or 2.94 *10^4 photons*s^{-1}*$receptor^{-1}$, which moved onto backgrounds that were five times as bright as the corresponding edges.

2. Mixed-contrast edges: The set comprised of six distinct epochs, each with a different Weber contrast value (50%, 66%, 75%, 80%, 83% and 87%). Here, the edge luminance was maintained constant at 7% of the highest LED intensity, across epochs, and the background luminance varied.

Behavioral data analysis

Fly turning behavior was defined as yaw velocities that were derived as described in (Seelig et al., 2010), leading to a positive turn when flies turned in the direction of the stimulation and to a negative turn in the opposite case. Turning elicited by the same epoch moving either to the right or to the left were aggregated to compute the mean response of the fly to that epoch. Time traces of turning responses are presented as angular velocities (rad/s) averaged across flies ± SEM.

Total turning responses of flies were calculated over the stimulus motion period (750ms), shifted by 100 ms to account for a response delay. Total turning was first tested for normal distribution using a Kolmogorov-Smirnov test. Two-tailed Student's t tests subsequently examined statistical differences between genotypes. Data points were considered significantly different only when the experimental group significantly differed from both genetic controls. Flies with a forward walking speed less than 3 mm/s, computed in the last 200 ms of the inter-trial interval, were discarded from the analysis. This resulted in rejection of approximately 15% of all flies.

Two-photon imaging

Female flies were anesthetized on ice before placing them onto a sheet of stainless-steel foil bearing a hole that fit the thorax and head of the flies. Flies they were head fixated using UV-sensitive glue (Bondic). The head of the fly was tilted downward, looking toward the stimulation screen and the back of the head was exposed to the microscope objective. To optically access the optic lobe, a small window was cut in the cuticle on the back of the head using fine blade and sharp forceps. During imaging, the brain was perfused with a carboxygenated saline-sugar solution composed of 103 mM NaCl, 3 mM KCl, 5 mM TES, 1 mM NaH2PO4, 4 mM MgCl2, 1.5 mM CaCl2,10 mM trehalose, 10 mM glucose, 7 mM sucrose, and 26 mM NaHCO3. For dissections, the same solution lacking calcium and sugars was used. The pH of the saline equilibrated near 7.3 when bubbled with 95% O2 / 5% CO2. The two-photon experiments were performed using a Bruker Investigator microscope (Bruker, Madison, WI, USA), equipped with a 25x/NA1.1 objective (Nikon, Minato, Japan). An excitation laser (Spectraphysics Insight DS+) tuned to 920 nm was used to excite GCaMP6f, applying 5-15 mW of power at the sample. Emitted light was sent through a SP680 short pass filter, a 560 lpxr dichroic filter and a 525/70 emission filter. Data was acquired using PrairieView software at a frame rate of 8 to 12 Hz.

Visual stimulation for imaging

For comparability between behavior and physiology, stimuli for imaging experiments were shown using a cylindrical LED panels arena with same dimensions as the one used for behavior. The arena (IO Rodeo, CA, USA) consisted of 470 nm LEDs with pixel resolution of ~2º at its center. The LEDs can show 16 different, linearly spaced intensity levels. The arena was positioned below the stage of the two-photon microscope, such that fly position under the two-photon objective was approximately at the same height as that of the arena and at the center of its upper circular ring. Two layers of blue filter (Rosko, Indigo no. 59) and a 0.6 neutral density (ND) filter foil (Lee filters) were placed in front of the arena to attenuate its intensity, such that the maximum luminance (highest LED level in the regime ND 0) was $2.43 * 10^5$ photons * s^{-1} * $photoreceptor^{-1}$. Further neutral density filters were added to achieve dimmer luminance regimes. MATLAB coupled with a data acquisition device (National Instruments, NI USB-6211) coordinated stimulus presentation, stimulus data acquisition and a start trigger to the microscope software to synchronize imaging with stimulus presentation.

All stimuli were full-field flashes. For L2 imaging, a set of contrast steps was shown at five luminance regimes ND 0 (the brightest), ND 0.6, ND 1.2, ND 1.8 and ND 2.4 (the dimmest). In each regime, 30 s long exposure to 53% of the maximum luminance was alternated with 30 s long ON or OFF of contrast

steps, where the contrast value was one of -100%, -87.5%, -75%, -62.5%, -50%, -25%, 25% and 50% Weber contrasts, randomly chosen. Each step was shown once, thus imaging time per luminance regime was ~8 minutes. Sequence of the luminance regimes was also randomized for each fly.

For L3 imaging, the stimulus was made of a dark 3s interval of ~zero luminance alternating with five luminances, each shown for 30 s. The luminances were 7%, 14%, 27%, 53% or 100% of the luminance of the highest LED level in each of the four luminance regimes ND 0, ND 0.9, ND 1.8 and ND 2.7. Sequence of the regimes as well as sequence of the luminances in each regime was randomized for each fly. The five luminances were shown three times each, thus imaging time per luminance regime was ~8:15 minutes.

Imaging data analysis

Two-photon data were analyzed using Matlab. Images were corrected for fly movements using cross-correlation upon Fourier transformation, and aligned to a reference image that was maximum intensity projection of the first 30 images. Regions of interest (ROIs) were selected manually from an averaged aligned image such that each ROI enclosed an axon terminal. Average fluorescence intensity of each ROI was calculated for each frame to acquire fluorescence time traces. Fluorescence time trace of a background region was subtracted from the time trace of each ROI. Such background-subtracted signals and stimulus traces were then interpolated to 10 Hz and trial averaged. Normalized signal was calculated for each ROI as $(dF/F) = (F - F_0)/ F_0$, where F is the fluorescence at each time point and F_0 was defined separately for each experiment as described below.

L2 imaging: F_0 equaled mean fluorescence of the entire time series of the ROI.

L3 imaging: Mean fluorescence intensity of the ROI during the dark epochs was used as F_0.

For both L2 and L3, single ROI signals having negative correlation with stimulus were chosen for further analysis. A minority of ROIs were positively correlated with stimulus, as described previously (Fisher et al. 2015). These ROIs have receptive field outside the stimulation area, and were thus discarded. Responses of the chosen ROIs were averaged for each fly, and the fly means were further averaged to obtain mean response traces, shown in Figure 1 and Figure 4 as mean ± SEM.

The luminance-contrast integration model

1. Data pre-processing

Integrated turning was calculated from 100 ms post the edge motion onset (to account for response latency) and over next 0.96 s, the approximate time it took for the flies to stop turning (i.e. return to zero velocity line). Quantification of integrated turning offered a relatively noise-free metric, considering flies did not make much net directional movement in some trials. Integrated turns were averaged across trials of same stimulus epoch for each fly, and these data points were fit by the model.

2. Modeling L2 response

LMCs were assumed to compute contrast relative to mean luminance over the time of experiment. The reference luminance I_{adapt} was thus calculated as temporal average of different luminance values shown within a luminance regime. Precisely,

$$I_{adapt} = \frac{\left[\left(T_{static} + \frac{T_{motion}}{2}\right) * I_{m\_bg} + \frac{T_{motion}}{2} * I_{m\_edge} + T_{interval} * I_{interval}\right]}{T_{static} + T_{motion} + T_{interval}}$$

Where static background duration T_{static}= 0.5 s, edge motion duration T_{motion}= 0.75 s, inter-trial interval $T_{interval}$= 0.75 s, and luminance of the inter-trial $I_{interval}$=0. I_{m_edge} is the mean luminance of OFF edges and I_{m_bg} is the mean luminance of the backgrounds specific to the experiments. Contrast of each edge apparent to the LMCs $C_{apparent}$ was calculated as

where $I_{background}$ and I_{edge} are the background and edge luminances, respectively, specific to each edge.

L2 responses to the apparent contrast were calculated using a model we designed based on (Laughlin et al. 1987). We allowed parameters to be flexible to adjust for the specific properties of *Drosophila melanogaster* as compared to *Calliphora vicina* (Figure M1A). As described in (Laughlin et al. 1987), the L2 response can be fit with a sigmoidal function of contrast, of which the gain k can also be fit using a sigmoidal function of $logI$. Thus, L2 response to any contrast C was formulated as:

$$L2 = \frac{1}{1 + \exp(kC)} - 0.5, \qquad k = \frac{a}{1 + \exp(-b(logI - logI_0))}.$$

We adjusted the parameters of the L2 model in order to optimize the performance of the entire luminance-contrast integration model. In the end, the optimized parameters were $a = 3.5723, b = 1.423$, and $\log I_0 = 4.505$. Example contrast vs response curves calculated with these fits (Figure M1B) are comparable to the measured curves in (Laughlin et al 1987).

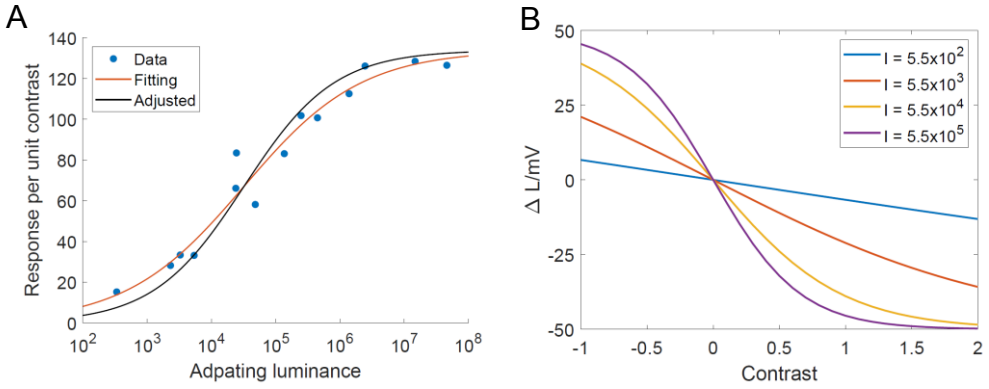

Figure M1: Modelling L2 responses. (A) Sigmoidal fit to the response per unit contrast vs log(luminance); data from Laughlin et al 1987 (blue dots and red fit) and the fit adjusted for

Drosophila melanogaster (black curve). (B) response vs contrast curves calculated for different adapting intensities using the adjusted k values.

3. Modelling the luminance-based dichotomy

The dichotomy in the L3 contribution was modelled as a sigmoidal function of luminance $f(I)$ formulated as

$$f(I) = \frac{1}{1 + \exp(-k_I(I/I_m - 1))}.$$

We always use $k_I = 1.0$ and $I_m = 10^3$ were used.

4. Model trained on the uniform-contrast datasets

Based on the dichotomy, the model (equation 2) was written as

$$Turn = a_0 + a_1 L_2 + a_2 + a_3(1 - b_0 L_2) f(I) + a_4\big(1 - f(I)\big)\log I - a_5 \log I_{edge} \tanh I_{edge}$$

where different colors indicate multiple sources of information that contribute to the turn. The green color corresponds to L2-driven i.e. L3 silenced behavior, the blue color represents terms with background luminance (L3) contribution, and the black color represents the inhibition from the edge luminance. Thus, the blue and black terms contributed to control behavior only, where L3 was functional.

The model was trained on the uniform-contrast datasets. Parameter estimates obtained by fitting are shown in the Table S1. Overall fit accuracy was $R^2 = 0.882, p = 7.38 \times 10^{-64}$. Dataset-wise accuracies were: $R^2 = 0.871$ (-50% uniform-contrast set), $R^2 = 0.853$,(-80% uniform-contrast set) and $R^2 = 0.864$ (-100% uniform-contrast set).

We then used this model to predict responses to the mixed-contrast stimuli, which gave a performance of $R^2 = 0.848$.

5. Model trained on mixed-contrast dataset

The same model (equation 2) was trained on mixed-contrast dataset and validated on the uniform-contrast datasets.

Parameter estimates obtained by fitting are shown in the Table S2. Fit accuracy was $R^2 = 0.971, p = 6.07 \times 10^{-39}$. When predicting responses to uniform contrasts datasets, the model performed with overall accuracy $R^2 = 0.748$ (50% contrast - $R^2 = 0.783$, 80% contrast - $R^2 = 0.658$, 100% - contrast $R^2 = 0.691$).

6. Model fit on both datasets (uniform-contrast and mixed-contrast data)

To account for the contrast sensitization effects, we further revised the model, for which we needed to find which term of equation 2 is influenced by this sensitization effect. Thus, we added a group of dummy variables which directly corresponded to the variables in equation 2. The terms associated

with the dummy variables only contributed to the mixed-contrast data. The new model was given by

$$Turn = a_0 + a_1 L_2 + a_2 + a_3(1 - b_0 L_2) f(I) + a_4\big(1 - f(I)\big)\log I - a_5 \log I_{edge} \tanh I_{edge}$$
$$+ a_0' + a_1' L_2 + a_2' + a_3'(1 - b_0' L_2) f(I) + a_4'\big(1 - f(I)\big)\log I - a_5' \log I_{edge} \tanh I_{edge} \quad \text{.....(2.1)}$$

Fitting performance was $R^2 = 0.905, p = 8.66 \times 10^{-93}$. Parameter estimates are in Table S3.

We then retained only the dummy variables with p < 0.5. The only significant variable was a_1', which is the coefficient of L2-only term. This suggested that the L2-only term was significantly influenced when there were multiple Weber contrasts in the experiment. When the other dummy variables were removed, we obtained the following equation

$$Turn = a_0 + a_1 L_2 + a_2 + a_3(1 - b_0 L_2) f(I) + a_4\big(1 - f(I)\big)\log I - a_5 \log I_{edge} \tanh I_{edge} + a_1' L_2 \quad \text{..... (2.2)}$$

This model accounted for most (72.3%) of the difference of RSS (residual sum of squares) between the model with all dummy variables and the one without dummy variables.

We hypothesized that the mixed contrasts play a role of sensitization. Since the flies are exposed to multiple Weber contrasts randomly, they become more sensitive to contrasts, which corresponds to a larger L2 term in the model. To represent this hypothesis, we rewrote the model as

$$Turn = a_0 + a_1 L_2 + a_2 + a_3(1 - b_0 L_2) f(I) + a_4\big(1 - f(I)\big)\log I - a_5 \log I_{edge} \tanh I_{edge}$$
$$+ k_{adapt} a_1 L_2.$$

The last term was only functional when responses with mixed contrasts were predicted. The value of k_{adapt} was optimized before fitting other coefficients. The optimization was done by maximizing the R^2 of the final model.

We also included the dummy variables to check if this additional coefficient k_{adapt} captured the main difference between the uniform contrasts dataset and the mixed contrasts dataset. With dummy variables, the equation was as follows.

$$Turn = a_0 + a_1 L_2 + a_2 + a_3(1 - b_0 L_2) f(I) + a_4\big(1 - f(I)\big)\log I - a_5 \log I_{edge} \tanh I_{edge}$$
$$+ k_{adapt} a_1 L_2 + a_0' + a_1' L_2 + a_2' + a_3'(1 - b_0' L_2) f(I) + a_4'\big(1 - f(I)\big)\log I - a_5' \log I_{edge} \tanh I_{edge}.$$

The results are shown in the tables S4. No dummy variables were significant. Also, there was no significant difference between the performances of these two models, with and without dummy variables (F-test, p = 0.06), which confirmed that the difference between the uniform contrasts response and the mixed contrasts response was mainly an additional coefficient of the L2 response. With fitting procedure, this coefficient was found as $k_{adapt} = 0.17$. Model performance without dummy variables was $R^2 = 0.899, p = 4.46 \times 10^{-98}$.

7. Revised model fit on uniform contrasts data

Enlightened by the above analysis, we repeated the fitting procedure with the revised model given as

$$Turn = a_0 + a_1 L_2 + a_2 + a_3(1 - b_0 L_2) f(I) + a_4\big(1 - f(I)\big)\log I \; - a_5 \log I_{edge} \tanh I_{edge} + k_{adapt} a_1 L_2.$$

The model was fit to the uniform-contrasts datasets and validated on the mixed-contrast dataset. Prediction improved significantly from $R^2 = 0.848$ to $R^2 = 0.925$ (p = 1.61e-9, F-test).

Supplemental Information

1. Supplemental figures

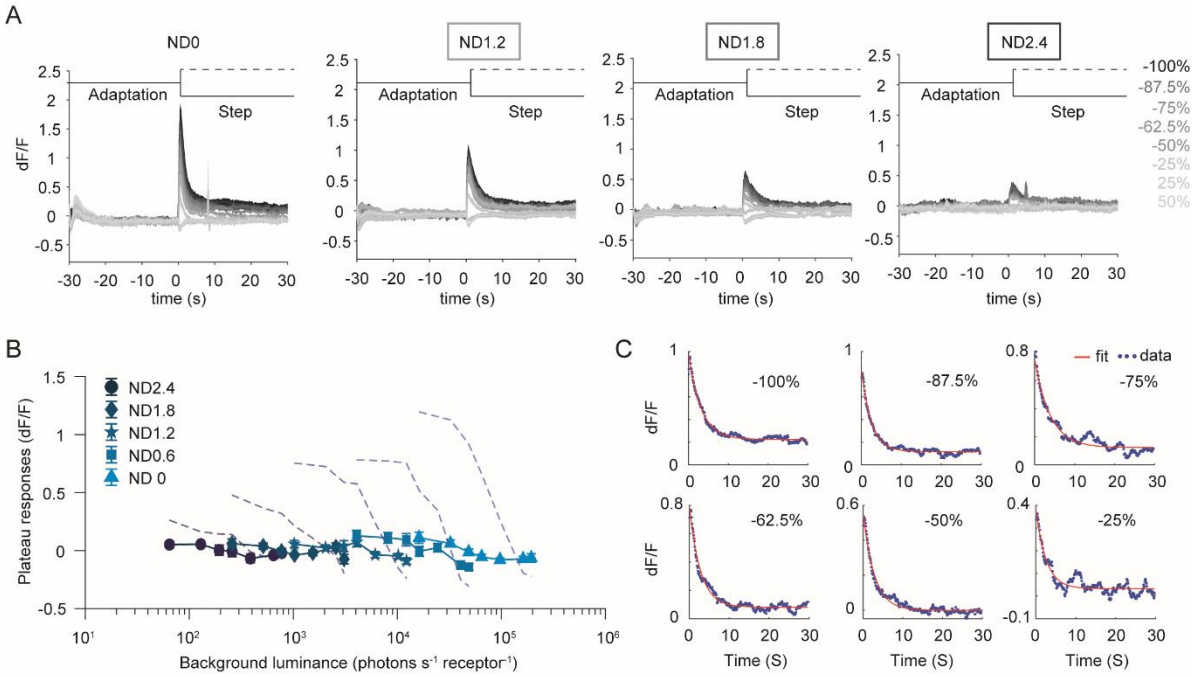

Figure S1: L2 responses to a range of contrast across different adapting luminances. (A) L2 calcium response time traces in the luminance regimes ND 0 (the brightest), ND 1.2, ND 1.8 and ND 2.4 (the dimmest). Gray shades represent contrasts. Black trace represents stimulus. (B) L2 plateau responses quantified over the last second of the 30s epochs, plotted against log(luminance), in five luminance regimes. Dashed lines represent the peak responses as in Figure 1E, replotted for comparison. (C) Example exponential fits to mean OFF step response traces in the luminance regime ND 0.6 Sample size is n=10 (136), #flies (#ROIs). Traces and plots in A and B show mean ± SEM.

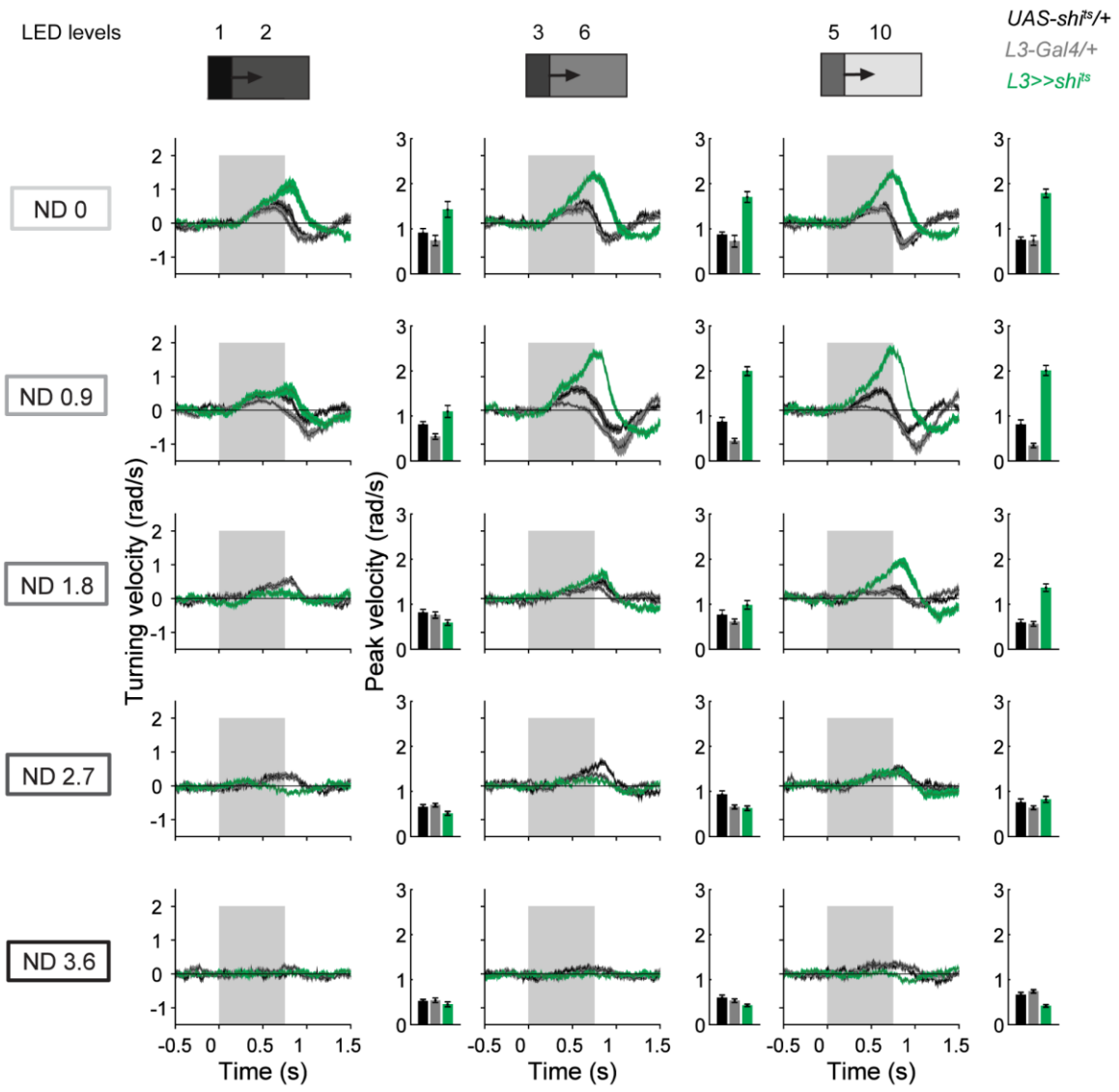

Figure S2: At -50% contrast, responses of L3 silenced flies underestimates stimuli in low luminance regimes and overestimates them in the bright regimes. Time traces and peak turning velocities of control and L3-silenced flies to the uniform-contrast stimuli at -50% contrast. The columns represent three of the five edges (the dimmest, intermediate and the brightest) shown in each regime. Rows correspond to five different adaptation states, generated by ND filters. Sample size in N=10 per plot. Traces and plots in show mean ± SEM.

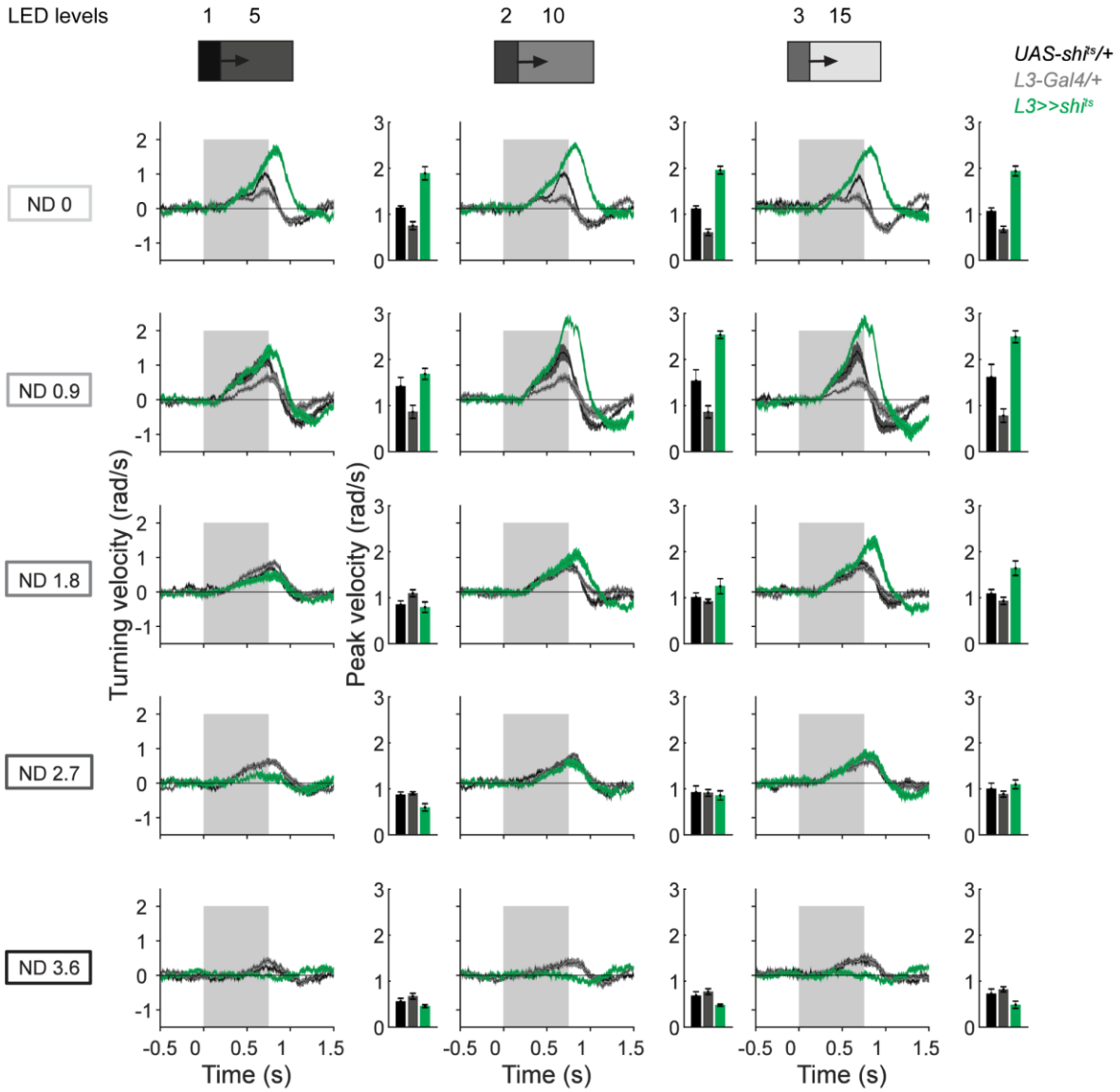

Figure S3: At -80% contrast, responses of L3 silenced flies underestimates stimuli in low luminance regimes and overestimates them in the bright regimes. Time traces and peak turning velocities of control and L3-silenced flies to the uniform-contrast stimuli at -80% contrast. The columns represent the three edges shown in each regime. Rows correspond to five different adaptation states, generated by ND filters. Sample size in N=10 per plot. Traces and plots in show mean ± SEM.

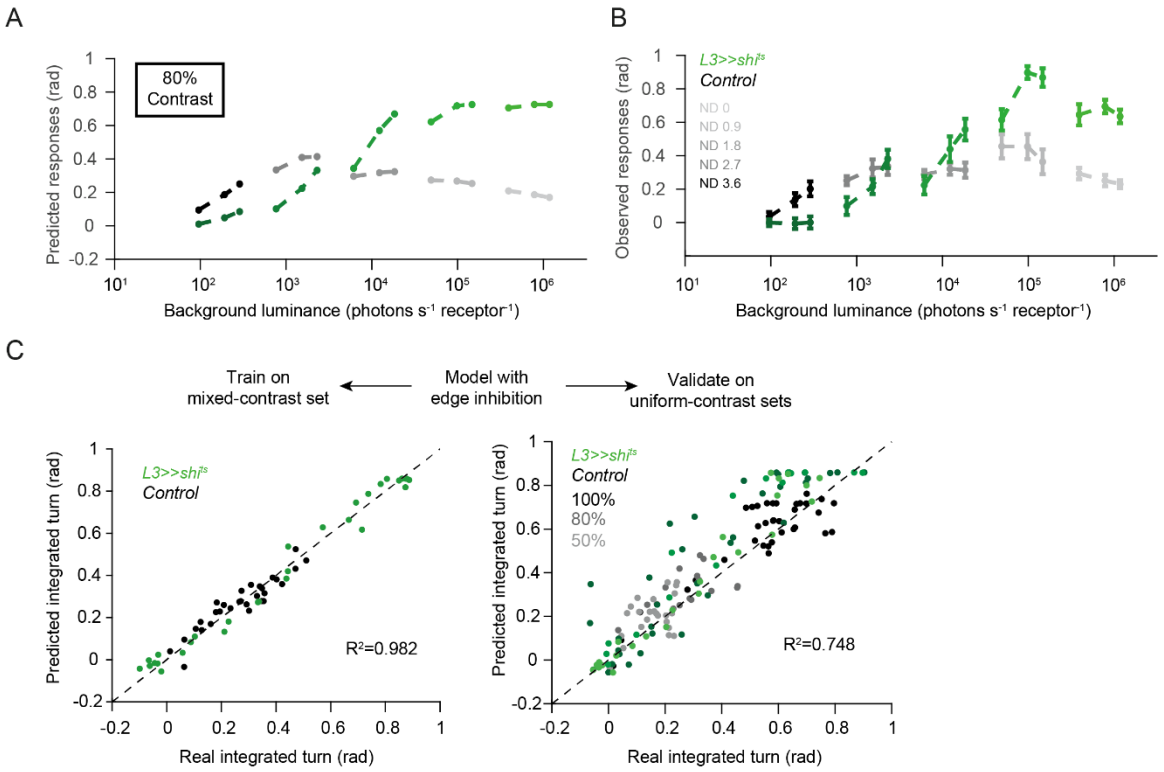

Figure S4: Model trained on mixed-contrast dataset predicts responses to uniform contrasts with high accuracy. (A) Behavior of control and L3-silenced flies in response to -80% contrast stimuli as predicted by the revised model (eqution 2). (B) The corresponding observed behavioral responses are shown for comparison. (C) The model including edge inhibition (equation 2) was trained on responses to the mixed-contrast stimuli and validated on responses to the uniform-contrast stimuli. Predicted vs observed responses are plotted separately for the training set (left) and the test set (right). Prediction accuracies are represented by the R-squared values. Dashed lines are unity lines.

2. Supplemental tables

Table S1: Model (2) fit on the uniform-contrast data – parameter estimates

Coefficient	Estimate	SE	p-Value
a_0	-0.782	0.045	4e-37
a_1	1.508	0.059	1e-55
a_2	-0.704	0.132	4e-7
a_3	1.806	0.151	3e-23
$a_3 b_0$	1.161	0.125	2e-16
a_4	0.399	0.058	2e-10
a_5	0.093	0.006	2e-34

Table S2: Model (2) fit on the mixed-contrast data – parameter estimates

Coefficient	Estimate	SE	p-Value
a_0	-0.997	0.038	4e-32
a_1	1.857	0.048	2e-40
a_2	-0.719	0.113	5e-8
a_3	1.602	0.146	3e-15
$a_3 b_0$	1.024	0.147	5e-9
a_4	0.486	0.053	2e-12
a_5	0.090	0.020	4e-5

Table S3: Model (2.1) fit on all datasets together (uniform-contrast and mixed-contrast sets) – parameter estimates.

Coefficient	Estimate	SE	p-Value
a_0	-0.028	0.017	0.093
a_1	1.508	0.054	4e-70
a_2	-0.704	0.122	3e-08
a_3	1.225	0.120	8e-20
$a_3 b_0$	1.161	0.116	2e-19
a_4	0.399	0.053	3e-12
a_5	0.093	0.005	2e-42
a_0'	-0.011	0.030	0.727
a_1'	0.411	0.100	6e-05
a_2'	-0.079	0.225	0.727
a_3'	0.027	0.252	0.915
$a_3' b_0'$	0.016	0.250	0.950
a_4'	0.095	0.102	0.355
a_5'	0.003	0.034	0.934

Table S4: Model (3) fit on on all datasets together (uniform-contrast and mixed-contrast sets) – parameter estimates.

Coefficient	Estimate	SE	p-Value
$\boldsymbol{a_0}$	-0.031	0.014	0.026
$\boldsymbol{a_1}$	1.550	0.044	4e-89
$\boldsymbol{a_2}$	-0.721	0.104	5e-11
$\boldsymbol{a_3}$	1.219	0.103	6e-25
$\boldsymbol{a_3 b_0}$	1.155	0.100	5e-24
$\boldsymbol{a_4}$	0.425	0.046	2e-17
$\boldsymbol{a_5}$	0.096	0.005	8e-49

General discussion

Objects reflect different amounts of light under different illumination, but our eyes and brain have to interpret these light signals as coming from the same objects. The influence of changing illumination is counteracted by a luminance gain. The ideal case of luminance gain control from the perspective of object recognition is to attain luminance-invariant contrast sensitivity. Whereas photoreceptors control their gain to remain sensitive to input changes across illumination levels, they and the first-order interneurons do not achieve luminance invariance to an extent that their contrast sensitivity alone can support perceptual constancy. If guided by peripheral contrast computation, perception and behavior would deviate from constancy, especially when self-motion imposes a challenge of adapting the sensitivity quickly. This thesis investigates strategies of the first-order interneurons in the fly eye – the LMCs – to enable appropriate contrast computation in the downstream circuitry. LMCs acquire physiological specializations to segregate photoreceptor signals into distinct features, luminance and contrast. In Manuscript 2, I showed that both features, or rather their differently filtered, linear and non-linear transformations, are relayed to both ON and OFF pathways. Manuscripts 1 and 3 show that within the OFF pathway, the features interact to achieve a contrast-constant estimate useful to guide behavior. Manuscript 1 uncovers the specific role of luminance information in enhancing contextual dim cues, when poorly adjusted LMC gain underestimates the cues. Manuscript 3 demonstrates how the corrective role of luminance signals generalizes across contrasts and luminances, as well as fast and slow timescales. LMCs fail to both enhance and reduce gain at fast timescales, and consequently underestimate cues of high behavioral relevance (i.e. high contrast) and overestimate cues of lower relevance. Luminance signals enable a two-way gain correction to correct for these deviations from contrast constancy. In very dim conditions, the same luminance-sensitive pathway enhances detection of stimuli. In sum, we found that the LMCs do not aim to achieve a behaviorally relevant contrast sensitivity themselves but adopt information processing strategies to enable accurate contrast estimation in the downstream circuitry.

In the following sections, I will discuss how our findings add to the wealth of knowledge about visual strategies in both flies and vertebrate retina. First, I will discuss a common role of luminance signals in establishing perceptual constancy – the goal of luminance gain control I so far focused on. I will next discuss how the fly LMC strategy, namely feature diversification downstream of receptors, generalizes across species as well as sensory modalities. Following that, I will elucidate how ON and OFF pathways compare in terms of how they guide behavior and how they employ luminance signals for gain correction. Finally, I will elaborate on how the post-LMC gain control described in this study relates to the diversity of known post-receptor gain control mechanisms.

1. Universal role of luminance signals in visual constancy

As argued early on, luminance difference rather than mere luminance provides useful information for image processing. Also, from a predictive coding perspective, steady background luminance signals are redundant. They mostly correlate with illuminant properties, and tell little about object properties such

as reflectances. Contrast on the other hand correlates with reflectances, when computed in a luminance-invariant manner. In line with this, fly LMCs were thought to capture predominantly contrast-sensitive signals from photoreceptors, and reduce transmission of the sustained steady-state receptor signal (Laughlin, 1989). Such predictive coding strategy would ensure that contrast signals are relayed with greater coding capacity offered by the neurons' full operating range (Laughlin, 1981; Srinivasan et al., 1982). Purely contrast-sensitive neurons like L2 indeed discard luminance information, and do not show a luminance-dependent baseline. Among processes that confer this property to L2, lateral inhibition enables subtraction of spatially redundant luminance information from L2 responses (Freifeld et al., 2013a; Laughlin and Osorio, 1989; Mimura, 1974). However, subtraction of temporally redundant information relies mostly on the neuron's temporal filtering properties. When considerably long luminance history shapes gain control, contrast computation cannot achieve invariance with regard to rapidly changing luminance. Our data show that LMC transient signals are not fully luminance invariant, in both slowly and rapidly changing environments, and thus luminance information can no longer be considered redundant. In fact, luminance signals are required as a reference for downstream contrast correction. L3 and also L1 neurons relay luminance signals in parallel to contrast signals and help achieve contrast constancy at a proximal processing site. Sustained luminance-sensitive signals are found at various stages of vertebrate visual processing, including bipolar cells (Awatramani and Slaughter, 2000; Ichinose and Hellmer, 2016; Oesch and Diamond, 2011; Werblin, 1974), horizontal cells (Werblin, 1974), RGCs (Baden et al., 2020; Ikeda and Wright, 1972) and even V1 neurons (Huang and Paradiso, 2008). Sustained signals in the rod bipolar cells are thought to enter the cone pathway via AII amacrine cells, where they can enable contrast computation in scotopic condition, thus potentially enhancing dim light vision (Oesch and Diamond, 2011). Sustained and transient RGCs are thought to convey spatial contrast and orientation/motion features, respectively (Ikeda and Wright, 1972). However, behavioral relevance of these associations is unknown. Given that the cellular and environmental constraints are common for all peripheral visual systems, and that post-receptor luminance gain controls exist in vertebrate systems as well (Dunn et al., 2007; Rieke and Rudd, 2009a), luminance information may shape stable contrast computation in vertebrate visual systems too.

Luminance signals potentially correct deficits in contrast computation in both spatial and temporal domains. As columnar neurons that directly communicate with downstream columnar neurons, both L1 and L3 can influence downstream localized contrast processing with their differentially filtered luminance input. On the other hand, availability of luminance information past photoreceptors allows another instance of lateral inhibition which, unlike at the photoreceptor-LMC synapse, can benefit from luminance integrated over a larger area by means of wide-field neurons. However, even the signals serving as substrate for spatial integration evolve over time, making it less likely that lateral inhibition will fully account for the gain correction in dynamic conditions. I speculate that the spatial integration processes mainly compensate the deficits in LMC contrast coding observed at slowly changing conditions, whereas the additional gain control challenges posed by dynamic conditions are further tackled by local interactions of luminance- and contrast- sensitive components downstream of LMCs.

We showed that luminance information is necessary for constant perception of both ON and OFF contrasts, and that encoding of both contrast polarities in LMCs is similarly challenged by rapid luminance changes. Surprisingly, in bigger flies, luminance increments were linked to comparatively faster timescales of LMC adaptation than the ones observed with luminance decrements (Laughlin and Hardie, 1978). Also, ON RGCs are more likely to encode luminance-invariant contrast than OFF RGCs, under similar conditions (Idrees and Münch, 2020). However, contrast-sensitive LMCs L1 and L2 in *Drosophila* exhibit linear response properties with respect to contrast (Clark et al., 2011a), supporting the predominantly symmetrical ON-OFF contrast computation apparent in our data, and a common luminance-dependent mechanism tackles the challenges faced by the two pathways. Interestingly, this implies luminance encoding too has to work symmetrically. L3 encodes absolute luminance at least over a few orders of luminance, satisfying this requirement. L1 luminance signals also appear symmetrical in response to the staircase stimulus, however if L1 encodes absolute luminance remains to be determined.

Interestingly, color contrast also needs to be perceived stably to be a useful cue under varying illumination. Like achromatic vision, color vision was thought to be discounting illuminant information through chromatic receptor adaptation, commonly referred to as Von Kries adaptation after (von Kries, 1905). However, some of the underlying adaptation mechanisms are also slow and cannot explain how we exhibit color constancy almost instantaneously with the illumination change (Chittka et al., 2014; Lotto and Chittka, 2005). In addition, information about the illuminant spectrum in natural scenes is useful in many ways, for e.g. to recognize time of the day, and animals including us are aware of this information. Studies of bumblebee color vision reveal compelling evidence that the illuminant information is retained in the brain and even used as a contextual cue towards achieving color constancy (Dyer, 2006; Lotto and Chittka, 2005). Bees prominently rely on color cues to identify flower species, and also exhibit color-constant behavior immediately after a switch in illuminant (Neumeyer, 1981), in line with evidences that several post-receptor mechanisms contribute to establishing color constancy (Chittka et al., 2014). Together, this suggests involvement of luminance-sensitive neurons in achieving color constancy, besides contrast constancy. L3 makes a promising candidate to relay luminance information to the chromatic pathway is *Drosophila*, since it innervates Tm9 and Tm5 neurons where it interacts with R8 and R7 output – photoreceptors of the chromatic pathway (Gao et al., 2008; Takemura et al., 2013a). Besides, a multi-columnar neuron Dm9 integrates inputs from L3 and R7, R8 (Heath et al 2020). L3 also itself receives input from R8, and synapses with Tm20 neurons, thus multiple interactions with chromatic channels are possible (Gao et al., 2008; Lin et al., 2016; Melnattur et al., 2014; Takemura et al., 2013a). Color contrast guides *Drosophila* behavior, and color discrimination is important not only for phototaxis but also for mating choices (Fischbach, 1979; Gao et al., 2008; Katayama et al., 2014; Schnaitmann et al., 2020), suggesting color constancy is behaviorally useful. Recent advances uncovering elaborate color processing circuitry in *Drosophila* can be combined with behavioral assays (Heath et al., 2020; Pagni et al., 2021; Schnaitmann et al., 2018), to explore the role of luminance-sensitive neurons in insect color constancy.

2. Diversification of features downstream of receptors – common sensory principle

2.1 Diversification of luminance and contrast in the fly LMCs

Three LMC classes in *Drosophila* filter the same photoreceptor input differently (Figure 4). The achromatic photoreceptors R1-R6 encode both contrast and luminance. L1 acquires an amplified contrast signal and also retains a luminance-sensitive baseline, whereas L2 acquires a similarly amplified contrast component alone. L3 conspicuously retains luminance information, although it does not fully discard contrast information (Ketkar et al., 2020). L3 non-linearly amplifies low luminances unlike L1, arguing that these two neurons in fact encode two different features in their baseline (Figure 4C, D). As discussed in Manuscript 3, the two luminance features are of distinct behavioral relevance. Below I consider how contrast encoded by different LMC classes could also correspond to different features, unlike the current view.

We relate L1's different luminance sensitivity to the coexisting contrast sensitivity, in that only a fraction of its operating range can be used for luminance coding. Likewise, L1 also allocates only a part of its operating range for contrast coding, and thus may differ from L2. Given the high-gain photoreceptor-LMC synapse, L1 may not be able to capture the entire range of photoreceptor responses, or the synaptic amplification would be smaller than L2 (Laughlin, 1989). In bigger flies, where the LMCs were earlier characterized, contrast encoding between L1 and L2 is not reliably compared without cell-type specific access (Juusola et al., 1995; Laughlin et al., 1987). Thus, how L1 contrast sensitivity compares with that of the photoreceptors on the one hand and L2 on the other hand remains to be explicitly tested. Nevertheless, L1 and L2 function is differently required for motion detection in different contrast ranges (Rister et al., 2007), further supporting the idea of differential contrast coding in L1 and L2.

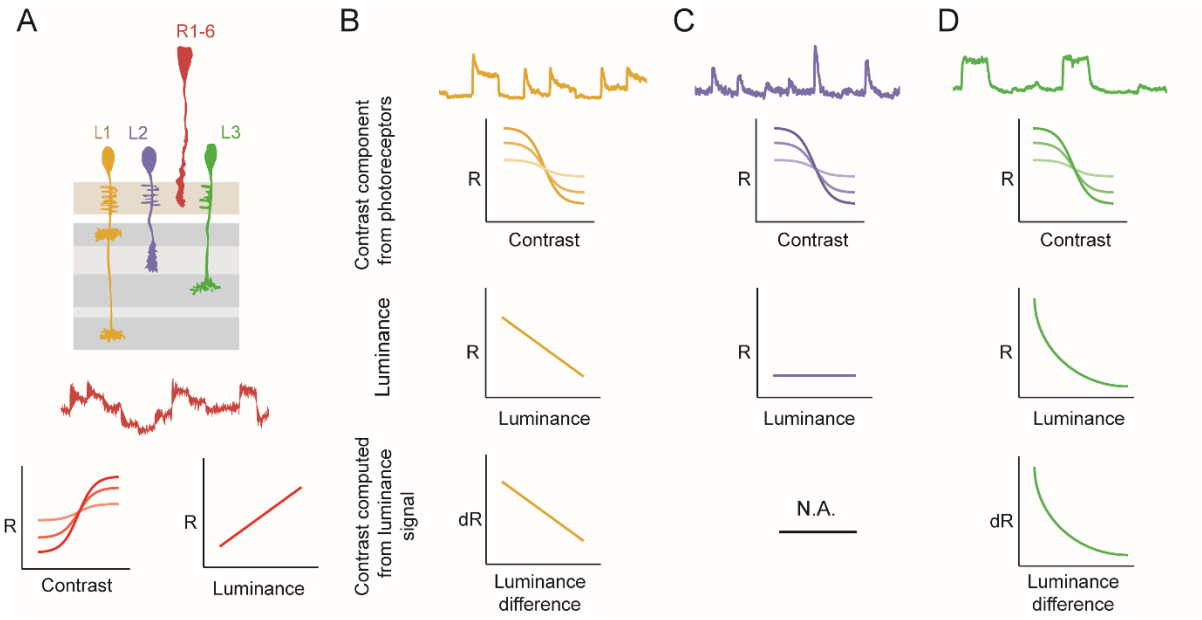

Figure 4: *Drosophila* LMCs specialize in the extraction of luminance and contrast features. (A) LMCs L1, L2 and L3 photoreceptors receive the same photoreceptor input (red), which contains contrast as well as luminance signals. Contrast sensitivity increases with luminance for a certain range of luminance, giving steeper contrast-response curves with increasing luminance (darker shade corresponds to higher background luminance). Luminance signals vary linearly over some orders of luminance (before they attain a fixed value). (B) L1 captures inverted versions of both contrast and luminance signals (orange). Contrast signals are amplified presumably with a uniform gain across luminance, and luminance encoding is predominantly linear. If a neuron downstream of L1 computes contrast from the luminance signals, it will thus be proportional to a linear L1 response difference. (C) L2 captures contrast signals in an inverted and amplified manner (purple), similar to L1. The constant baseline does not encode any luminance. (D) L3 has small contrast-sensitive components that potentially match photoreceptor contrast components, however it encodes mainly luminance (green). Low luminances elicit non-linearly high responses. If a post-synaptic neuron computes contrast from the L3 luminance signals, it will be proportional to the non-linear L3 response difference. Thus, resolution of contrasts in low luminance computed downstream of L3 would be fundamentally different from L3's own contrast sensitivity.

Does L3 also contribute to contrast diversification? We observed that L3 is sufficient for behavior in both the ON and OFF pathways. Since contrast is the most basic visual cue, the L3 pathway must compute contrast (Manuscript 2,(Ketkar et al., 2020)). This can happen within L3 or in a downstream neuron. L3 responses themselves comprise a fast transient component, which is often indiscernible in calcium signals due to their slow dynamics, but certainly visible in voltage recordings (Hardie and Weckström, 1990; Juusola et al., 1995). We also could see transient components in L3 response when using the genetically encoded voltage indicator ASAP2, arguing that L3 itself can relay contrast signals (Ketkar et al., 2020) that are less amplified than L1 and L2. However, we hypothesize a neuron downstream of L3 to derive a clearer and stronger contrast signal by means of its own temporal filtering, rather than merely inheriting the L3 contrast signals. For one, purely L3-driven behavior seems to mirror the luminance-coding L3 properties, such that the particularly dim stimuli are non-linearly amplified. This can be achieved when a downstream neuron is sensitive to the changes in L3 baseline (Figure 4D). Secondly, amplification of contrast signals at the photoreceptor-LMCs synapse is constant across luminances (Laughlin et al., 1987). If this also applied to the photoreceptor-L3 synapse, L3 would

encode stimuli as a sigmoidal function of luminance, thus encoding extreme luminances with reduced sensitivity, contradicting the high sensitivity for dim stimuli observed in behavior. These evidences together support our hypothesis that contrast signals in L3 pathway, supporting behavior, emerge downstream of L3. Most prominent post-synaptic partners of L3 in both ON and OFF pathways – Mi9 and Tm9 – are rather sustained, and their contrast-coding properties remain to be systematically explored. Nevertheless, contrast signals in the L3 pathway still result from the diversity of temporal filtering properties downstream of photoreceptors, while also providing behavioral evidence that such diversification is beneficial.

2.2 Diversification in other visual systems and modalities

Like Dipteran LMCs, first-order interneurons of many other insects have been described to differ in their filtering properties. For example, bumblebee LMCs show different transient and sustained characteristics (Rusanen and Weckström, 2016). Butterfly LMCs have spiking and non-spiking types, with the spiking types changing their coding strategy with light intensity (Rusanen et al., 2018). Importantly, bipolar cells – the first-order interneurons in vertebrate retina – show exceptional diversity of spatial and temporal filtering properties (Baden et al., 2013; Euler and Masland, 2000; Euler et al., 2014a; Schreyer and Gollisch, 2021). Rod bipolar cells show sustained characteristics but also a transient component, whereas cone bipolar cells have both transient and sustained classes, and the transient cells have different adaptation time constants and tonic-to-phasic ratios (Awatramani and Slaughter, 2000; Euler and Masland, 2000; Ichinose and Hellmer, 2016; Ichinose et al., 2014; Odermatt et al., 2012; Oesch and Diamond, 2011). Moreover, some bipolar cells can have nonlinear synapses that can increase the dynamic range for encoding luminance past phototransduction (Odermatt et al., 2012). Thus, many parallels exist between the diversification of coding strategies between first order visual interneurons in vertebrates and invertebrates. The bipolar cell diversity is known to shape temporal diversity in RGCs, and as a result, RGC types can perform a diverse array of highly complex tasks including motion discrimination and motion prediction (Gollisch and Meister, 2010). However, the impact of the diverse RGC functions on behavior is not explicitly tested.

A straightforward advantage of diversified temporal filtering is to achieve differential temporal frequency (TF) tuning and speed tuning in the downstream circuitry. Neurons with different temporal filter properties are essential to implement motion detection algorithms, and speed tuning models rely on differently TF-tuned motion detectors (Arenz et al., 2017; Behnia et al., 2014a; Creamer et al., 2018). These aspects of visual processing are well-studied in fruit flies, and the behaviorally relevant temporal properties were observed in second-order interneurons presynaptic to the elementary motion detectors of the fly eye – T4/T5 cells (Arenz et al., 2017; Serbe et al., 2016; Strother et al., 2017). We now show that a diversity of temporal filtering properties already emerges at the first-order interneurons – LMCs, and the different LMC properties translate to behavior many synapses downstream of LMCs.

Interestingly, most other sensory modalities also need to differentially filter receptor input to extract distinct temporal information. Local interneurons of the *Drosophila* antennal lobe specialize to detect

rapid and slow fluctuations in olfactory input (Nagel and Wilson, 2016). Mechanosensory neurons with different temporal properties in the *Drosophila* Johnston's organ detect vibration and deflection of antennae (Kamikouchi et al., 2009). Also, *Drosophila* proprioception encodes joint movement and position with phasic and tonic responses, respectively (Mamiya et al., 2018). Lastly, recognition of conspecific in many insect species relies on detection of temporal patterns in calling songs (Ai et al., 2018; Clemens and Hennig, 2020). Thus, differential temporal filtering at a peripheral processing stage is fundamental to the function of many sensory systems.

3. Parallels and differences between ON and OFF pathways

Both ON and OFF motion-guided behaviors are nearly contrast constant, whereas the principal contrast-sensitive inputs to both pathways, i.e. L1 and L2, scale their contrast responses with contextual luminance. In line with this, both ON and OFF pathways require luminance signals to guide contrast-constant behavior. Despite these similarities, the two pathways are not exactly mirror-symmetric.

First, the residual luminance dependence seen in wild-type behavior shows opposite trends in the two pathways: responses to -100% contrast stimuli vary slightly positively with contextual luminance, whereas responses to +100% contrast stimuli vary negatively with contextual luminance. Thus, ON and OFF contrasts of the same strength do not have comparable behavioral relevance when matched across luminances. In this regard, the ON stimuli rather resemble low-contrast OFF stimuli. These two stimulus settings further resemble in terms of an inhibitory contribution from L3. We attribute these striking similarities between dissimilar ON and OFF contrasts to their edge luminances. Both low-contrast moving OFF edges as well as ON edges with any contrast vary in luminance. L3 inhibition based on edge luminance thus seems a general principle across pathways.

Why would any behavioral response scale inversely with luminance? In our behavioral assay comprising single moving OFF edges, the responses may include a phototactic component in addition to the motion-driven i.e. optomotor component. Flies generally show positive phototaxis, however the choice is a complex function of light intensity (Fischbach, 1979; Jacob et al., 1977). When using wavelengths similar to those in our stimuli, the light source attracts flies progressively more with increasing light intensity, but very high intensities are less attractive or even repulsive. Our OFF stimuli with low contrast may offer a phototactic choice wherein bright edge luminances are more attractive than their brighter backgrounds, and the resulting phototactic direction is opposite to the optomotor direction. On the other hand, our ON edge stimuli comprise multiple edges and offer little scope for phototactic influence. We speculate that the negative luminance correlation of ON responses is due to luminance-dependent startle, however, this hypothesis needs further verification. Nevertheless, traits such as phototaxis underline the differential behavioral relevance of ON and OFF contrasts, reflected in their different circuit architectures and physiology.

We found that both L1 and L3 luminance signals are required in both ON and OFF pathways. Among them, L3 has a conserved function in both pathways, in that L3 signaling always enhances responses to

stimuli in contextual dim light. However, as a second instance of asymmetry, the extent to which the L1 and L3 signals contribute to constancy differs across ON and OFF pathways. ON edge-driven behavior can still handle the challenges of dynamic conditions, if one of the two luminance inputs are blocked. Only when both L1 and L3 are blocked, the flies underestimate contextual dim edges. In contrast, the OFF pathway requires both L1 and L3 signals for contrast constancy, individually. Interestingly, a different number of circuit components relay the two luminance inputs, separately and in combination, in the two pathways (Figure 5). In the ON pathway, Mi9 relays L3 input, Mi1 integrates L1 and L3 inputs, whereas many neurons including Tm3 and L5 are postsynaptic to only L1 (Shinomiya et al., 2019; Strother et al., 2017; Takemura et al., 2013a). In the OFF pathway, Tm9 neurons integrate L1 and L3 signals, and L1 contributes through yet another indirect channel (Fisher et al., 2015b)(Fisher et al 2015). However, a channel relaying excitatory L3 contribution alone is not known, and thus L3 may only act via Tm9 in an L1-dependent way. Whether L1 is also required for gain reduction in the OFF pathway, like L3, remains to be explored.

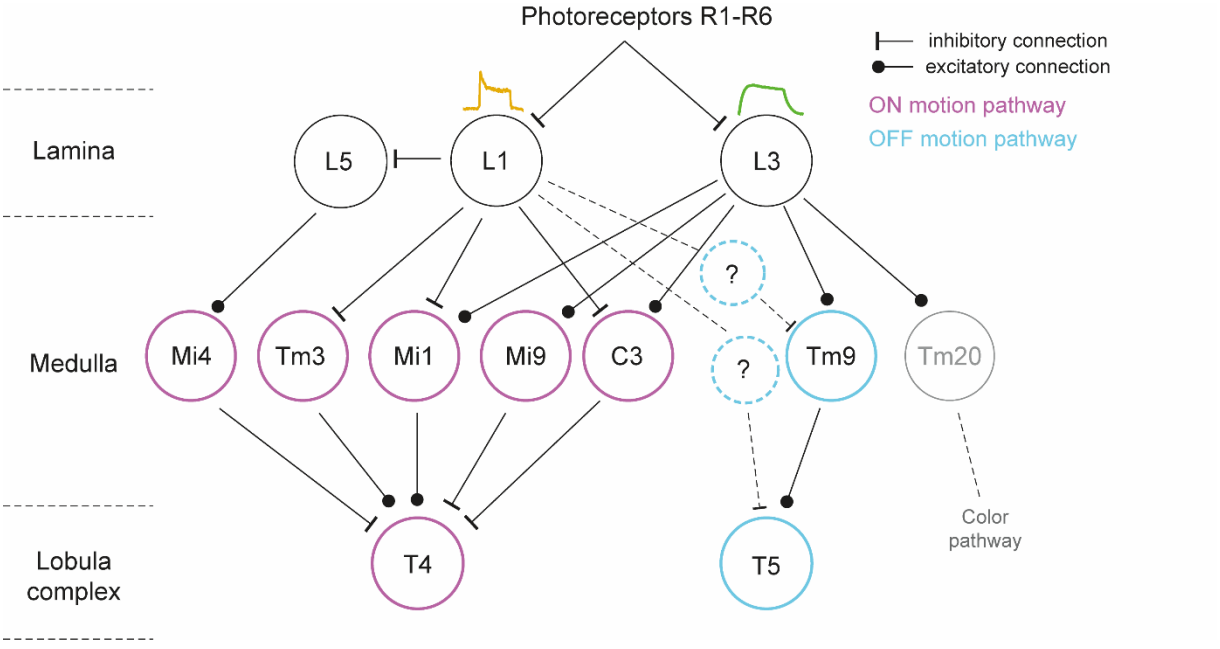

Figure 5: Luminance information from L1 and L3 is conveyed to both ON and OFF motion-sensitive neurons. Downstream of the photoreceptors R1-R6, L1 and L3 capture luminance information differently. L1 luminance signals can reach the ON motion-sensitive T4 cells via multiple channels, including L5→ Mi4 channel, Tm3, Mi1, C3. Among these, Mi1 and C3 integrate L3 luminance signals as well, and L3 signals are separately conveyed by Mi9 neurons. In the OFF pathway, only Tm9 is known to convey direct L3 signals to the OFF motion-sensitive T5 neurons. Tm9 neurons also indirectly receive L1 luminance input, and L1 is known to communicate with T5 via yet unknown connections. Certain neurons post-synaptic to L3, including Tm20, convey luminance information to the color pathway, too.

4. Post-receptor luminance gain control across invertebrates and vertebrates

Our data reveal the requirement of post-receptor gain control in flies, and the LMC signals containing the information for these gain control operations. The exact location where the gain control leading to contrast constancy happens remains to be explored. However, diverse gain control processes at many

processing stages have been studied in different species, including several vertebrate species. For example, gain control is evident at every retinal stage including photoreceptors, horizontal cells, bipolar cells, amacrine cells and RGCs, and even in LGN and V1 neurons (Alitto et al., 2019; Carandini et al., 1997; Schwartz and Rieke, 2013; Shapley and Enroth-Cugell, 1984).. Seldom are the post-receptor stages linked to visual constancy, with few exceptions including (MacEvoy and Paradiso, 2001). However, their contribution to luminance gain control is well-accepted, especially to improve signal processing reliability. Peripheral luminance gain control in dim light is especially risky, in that it can result in detection and subsequent amplification of spurious signals embedded in high levels of noise (Rieke and Rudd, 2009a). In such case, rapid gain control rather emerges at a later retinal stage where a low-noise signal is available due to increased spatial summation (Dunn et al., 2007). As we noted in Manuscript 3, *Drosophila* contrast processing also generally needs corrective amplification in dim conditions, and in rapidly changing conditions, and hence the post-receptor gain control we proposed has shared function with that observed in vertebrates. However, the corrective gain control in *Drosophila* is required also in contextual and absolute bright light, where noise is less likely to be a limiting factor for the peripheral processing stages. Why is a post-receptor site beneficial for gain control over a broad range of conditions, and why is such generalized limitation of peripheral gain control not observed in other visual systems? While these questions have to be separately and extensively addressed, we first speculate that specifically addressing contrast constancy instead of sensitivity thresholds may have revealed further limitations of the peripheral processing stage. Secondly, it is possible that calcium imaging revealed different temporal properties than electrophysiology that was widely employed in earlier studies concerning peripheral adaptation, since the two recording techniques have distinct biases (Ali and Kwan, 2020; Siegle et al., 2021; Wei et al., 2020b). Lastly, we propose that a conspicuous limitation of the fly visual periphery was evident solely because behavior could be causally linked to the function of neurons, through genetic access to specific cell types. Linking neuronal function to behavior in other model systems is usually done by independently measuring physiology and behavior, which unavoidably require different experimental conditions. Therefore, similar peripheral mechanisms might be in place in other species, but could have been overlooked due to the methodological limitations. Our study, in addition to examining physiology and behavior under identical stimulus conditions, also establishes a causal connection between the two with genetic silencing experiments. Thus, the study highlights unique advantages of the *Drosophila* genetic toolkit available to dissect a versatile visual circuitry.

Importantly, some of the post-receptor gain controls are linked to contrast adaptation, another important mechanism that enables optimal use of neuronal operating range to encode prevailing variance in luminance (Carandini and Heeger, 2012; Laughlin, 1981). Multiple bipolar and RGC types in vertebrates as well as certain second-order interneurons in *Drosophila* vision implement contrast gain control (Brown and Masland, 2001; Drews et al., 2020; Garvert and Gollisch, 2013; Khani and Gollisch, 2017; Matulis et al., 2020a), and adaptation to contrast is considered an efficient coding strategy (Laughlin, 1981; Yedutenko et al., 2021). Does the corrective gain control proposed by our data coincide with contrast gain control? We think it is rather a distinct luminance gain control, for several reasons.

First, the corrective role of luminance led to constant behavioral responses to (Weber) contrast values, whether presented at different luminances or with different contrasts. Contrast adaptation instead changes behavioral relevance of contrast values, and thus leads to deviations from constancy (Webster and Mollon, 1995). Secondly, the luminance-sensitive L3 neurons or their post-synaptic partners are not strongly implicated in contrast adaptation, and circuit components underlying contrast and luminance gain are rather mutually exclusive (Matulis et al., 2020a)(Gür and Silies, unpublished). However, Mi1 neurons post-synaptic to L1 rapidly adapt to contrast, suggesting gain correction post L1 may deal with contrast gain. Lastly, contrast and luminance statistics independently vary in visual scenes, and adaptation to them likely occurs in independent parallel channels (Frazor and Geisler, 2006; Mante et al., 2005). Together, we suggest that the gain correction mediated by L3 pathway at least is to compensate for the limitations of peripheral luminance gain control, and aims for contrast constancy in behavior.

Conclusions and outlook

Sighted animals including humans live in a world with different reflecting surfaces. Brains can base visual identification of objects on their different reflecting properties if they accurately compute the feature representative of these properties - Weber (or Michelson) contrast. Estimating such luminance-invariant contrast within the peripheral processing stages is not feasible due to cellular constraints, and furthermore, it may not be an optimal and reliable strategy in dynamic environments. However, the peripheral stages can ensure that the downstream processes have access to relevant information to compensate for the peripheral limitations. This thesis, investigating contrast computation in the peripheral visual system of *Drosophila* from a behavioral perspective, concludes that

1. The photoreceptor and LMC gain is not optimally adjusted for contrast constancy in behavior, in both slowly and quickly changing conditions. However, LMCs adopt a strategy of preserving luminance information in parallel to contrast information, allowing additional luminance gain control in the downstream circuitry.
2. The peripheral processing stages also split into ON and OFF pathways, and both pathways require luminance and contrast information for constancy in behavior. LMC classes individually specialize in segregating luminance and contrast features and relay them to both ON and OFF pathways emerging downstream. Two LMC classes in fact encode two distinct functions of luminance, reminiscent of the signal diversification strategy implemented by the first-order interneuron population in vertebrate retina.
3. Post-LMC luminance gain control has to fulfill differential requirements of gain reduction and enhancement across luminance-contrast space as well as at fast and slow timescales. Each requirement is met by distinct processing of contrast and luminance signals, or their interaction. The circuitry downstream of LMCs likely hosts these operations in parallel streams, before the output of these parallel streams is combined to achieve a contrast-constant estimate useful for behavior.
4. One of the post-LMC gain correction operations is aimed at enhancing dim light vision. The luminance-sensitive neurons L3 are physiologically suited to amplify dim stimuli, indicating a strategy of the insect brains to support vision across broad luminance range before the evolution of rod-cone bifurcation.
5. Organizing rapid gain control mechanisms at post-receptor sites can be a conserved information processing strategy across visual systems, since these sites can provide a noise-free substrate past spatial summation stages for a more reliable gain control.

The study opens up the possibility to acquire a detailed understanding of these strategies at biophysical and circuit levels, and across different species.

Neural correlates of post-LMC gain correction in both OFF and ON pathways

The visual system of *Drosophila* is thoroughly explored at the anatomical, cellular and circuit levels. Therefore, the system offers a promising opportunity to understand the location as well as the

molecular and circuit mechanisms underlying the post-LMC gain control operations discussed in this thesis. The algorithmic model in Manuscript 3 proposes a multi-channel circuit for the integration of luminance and contrast signals in the OFF pathway, where different channels process contrast, background luminance, edge luminance and contrast-luminance interaction (Figure 7). The model can guide an experimental search for the neural correlates of its component channels. Second-order interneurons upstream of the OFF motion-selective T5 neurons can constitute these parallel channels, and T5 neurons can integrate their output. Preliminary data in the Silies lab indeed support the idea that T5 neurons are contrast constant (Gür and Silies, unpublished), and this hypothesis should further be validated by testing the extent of contrast constancy as well as dim-light efficiency achieved at the level of T5 neurons. If T5 neurons occupy the niche of integrators, the computation in upstream interneurons can be matched with the distinct channels of the model. This can be done with both physiological and behavioral tests. For example, genetically blocking the output of a neuron type that relays information about edge luminance would abolish the post-receptor gain decrement at low contrasts, leading to overestimation of stimuli by behavioral responses as well as T5 calcium responses.

Connectomics studies can further guide the hypotheses about the match between the second-order interneurons and the model components (Shinomiya et al., 2014b, 2019; Takemura et al., 2013b, 2017b). Some hypotheses are already discussed in Manuscript 3. However, some indirect connections between the LMCs and second-order interneurons, not revealed by the connectomics approach, are important too. For example, L1 is an indirect upstream connection of Tm9 – a crucial T5 input (Fisher et al., 2015d), and we also showed that L1 function is required for contrast-constant OFF pathway behavior (Manuscript 2). Moreover, L1 has both contrast and luminance components in its response. Our model so far does not account for the nature of L1 contribution to the OFF-pathway gain control, neither does it estimate which of the contrast and luminance components are required. Determining the computational correlate of Tm9 may open up the possibility to pinpoint the physiological contribution of L1 in the OFF pathway. Nevertheless, further links of L1 to the OFF pathway, including the GABAergic C2 and C3 neurons, imply a more complex L1 involvement that can be unraveled only upon a detailed characterization of behavior in absence of L1 function.

Coming to the ON pathway, a thorough characterization of behavior across luminance-contrast space is a prerequisite to capture all post-LMC gain control operations. However, the observed behavioral responses to 100% ON contrast revealed that both L1 and L3 pathways contribute contrast information that is individually sufficient, whereas their combined (potentially luminance) information regulates gain enhancement in contextual dim light (Manuscript 2). Furthermore, L3 individually contributes inhibitory signals to ON pathway. These findings together highlight computational similarities between the ON and OFF pathways, based on which a multi-channel integration of luminance and contrast signals can be hypothesized to occur downstream of LMCs. Assuming the ON motion-selective T4 neurons integrate differently processed luminance/contrast information, analogous to the OFF-pathway T5, the second-order interneurons presynaptic to T4 can be explored for their luminance-contrast integrating functions. Among the candidate neurons, Mi1 receives input from both L1 and L3, and thus could mediate their combined excitatory contribution to behavior (Takemura et al., 2013b).

Mi9 is a postsynaptic partner of L3 and is inhibitory, making it a strong candidate for L3-mediated inhibition (Strother et al., 2017; Takemura et al., 2013b).

Neural correlates of spatial pooling

Spatial summation proposed to occur downstream of the LMCs is crucial for both amplification of very dim stimuli and rapid gain modulation in a noise-free environment. Moreover, we also speculate that L3's functional dichotomy originates in the extent of spatial summation. Neural correlates of spatial summation can be searched within Dm neurons, as discussed in Manuscript 3. Whereas some Dm neuron types are likely to sample L3 output based on anatomical location of their dendrites, physiology of the postsynaptic partners of Dm neurons will validate our hypothesis that spatial pooling implements contrast correction. The postsynaptic connections of Dm neurons with T5 or its presynaptic partners can be explored, for example, through optogenetic activation of Dm neurons and physiological recordings of the postsynaptic candidate responses. Once the candidate Dm classes are narrowed down, it can further be tested if and how their summation extent is influenced by luminance.

Although a greater extent of pooling results in less noise, pool size must be restricted to allow for an acceptable spatial resolution of gain control (Rieke and Rudd, 2009a). The acceptable level of resolution will ultimately depend on spatial luminance structure of natural scenes. This hypothesis can now be tested downstream of L3. The extent of spatial pooling can be evaluated using local stimulation of L3 neurons from adjacent cartridges and simultaneously recording activity of Tm9. Pooling area thus determined can be compared with a theoretically obtained estimate of pooling area that optimally settles the tradeoff between spatial resolution and noise levels in natural scenes.

If and how luminance values influence the extent of spatial pooling can be determined through a characterization of behavior against stimulus parameters such as size or spatial frequency coupled with luminance variations. Integration of moving stimuli over greater spatial extent has been observed at lower mean luminances, in the behavior of bigger fly species (Pick and Buchner, 1979). The same study predicted an influence of luminance on temporal summation too. In line with this, transience of both photoreceptor and LMC responses goes down with decreasing luminance, and thus the extent of temporal summation goes up (Laughlin, 1989; Laughlin and Hardie, 1978). This possibility too can be tested in *Drosophila* behavior, by varying exposure times of dim and bright stimuli.

Generalized requirement of post-receptor gain control across insect species

Since contrast-sensitive LMCs in different fly species show similar limitations in contrast coding (Laughlin and Hardie, 1978; Laughlin et al., 1987)(Manuscript 3), post-LMC gain correction is likely a generalized requirement across species. However, different species, even the closely related ones from the *melanogaster* subgroup may require a different nature or extent of gain correction, depending on the specific challenges of their visuo-ecological niches. *D. melanogaster* occupy vastly differing habitats and thus are likely to face many different luminance-contrast distributions, whereas forest-dwelling species such as *D. teisseiri* may face high variation of contrasts at low luminance, on fast timescales (Lachaise et al., 1988). On the contrary, closely related *D. yakuba* that inhabit the savanna face bright

conditions but less variation on fast timescales. Thus, *D. teisseiri* may require stronger gain increments and decrements at contextual light fluctuations, possibly starting at a lower absolute luminance, than *D. yakuba* would require. Comparing contrast constancy in behavior of these species will shed light on the role of environments in shaping visual physiology and, in the long run, on the evolution of the putative physiological differences.

Our data implicate post-receptor gain control processes also in enhancing dim light vision. Whereas Drosophila are crepuscular organisms and may require limited dim light vision, it will be interesting to test if luminance information is preserved and utilized even more prominently in nocturnal insect species. From morphological observations, LMCs themselves are shown to be involved in spatial pooling in certain species. For example, dendrites of LMC subtypes in many nocturnal insects span a wider area or more eye columns than their diurnal counterparts (Greiner et al., 2004; Ohly, 1975; Ribi, 1977; Stöckl et al., 2016b; Strausfeld and Blest, 1970; Warrant, 2017). However, further possibilities of spatiotemporal summation downstream of LMCs remain to be explored. Notably, specific LMC classes in Hawkmoth species show L3-like dendritic morphology. Whereas cell-type specific investigations to probe the physiological relevance of LMC subtypes may not be currently feasible in other insects, nocturnal Drosophila individuals found in the wild may provide an immediate possibility in this regard (Pegoraro et al., 2020).

Mechanisms underlying LMC physiological specializations

LMCs L1, L2 and L3 all receive input from the same receptors, but develop distinct physiological properties (Manuscript 2). The specializations can emerge cell-autonomously, as a result of distinct membrane properties, or can additionally be shaped by lateral circuit interactions. L3 has been distinguished from L1 and L2 on the basis of potassium conductances, where L3 predominantly uses a delayed rectifier current K_d known for its sustained nature (Hardie and Weckström, 1990). L1 and L2 owe their transient properties to rapidly inactivating A-type currents (K_a), and certain species of K_a channels distinguishing L2 from L3 have been identified in terms of both expression levels and physiological impact (Gür et al., 2020). However, K_a channels do not fully account for L2 transience, suggesting further mechanisms at work. Some of the transience can be attributed to lateral inhibition, since center-surround receptive fields have been described for LMCs, and they affect response kinetics (Freifeld et al., 2013b; Laughlin and Osorio, 1989; Mimura, 1974). Our finding, that L1 – considered an L2 sibling even at the transcriptome level – differs physiologically from L2, corroborates the hypothesis about lateral inhibition as the distinguishing mechanism (Tan et al., 2015b). In line with this, L2 is proposed to be receiving stronger lateral antagonism than both L1 and L3 (Laughlin and Osorio, 1989).

The role of circuit interactions can be tested by genetically isolating individual lamina neuron types and examining their responses. Lateral connections with first-order interneurons can be silenced using an *ort* mutant background to block transmission between photoreceptors and these parallel channels (Gengs et al., 2002; Ketkar et al., 2020). Feedback loops can be silenced by blocking the synaptic output, using conditional blocking techniques such as cell-type specific $Shibire^{ts}$ (Kitamoto) expression. In addition to circuit connections, extracellular field potentials are implicated in determining LMC

response properties, especially in the subtraction of low-frequency components i.e. sustained components (Weckström and Laughlin, 2010). How the extracellular potentials affect the LMC types differently is also an open question. It can be tested if the different medulla layers hosting L1-L3 neuronal projections provide environments with different field potentials. For example, layer specificity of L3 axons can be altered by knocking down a transcription factor *dFezf* that is specifically expressed in L3 (Peng et al., 2018; Santiago et al., 2021). L3 axon terminals, innervating medulla layers M1 and M2 instead of M3 on *dFezf* loss, can be examined for having developed L1- or L2-like temporal filtering properties. However, a change of location may also result in a change of post-synaptic partners; thus, the *dFezf* loss-of-function approach can be combined with cell type isolation approach, to differentiate between the possible underlying mechanisms. Taken together, elucidating the mechanisms underlying contrast constancy in *Drosophila* might allow to link molecular specializations and circuit interactions to cell-type specific physiological properties. Such investigation will ultimately further our understanding of how visual systems evolved to support visual behaviors, in the laboratory as well as natural habitats.

References

Abbas, F., and Vinberg, F. (2021). Transduction and Adaptation Mechanisms in the Cilium or Microvilli of Photoreceptors and Olfactory Receptors From Insects to Humans. Front. Cell. Neurosci. *15*, 84.

Adelson, E.H. (1982). Saturation and adaptation in the rod system. Vision Res. *22*, 1299–1312.

Adelson, E.H. (2000). Lightness perception and lightness illusions. In The New Cognitive Neurosciences, (Cambridge: MIT Press), pp. 339–351.

Agi, E., Langen, M., Altschuler, S.J., Wu, L.F., Zimmermann, T., and Hiesinger, P.R. (2014). The evolution and development of neural superposition. J. Neurogenet. *28*, 216–232.

Aguilar, M., and Stiles, W.S. (1954). Saturation of the Rod Mechanism of the Retina at High Levels of Stimulation. Opt. Acta Int. J. Opt. *1*, 59–65.

Ai, H., Kumaraswamy, A., Kohashi, T., Ikeno, H., and Wachtler, T. (2018). Inhibitory Pathways for Processing the Temporal Structure of Sensory Signals in the Insect Brain. Front. Psychol. *9*, 1517.

Ali, F., and Kwan, A.C. (2020). Interpreting in vivo calcium signals from neuronal cell bodies, axons, and dendrites: a review. Neurophotonics *7*, 011402.

Alitto, H.J., Rathbun, D.L., Fisher, T.G., Alexander, P.C., and Usrey, W.M. (2019). Contrast gain control and retinogeniculate communication. Eur. J. Neurosci. *49*, 1061–1068.

Andrews, T.J., and Coppola, D.M. (1999). Idiosyncratic characteristics of saccadic eye movements when viewing different visual environments. Vision Res. *39*, 2947–2953.

Arenz, A., Drews, M.S., Richter, F.G., Ammer, G., and Borst, A. (2017). The Temporal Tuning of the Drosophila Motion Detectors Is Determined by the Dynamics of Their Input Elements. Curr. Biol. *27*, 929–944.

Asteriti, S., Liu, C.H., and Hardie, R.C. (2017). Calcium signalling in Drosophila photoreceptors measured with GCaMP6f. Cell Calcium *65*, 40–51.

Awatramani, G.B., and Slaughter, M.M. (2000). Origin of Transient and Sustained Responses in Ganglion Cells of the Retina. J. Neurosci. *20*, 7087–7095.

Baden, T., Schubert, T., Chang, L., Wei, T., Zaichuk, M., Wissinger, B., and Euler, T. (2013). A tale of two retinal domains: Near-Optimal sampling of achromatic contrasts in natural scenes through asymmetric photoreceptor distribution. Neuron *80*, 1206–1217.

Baden, T., Schubert, T., Berens, P., and Euler, T. (2018). The Functional Organization of Vertebrate Retinal Circuits for Vision.

Baden, T., Euler, T., and Berens, P. (2020). Understanding the retinal basis of vision across species. Nat. Rev. Neurosci. *21*, 5–20.

Bahl, A., Ammer, G., Schilling, T., and Borst, A. (2013). Object tracking in motion-blind flies. Nat. Neurosci. *16*, 730–738.

Barlow, H.B. (1957). Increment thresholds at low intensities considered as signal/noise discriminations. J. Physiol. *136*, 469–488.

Barlow, H.B. (1965). Optic nerve impulses and Weber's law. Cold Spring Harb. Symp. Quant. Biol. *30*, 539–546.

Barlow, H.B., and Levick, W.R. (1969). Three factors limiting the reliable detection of light by retinal ganglion cells of the cat. J. Physiol. *200*, 1–24.

Baylor, D.A., and Hodgkin, A.L. (1974). Changes in time scale and sensitivity in turtle photoreceptors. J. Physiol. *242*, 729–758.

Baylor, D.A., Matthews, G., and Yau, K.W. (1980). Two components of electrical dark noise in toad retinal rod outer segments. J. Physiol. *309*, 591–621.

Beaudoin, D.L., Borghuis, B.G., and Demb, J.B. (2007). Cellular Basis for Contrast Gain Control over the Receptive Field Center of Mammalian Retinal Ganglion Cells. J. Neurosci. *27*, 2636–2645.

Behnia, R., Clark, D.A., Carter, A.G., Clandinin, T.R., and Desplan, C. (2014a). Processing properties of ON and OFF pathways for Drosophila motion detection. Nature *512*, 427–430.

Behnia, R., Clark, D.A., Carter, A.G., Clandinin, T.R., and Desplan, C. (2014b). Processing properties of on and off pathways for Drosophila motion detection. Nature.

Bennet MVL (1971). Electrolocation in fish. Ann. N. Y. Acad. Sci. *V*, 347–491.

Blakeslee, B., and McCourt, M.E. (2015). What visual illusions tell us about underlying neural mechanisms and observer strategies for tackling the inverse problem of achromatic perception. Front. Hum. Neurosci. *9*.

Boergens, K.M., Kapfer, C., Helmstaedter, M., Denk, W., and Borst, A. (2018). Full reconstruction of large lobula plate tangential cells in Drosophila from a 3D EM dataset. PLoS ONE.

Borst, A. (2009). Drosophila's View on Insect Vision. Curr. Biol. *19*.

Borst, A. (2014). In search of the holy grail of fly motion vision. Eur. J. Neurosci. *40*, 3285–3293.

Boynton, R.M., Ikeda, M., and Stiles, W.S. (1964). Interactions among chromatic mechanisms as inferred from positive and negative increment thresholds. Vision Res. *4*, 87–117.

Brown, L.G., and Rudd, M.E. (1998). Evidence for a noise gain control mechanism in human vision. Vision Res. *38*, 1925–1933.

Brown, S.P., and Masland, R.H. (2001). Spatial scale and cellular substrate of contrast adaptation by retinal ganglion cells. Nat. Neurosci. *4*, 44–51.

Brown, T.M., Tsujimura, S., Allen, A.E., Wynne, J., Bedford, R., Vickery, G., Vugler, A., and Lucas, R.J. (2012). Melanopsin-Based Brightness Discrimination in Mice and Humans. Curr. Biol. *22*, 1134–1141.

Buchner, E. (1976). Elementary movement detectors in an insect visual system. Biol. Cybern. *24*, 85–101.

Burkhardt, D.A. (1994). Light adaptation and photopigment bleaching in cone photoreceptors in situ in the retina of the turtle. J. Neurosci. *14*, 1091–1105.

Burkhardt, D.A., Gottesman, J., Kersten, D., and Legge, G.E. (1984). Symmetry and constancy in the perception of negative and positive luminance contrast. J. Opt. Soc. Am. A *1*, 309.

Busse, L., Ayaz, A., Dhruv, N.T., Katzner, S., Saleem, A.B., Schölvinck, M.L., Zaharia, A.D., and Carandini, M. (2011). The Detection of Visual Contrast in the Behaving Mouse. J. Neurosci. *31*, 11351–11361.

Carandini, M., and Heeger, D.J. (2012). Normalization as a canonical neural computation. Nat. Rev. Neurosci. *13*, 51–62.

Carandini, M., Heeger, D.J., and Movshon, J.A. (1997). Linearity and normalization in simple cells of the macaque primary visual cortex. J. Neurosci. Off. J. Soc. Neurosci. *17*, 8621–8644.

Carandini, M., Heeger, D.J., and Anthony Movshon, J. (1999). Linearity and Gain Control in V1 Simple Cells. In Models of Cortical Circuits, P.S. Ulinski, E.G. Jones, and A. Peters, eds. (Boston, MA: Springer US), pp. 401–443.

Chakravarthi, A., Baird, E., Dacke, M., and Kelber, A. (2016). Spatial Vision in Bombus terrestris. Front. Behav. Neurosci. *10*, 17.

Chiappe, M.E., Seelig, J.D., Reiser, M.B., and Jayaraman, V. (2010). Walking modulates speed sensitivity in drosophila motion vision. Curr. Biol. *20*, 1470–1475.

Chichilnisky, E.J., and Kalmar, R.S. (2002). Functional Asymmetries in ON and OFF Ganglion Cells of Primate Retina. J. Neurosci. *22*, 2737–2747.

Chittka, L., Faruq, S., Skorupski, P., and Werner, A. (2014). Colour constancy in insects. J. Comp. Physiol. A *200*, 435–448.

Chou, W.H., Hall, K.J., Wilson, D.B., Wideman, C.L., Townson, S.M., Chadwell, L.V., and Britt, S.G. (1996). Identification of a novel Drosophila opsin reveals specific patterning of the R7 and R8 photoreceptor cells. Neuron *17*, 1101–1115.

Clark, D.A., Bursztyn, L., Horowitz, M.A., Schnitzer, M.J., and Clandinin, T.R. (2011a). Defining the Computational Structure of the Motion Detector in Drosophila. Neuron.

Clark, D.A., Bursztyn, L., Horowitz, M.A., Schnitzer, M.J., and Clandinin, T.R. (2011b). Defining the Computational Structure of the Motion Detector in Drosophila. Neuron *70*, 1165–1177.

Clark, D.A., Benichou, R., Meister, M., and Azeredo da Silveira, R. (2013). Dynamical adaptation in photoreceptors. PLoS Comput. Biol. *9*, e1003289.

Clark, D.A., Fitzgerald, J.E., Ales, J.M., Gohl, D.M., Silies, M.A., Norcia, A.M., and Clandinin, T.R. (2014). Flies and humans share a motion estimation strategy that exploits natural scene statistics. Nat. Neurosci. *17*, 296–303.

Clemens, J., and Hennig, R.M. (2020). 2.08 - Coding Strategies in Insects. In The Senses: A Comprehensive Reference (Second Edition), B. Fritzsch, ed. (Oxford: Elsevier), pp. 100–113.

Crawford, B.H. (1947). Visual adaptation in relation to brief conditioning stimuli | Proceedings of the Royal Society of London. Series B - Biological Sciences.

Creamer, M.S., Mano, O., and Clark, D.A. (2018). Visual Control of Walking Speed in Drosophila. Neuron *100*, 1460-1473.e6.

Dakin, S.C., and Turnbull, P.R.K. (2016). Similar contrast sensitivity functions measured using psychophysics and optokinetic nystagmus. Sci. Rep. *6*, 34514.

Do, M.T.H., and Yau, K.-W. (2013). Adaptation to steady light by intrinsically photosensitive retinal ganglion cells. Proc. Natl. Acad. Sci. *110*, 7470–7475.

Drews, M.S., Leonhardt, A., Pirogova, N., Richter, F.G., Schuetzenberger, A., Braun, L., Serbe, E., and Borst, A. (2020). Dynamic Signal Compression for Robust Motion Vision in Flies. Curr. Biol. *30*, 209-221.e8.

Dubs, A., Laughlin, S.B., and Srinivasan, M.V. (1981). Single photon signals in fly photoreceptors and first order interneurones at behavioral threshold. J. Physiol. *317*, 317–334.

Dunn, F.A., Lankheet, M.J., and Rieke, F. (2007). Light adaptation in cone vision involves switching between receptor and post-receptor sites. Nature *449*, 603–606.

Dyakova, O., and Nordström, K. (2017). Image statistics and their processing in insect vision. Curr. Opin. Insect Sci. *24*, 7–14.

Dyer, A.G. (2006). Bumblebees directly perceive variations in the spectral quality of illumination. J. Comp. Physiol. A *192*, 333.

Egelhaaf, M., and Reichardt, W. (1987). Dynamic response properties of movement detectors: Theoretical analysis and electrophysiological investigation in the visual system of the fly. Biol. Cybern. *56*, 69–87.

Enroth-Cugell, C., and Lennie, P. (1975). The control of retinal ganglion cell discharge by receptive field surrounds. J. Physiol. *247*, 551–578.

Enroth-Cugell, C., and Shapley, R.M. (1973). Adaptation and dynamics of cat retinal ganglion cells. J. Physiol. *233*, 271–309.

Euler, T., and Masland, R.H. (2000). Light-Evoked Responses of Bipolar Cells in a Mammalian Retina. J. Neurophysiol. *83*, 1817–1829.

Euler, T., Haverkamp, S., Schubert, T., and Baden, T. (2014a). Retinal bipolar cells: elementary building blocks of vision. Nat. Rev. Neurosci. *15*, 507–519.

Euler, T., Haverkamp, S., Schubert, T., and Baden, T. (2014b). Retinal bipolar cells: Elementary building blocks of vision. Nat. Rev. Neurosci. *15*, 507–519.

Fain, G.L., Matthews, H.R., Cornwall, M.C., and Koutalos, Y. (2001). Adaptation in Vertebrate Photoreceptors. Physiol. Rev. *81*, 117–151.

Fischbach, K.F. (1979). Simultaneous and successive colour contrast expressed in “slow” phototactic behaviour of walkingDrosophila melanogaster. J. Comp. Physiol. *130*, 161–171.

Fischbach, K.F., and Dittrich, A.P.M. (1989). The optic lobe of Drosophila melanogaster. I. A Golgi analysis of wild-type structure. Cell Tissue Res.

Fisher, Y.E., Silies, M., and Clandinin, T.R. (2015a). Orientation Selectivity Sharpens Motion Detection in Drosophila. Neuron.

Fisher, Y.E., Leong, J.C.S., Sporar, K., Ketkar, M.D., Gohl, D.M., Clandinin, T.R., and Silies, M. (2015b). A Class of Visual Neurons with Wide-Field Properties Is Required for Local Motion Detection. Curr. Biol.

Fisher, Y.E., Leong, J.C.S., Sporar, K., Ketkar, M.D., Gohl, D.M., Clandinin, T.R., and Silies, M. (2015c). A Class of Visual Neurons with Wide-Field Properties Is Required for Local Motion Detection. Curr. Biol. *25*, 3178–3189.

Fisher, Y.E., Silies, M., and Clandinin, T.R. (2015d). Orientation Selectivity Sharpens Motion Detection in Drosophila. Neuron *88*, 390–402.

Frazor, R.A., and Geisler, W.S. (2006). Local luminance and contrast in natural images. Vision Res. *46*, 1585–1598.

Freifeld, L., Clark, D.A., Schnitzer, M.J., Horowitz, M.A., and Clandinin, T.R. (2013a). GABAergic Lateral Interactions Tune the Early Stages of Visual Processing in Drosophila. Neuron.

Freifeld, L., Clark, D., Schnitzer, M., Horowitz, M., and Clandinin, T. (2013b). GABAergic Lateral Interactions Tune the Early Stages of Visual Processing in Drosophila. Neuron *78*, 1075–1089.

French, A.S., Korenberg, M.J., Järvilehto, M., Kouvalainen, E., Juusola, M., and Weckström, M. (1993). The dynamic nonlinear behavior of fly photoreceptors evoked by a wide range of light intensities. Biophys. J. *65*, 832–839.

Frixione, E., and Pérez-Olvera, O. (1991). Light-adapting migration of the screening-pigment in crayfish photoreceptors is a two-stage movement comprising an all-or-nothing initial phase. J. Neurobiol. *22*, 238–248.

Gallio, M., Ofstad, T.A., Macpherson, L.J., Wang, J.W., and Zuker, C.S. (2011). The Coding of Temperature in the Drosophila Brain. Cell *144*, 614–624.

Gao, S., Takemura, S. ya, Ting, C.Y., Huang, S., Lu, Z., Luan, H., Rister, J., Thum, A.S., Yang, M., Hong, S.T., et al. (2008). The Neural Substrate of Spectral Preference in Drosophila. Neuron *60*, 328–342.

Garvert, M.M., and Gollisch, T. (2013). Local and global contrast adaptation in retinal ganglion cells. Neuron *77*, 915–928.

Gengs, C., Leung, H.T., Skingsley, D.R., Iovchev, M.I., Yin, Z., Semenov, E.P., Burg, M.G., Hardie, R.C., and Pak, W.L. (2002). The target of Drosophila photoreceptor synaptic transmission is a histamine-gated chloride channel encoded by ort (hclA). J. Biol. Chem. *277*, 42113–42120.

Gjorgjieva, J., Sompolinsky, H., and Meister, M. (2014). Benefits of Pathway Splitting in Sensory Coding. J. Neurosci. *34*, 12127–12144.

Gollisch, T., and Meister, M. (2008). Modeling convergent ON and OFF pathways in the early visual system. Biol. Cybern. *99*, 263–278.

Gollisch, T., and Meister, M. (2010). Eye Smarter than Scientists Believed: Neural Computations in Circuits of the Retina. Neuron *65*, 150–164.

Gonzalez-Bellido, P.T., Wardill, T.J., and Juusola, M. (2011). Compound eyes and retinal information processing in miniature dipteran species match their specific ecological demands. Proc. Natl. Acad. Sci. *108*, 4224–4229.

Götz, K.G. (1964). Optomotorische Untersuchung des visuellen systems einiger Augenmutanten der Fruchtfliege Drosophila. Kybernetik *2*, 77–92.

Greiner, B., Ribi, W.A., Wcislo, W.T., and Warrant, E.J. (2004). Neural organisation in the first optic ganglion of the nocturnal bee Megalopta genalis. Cell Tissue Res. *318*, 429–437.

Gu, Y., Oberwinkler, J., Postma, M., and Hardie, R.C. (2005). Mechanisms of Light Adaptation in Drosophila Photoreceptors. Curr. Biol. *15*, 1228–1234.

Gür, B., Sporar, K., Lopez-Behling, A., and Silies, M. (2020). Distinct expression of potassium channels regulates visual response properties of lamina neurons in Drosophila melanogaster. J. Comp. Physiol. A *206*, 273–287.

Hardie, R.C., and Weckström, M. (1990). Three classes of potassium channels in large monopolar cells of the blowfly Calliphora vicina. J. Comp. Physiol. A *167*, 723–736.

Hayhoe, M., and Wenderoth, P. (1991). Adaptation Mechanisms in Color and Brightness. In From Pigments to Perception: Advances in Understanding Visual Processes, A. Valberg, and B.B. Lee, eds. (Boston, MA: Springer US), pp. 353–367.

Hayhoe, M.M., Benimoff, N.I., and Hood, D.C. (1987). The time-course of multiplicative and subtractive adaptation process. Vision Res. *27*, 1981–1996.

Heath, S.L., Christenson, M.P., Oriol, E., Saavedra-Weisenhaus, M., Kohn, J.R., and Behnia, R. (2020). Circuit Mechanisms Underlying Chromatic Encoding in Drosophila Photoreceptors. Curr. Biol. *30*, 264-275.e8.

Heisenberg, M., and Buchner, E. (1977). The rôle of retinula cell types in visual behavior of Drosophila melanogaster. J. Comp. Physiol. A *117*, 127–162.

Huang, X., and Paradiso, M.A. (2008). V1 Response Timing and Surface Filling-In. J. Neurophysiol. *100*, 539–547.

Hubel, D.H., and Wiesel, T.N. (1962). Receptive fields, binocular interaction and functional architecture in the cat's visual cortex. J. Physiol. *160*, 106–154.

Ibbotson, M.R., and Clifford, C.W.G. (2001). Characterising temporal delay filters in biological motion detectors. Vision Res. *41*, 2311–2323.

Ichinose, T., and Hellmer, C.B. (2016). Differential signalling and glutamate receptor compositions in the OFF bipolar cell types in the mouse retina: Temporal coding in the retinal OFF bipolar cells. J. Physiol. *594*, 883–894.

Ichinose, T., and Lukasiewicz, P.D. (2007). Ambient Light Regulates Sodium Channel Activity to Dynamically Control Retinal Signaling. J. Neurosci. *27*, 4756–4764.

Ichinose, T., Fyk-Kolodziej, B., and Cohn, J. (2014). Roles of ON Cone Bipolar Cell Subtypes in Temporal Coding in the Mouse Retina. J. Neurosci. *34*, 8761–8771.

Idrees, S., and Münch, T.A. (2020). Different contrast encoding in ON and OFF visual pathways (Neuroscience).

Ikeda, H., and Wright, M.J. (1972). Receptive field organization of `sustained' and `transient' retinal ganglion cells which subserve different functional roles. J. Physiol. *227*, 769–800.

Jacob, K.G., Willmund, R., Folkers, E., Fischbach, K.F., and Spatz, H.Ch. (1977). T-maze phototaxis ofDrosophila melanogaster and several mutants in the visual systems. J. Comp. Physiol. *116*, 209–225.

Jin, J., Wang, Y., Lashgari, R., Swadlow, H.A., and Alonso, J.-M. (2011). Faster Thalamocortical Processing for Dark than Light Visual Targets. J. Neurosci. *31*, 17471–17479.

Joesch, M., Schnell, B., Raghu, S.V., Reiff, D.F., and Borst, A. (2010). ON and off pathways in Drosophila motion vision. Nature.

Juusola, M., and Hardie, R.C. (2001). Light adaptation in Drosophila photoreceptors: I. Response dynamics and signaling efficiency at 25 degrees C. J. Gen. Physiol. *117*, 3–25.

Juusola, M., Uusitalo, R.O., and Weckström, M. (1995). Transfer of graded potentials at the photoreceptor-interneuron synapse. J. Gen. Physiol. *105*, 117–148.

Kamikouchi, A., Inagaki, H.K., Effertz, T., Hendrich, O., Fiala, A., Göpfert, M.C., and Ito, K. (2009). The neural basis of Drosophila gravity-sensing and hearing. Nature *458*, 165–171.

Kaplan, E. (2008). Luminance Sensitivity and Contrast Detection. In The Senses: A Comprehensive Reference, (Elsevier), pp. 29–43.

Kaplan, E., Marcus, S., and So, Y.T. (1979). Effects of dark adaptation on spatial and temporal properties of receptive fields in cat lateral geniculate nucleus. J. Physiol. *294*, 561–580.

Katayama, N., Abbott, J.K., Kjærandsen, J., Takahashi, Y., and Svensson, E.I. (2014). Sexual selection on wing interference patterns in Drosophila melanogaster. Proc. Natl. Acad. Sci. *111*, 15144–15148.

Katz, B., and Minke, B. (2009). Drosophila photoreceptors and signaling mechanisms. Front. Cell. Neurosci. *3*.

Keleş, M.F., and Frye, M.A. (2017). Object-Detecting Neurons in Drosophila. Curr. Biol. *27*, 680–687.

Keleş, M.F., Mongeau, J.M., and Frye, M.A. (2019). Object features and T4/T5 motion detectors modulate the dynamics of bar tracking by Drosophila. J. Exp. Biol.

Kelly, D.H. (1972). Adaptation effects on spatio-temporal sine-wave thresholds. Vision Res. *12*, 89–101.

Ketkar, M.D., Sporar, K., Gür, B., Ramos-Traslosheros, G., Seifert, M., and Silies, M. (2020). Luminance Information Is Required for the Accurate Estimation of Contrast in Rapidly Changing Visual Contexts. Curr. Biol.

Khani, M.H., and Gollisch, T. (2017). Diversity in spatial scope of contrast adaptation among mouse retinal ganglion cells. J. Neurophysiol. *118*, 3024–3043.

Kirschfeld, K. (1967). Die projektion der optischen umwelt auf das raster der rhabdomere im komplexauge von Musca. Exp. Brain Res. *3*, 248–270.

Kirschfeld, K. (1976). The Resolution of Lens and Compound Eyes. In Neural Principles in Vision, F. Zettler, and R. Weiler, eds. (Berlin, Heidelberg: Springer), pp. 354–370.

Kirschfeld, K., and Franceschini, N. (1969). Ein Mechanismus zur Steuerung des Lichtflusses in den Rhabdomeren des Komplexauges von Musca. Kybernetik *6*, 13–22.

Kitamoto, T. (2001). Conditional modification of behavior inDrosophila by targeted expression of a temperature-sensitiveshibire allele in defined neurons. J. Neurobiol. *47*, 81–92.

Koenderink, J.J., and van Doorn, A.J. (1978). Visual detection of spatial contrast; Influence of location in the visual field, target extent and illuminance level. Biol. Cybern. *30*, 157–167.

Krauskopf, J. (1980). Discrimination and detection of changes in luminance. Vision Res. *20*, 671–677.

von Kries, J. (1905). Die Gesichtsempfindungen. In: Nagel W (ed) Handbuch der Physiologie des Menschen, vol 3. (Braunschweig: Vieweg), pp. 109–282.

Lachaise, D., Cariou, M., David, J.R., Lemeunier, F., Tsacas, L., and Ashburner, M. (1988). Historical biogeography of the Drosophila melanogaster species subgroup. Evol. Biol. *22*, 159–225.

Laughlin, S. (1981). A simple coding procedure enhances a neuron's information capacity. Z. Naturforschung - Sect. C J. Biosci. *doi:10.151*, 1981-9–1040.

Laughlin, S.B. (1989). The role of sensory adaptation in the retina. Exp Biol *146*, 39–62.

Laughlin, S.B., and Hardie, R.C. (1978). Common strategies for light adaptation in the peripheral visual systems of fly and dragonfly. J. Comp. Physiol. *128*, 319–340.

Laughlin, S.B., and Osorio, D. (1989). Mechanisms for Neural Signal Enhancement in the Blowfly Compound Eye. J. Exp. Biol. *144*, 113–146.

Laughlin, S.B., Howard, J., and Blakeslee, B. (1987). Synaptic limitations to contrast coding in the retina of the blowfly Calliphora. Proc. R. Soc. Lond. Ser. B Contain. Pap. Biol. Character R. Soc. G. B. *231*, 437–467.

Lee, B.B., Dacey, D.M., Smith, V.C., and Pokorny, J. (2003). Dynamics of sensitivity regulation in primate outer retina: The horizontal cell network. J. Vis. *3*, 5–5.

Leong, J.C.S., Esch, J.J., Poole, B., Ganguli, S., and Clandinin, T.R. (2016). Direction Selectivity in Drosophila Emerges from Preferred-Direction Enhancement and Null-Direction Suppression. J. Neurosci. *36*, 8078–8092.

Leonhardt, A., Ammer, G., Meier, M., Serbe, E., Bahl, A., and Borst, A. (2016). Asymmetry of Drosophila on and off motion detectors enhances real-world velocity estimation. Nat. Neurosci.

Lin, T.-Y., Luo, J., Shinomiya, K., Ting, C.-Y., Lu, Z., Meinertzhagen, I.A., and Lee, C.-H. (2016). Mapping chromatic pathways in the *Drosophila* visual system: Chromatic Visual Circuits in the Fly's Lobula. J. Comp. Neurol. *524*, 213–227.

Lotto, R.B., and Chittka, L. (2005). Seeing the light: Illumination as a contextual cue to color choice behavior in bumblebees. Proc. Natl. Acad. Sci. *102*, 3852–3856.

MacEvoy, S.P., and Paradiso, M.A. (2001). Lightness constancy in primary visual cortex. Proc. Natl. Acad. Sci. *98*, 8827–8831.

Maddess, T., and Laughlin, S.B. (1985). Adaptation of the Motion-Sensitive Neuron H1 is Generated Locally and Governed by Contrast Frequency. Proc. R. Soc. Lond. B Biol. Sci. *225*, 251–275.

Maisak, M.S., Haag, J., Ammer, G., Serbe, E., Meier, M., Leonhardt, A., Schilling, T., Bahl, A., Rubin, G.M., Nern, A., et al. (2013). A directional tuning map of Drosophila elementary motion detectors. Nature.

Mamiya, A., Gurung, P., and Tuthill, J.C. (2018). Neural Coding of Leg Proprioception in Drosophila. Neuron *100*, 636–650.

Manookin, M.B., Beaudoin, D.L., Ernst, Z.R., Flagel, L.J., and Demb, J.B. (2008). Disinhibition Combines with Excitation to Extend the Operating Range of the OFF Visual Pathway in Daylight. J. Neurosci. *28*, 4136–4150.

Mante, V., Frazor, R.A., Bonin, V., Geisler, W.S., and Carandini, M. (2005). Independence of luminance and contrast in natural scenes and in the early visual system. Nat. Neurosci. *8*, 1690–1697.

Matulis, C.A., Chen, J., Gonzalez-Suarez, A.D., Behnia, R., and Clark, D.A. (2020a). Heterogeneous Temporal Contrast Adaptation in Drosophila Direction-Selective Circuits. Curr. Biol.

Matulis, C.A., Chen, J., Gonzalez-Suarez, A.D., Behnia, R., and Clark, D.A. (2020b). Heterogeneous Temporal Contrast Adaptation in Drosophila Direction-Selective Circuits. Curr. Biol. CB *30*, 222-236.e6.

Meinertzhagen, I.A., and O'Neil, S.D. (1991). Synaptic organization of columnar elements in the lamina of the wild type in Drosophila melanogaster. J. Comp. Neurol. *305*, 232–263.

Melnattur, K.V., Pursley, R., Lin, T.-Y., Ting, C.-Y., Smith, P.D., Pohida, T., and Lee, C.-H. (2014). Multiple redundant medulla projection neurons mediate color vision in Drosophila. J. Neurogenet. *28*, 374–388.

Milner, E.S., and Do, M.T.H. (2017). A Population Representation of Absolute Light Intensity in the Mammalian Retina. Cell *171*, 865-876.e16.

Mimura, K. (1974). Analysis of visual information in lamina neurones of the fly. J. Comp. Physiol. *88*, 335–372.

Molina-Obando, S., Vargas-Fique, J.F., Henning, M., Gür, B., Schladt, M., Akhtar, J., Berger, T.K., and Silies, M. (2019). ON selectivity in the Drosophila visual system is a multisynaptic process involving both glutamatergic and GABAergic inhibition.

Nagel, K.I., and Wilson, R.I. (2016). Mechanisms Underlying Population Response Dynamics in Inhibitory Interneurons of the Drosophila Antennal Lobe. J. Neurosci. *36*, 4325–4338.

Naka, K.I., and Rushton, W.A.H. (1966). S-potentials from luminosity units in the retina of fish (Cyprinidae). J. Physiol. *185*, 587–599.

Nern, A., Pfeiffer, B.D., and Rubin, G.M. (2015a). Optimized tools for multicolor stochastic labeling reveal diverse stereotyped cell arrangements in the fly visual system. Proc. Natl. Acad. Sci. *112*, E2967–E2976.

Nern, A., Pfeiffer, B.D., and Rubin, G.M. (2015b). Optimized tools for multicolor stochastic labeling reveal diverse stereotyped cell arrangements in the fly visual system. Proc. Natl. Acad. Sci. *112*, E2967–E2976.

Nes, F.L.V., and Bouman, M.A. (1967). Spatial Modulation Transfer in the Human Eye. JOSA *57*, 401–406.

Neumeyer, C. (1981). Chromatic adaptation in the honeybee: Successive color contrast and color constancy. J. Comp. Physiol. *144*, 543–553.

Nicholas, S., and Nordström, K. (2020). Persistent Firing and Adaptation in Optic-Flow-Sensitive Descending Neurons. Curr. Biol. CB *30*, 2739-2748.e2.

Nikolaev, A., Zheng, L., Wardill, T.J., O'Kane, C.J., de Polavieja, G.G., and Juusola, M. (2009). Network adaptation improves temporal representation of naturalistic stimuli in Drosophila eye: II mechanisms. PloS One *4*, e4306.

Nilsson, D.-E. (1989). Optics and Evolution of the Compound Eye. In Facets of Vision, D.G. Stavenga, and R.C. Hardie, eds. (Berlin, Heidelberg: Springer), pp. 30–73.

Normann, R.A., and Perlman, I. (1979). The effects of background illumination on the photoresponses of red and green cones. J. Physiol. *286*, 491–507.

Normann, R.A., and Werblin, F.S. (1974). Control of Retinal Sensitivity I . Light and Dark Adaptation of. J. Gen. Physiol. *63*, 37–61.

Odermatt, B., Nikolaev, A., and Lagnado, L. (2012). Encoding of Luminance and Contrast by Linear and Nonlinear Synapses in the Retina. Neuron *73*, 758–773.

Oesch, N.W., and Diamond, J.S. (2011). Ribbon synapses compute temporal contrast and encode luminance in retinal rod bipolar cells. Nat. Neurosci. *14*, 1555–1561.

Ohly, K.P. (1975). The neurons of the first synaptic region of the optic neuropil of the firefly, Phausis splendidula l. (Coleoptera). Cell Tissue Res. *158*, 89–109.

Pagni, M., Haikala, V., Oberhauser, V., Meyer, P.B., Reiff, D.F., and Schnaitmann, C. (2021). Interaction of "chromatic" and "achromatic" circuits in Drosophila color opponent processing. Curr. Biol. CB *31*, 1687-1698.e4.

Palmer, C., Cheng, S.-Y., and Seidemann, E. (2007). Linking Neuronal and Behavioral Performance in a Reaction-Time Visual Detection Task. J. Neurosci. *27*, 8122–8137.

Pasternak, T., and Merigan, W.H. (1981). The luminance dependence of spatial vision in the cat. Vision Res. *21*, 1333–1339.

Pegoraro, M., Flavell, L.M.M., Menegazzi, P., Colombi, P., Dao, P., Helfrich-Förster, C., and Tauber, E. (2020). The genetic basis of diurnal preference in Drosophila melanogaster. BMC Genomics *21*, 596.

Peirce, J.W. (2008). Generating stimuli for neuroscience using PsychoPy. Front. Neuroinformatics *2*.

Peng, J., Santiago, I.J., Ahn, C., Gur, B., Tsui, C.K., Su, Z., Xu, C., Karakhanyan, A., Silies, M., and Pecot, M.Y. (2018). Drosophila fezf coordinates laminar-specific connectivity through cell-intrinsic and cell-extrinsic mechanisms. ELife *7*, e33962–e33962.

Pick, B., and Buchner, E. (1979). Visual movement detection under light- and dark-adaptation in the fly, Musca domestica. J. Comp. Physiol. *134*, 45–54.

Popova, E. (2015). ON-OFF Interactions in the Retina: Role of Glycine and GABA. Curr. Neuropharmacol. *12*, 509–526.

Pouli, T., Cunningham, D., and Reinhard, E. (2010). Statistical regularities in low and high dynamic range images. In Proceedings of the 7th Symposium on Applied Perception in Graphics and Visualization - APGV '10, (Los Angeles, California: ACM Press), p. 9.

Ramos-Traslosheros, G., and Silies, M. (2021). The physiological basis for contrast opponency in motion computation in Drosophila. Nat. Commun. *12*, 1–16.

Ramos-Traslosheros, G., Henning, M., and Silies, M. (2018). Motion detection: Cells, circuits and algorithms. Neuroforum *24*, A61–A72.

Ratliff, C.P., Borghuis, B.G., Kao, Y.-H., Sterling, P., and Balasubramanian, V. (2010). Retina is structured to process an excess of darkness in natural scenes. Proc. Natl. Acad. Sci. *107*, 17368–17373.

Reiser, M.B., and Dickinson, M.H. (2008). A modular display system for insect behavioral neuroscience. J. Neurosci. Methods *167*, 127–139.

Ribi, W.A. (1977). Fine structure of the first optic ganglion (lamina) of the cockroach, Periplaneta americana. Tissue Cell *9*, 57–72.

Rieke, F., and Rudd, M.E. (2009a). The Challenges Natural Images Pose for Visual Adaptation. Neuron *64*, 605–616.

Rieke, F., and Rudd, M.E. (2009b). The Challenges Natural Images Pose for Visual Adaptation. Neuron *64*, 605–616.

Rinner, O., Rick, J.M., and Neuhauss, S.C.F. (2005). Contrast Sensitivity, Spatial and Temporal Tuning of the Larval Zebrafish Optokinetic Response. Invest. Ophthalmol. Vis. Sci. *46*, 137–142.

Rister, J., Pauls, D., Schnell, B., Ting, C.Y., Lee, C.H., Sinakevitch, I., Morante, J., Strausfeld, N.J., Ito, K., and Heisenberg, M. (2007). Dissection of the Peripheral Motion Channel in the Visual System of Drosophila melanogaster. Neuron *56*, 155–170.

Ross, B.C. (2014). Mutual information between discrete and continuous data sets. PLoS ONE *9*, e87357–e87357.

Ruderman, D.L., and Bialek, W. (1994). Statistics of natural images: Scaling in the woods. Phys. Rev. Lett. *73*, 814–817.

Rusanen, J., and Weckström, M. (2016). Frequency-selective transmission of graded signals in large monopolar neurons of blowfly Calliphora vicina compound eye. J. Neurophysiol. *115*, 2052–2064.

Rusanen, J., Vähäkainu, A., Weckström, M., and Arikawa, K. (2017). Characterization of the first-order visual interneurons in the visual system of the bumblebee (Bombus terrestris). J. Comp. Physiol. A Neuroethol. Sens. Neural. Behav. Physiol. *203*, 903–913.

Rusanen, J., Frolov, R., Weckström, M., Kinoshita, M., and Arikawa, K. (2018). Non-linear amplification of graded voltage signals in the first-order visual interneurons of the butterfly Papilio xuthus. J. Exp. Biol. *221*, jeb179085–jeb179085.

Rushton, W.A. (1965). VISUAL ADAPTATION. Proc. R. Soc. Lond. B Biol. Sci. *162*, 20–46.

Salazar-Gatzimas, E., Agrochao, M., Fitzgerald, J.E., and Clark, D.A. (2018). The Neuronal Basis of an Illusory Motion Percept Is Explained by Decorrelation of Parallel Motion Pathways. Curr. Biol.

Salcedo, E., Huber, a, Henrich, S., Chadwell, L.V., Chou, W.H., Paulsen, R., and Britt, S.G. (1999). Blue- and green-absorbing visual pigments of Drosophila: ectopic expression and physiological characterization of the R8 photoreceptor cell-specific Rh5 and Rh6 rhodopsins. J. Neurosci. Off. J. Soc. Neurosci. *19*, 10716–10726.

Santiago, I.J., Zhang, D., Saras, A., Pontillo, N., Xu, C., Chen, X., Weirauch, M.T., Mistry, M., Ginty, D.D., Pecot, M.Y., et al. (2021). Drosophila Fezf functions as a transcriptional repressor to direct layer-specific synaptic connectivity in the fly visual system. Proc. Natl. Acad. Sci. *118*.

Schnaitmann, C., Haikala, V., Abraham, E., Oberhauser, V., Thestrup, T., Griesbeck, O., and Reiff, D.F. (2018). Color Processing in the Early Visual System of Drosophila. Cell *172*, 318-318.e18.

Schnaitmann, C., Pagni, M., and Reiff, D.F. (2020). Color vision in insects: insights from Drosophila. J. Comp. Physiol. A *206*, 183–198.

Schnapf, J.L., Nunn, B.J., Meister, M., and Baylor, D.A. (1990). Visual transduction in cones of the monkey Macaca fascicularis. J. Physiol. *427*, 681–713.

Schnell, B., Joesch, M., Forstner, F., Raghu, S.V., Otsuna, H., Ito, K., Borst, A., and Reiff, D.F. (2010). Processing of horizontal optic flow in three visual interneurons of the Drosophila brain. J. Neurophysiol.

Scholl, B., Gao, X., and Wehr, M. (2010). Nonoverlapping Sets of Synapses Drive On Responses and Off Responses in Auditory Cortex. Neuron *65*, 412–421.

Schreyer, H.M., and Gollisch, T. (2021). Nonlinear spatial integration in retinal bipolar cells shapes the encoding of artificial and natural stimuli. Neuron *109*, 1692-1706.e8.

Schwartz, G.W., and Rieke, F. (2013). Controlling gain one photon at a time. ELife *2*, e00467.

Seelig, J.D., Chiappe, M.E., Dutta, A., Osborne, J.E., Reiser, M.B., and Jayaraman, V. (2010). Two-photon calcium imaging from head-fixed Drosophila during optomotor walking behavior. Nat. Methods *7*, 535–540.

Serbe, E., Meier, M., Leonhardt, A., and Borst, A. (2016). Comprehensive Characterization of the Major Presynaptic Elements to the Drosophila OFF Motion Detector. Neuron *89*, 829–841.

Shapley, R., and Enroth-Cugell, C. (1984). Chapter 9 Visual adaptation and retinal gain controls. Prog. Retin. Res. *3*, 263–346.

Shapley, R., Enroth-Cugell, C., Bonds, A.B., and Kirby, A. (1972). Gain Control in the Retina and Retinal Dynamics. Nature *236*, 352–353.

Shinomiya, K., Karuppudurai, T., Lin, T.Y., Lu, Z., Lee, C.H., and Meinertzhagen, I.A. (2014a). Candidate neural substrates for off-edge motion detection in drosophila. Curr. Biol. *24*, 1062–1070.

Shinomiya, K., Karuppudurai, T., Lin, T.Y., Lu, Z., Lee, C.H., and Meinertzhagen, I.A. (2014b). Candidate neural substrates for off-edge motion detection in drosophila. Curr. Biol.

Shinomiya, K., Huang, G., Lu, Z., Parag, T., Xu, C.S., Aniceto, R., Ansari, N., Cheatham, N., Lauchie, S., Neace, E., et al. (2019). Comparisons between the ON- and OFF-edge motion pathways in the Drosophila brain. ELife *8*, e40025.

Siegle, J.H., Ledochowitsch, P., Jia, X., Millman, D.J., Ocker, G.K., Caldejon, S., Casal, L., Cho, A., Denman, D.J., Durand, S., et al. (2021). Reconciling functional differences in populations of neurons recorded with two-photon imaging and electrophysiology. ELife *10*, e69068.

Silies, M., Gohl, D.M., Fisher, Y.E., Freifeld, L., Clark, D.A., and Clandinin, T.R. (2013a). Modular Use of Peripheral Input Channels Tunes Motion-Detecting Circuitry. Neuron.

Silies, M., Gohl, D., Fisher, Y., Freifeld, L., Clark, D., and Clandinin, T.R. (2013b). Modular Use of Peripheral Input Channels Tunes Motion-Detecting Circuitry. Neuron *79*, 111–127.

Silies, M., Gohl, D.M., and Clandinin, T.R. (2014). Motion-Detecting Circuits in Flies: Coming into View. Annu. Rev. Neurosci. *37*, 307–327.

Song, Z., and Juusola, M. (2017). A biomimetic fly photoreceptor model elucidates how stochastic adaptive quantal sampling provides a large dynamic range. J. Physiol. *595*, 5439–5456.

Spitschan, M., Aguirre, G.K., Brainard, D.H., and Sweeney, A.M. (2016). Variation of outdoor illumination as a function of solar elevation and light pollution. Sci. Rep. *6*, 26756.

Srinivasan, M.V., Laughlin, S.B., Dubs, A., and Horridge, G.A. (1982). Predictive coding: a fresh view of inhibition in the retina. Proc. R. Soc. Lond. B Biol. Sci. *216*, 427–459.

Stöckl, A.L., O'Carroll, D.C., and Warrant, E.J. (2016a). Neural summation in the hawkmoth visual system extends the limits of vision in dim light. Curr. Biol.

Stöckl, A.L., O'Carroll, D.C., and Warrant, E.J. (2016b). Neural summation in the hawkmoth visual system extends the limits of vision in dim light. Curr. Biol. *26*, 821–826.

Strausfeld, N.J., and Blest, A.D. (1970). Golgi studies on insects Part I. The optic lobes of Lepidoptera. Philos. Trans. R. Soc. Lond. B Biol. Sci. *258*, 81–134.

Strother, J.A., Wu, S.T., Wong, A.M., Nern, A., Rogers, E.M., Le, J.Q., Rubin, G.M., and Reiser, M.B. (2017). The Emergence of Directional Selectivity in the Visual Motion Pathway of Drosophila. Neuron *94*, 168-182.e10.

Takemura, S., Bharioke, A., Lu, Z., Nern, A., Vitaladevuni, S., Rivlin, P.K., Katz, W.T., Olbris, D.J., Plaza, S.M., Winston, P., et al. (2013a). A visual motion detection circuit suggested by Drosophila connectomics. Nature *500*, 175–181.

Takemura, S., Bharioke, A., Lu, Z., Nern, A., Vitaladevuni, S., Rivlin, P.K., Katz, W.T., Olbris, D.J., Plaza, S.M., Winston, P., et al. (2013b). A visual motion detection circuit suggested by Drosophila connectomics. Nature.

Takemura, S., Xu, C.S., Lu, Z., Rivlin, P.K., Parag, T., Olbris, D.J., Plaza, S., Zhao, T., Katz, W.T., Umayam, L., et al. (2015). Synaptic circuits and their variations within different columns in the visual system of Drosophila. Proc. Natl. Acad. Sci. *112*, 13711–13716.

Takemura, S. ya, Nern, A., Chklovskii, D.B., Scheffer, L.K., Rubin, G.M., and Meinertzhagen, I.A. (2017a). The comprehensive connectome of a neural substrate for 'ON' motion detection in Drosophila. ELife *6*, e24394–e24394.

Takemura, S.Y., Nern, A., Chklovskii, D.B., Scheffer, L.K., Rubin, G.M., and Meinertzhagen, I.A. (2017b). The comprehensive connectome of a neural substrate for 'ON' motion detection in Drosophila. ELife.

Tan, L., Zhang, K.X., Pecot, M.Y., Nagarkar-Jaiswal, S., Lee, P.T., Takemura, S.Y., McEwen, J.M., Nern, A., Xu, S., Tadros, W., et al. (2015a). Ig Superfamily Ligand and Receptor Pairs Expressed in Synaptic Partners in Drosophila. Cell *163*, 1756–1769.

Tan, L., Zhang, K.X., Pecot, M.Y., Nagarkar-Jaiswal, S., Lee, P.-T., Takemura, S., McEwen, J.M., Nern, A., Xu, S., Tadros, W., et al. (2015b). Ig Superfamily Ligand and Receptor Pairs Expressed in Synaptic Partners in Drosophila. Cell *163*, 1756–1769.

Thibos, L.N., and Werblin, F.S. (1978). The response properties of the steady antagonistic surround in the mudpuppy retina. J. Physiol. *278*, 79–99.

Thoreson, W.B., and Dacey, D.M. (2019). Diverse Cell Types, Circuits, and Mechanisms for Color Vision in the Vertebrate Retina. Physiol. Rev. *99*, 1527–1573.

Tichy, H., and Hellwig, M. (2018). Independent processing of increments and decrements in odorant concentration by ON and OFF olfactory receptor neurons. J. Comp. Physiol. A *204*, 873–891.

Timofeev, K., Joly, W., Hadjieconomou, D., and Salecker, I. (2012). Localized netrins act as positional cues to control layer-specific targeting of photoreceptor axons in drosophila. Neuron *75*, 80–93.

Tuthill, J.C., Nern, A., Holtz, S.L., Rubin, G.M., and Reiser, M.B. (2013). Contributions of the 12 Neuron Classes in the Fly Lamina to Motion Vision. Neuron *79*, 128–140.

Van Hateren, J.H. (1997). Processing of natural time series of intensities by the visual system of the blowfly. Vision Res. *37*, 3407–3416.

Vaney, D.I., Sivyer, B., and Taylor, W.R. (2012). Direction selectivity in the retina: symmetry and asymmetry in structure and function. Nat. Rev. Neurosci. *13*, 194–208.

Wark, B., Fairhall, A., and Rieke, F. (2009). Timescales of inference in visual adaptation. Neuron *61*, 750–761.

Warrant, E.J. (2017). The remarkable visual capacities of nocturnal insects: Vision at the limits with small eyes and tiny brains. Philos. Trans. R. Soc. B Biol. Sci. *372*, 20160063–20160063.

Warrant, E.J., and McIntyre, P.D. (1992). The Trade-Off Between Resolution and Sensitivity in Compound Eyes. In Nonlinear Vision: Determination of Neural Receptive Fields, Function, and Networks, (Boca Raton, FL: CRC Press Inc), pp. 391–421.

Wässle, H., and Boycott, B.B. (1991). Functional architecture of the mammalian retina. Physiol. Rev. *71*, 447–480.

Webster, M.A., and Mollon, J.D. (1995). Colour constancy influenced by contrast adaptation. Nature *373*, 694–698.

Weckström, M., and Laughlin, S. (2010). Extracellular potentials modify the transfer of information at photoreceptor output synapses in the blowfly compound eye. J. Neurosci. Off. J. Soc. Neurosci. *30*, 9557–9566.

Wei, H., Kyung, H.Y., Kim, P.J., and Desplan, C. (2020a). The diversity of lobula plate tangential cells (LPTCs) in the Drosophila motion vision system. J. Comp. Physiol. A Neuroethol. Sens. Neural. Behav. Physiol.

Wei, Z., Lin, B.-J., Chen, T.-W., Daie, K., Svoboda, K., and Druckmann, S. (2020b). A comparison of neuronal population dynamics measured with calcium imaging and electrophysiology. PLOS Comput. Biol. *16*, e1008198.

Werblin, F.S. (1974). Control of Retinal Sensitivity. J. Gen. Physiol. *63*, 62–87.

Werblin, F.S., and Dowling, J.E. (1969). Organization of the retina of the mudpuppy, Necturus maculosus. II. Intracellular recording. J. Neurophysiol. *32*, 339–355.

Whittle, P., and Challands, P.D.C. (1969). The effect of background luminance on the brightness of flashes. Vision Res. *9*, 1095–1110.

Wienbar, S., and Schwartz, G.W. (2018). The dynamic receptive fields of retinal ganglion cells. Prog. Retin. Eye Res. *67*, 102–117.

Wienecke, C.F.R., Leong, J.C.S., and Clandinin, T.R. (2018). Linear Summation Underlies Direction Selectivity in Drosophila. Neuron *99*, 680-688.e4.

Yang, H.H., and Clandinin, T.R. (2018). Elementary Motion Detection in Drosophila : Algorithms and Mechanisms. Annu. Rev. Vis. Sci. *4*, 143–163.

Yang, H.H.H., St-Pierre, F., Sun, X., Ding, X., Lin, M.Z.Z., and Clandinin, T.R.R. (2016). Subcellular Imaging of Voltage and Calcium Signals Reveals Neural Processing In Vivo. Cell *166*, 245–257.

Yedutenko, M., Howlett, M.H.C., and Kamermans, M. (2021). High Contrast Allows the Retina to Compute More Than Just Contrast. Front. Cell. Neurosci. *14*, 481.

Zele, A.J., Feigl, B., Adhikari, P., Maynard, M.L., and Cao, D. (2018). Melanopsin photoreception contributes to human visual detection, temporal and colour processing. Sci. Rep. *8*, 3842.

Zheng, L., de Polavieja, G.G., Wolfram, V., Asyali, M.H., Hardie, R.C., and Juusola, M. (2006). Feedback Network Controls Photoreceptor Output at the Layer of First Visual Synapses in Drosophila. J. Gen. Physiol. *127*, 495–510.

Acknowledgements

I am among the luckiest PhD students, no exaggeration, all thanks to the people who made the past years a perfect package of rewarding and memorable experiences. The list below is not quite complete, but one that fits in the finiteness of this thesis. I owe my earnest thanks to:

First and foremost, my advisor Marion Silies, whose ideas formed the basis of not only this work but also my thought process in general. Marion, thank you for being a passionate teacher and a constant motivator. From formulating the question to communicating the results, I could learn every aspect of Science from you. Thanks for the enormous freedom in shaping my projects and ample opportunities to make mistakes, and yet being there to guide me every time I faltered. Professors belonged to another world, until I witnessed you become one and still remain incredibly accessible and real. Furthermore, having seen the mentor and the well-wisher in you dominating the boss has amended the definition of leadership known to me. Lastly, thanks for demonstrating how being an expert and being vulnerable to new ideas is actually complementary, and not mutually exclusive. Research wouldn't have been as exciting without all the rigorous discussions with you, where even my raw arguments were encouraged and addressed with utmost seriousness. Undoubtedly, pursuing a PhD in this lab is among the best decisions I have made so far. Coming to decision making, there are more than one correct choices as you said, indeed, but rarely was I so convinced of having chosen a right path. Truly, the time spent with you will remain a forever source of inspiration to me.

Tim Gollisch and Viola Priesemann, for taking time out for the annual committee meetings and for your valuable feedback. Your different perspectives on my ongoing work always bettered my then future plans. Thank you, also for your caring attention that the course of my PhD fell in line with my expectations. Special thanks to Viola, for being my *SmartStart* mentor and for the guidance and support you extended even through my changing project interests. Moreover, several resources of the institute that you made available to me have made parts of this work smoother.

Tobias Moser, Martin Göpfert and Jan Clemens, for evaluating my thesis as my extended thesis examination board. It is an honor to have your expert comments on my thesis.

Julijana Gjorgjieva and Shuai Shao, for being excellent collaborators in figuring out some of the most exciting findings in this work. I am grateful to Julijana first for hosting my *SmartStart* rotation, and then mentoring our joint project that helped me see a more complete picture behind the data. Thanks Shuai, for your outstanding modelling ideas and for being patient with my experiments and naïve suggestions.

Jan Benda, for your generous insights on neural adaptation. Your remote guidance was as effective as a hands-on training, where I learnt some concepts central to my research topic.

All my colleagues from the Silies Lab (now department!) for the great work atmosphere and fruitful discussions during and outside the lab meetings. Whereas every member has direct or indirect contributions to my projects, here are some specific mentions: Katja, thank you for an awesome collaboration that got me started with this work. Without your key experiments, the topics I delved into would be non-existent. Luis, thank you for opening your treasures of knowhow for each of my queries. Our extensive discussions are where much of my conceptual understanding comes from.

Sebastian and Burak, working with you have been a wonderful experience, given your constructively critical approach. Miriam, thanks for entertaining my enthusiastic probes into your project and for being a sympathetic personality. Carlotta, thanks for taking time out to solve my random doubts in random analyses. Christine, from taking care of flies to dropping me to the train station, you have supported me across a range of activities, and I am thankful for all of them. Also thanks to Luis, Christine and Juan for making superb office partners across the cities. At last, thanks to all my friends from the department who make the lunch breaks and social events so much fun!

My students, especially Deniz, Jannik, Renee and Maria, who invested their sincere efforts and did not give up on their questions until I was pushed to clear my mind and provide a satisfactory answer. Thanks to their cooperation and patience, my experience of the 'other side of teaching' was quite promising. I take this moment to also remember the scientists-in-training who invested their precious PhD times to train a fresh student like me from scratch.

The IMPRS Neuroscience office for the support in all matters concerning my MSc and PhD years. Jonas, Sandra and Franziska, the extent of your help is exceptional, and leaves very little among the official things for us to worry about. Further thanks to the GGNB office, for organizing diverse courses to enrich our PhD learning experience. I would also like to thank the Bernstein Network for Computational Neuroscience (BCCN) for the *SmartStart* training opportunity, which expanded my knowledge of computational resources and the interdisciplinary network at the very beginning of my PhD journey.

All the known and unknown organizers of the conferences and symposia, for providing me with diverse opportunities of discussing my work with the worldwide neuroscience community. This has played a major role in boosting my confidence as well as in widening my network. Thank you, also for bringing the conference platforms online during the pandemic.

My teachers from all steps of education, who get the credit for my sustained interest in figuring out the unknowns in Biology. Among them are my Science teachers from the school years, especially Mrs. Madhumati Bhagwat and Mrs. Madhuri Gharpure, and the NIT Warangal faculty, especially Dr. Onkara Perumal. Furthermore, my sincere thanks to the Neurasmus faculty from Göttingen, Bordeaux and Berlin for introducing me to various streams of neuroscience and specifically, allowing me sufficient exposure to narrow down my long-term research interest.

My parents, for giving me all the freedom in identifying my interests and deciding my career path, and for the strength to follow this path consistently. Thanks to my sister and my grandparents, for having an open ear to my comic complaints such as 'the flies don't walk!', and also to my extended family for appreciating my work even after my largely incomprehensible descriptions!

My friends from all walks of life. To keep the long list short: Thanks to "mmrta", for the sustained connections dating back to my childhood. Thanks to all the Warangal folks who still remind me of the "Lite teesko" philosophy. Thanks to the IMPRS "Neuros", for making Göttingen a home away from home. Thanks to the Berlin "Foodies", the coolest group that shares moments of pure joy with me, looking forward to more of them! Very special thanks to Pramod, for his unfailing and unconditional support on both emotional and intellectual levels, and for keeping me going specifically in my PhD 'Endgame'. I have come to believe that the world is a small place, for minds that are not even femtometers away.

Appendix

1. List of Abbreviations

BPC	Bipolar Cell
DC	Direct current
Dm	Dorsal medulla
GABA	Gamma-Aminobutyric acid
L	Lamina
LMC	Lamina Monopolar Cell
Lo	Lobula
LP	Lobula Plate
LPTC	Lobula Plate Tangential Cell
Mi	Medulla-intrinsic
PR	Photoreceptor
R	Retina
RGC	Retinal Ganglion Cell
Tm	Transmedullary

2. List of Figures

Figures for Introduction and General Discussion:

Figures from the manuscripts: (Published Manuscript excluded)

Manuscript 2

Manuscript 3:

List of tables for Manuscript 3:

Declaration

Herewith I declare, that I prepared the Doctoral Thesis '**Strategies for dynamic vision in the Drosophila peripheral visual system**' on my own and with no other sources and aids than quoted.

Mainz, 31.08.2021

Madhura D. Ketkar